

JOURNAL OF

CHROMATOGRAPHY

INCLUDING ELECTROPHORESIS AND OTHER SEPARATION METHODS

EDITORS

R. W. Giese (Boston, MA)
 J. K. Haken (Kensington, N.S.W.)
 K. Macek (Prague)
 L. R. Snyder (Orinda, CA)

EDITORS, SYMPOSIUM VOLUMES.

E. Heftmann (Orinda, CA), Z. Deyl (Prague)

EDITORIAL BOARD

D. W. Armstrong (Rolla, MO)
 W. A. Aue (Halifax)
 P. Božek (Brno)
 A. A. Boulton (Saskatoon)
 P. W. Carr (Minneapolis, MN)
 N. H. C. Cooke (San Ramon, CA)
 V. A. Davankov (Moscow)
 Z. Deyl (Prague)
 S. Dilli (Kensington, N.S.W.)
 F. Erni (Basle)
 M. B. Evans (Hatfield)
 J. L. Glajch (N. Billerica, MA)
 G. A. Guiochon (Knoxville, TN)
 P. R. Haddad (Kensington, N.S.W.)
 I. M. Hais (Hradec Králové)
 W. S. Hancock (San Francisco, CA)
 S. Hjertén (Uppsala)
 Cs. Horváth (New Haven, CT)
 J. F. K. Huber (Vienna)
 K.-P. Hupe (Waldbronn)
 T. W. Hutchens (Houston, TX)
 J. Janák (Brno)
 P. Jandera (Pardubice)
 B. L. Karger (Boston, MA)
 J. J. Kirkland (Wilmington, DE)
 E. sz. Kováts (Lausanne)
 A. J. P. Martin (Cambridge)
 L. W. McLaughlin (Chestnut Hill, MA)
 E. D. Pearson (Keele)
 J. D. Pearson (Kalamazoo, MI)
 H. Poppe (Amsterdam)
 F. E. Regnier (West Lafayette, IN)
 P. G. Righetti (Milan)
 P. Schoenmakers (Eindhoven)
 R. Schwarzenbach (Dübendorf)
 R. E. Shoup (West Lafayette, IN)
 A. M. Siouffi (Marseille)
 D. J. Strydom (Boston, MA)
 N. Tanaka (Kyoto)
 S. Terabe (Hyogo)
 K. K. Unger (Mainz)
 R. Verpoorte (Leiden)
 Gy. Vigh (College Station, TX)
 J. T. Watson (East Lansing, MI)
 B. D. Westerlund (Uppsala)

EDITORS, BIBLIOGRAPHY SECTION

Z. Deyl (Prague), J. Janák (Brno), V. Schwarz (Prague), K. Macek (Prague)

JOURNAL OF CHROMATOGRAPHY

INCLUDING ELECTROPHORESIS AND OTHER SEPARATION METHODS

Scope. The *Journal of Chromatography* publishes papers on all aspects of chromatography, electrophoresis and related methods. Contributions consist mainly of research papers dealing with chromatographic theory, instrumental development and their applications. The section *Biomedical Applications*, which is under separate editorship, deals with the following aspects: developments in and applications of chromatographic and electrophoretic techniques related to clinical diagnosis or alterations during medical treatment; screening and profiling of body fluids or tissues with special reference to metabolic disorders; results from basic medical research with direct consequences in clinical practice; drug level monitoring and pharmacokinetic studies; clinical toxicology; analytical studies in occupational medicine.

Submission of Papers. Manuscripts (in English; four copies are required) should be submitted to: Editorial Office of *Journal of Chromatography*, P.O. Box 681, 1000 AR Amsterdam, Netherlands, Telefax (+31-20) 5862 304, or to: The Editor of *Journal of Chromatography*, *Biomedical Applications*, P.O. Box 681, 1000 AR Amsterdam, Netherlands. Review articles are invited or proposed by letter to the Editors. An outline of the proposed review should first be forwarded to the Editors for preliminary discussion prior to preparation. Submission of an article is understood to imply that the article is original and unpublished and is not being considered for publication elsewhere. For copyright regulations, see below.

Publication. The *Journal of Chromatography* (incl. *Biomedical Applications*) has 39 volumes in 1992. The subscription prices for 1992 are:

J. Chromatogr. (incl. *Cum. Indexes, Vols. 551-600*) + *Biomed. Appl.* (Vols. 573-611):

Dfl. 7722.00 plus Dfl. 1209.00 (p.p.h.) (total ca. US\$ 4421.25)

J. Chromatogr. (incl. *Cum. Indexes, Vols. 551-600*) only (Vols. 585-611):

Dfl. 6210.00 plus Dfl. 837.00 (p.p.h.) (total ca. US\$ 3488.50)

Biomed. Appl. only (Vols. 573-584):

Dfl. 2760.00 plus Dfl. 372.00 (p.p.h.) (total ca. US\$ 1550.50)

Subscription Orders. The Dutch guilder price is definitive. The US\$ price is subject to exchange-rate fluctuations and is given as a guide. Subscriptions are accepted on a prepaid basis only, unless different terms have been previously agreed upon. Subscription orders can be entered only by calendar year (Jan.-Dec.) and should be sent to Elsevier Science Publishers, Journal Department, P.O. Box 211, 1000 AE Amsterdam, Netherlands, Tel. (+31-20) 5803 642, Telefax (+31-20) 5803 598, or to your usual subscription agent. Postage and handling charges include surface delivery except to the following countries where air delivery via SAL (Surface Air Lift) mail is ensured: Argentina, Australia, Brazil, Canada, Hong Kong, India, Israel, Japan*, Malaysia, Mexico, New Zealand, Pakistan, China, Singapore, South Africa, South Korea, Taiwan, Thailand, USA. *For Japan air delivery (SAL) requires 25% additional charge of the normal postage and handling charge. For all other countries airmail rates are available upon request. Claims for missing issues must be made within three months of our publication (mailing) date, otherwise such claims cannot be honoured free of charge. Back volumes of the *Journal of Chromatography* (Vols. 1-572) are available at Dfl. 208.00 (plus postage). Customers in the USA and Canada wishing information on this and other Elsevier journals, please contact Journal Information Center, Elsevier Science Publishing Co. Inc., 655 Avenue of the Americas, New York, NY 10010, USA, Tel. (+1-212) 633 3750, Telefax (+1-212) 633 3764.

Abstracts/Contents Lists published in Analytical Abstracts, Biochemical Abstracts, Biological Abstracts, Chemical Abstracts, Chemical Titles, Chromatography Abstracts, Clinical Chemistry Lookout, Current Contents/Life Sciences, Current Contents/Physical, Chemical & Earth Sciences, Deep-Sea Research/Part B: Oceanographic Literature Review, Excerpta Medica, Index Medicus, Mass Spectrometry Bulletin, PASCAL-CNRS, Pharmaceutical Abstracts, Referativnyi Zhurnal, Research Alert, Science Citation Index and Trends in Biotechnology.

See inside back cover for Publication Schedule, Information for Authors and information on Advertisements.

© ELSEVIER SCIENCE PUBLISHERS B.V. — 1991

0021-9673/91/803.50

All rights reserved. No part of this publication may be reproduced, stored in a retrieval system or transmitted in any form or by any means, electronic, mechanical, photocopying, recording or otherwise, without the prior written permission of the publisher, Elsevier Science Publishers B.V., Permissions Department, P.O. Box 521, 1000 AN Amsterdam, Netherlands.

Upon acceptance of an article by the journal, the author(s) will be asked to transfer copyright of the article to the publisher. The transfer will ensure the widest possible dissemination of information.

Submission of an article for publication entails the authors' irrevocable and exclusive authorization of the publisher to collect any sums or considerations for copying or reproduction payable by third parties (as mentioned in article 17 paragraph 2 of the Dutch Copyright Act of 1912 and the Royal Decree of June 20, 1974 (S. 351) pursuant to article 16 b of the Dutch Copyright Act of 1912) and/or to act in or out of Court in connection therewith.

Special regulations for readers in the USA. This journal has been registered with the Copyright Clearance Center, Inc. Consent is given for copying of articles for personal or internal use, or for the personal use of specific clients. This consent is given on the condition that the copier pays through the Center the per-copy fee stated in the code on the first page of each article for copying beyond that permitted by Sections 107 or 108 of the US Copyright Law. The appropriate fee should be forwarded with a copy of the first page of the article to the Copyright Clearance Center, Inc., 27 Congress Street, Salem, MA 01970, USA. If no code appears in an article, the author has not given broad consent to copy and permission to copy must be obtained directly from the author. All articles published prior to 1980 may be copied for a per-copy fee of US\$ 2.25, also payable through the Center. This consent does not extend to other kinds of copying, such as for general distribution, resale, advertising and promotion purposes, or for creating new collective works. Special written permission must be obtained from the publisher for such copying.

No responsibility is assumed by the Publisher for any injury and/or damage to persons or property, as a matter of products liability, negligence or otherwise, or from any use or operation of any methods, products, instructions or ideas contained in the materials herein. Because of rapid advances in the medical sciences, the Publisher recommends that independent verification of diagnoses and drug dosages should be made.

Although all advertising material is expected to conform to ethical (medical) standards, inclusion in this publication does not constitute a guarantee or endorsement of the quality or value of such product or of the claims made of it by its manufacturer.

This issue is printed on acid-free paper.

Printed in the Netherlands

CONTENTS

(Abstracts/Contents Lists published in Analytical Abstracts, Biochemical Abstracts, Biological Abstracts, Chemical Abstracts, Chemical Titles, Chromatography Abstracts, Current Contents/Life Sciences, Current Contents/Physical, Chemical & Earth Sciences, Deep-Sea Research/Part B: Oceanographic Literature Review, Excerpta Medica, Index Medicus, Mass Spectrometry Bulletin, PASCAL-CRNS, Referativnyi Zhurnal, Research Alert and Science Citation Index)

REGULAR PAPERS

Column Liquid Chromatography

- UNIFAC model as a heuristic guide for estimating retention in chromatography
by J. H. Park, J. E. Lee and M. D. Jang (Kyongsan, South Korea) and J.-J. Li and P. W. Carr (Minneapolis, MN, USA)
(Received June 18th, 1991) 1
- Simultaneous optimization of several chromatographic performance goals using Derringer's desirability function
by B. Bourguignon and D. L. Massart (Brussels, Belgium) (Received June 18th, 1991) 11
- Continuous beds for standard and micro high-performance liquid chromatography
by J.-L. Liao, R. Zhang and S. Hjertén (Uppsala, Sweden) (Received May 27th, 1991) 21
- Protein adsorption capacity of a porous phenylalanine-containing membrane based on a polyethylene matrix
by M. Kim, K. Saito and S. Furusaki (Tokyo, Japan) and T. Sugo and I. Ishigaki (Gunma, Japan) (Received June 17th,
1991) 27
- Two-dimensional mapping by high-performance liquid chromatography of pyridylamino oligosaccharides from various gly-
cosphingolipids
by K. Ohara, M. Sano, A. Kondo and I. Kato (Shiga, Japan) (Received June 3rd, 1991) 35
- Retention behaviour of a template-assembled synthetic protein and its amphiphilic building blocks on reversed-phase columns
by V. Steiner, M. Schär and K. O. Börnsen (Basel, Switzerland) and M. Mutter (Lausanne, Switzerland) (Received June
24th, 1991) 43
- High-performance affinity chromatography of NADP⁺ dehydrogenases from cell-free extracts using a nucleotide analogue as
general ligand
by J. Alhama, J. López-Barea and F. Toribio (Córdoba, Spain) (Received June 10th, 1991) 51
- Determination of metacycline and related substances by column liquid chromatography on poly(styrene-divinylbenzene)
by W. Naidong, K. Verresen, E. Roets and J. Hoogmartens (Leuven, Belgium) (Received June 13th, 1991) 61
- Isolation of doxycycline, 6-epidoxycycline and 2-acetyl-2-decarboxamidometacycline from commercial metacycline by prepara-
tive column liquid chromatography on silica gel
by W. Naidong, K. Verresen, R. Busson, E. Roets and J. Hoogmartens (Leuven, Belgium) (Received June 13th, 1991) 67
- Analysis of dyes extracted from textile fibers by thermospray high-performance liquid chromatography-mass spectrometry
by J. Yinon (Rehovot, Israel) and J. Saar (Beer Sheva, Israel) (Received June 28th, 1991) 73
- Gas Chromatography*
- Prediction of retention indexes. II. Structure-retention index relationship on polar columns
by C. T. Peng and Z. C. Yang (San Francisco, CA, USA) and S. F. Ding (Beijing, China) (Received June 4th, 1991) 85
- Prediction of retention indexes. III. Silylated derivatives of polar compounds
by C. T. Peng, Z. C. Yang and D. Maltby (San Francisco, CA, USA) (Received June 4th, 1991) 113
- Gas chromatography for measurement of hydrogen isotopes at tritium processing
by T. Uda, K. Okuno, T. Suzuki and Y. Narusa (Ibaraki-ken, Japan) (Received July 1st, 1991) 131
- Enantiomeric separation of α -phenylethylamine and its substituted isomers by gas chromatography
by X. Lou, X. Liu, S. Zhang and L. Zhou (Dalian, China) (Received June 21st, 1991) 139

(Continued overleaf)

SHORT COMMUNICATIONS

Column Liquid Chromatography

High-performance liquid chromatography of peptides at reduced temperatures: separation of isomers
by M. Lebl, S. Fang and V. J. Hruby (Tucson, AZ, USA) (Received June 6th, 1991) 145

Determination of cimetidine and related impurities in pharmaceutical formulations by high-performance liquid chromatography
by P. Betto, E. Ciranni-Signoretti and R. Di Fava (Rome, Italy) (Received July 11th, 1991) 149

High-performance liquid chromatography of thiazolidinic compounds obtained by condensation of pyridoxal 5'-phosphate or
pyridoxal with aminothiols (L- or D-cysteine, cysteamine, L-cysteine ethyl ester)
by L. Terzuoli, R. Leoncini, D. Vannoni, E. Marinello and R. Pagani (Siena, Italy) (Received July 16th, 1991) 153

Liquid chromatographic determination of ethylenethiourea using pulsed amperometric detection
by D. R. Doerge and A. B. K. Yee (Honolulu, HI, USA) (Received June 11th, 1991) 158

Gas Chromatography

Determination of specific retention volumes at 20°C for hydrocarbons on microporous carbons
by X.-L. Cao (Uxbridge, UK) (July 31st, 1991) 161

Identification of enzymatic degradation products from synthesized glucobrassicin by gas chromatography-mass spectrometry
by L. Latxague and C. Gardrat (Talence, France), J. L. Coustille (Pessac, France) and M. C. Viaud and P. Rollin (Orléans,
France) (Received July 19th, 1991) 166

Fast separation of polymethoxylated flavones by carbon dioxide supercritical fluid chromatography
by Ph. Morin (Orléans, France), A. Gallois and H. Richard (Massy, France) and E. Gaydou (Marseille, France) (Received
July 16th, 1991) 171

Determination of cimetidine in pharmaceutical preparations by capillary zone electrophoresis
by S. Arrowood and A. M. Hoyt, Jr. (Conway, AR, USA) (Received August 9th, 1991) 177

* In articles with more than one author, the name of the author to whom correspondence should be addressed is indicated *
* in the article heading by a 6-pointed asterisk (*) *

An authoritative review... highly recommended...

Optimization of Chromatographic Selectivity

A Guide to Method Development

by P. Schoenmakers, *Philips Research Laboratories, Eindhoven, The Netherlands*

(Journal of Chromatography Library, 35)

"The contents of this book have been put together with great expertise and care, and represent an authoritative review of this very timely topic... highly recommended to practising analytical chemists and to advanced students." (Jnl. of Chromatography)

"...an important contribution by a worker who has been in the field almost from its inception and who understands that field as well as anyone. If one is serious about method development, particularly for HPLC, this book will well reward a careful reading and will continue to be useful for reference purposes." (Mag. of Liquid & Gas Chromatography)

This is the first detailed description of method development in chromatography - the overall process of which may be summarized as: method selection, phase selection, selectivity optimization, and system optimization. All four aspects receive attention in this eminently readable book.

The first chapter describes chromatographic theory and nomenclature and outlines the method development process. Guidelines are then given for method selection and quantitative concepts for characterizing and classifying chromatographic phases. Selective separation methods (from both GC and LC) are

given - the main parameters of each method are identified and simple, quantitative relations are sought to describe their effects. Criteria by which to judge the quality of separation are discussed with clear recommendations for different situations. The specific problems involved in the optimization of chromatographic selectivity are explained. Optimization procedures, illustrated by examples, are described and compared on the basis of a number of criteria. Suggestions are made both for the application of different procedures and for further research. The optimization of programmed analysis receives special attention, and the last chapter summarizes the optimization of the chromatographic system, including the optimization of the efficiency, sensitivity and instrumentation.

Those developing chromatographic methods or wishing to improve existing methods will value the detailed, structured way in which the subject is presented. Because optimization procedures and criteria are described as elements of a complete optimization package, the book will help the reader to understand, evaluate and select current and future commercial systems.

Contents: 1. Introduction. 2. Selection of Methods. 3. Parameters Affecting Selectivity. 4. Optimization Criteria. 5. Optimization Procedures. 6. Programmed Analysis. 7. System Optimization. Indexes.

1986 1st repr. 1987 xvi + 346 pages
US\$ 110.50 / Dfl. 210.00
ISBN 0-444-42681-7



ELSEVIER SCIENCE PUBLISHERS

P.O. Box 211, 1000 AE Amsterdam, The Netherlands
P.O. Box 882, Madison Square Station, New York, NY 10159, USA

THE STANDARD TEXT ON THE SUBJECT...

Chemometrics: a textbook

D.L. Massart, *Vrije Universiteit Brussel, Belgium*,
B.G.M. Vandeginste, *Katholieke Universiteit Nijmegen, The Netherlands*,
S.N. Deming, *Dept. of Chemistry, University of Houston, TX, USA*,
Y. Michotte and L. Kaufman, *Vrije Universiteit Brussel, Belgium*

(Data Handling in Science and Technology, 2)

Most chemists, whether they are biochemists, organic, analytical, pharmaceutical or clinical chemists and many pharmacists and biologists need to perform chemical analyses. Consequently, they are not only confronted with carrying out the actual analysis, but also with problems such as method selection, experimental design, optimization, calibration, data acquisition and handling, and statistics in order to obtain maximum relevant chemical information. In other words: they are confronted with chemometrics.

This book, written by some of the leaders in the field, aims to provide a thorough, up-to-date introduction to this subject. The reader is given the opportunity to acquaint himself with the tools used in this discipline and the way in which they are applied. Some practical examples are given and the reader is shown how to select the appropriate tools in a given situation. The book thus provides the means to approach and solve analytical problems strategically and systematically, without the need for the reader to become a fully-fledged chemometrician.

Contents: Chapter 1. Chemometrics and the Analytical Process. 2. Precision and Accuracy. 3. Evaluation of Precision and Accuracy. Comparison of Two Procedures. 4. Evaluation of Sources of Variation in Data. Analysis of Variance. 5. Calibration. 6. Reliability and Drift. 7. Sensitivity and Limit of Detection. 8. Selectivity and Specificity. 9. Information. 10. Costs. 11. The Time Constant. 12. Signals and Data. 13. Regression Methods. 14. Correlation Methods. 15. Signal Processing. 16. Response Surfaces and Models. 17. Exploration of Response Surfaces. 18. Optimization of Analytical Chemical Methods. 19. Optimization of Chromatographic Methods. 20. The Multivariate Approach. 21. Principal Components and Factor Analysis. 22. Clustering Techniques. 23. Supervised Pattern Recognition. 24. Decisions in the Analytical Laboratory. 25. Operations Research. 26. Decision Making. 27. Process Control. Appendix. Subject Index.

"...it is apparent that the book is the most comprehensive available on chemometrics. Beginners and those more familiar with the field will find the book a great benefit because of that breadth, and especially because of the clarity and relative uniformity of presentation. Like its predecessor, this book will be the standard text on the subject for some time." (Trends in Analytical Chemistry)

1988 485 pages US\$ 85.25 / Dfl. 175.00 ISBN 0-444-42660-4

ELSEVIER SCIENCE PUBLISHERS

P.O. Box 211, 1000 AE Amsterdam, The Netherlands

P.O. Box 1663, Grand Central Station, New York, NY 10163, USA

7385A

JOURNAL OF CHROMATOGRAPHY

VOL. 586 (1991)

JOURNAL of CHROMATOGRAPHY

INCLUDING ELECTROPHORESIS AND OTHER SEPARATION METHODS

EDITORS

R. W. GIESE (Boston, MA), J. K. HAKEN (Kensington, N.S.W.), K. MACEK (Prague), L. R. SNYDER (Orinda, CA)

EDITORS, SYMPOSIUM VOLUMES

E. HEFTMANN (Orinda, CA), Z. DEYL (Prague)

EDITORIAL BOARD

D. W. Armstrong (Rolla, MO), W. A. Aue (Halifax), P. Boček (Brno), A. A. Boulton (Saskatoon), P. W. Carr (Minneapolis, MN), N. H. C. Cooke (San Ramon, CA), V. A. Davankov (Moscow), Z. Deyl (Prague), S. Dilli (Kensington, N.S.W.), F. Erni (Basle), M. B. Evans (Hatfield), J. L. Glajch (N. Billerica, MA), G. A. Guiochon (Knoxville, TN), P. R. Haddad (Kensington, N.S.W.), I. M. Hais (Hradec Králové), W. S. Hancock (San Francisco, CA), S. Hjertén (Uppsala), Cs. Horváth (New Haven, CT), J. F. K. Huber (Vienna), K.-P. Hupe (Waldbronn), T. W. Hutchens (Houston, TX), J. Janák (Brno), P. Jandera (Pardubice), B. L. Karger (Boston, MA), J. J. Kirkland (Wilmington, DE), E. sz. Kováts (Lausanne), A. J. P. Martin (Cambridge), L. W. McLaughlin (Chestnut Hill, MA), E. D. Morgan (Keele), J. D. Pearson (Kalamazoo, MI), H. Poppe (Amsterdam), F. E. Regnier (West Lafayette, IN), P. G. Righetti (Milan), P. Schoenmakers (Eindhoven), R. Schwarzenbach (Dübendorf), R. E. Shoup (West Lafayette, IN), A. M. Siouffi (Marseille), D. J. Strydom (Boston, MA), N. Tanaka (Kyoto), S. Terabe (Hyogo), K. K. Unger (Mainz), R. Verpoorte (Leiden), Gy. Vigh (College Station, TX), J. T. Watson (East Lansing, MI), B. D. Westerlund (Uppsala)

EDITORS, BIBLIOGRAPHY SECTION

Z. Deyl (Prague), J. Janák (Brno), V. Schwarz (Prague), K. Macek (Prague)



ELSEVIER
AMSTERDAM — LONDON — NEW YORK — TOKYO

J. Chromatogr., Vol. 586 (1991)

All rights reserved. No part of this publication may be reproduced, stored in a retrieval system or transmitted in any form or by any means, electronic, mechanical, photocopying, recording or otherwise, without the prior written permission of the publisher, Elsevier Science Publishers B.V., Permissions Department, P.O. Box 521, 1000 AN Amsterdam, Netherlands.

Upon acceptance of an article by the journal, the author(s) will be asked to transfer copyright of the article to the publisher. The transfer will ensure the widest possible dissemination of information.

Submission of an article for publication entails the authors' irrevocable and exclusive authorization of the publisher to collect any sums or considerations for copying or reproduction payable by third parties (as mentioned in article 17 paragraph 2 of the Dutch Copyright Act of 1912 and the Royal Decree of June 20, 1974 (S. 351) pursuant to article 16 b of the Dutch Copyright Act of 1912) and/or to act in or out of Court in connection therewith.

Special regulations for readers in the USA. This journal has been registered with the Copyright Clearance Center, Inc. Consent is given for copying of articles for personal or internal use, or for the personal use of specific clients. This consent is given on the condition that the copier pays through the Center the per-copy fee stated in the code on the first page of each article for copying beyond that permitted by Sections 107 or 108 of the US Copyright Law. The appropriate fee should be forwarded with a copy of the first page of the article to the Copyright Clearance Center, Inc., 27 Congress Street, Salem, MA 01970, USA. If no code appears in an article, the author has not given broad consent to copy and permission to copy must be obtained directly from the author. All articles published prior to 1980 may be copied for a per-copy fee of US\$ 2.25, also payable through the Center. This consent does not extend to other kinds of copying, such as for general distribution, resale, advertising and promotion purposes, or for creating new collective works. Special written permission must be obtained from the publisher for such copying.

No responsibility is assumed by the Publisher for any injury and/or damage to persons or property as a matter of products liability, negligence or otherwise, or from any use or operation of any methods, products, instructions or ideas contained in the materials herein. Because of rapid advances in the medical sciences, the Publisher recommends that independent verification of diagnoses and drug dosages should be made.

Although all advertising material is expected to conform to ethical (medical) standards, inclusion in this publication does not constitute a guarantee or endorsement of the quality or value of such product or of the claims made of it by its manufacturer.

This issue is printed on acid-free paper.

UNIFAC model as a heuristic guide for estimating retention in chromatography

Jung Hag Park*, Jung Eun Lee and Myung Duk Jang

Department of Chemistry, Yeungnam University, Kyongsan 712-749 (South Korea)

Jian-Jun Li and Peter W. Carr

Department of Chemistry, University of Minnesota, 207 Pleasant Street S. E., Minneapolis, MN 55455 (USA)

(First received February 8th, 1991; revised manuscript received June 18th, 1991)

ABSTRACT

The usefulness of the UNIFAC activity coefficient estimation method for understanding the magnitude of solute–solvent interactions in gas and liquid chromatography has been investigated. To demonstrate the power of UNIFAC it was used to investigate the origin of the Martin equation, to explore the methylene group selectivity and relative retention in reversed-phase liquid–liquid partition chromatography, to examine solute–solvent interactions in eluents in normal-phase liquid chromatography and to examine mixed stationary phase effects in gas–liquid chromatography. Although not accurate enough to be useful for quantitative predictions of retention, UNIFAC is fairly useful in explaining a wide variety of issues of general importance in chromatography such as the prediction of the order of elution of polar *versus* non-polar solutes and the relative strengths of solvents in all types of chromatography.

INTRODUCTION

The UNIFAC (*UNIQUAC* functional group activity coefficient) model is an activity coefficient estimation scheme that is used generally in chemical engineering [1]. Its major use is for the prediction of vapour–liquid [2] and liquid–liquid equilibria [3]. There have only been a few studies on the application of UNIFAC to chromatography [4–6]. It has not been systematically explored, nor is it widely appreciated how generally applicable UNIFAC is as a guide to understanding the magnitude of solute–solvent interactions in chromatography.

As UNIFAC is a method oriented towards functional groups, it is broadly applicable in a predictive sense. Forty-four different “main” groups have been defined and the relevant interaction parameters made available. Thus, in principle, the activity coefficients in any mixture of species consisting of molecules containing these functional groups can

be computed. This makes the UNIFAC method far more powerful in terms of its generality than other approaches such as those based on the separation of cohesive energy densities which are used frequently in chromatography [7–9]. As has been shown, UNIFAC is not accurate enough, at this stage of its development, to be useful for the quantitative prediction of retention [10]. As chromatographic separation is able to distinguish between two types of solute molecules that differ in the strength of their interactions with the mobile and stationary phases by only around 10 joules per mole, there is as yet no general predictive method that suffices for use in chromatography. Nonetheless UNIFAC is sufficiently accurate that it is useful for the prediction of the relative retention of polar *versus* non-polar compounds, the relative strengths of solvents and other important chromatographic properties.

The purpose of this paper is to introduce the UNIFAC method, to show how it can be applied to

a wide variety of issues of general importance in chromatography and to use it to explain a number of important chromatographic observations.

UNIFAC METHOD

UNIFAC combines the UNIQUAC model of solutions [11] and the so-called analytical solution of group (ASOG) concept [12]. UNIQUAC (*universal quasi-chemical*) is an approximate model of liquid mixtures developed by the application of Guggenheim's quasi-chemical lattice model of liquid mixtures [13] through the use of a component's local area fraction as the main concentration variable. In essence this approach is a simple alternative to the highly unrealistic random mixing model which is the basis for regular solution theory. The ASOG approach is based on the idea that a solution can be viewed as a mixture of independent functional groups of all the individual components, and assumes that the contribution any functional group makes to the activity coefficient of a molecule is independent of any other functional group in that molecule, that is, the free energy of interaction of one species with a second species is assumed to be the additive sum of independent functional group contributions. Thus, in principle, the ASOG method can be made more realistic by simply redefining the set of functional groups to contain a larger and more complex group of units until the set includes all possible molecules. The UNIQUAC equation for the activity coefficient of component i is:

$$\ln \gamma_i = \ln \gamma_i^C + \ln \gamma_i^R \quad (1)$$

combinatorial residual

where

$$\ln \gamma_i^C = \ln(\varphi_i/x_i) + (z/2) q_i \ln(\theta_i/\varphi_i) + l_i - \varphi_i/x_i \sum_{i=1}^n x_i l_i \quad (2)$$

$$\ln \gamma_i^R = q_i \left[1 - \ln \left(\sum_{j=1}^n \theta_j \tau_{ji} \right) - \sum_{j=1}^n \left(\theta_j \tau_{ij} / \sum_{k=1}^n \theta_k \tau_{kj} \right) \right] \quad (3)$$

such that

$$l_i = (z/2)(r_i - q_i) - (r_i - 1); z = 10 \quad (4)$$

$$\theta_i = \left[q_i x_i / \sum_{j=1}^n q_j x_j \right]; \quad \varphi_i = \left[r_i x_i / \sum_{j=1}^n r_j x_j \right] \quad (5)$$

$$\tau_{ji} = \exp[-(u_{ji} - u_{ij})/RT] \quad (6)$$

In the above expressions, x_i is the mole fraction of component i , n is the number of components, θ_i is the area fraction of component i and φ_i is the segment (or volume) fraction of component i . The values of r_i and q_i are measures of pure component molecular Van der Waals volumes and surface areas. The two binary interaction parameters, τ_{ij} and τ_{ji} , are evaluated from experimental phase equilibrium data. The combinatorial term can be viewed as a slightly improved Flory-Huggins like athermal or entropic term. Similarly the residual term represents the enthalpic contributions to solution non-ideality. Thus the binary parameters τ_{ij} and τ_{ji} represent the energy of interaction of two separate molecules.

The UNIQUAC expression for the combinatorial activity coefficient term is used directly in the UNIFAC model. The r_i and q_i parameters are calculated in the UNIFAC model as the sum of the molecular i group volume and area parameters, R_k and Q_k [11].

$$r_i = \sum_{k=1}^g v_k^{(i)} R_k \quad \text{and} \quad q_i = \sum_{k=1}^g v_k^{(i)} Q_k \quad (7)$$

where g is the number of different groups in component i and v_k is the number of k -type groups in the molecule. These group volume and area parameters are obtained from the Van der Waals group volumes and surface areas V_{wk} and A_{wk} given by Bondi [14] and normalized by Abrams and Prausnitz [11] to best represent the true molecular volumes and surface areas.

The solution of groups concept is used in UNIFAC to determine the residual portion of the activity coefficient.

$$\ln \gamma_i^R = \sum_{k=1}^{g'} v_k^{(i)} [\ln \Gamma_k - \ln \Gamma_k^{(i)}] \quad (8)$$

where g' is the total number of different functional groups in the mixture, Γ_k is the group residual activity coefficient and $\Gamma_k^{(i)}$ is the activity coefficient of group k in a reference solution containing only molecules of type i . This reference term normalizes the

expression so that as x_i approaches unity, the activity coefficient of component i is forced to unity to obey the Raoult's law standard state.

The group residual activity coefficient (Γ_k) is calculated in a manner similar to the molecular residual activity coefficient in the UNIQUAC model:

$$\ln \Gamma_k = Q_k \left[1 - \ln \left(\sum_{m=1}^{g'} \theta_m \psi_{mk} \right) - \sum_{m=1}^{g'} \left(\theta_m \psi_{km} / \sum_{n=1}^{g'} \theta_n \psi_{nm} \right) \right] \quad (9)$$

where

$$\theta_m = (Q_m x_m) / \left(\sum_{n=1}^{g'} Q_n x_n \right) \quad (10)$$

$$\begin{aligned} \psi_{nm} &= \exp[-(u_{nm} - u_{mm})/RT] \\ &= \exp(-a_{mn}/RT) \end{aligned} \quad (11)$$

In the above expressions x_m is the mole fraction of group m in the mixture and u_{mn} is a measure of the interaction energy between groups m and n . The group interaction parameters, a_{mn} , are determined from banks of experimental phase equilibrium data [15]. Note a_{mn} is not equal to a_{nm} and, by definition, $a_{mm} = 0$. For the purpose of improving the group volumes and surface areas, a number of functional (main) groups are divided into "subgroups" and assigned subgroup R_k and Q_k values. The interaction parameters used in the residual activity coefficient term, however, are assigned only by main groups.

Recently two different modified UNIFAC methods, which show substantially improved accuracy for the prediction of γ^∞ , have been reported [16,17]. However, the two modified UNIFAC methods use six interaction parameters between two interacting groups, whereas only two parameters are used in the original version of UNIFAC, thus the flexibility of the modified methods is substantially reduced. In addition, the number of available group interaction parameters in the modified UNIFAC methods is smaller than in the original version of UNIFAC.

CALCULATIONS

All calculations were performed on an IBM compatible personal computer using programs written in GWBASIC. The double-precision option was

employed to improve the computational accuracy. For these calculations the original UNIFAC model with a combinatorial term modified as suggested by Kikic *et al.* [18] and the revised parameters for vapour-liquid equilibria by Gmehling *et al.* [15], Macedo *et al.* [19] and Tieggs *et al.* [20] were used.

RESULTS AND DISCUSSION

Martin equation

Most chromatographers are familiar with the Martin equation which states that in many forms of chromatography the logarithmic partition coefficient, and therefore the logarithmic capacity factor, is a linear function of the number of methylene groups within a homologous series of solutes.

$$\log K \text{ (or } k') = A + B \cdot n \quad (12)$$

where n denotes the homologue number. Agreement with this equation is so generally accepted that it is frequently used as the basis for estimating column dead volume in gas-liquid chromatography (GLC) and reversed-phase liquid chromatography (RPLC) [21]. The Kovats retention index is also largely based on the observed compliance with the Martin equation. Similarly Smith's scheme for establishing a retention index in RPLC relies in part on the linearity between $\log k'$ and n [22,23].

To assess the agreement between UNIFAC and the Martin equation in GLC two extreme types of common stationary phases were chosen, namely hexadecane and dimethyldodecylamine, and a homologous series of solutes. The logarithmic partition coefficients were then computed from the pure component vapour pressures via the equation:

$$\log K = \log RT - \log V_s - \log \gamma^\infty p^\circ \quad (13)$$

where V_s is the molar volume of the stationary phase, γ^∞ and p° are the infinite dilution activity coefficient and vapour pressure of the pure solute, respectively, and RT is the product of the gas constant and temperature in degrees Kelvin. As can be seen in Fig. 1, in all instances the computed partition coefficients are essentially linear functions of n . UNIFAC produces the desired qualitative result and if computed K values on hexadecane are compared with measured values, a fairly good quantitative

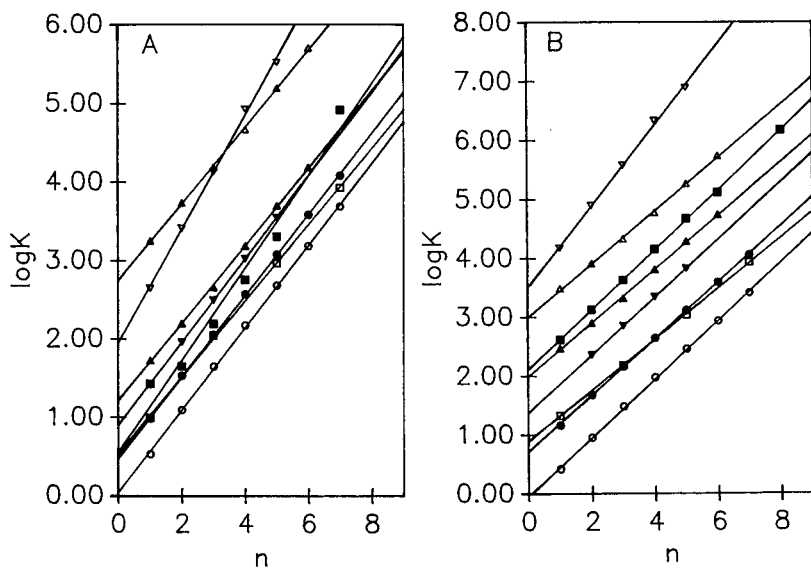


Fig. 1. Plots of calculated logarithmic gas-liquid partition coefficients (K) of homologous solutes versus n in (A) hexadecane and (B) dimethyldodecylamine at 298.15 K. Symbols: (○) alkanes, (●) alkenes, (△) alkylbenzenes, (▲) 2-ketones, (□) alkyl ethers, (■) 1-alcohols, (▽) carboxylic acids and (▼) 1-bromoalkanes.

tive agreement is observed, except for the carboxylic acids (inverse open triangle and dashed-crossed line in Fig. 2).

A similar analysis is carried out using estimates of the partition coefficients for transfer from water to hexadecane as an admittedly oversimplified and a very crude model of RPLC. In this instance the par-

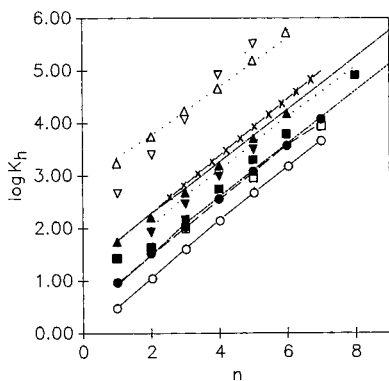


Fig. 2. Comparison of experimental (lines) and calculated (symbols) gas-liquid partition coefficients of homologous solutes in hexadecane (K_h) at 298.15 K. For symbols, see Fig. 1. Experimental data are from ref. 43: (—) alkanes, (---) alkenes, (····) alkylbenzenes, (-·-·-·) 2-ketones, (-----) alkyl ethers, (- - - -) 1-alcohols, (×-×-×) carboxylic acids, (....) 1-bromoalkanes.

tion coefficient is computed from the molar volumes of the two phases and the infinite dilution activity coefficients estimated by UNIFAC:

$$K_{h/w} = V_w \gamma_w^\infty / (V_h \gamma_h^\infty) \quad (14)$$

where V_h and V_w indicate the molar volume of hexadecane and water and γ_h^∞ and γ_w^∞ denote the computed infinite dilution activity coefficient of a solute in hexadecane and water, respectively. The results for several homologous series are shown in Fig. 3; linearity is once again observed. The computed logarithmic activity coefficients are not linear with n (Fig. 4), whereas the logarithms of the measured vapour pressures are linear (Fig. 5). It should be noted that the vapour pressure does not enter into the result, thus the linearity is not a consequence of an apparent linear variation in $\log p^\circ$ with n .

A detailed examination of the UNIQUAC-UNIFAC equations show two distinctly different causes of the fact that $\log \gamma^\infty$ is not a linear function of the homologue number. First, the combinatorial term used in UNIQUAC, and in the simple Flory-Huggins model, does not predict that $\log \gamma^\infty$ will be linear with n . For a solute at infinite dilution it is certainly true that the first term in eqn. 8 is linear with

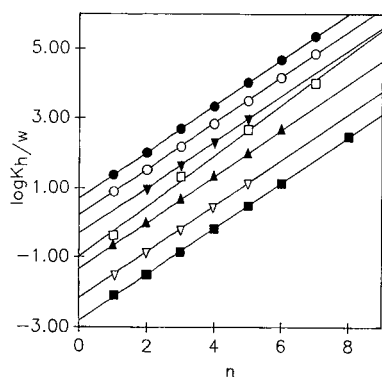


Fig. 3. Plots of calculated water-hexadecane partition coefficients ($K_{h/w}$) versus n at 298.15 K. For symbols, see Fig. 1.

the homologue number of the solute. This term represents the interactions of the solute with its surroundings. However, the second term in eqn. 8 represents the interaction of the pure solute with itself in the pure solute reference state. As the homologue number of the "solute" is varied, that of the reference "solvent" is also varied as in the reference state the "solute" and "solvent" are identical species. It follows that $\log \gamma^\infty$ is not a linear function of homologue number. Further there is no fundamental reason to think that $\log \gamma^\infty$ ought to be a linear function of homologue number. It must be understood that in many circumstances the combinatorial contribution to $\log \gamma^\infty$ will be small. Further, when the transfer of a solute at infinite dilution from one liquid to a second is considered, the reference state

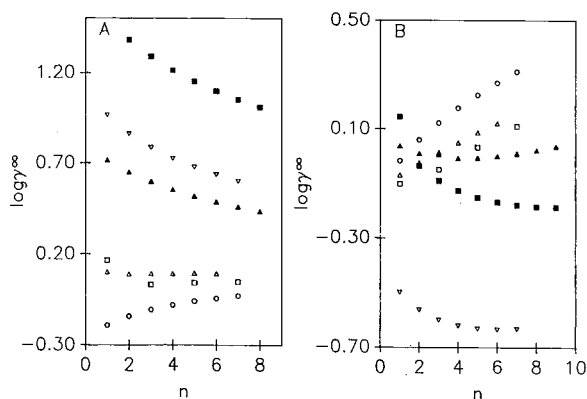


Fig. 4. Plots of calculated γ^∞ values versus n in (A) hexadecane and (B) dimethyldodecylamine at 298.15 K. For symbols, see Fig. 1.

term in eqn. 8 will exactly cancel. This leaves the first term in eqn. 8 as the dominant term in establishing $\log \gamma^\infty$ and this term is strictly linear with homologue number. Thus $\log K_{h/w}$ is linear with n .

It is noted, in agreement with Cheong and Carr [24] who measured activity coefficients in water and in aqueous mixtures of a variety of miscible solvents, that the activity coefficients of non-polar, non-hydrogen bonding solutes in water are large and vary greatly with n . In contrast, activity coefficients in non-polar solvents are small and are not very variable. The slopes of plots of $\log K_{h/w}$ versus n are greater than the slopes of plots of $\log K_n$ versus n .

UNIFAC can also cast some light on the importance of homologue number in normal-phase liquid chromatography. In normal-phase adsorption chromatography the Snyder model [25] is based in part on the assumption that solute-solvent interactions in a low-polarity mobile phase are negligible relative to the magnitude of solute and solvent interactions with a polar adsorbent such as silica. In essence Snyder argues that the principal effect of a change in the eluent phase is to modulate the solute interactions with the stationary phase; direct solute-eluent effects are said to be small. It will be shown here that the effect of solute homologue number in the mobile phase is fairly small, at least relative to the effect of homologue number in RPLC and GLC. For simplicity normal-phase partition chromatography is considered with hexane as the eluent and β, β' -oxydipropionitrile as the stationary

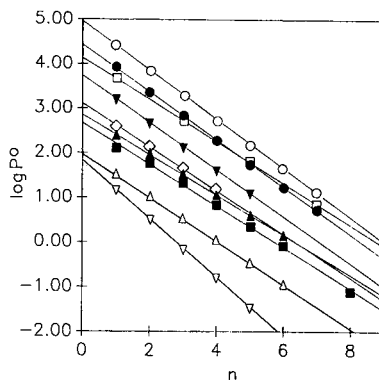


Fig. 5. Plots of vapour pressures of pure solutes (p^0) at 298.15 K versus n . For symbols, see Fig. 1.

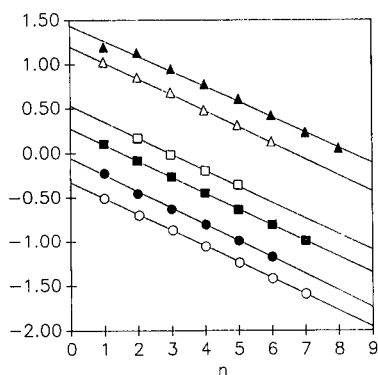


Fig. 6. Plots of calculated β,β' -oxydipropionitrile-hexane partition coefficients ($K_{o/h}$) versus n at 298.15 K. Symbols: (○) alkanes, (●) alkylbenzenes, (△) ketones, (▲) alcohols, (□) esters and (■) amines.

phase. Logarithms of estimated partition coefficients for the transfer from hexane to β,β' -oxydipropionitrile ($K_{o/h}$) are plotted versus n in Fig. 6. The change in $\log K_{o/h}$ with n and the parent functional groups are fairly small relative to the changes in RPLC. Thus in normal-phase liquid chromatography very minor differences in retention are expected between molecules that differ only by a methylene group as a result of solute-solvent interactions in the mobile phase.

Phase composition effects

Mixed liquid stationary phases in GC. Laub and co-workers introduced the concept of a diachoric solution in the mid-1970s [26–29]. In essence they observed that plots of the partition coefficient (K_M) of a solute distributed between a binary liquid stationary phase (B + C) and a gas phase versus the composition of the stationary phase were linear within experimental error (which in some instances reached $\pm 10\%$) with the volume fraction of the two solvents.

$$K_M = \phi_B K_B + \phi_C K_C \quad (15)$$

where Φ_i represents the volume fraction of solvent component i and K_i is the partition coefficient in either pure solvent. The system behaved as if the mixture of solvents was in fact not mixed. To investigate this effect plots of gas-liquid partition coefficients are presented for a variety of solutes in

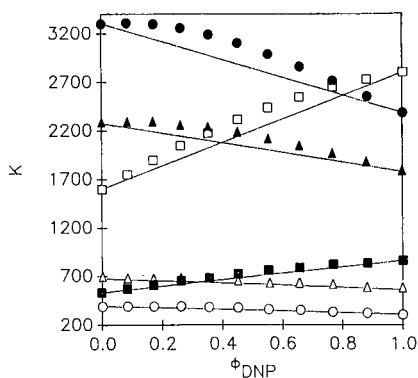


Fig. 7. Plots of calculated gas-liquid partition coefficients (K) of various solutes in mixtures of squalane with dinonyl phthalate (DNP) at 303.15 K versus volume fraction (ϕ) of the second solvent. Symbols: (○) hexane, (●) octane, (△) cyclohexane, (▲) methylcyclohexane, (□) toluene and (■) benzene.

mixed stationary phases of squalane and bis(3,5,5-trimethylhexyl)phthalate (dinonyl phthalate) (Fig. 7). The solid line shown in each figure is the line that connects the end-points of the plot. As can be seen there are systematic deviations that will be obscured by experimental imprecision. Martire [30] has shown that diachoric solution theory is valid only if any associations occurring between the solute and either stationary phase are of the 1:1 type and that the two stationary liquids form an ideal solution. Later Martire and co-workers [31,32] showed, both experimentally and theoretically, that plots of K_M versus Φ_C are curved and the extent of curvature depends on the strength of the interactions between the two solvents. UNIFAC can correctly predict curvature in such plots, as shown in Fig. 7.

Mobile phase effects in RPLC. Mobile phase composition effects are very important in liquid chromatography. The exact form of the relationship between k' and the volume fraction of a strong solvent in RPLC has been the subject of much debate. A linear relationship between $\log k'$ and volume percent is thought to be more accurate for methanol-water mixtures than for mixtures with other solvents [24]. Other workers, based on lattice theories [33] and simple regular solution theory [34], have advocated quadratic relationships. The displacement model of Geng and Regnier [35,36] argues for a linear relationship between $\log k'$ and the logarithm of the molar concentration of the modifier. The use of empirical parameters such as the

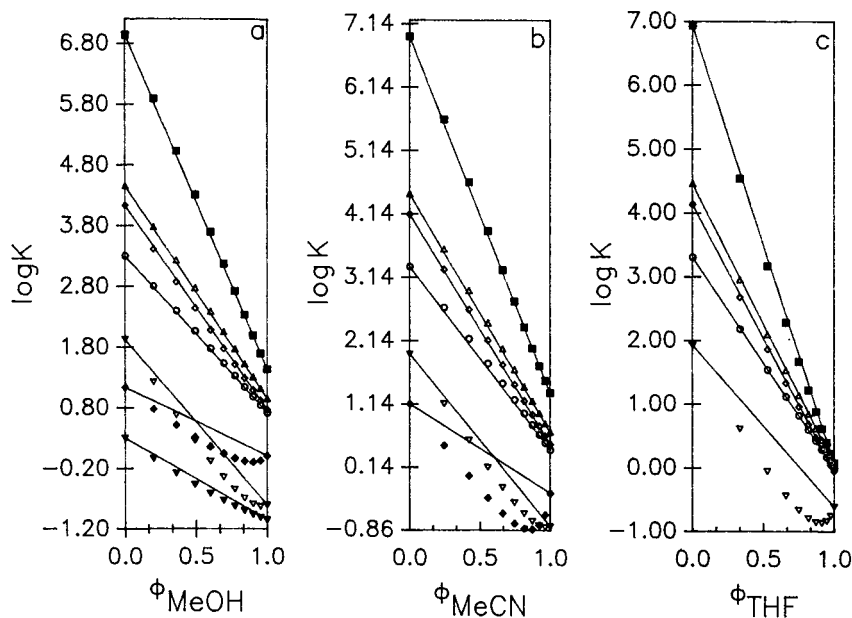


Fig. 8. Plots of calculated hexadecane–aqueous mixture partition coefficients (K) of various solutes *versus* volume fraction of (a) methanol, (b) acetonitrile and (c) tetrahydrofuran at 298.15 K. Symbols: (○) benzene, (△) ethylbenzene, (■) heptylbenzene, (▽) benzyl alcohol, (▼) phenol, (◇) chlorobenzene and (◆) aniline.

ET(30) scale to correlate retention in RPLC have been discussed at length [37,38].

Mobile phase effects in RPLC can be modelled using the UNIFAC approach by assuming, as above, that RPLC is a pure partition model. This is certainly not true [24]. For simplicity the effect of the organic solvent that partitions into the stationary phase will be neglected. This is a good approximation for methanol and acetonitrile mixtures with water if hexadecane is used as the stationary phase [39]. However, isopropanol and tetrahydrofuran are really fairly miscible with both water and hexadecane. Plots of $\log K$ *versus* composition for a judiciously selected series of solutes chosen to span a wide range in properties (dipolarity, hydrogen bond donor and acceptor strength, and size) are shown in Fig. 8. It is seen in this figure that UNIFAC can predict elution sequences. For example, UNIFAC predicts that the elution sequence in RPLC would be benzyl alcohol < chlorobenzene < ethyl benzene < naphthalene at a given mobile phase composition, as is invariably observed in RPLC. It should be pointed out that the solid lines are those connecting the end-points and not least-squares

lines. Clearly the plots are not precisely linear but there appears to be more curvature for the acetonitrile than the methanol mixtures. The slopes of the least-squares fits as well as the slopes of the lines shown in the figures are summarized in Tables I–III. Clearly the slopes vary almost linearly with the number of methylene groups or the number of aromatic rings. Also, as observed by many workers [40–42], there is a strong correlation between the intercept in pure water and the slope of the curves (Fig. 9). This correlation is forced on the system as follows. All solutes have very small activity coefficients of the order of unity in a pure organic mobile phase, whereas in water the activity coefficients are very large and very different. As in water all solutes start with large activity coefficients and end up with similar activity coefficients in the organic solvent, the slopes must correlate with the intercept.

For benzyl alcohol, phenol and aniline UNIFAC predicted a minimum in plots of $\log K$ *versus* volume fraction of modifier. This is in fact observed for these solutes in RPLC. Schoenmakers and co-workers [34,42] have shown that $\log k'$ varies non-linearly with the volume fraction of organic modifier

TABLE I

REGRESSION ANALYSIS OF EFFECT OF VOLUME FRACTION ON HEXADECANE-AQUEOUS METHANOL PARTITION COEFFICIENTS

The data are the results of regressing $\log K$ versus volume fraction for the organic solvent in the aqueous mixture. The number of data points is 11 in all regressions.

Solute	Intercept ^a	Slope ^a	<i>r</i>
Benzene	3.32(3.30)	2.60(2.59)	0.9999
Toluene	3.97(3.96)	3.19(3.18)	1.0000
Ethylbenzene	4.48(4.45)	3.52(3.61)	0.9999
Propylbenzene	4.99(4.96)	3.93(3.91)	0.9999
Pentylbenzene	6.00(5.90)	4.73(4.71)	0.9999
Heptylbenzene	6.99(6.94)	5.54(5.51)	0.9999
Naphthalene	4.86(4.82)	4.04(4.02)	0.9998
Anthracene	6.35(6.29)	5.48(5.46)	0.9998
Benzyl alcohol	1.74(1.13)	2.82(2.73)	0.9889
Phenol	0.23(0.30)	1.34(1.35)	0.9959
Chlorobenzene	4.10(4.13)	3.35(3.37)	0.9999
Aniline	0.99(1.14)	1.21(1.13)	0.9611

^a The numbers in parentheses are the intercepts and slopes for lines connecting end-points.

(Φ_0). The curvature is more pronounced for a less polar organic modifier and even in methanol-water the curvature is readily apparent if k' data are collected over a sufficiently wide range of φ_0 . For a given mobile phase system, the curvature is general-

TABLE II

REGRESSION ANALYSIS OF EFFECT OF VOLUME FRACTION ON HEXADECANE-AQUEOUS ACETONITRILE PARTITION COEFFICIENTS

Data calculated as in Table I.

Solute	Intercept	Slope	<i>r</i>
Benzene	3.36(3.30)	2.92(2.89)	0.9989
Toluene	3.99(3.96)	3.50(3.48)	0.9999
Ethylbenzene	4.50(4.45)	3.79(3.76)	0.9998
Propylbenzene	5.01(4.96)	4.17(4.13)	0.9998
Pentylbenzene	6.01(5.96)	4.93(4.88)	0.9999
Heptylbenzene	7.00(6.94)	5.69(5.63)	0.9999
Naphthalene	4.92(4.82)	4.49(4.44)	0.9994
Anthracene	6.42(6.29)	6.07(6.00)	0.9993
Benzyl alcohol	1.80(1.93)	2.82(2.73)	0.9922
Chlorobenzene	4.15(4.13)	3.64(3.63)	0.9999
Aniline	0.83(1.13)	1.74(1.41)	0.8855

TABLE III

REGRESSION ANALYSIS OF EFFECT OF VOLUME FRACTION ON HEXADECANE-AQUEOUS TETRAHYDROFURAN PARTITION COEFFICIENTS

Data calculated as in Table I.

Solute	Intercept	Slope	<i>r</i>
Benzene	3.29(3.30)	3.30(3.31)	0.9999
Toluene	3.94(3.96)	3.92(3.93)	0.9999
Ethylbenzene	4.42(4.45)	4.37(4.38)	0.9999
Propylbenzene	4.92(4.96)	4.86(4.88)	0.9999
Pentylbenzene	5.89(5.96)	5.86(5.87)	0.9998
Heptylbenzene	6.85(6.94)	6.84(6.86)	0.9997
Naphthalene	4.80(4.82)	4.91(4.92)	0.9999
Anthracene	6.25(6.29)	6.52(6.53)	0.9999
Benzyl alcohol	1.57(1.93)	2.62(2.54)	0.9544
Chlorobenzene	4.09(4.13)	4.16(4.18)	0.9999

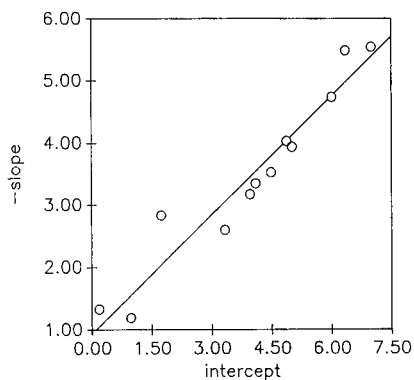


Fig. 9. Plot of slope versus intercept in the regression of effect of volume fraction on hexadecane-aqueous methanol partition coefficients. Data from Table I.

ly more pronounced for more polar solutes and a minimum is observed for a solute such as phenol which strongly associates. The predictions by UNIFAC is in agreement with the experimental observations.

CONCLUSIONS

As has been shown, UNIFAC is fairly useful in explaining a wide variety of issues of general importance in chromatography such as the prediction of elution order of polar versus non-polar compounds and the relative strengths of solvents in all types of

chromatography. It is, however, not accurate enough to be useful for the quantitative prediction of retention.

ACKNOWLEDGEMENT

Work at the University of Minnesota was supported in part by a grant from the National Science Foundation.

REFERENCES

- 1 J. M. Prausnitz, *Molecular Thermodynamics of Fluid Phase Equilibria*, Prentice Hall, Englewood Cliffs, NJ, 2nd ed., 1986.
- 2 A. Fredenslund, J. Gmehling and P. Rasmussen, *Vapor-Liquid Equilibria Using UNIFAC*, Elsevier, Amsterdam, 1977.
- 3 T. Magnussen, P. Rasmussen and A. Fredenslund, *Ind. Eng. Chem. Process Des. Dev.*, 20 (1981) 331.
- 4 M. Roth and J. Novak, *J. Chromatogr.*, 258 (1983) 23.
- 5 S. M. Petrovic, S. Lomic, and I. Sefer, *J. Chromatogr.*, 348 (1985) 49.
- 6 J. Gmehling and U. Weidlich, *Fluid Phase Equilib.*, 27 (1986) 171.
- 7 R. Tijssen, H. A. H. Billiet and P. J. Schoenmakers, *J. Chromatogr.*, 122 (1976) 185.
- 8 B. L. Karger, L. R. Snyder and C. Eon, *J. Chromatogr.*, 125 (1976) 71.
- 9 B. L. Karger, L. R. Snyder and C. Eon, *Anal. Chem.*, 50 (1978) 2126.
- 10 J. H. Park and P. W. Carr, *Anal. Chem.*, 59 (1987) 2596.
- 11 D. S. Abrams and J. M. Prausnitz, *AIChE J.*, 21 (1975) 116.
- 12 E. L. Derr and C. H. Deal, *I. Chem. E. Symp. Ser. No. 32 (Inst. Chem. Eng., London)*, 3 (1969) 40.
- 13 E. A. Guggenheim, *Mixtures*, Clarendon Press, Oxford, 1952.
- 14 A. Bondi, *Physical Properties of Molecular Crystals, Liquids, and Glasses*, Wiley, New York, 1968.
- 15 J. Gmehling, P. Rasmussen and A. Fredenslund, *Ind. Eng. Chem. Process Des. Dev.*, 21 (1982) 118.
- 16 U. Weidlich and J. Gmehling, *Ind. Eng. Chem. Res.*, 26 (1987) 1372.
- 17 B. L. Larson, P. Rasmussen and A. Fredenslund, *Ind. Eng. Chem. Res.*, 26 (1987) 2274.
- 18 I. Kikic, P. Alessi, P. Rasmussen and A. Fredenslund, *Can. J. Chem.*, 58 (1980) 253.
- 19 E. Macedo, U. Weidlich, J. Gmehling and P. Rasmussen, *Ind. Eng. Chem. Process Des. Dev.*, 22 (1983) 676.
- 20 D. Tiegs, J. Gmehling, P. Rasmussen and A. Fredenslund, *Ind. Eng. Chem. Res.*, 26 (1987) 159.
- 21 J. H. Knox and R. Kaliszán, *J. Chromatogr.*, 349 (1985) 211.
- 22 R. M. Smith, *J. Chromatogr.*, 236 (1982) 313.
- 23 R. M. Smith, *Adv. Chromatogr.*, 26 (1987) 277.
- 24 W. J. Cheong and P. W. Carr, *J. Chromatogr.*, 499 (1990) 373.
- 25 L. R. Snyder, *Principles of Adsorption Chromatography*, Marcel Dekker, New York, 1968.
- 26 J. H. Purnell and J. M. Vargas de Andrade, *J. Am. Chem. Soc.*, 97 (1975) 3585.
- 27 J. H. Purnell and J. M. Vargas de Andrade, *J. Am. Chem. Soc.*, 97 (1975) 3590.
- 28 R. J. Laub and J. H. Purnell, *J. Am. Chem. Soc.*, 98 (1976) 30.
- 29 R. J. Laub and J. H. Purnell, *J. Am. Chem. Soc.*, 98 (1976) 35.
- 30 D. E. Martire, *Anal. Chem.*, 48 (1976) 398.
- 31 R. J. Laub, D. E. Martire and J. H. Purnell, *J. Chem. Soc. Faraday Trans. 2*, 74 (1978) 213.
- 32 M. W. P. Harbison, R. J. Laub, D. E. Martire, J. H. Purnell and P. S. Williams, *J. Phys. Chem.*, 83 (1979) 1262.
- 33 D. E. Martire and R. E. Boehm, *J. Liq. Chromatogr.*, 3 (1980) 753.
- 34 P. J. Schoenmakers, H. A. H. Billiet, R. Tijssen and L. de Galan, *J. Chromatogr.*, 149 (1978) 519.
- 35 X. Geng and F. E. Regnier, *J. Chromatogr.*, 332 (1985) 147.
- 36 X. Geng and F. E. Regnier, *J. Chromatogr.*, 402 (1987) 41.
- 37 B. P. Johnson, M. G. Khaledi and J. G. Dorsey, *Anal. Chem.*, 58 (1986) 2354.
- 38 J. J. Michels and J. G. Dorsey, *J. Chromatogr.*, 457 (1988) 85.
- 39 A. J. Dallas, *PhD Thesis*, University of Minnesota, Minneapolis, MN, 1990.
- 40 D. J. Minick, D. A. Brent and J. Frenz, *J. Chromatogr.*, 461 (1989) 177.
- 41 M. A. Quarry, R. L. Grob, L. R. Snyder, J. W. Dolan and M. P. Rigney, *J. Chromatogr.*, 384 (1987) 163.
- 42 P. J. Schoenmakers, H. A. H. Billiet and L. de Galan, *J. Chromatogr.*, 185 (1979) 179.
- 43 M. H. Abraham, G. S. Whiting, R. Fuchs and E. J. Chambers, *J. Chem. Soc. Perkin Trans. 2*, (1990) 291.

Simultaneous optimization of several chromatographic performance goals using Derringer's desirability function

B. Bourguignon and D. L. Massart*

Vrije Universiteit Brussel, Farmaceutisch Instituut, Laarbeeklaan 103, B-1090 Brussels (Belgium)

(First received March 13th, 1991; revised manuscript received June 18th, 1991)

ABSTRACT

The desirability function, a multi-criterion decision-making method proposed by Derringer, was investigated to optimize different chromatographic performance goals. This function is a measure of overall quality and provides a convenient means to compare several chromatograms obtained by high-performance liquid chromatography (HPLC) and to select the separation with the most desirable properties. Other solutions to the problem of multi-criteria optimization in HPLC, such as the Pareto-optimality, chromatographic response functions and combined threshold criteria are compared with the proposed method, and the advantages and disadvantages of each are discussed.

INTRODUCTION

The optimization of strategies for high-performance liquid chromatography (HPLC) requires criteria to decide whether one chromatogram is superior to another. The selection of suitable criteria to achieve an optimum judgement may vary considerably from one example to another, according to the different goals that have to be met in the optimization process. This selection procedure is not clearly defined and an expert system has been proposed [1] to assist in it. Often a compromise between conflicting goals, such as maximizing the separation while minimizing the analysis time, has to be found. Balancing these goals against each other should result in the most acceptable solution to the optimization problem. Chromatographic optimization may therefore be considered as a multi-criterion problem. This paper reports an exploration of Derringer's desirability function [2], an approach from multi-criterion decision-making (MCDM), a branch of operations research, to tackle this chromatographic problem.

THEORY

One type of problem, which resembles the multi-criterion problem, arises in HPLC when a global separation criterion, *i.e.*, a criterion describing the separation between more than one pair of substances is to be developed. A well known approach was given by Drouen *et al.* [3]. They proposed using the calibrated normalized resolution product r^* , which is defined as

$$r^* = \prod_{i=0}^{n-1} (R_{s_{i,i+1}}/R_s) \quad (1)$$

where

$$\overline{R}_s = (1/n) \sum_{i=0}^{n-1} R_{s_{i,i+1}} \quad (2)$$

$R_{s_{i,i+1}}$ is the resolution between the i th and $(i+1)$ th peak and n is the number of peaks.

The aim of r^* is to achieve an equal distribution of peaks over the chromatogram. A very different method, with the same aim of obtaining an even

distribution of peaks, was proposed by Mazerolles *et al.* [4]. This method is based on information theory.

The problem becomes more difficult when criteria of a very different and nearly always conflicting nature are to be included, such as separation quality and time. In HPLC, there have been attempts to solve this problem using several different methods. The earliest approaches were modifications of Morgan and Deming's chromatographic response function (CRF) [5–9]. Such response functions consist of a factor related to time and another factor which describes the separation quality:

$$\text{CRF} = \text{"separation factor"} + X \text{"time factor"} \quad (3)$$

where X is a weighting factor.

If the sample consists of a mixture of an unknown number of components, new peaks may be discovered during optimization. In the response functions proposed by Wright *et al.* [10] and by Berridge [11], it is possible to consider simultaneously the resolution, time and number of peaks detected.

A time–separation quality compromise may also be achieved with a threshold approach [9,12–16]. First, using resolution-based criteria, solutions are defined where all the peaks are considered to be sufficiently separated, *i.e.*, they have at least a minimum resolution. From the set of acceptable solutions, that with the optimum analysis time is selected.

Another method of simultaneously optimizing different criteria, proposed by Smilde and co-workers [17–19] uses the concept of Pareto-optimality. This approach fits in with what is usually considered as MCDM by operations research specialists. Smilde and co-workers considered the minimum resolution as a measure of separation and the maximum capacity factor as a measure of analysis time. In the available factor space, the capacity factors of each solute can be predicted at any point using a model obtained from an experimental design plan. All predicted criteria values at each solvent composition are presented in a two-dimensional picture. The next step consists in establishing the Pareto-optimal points. A point is called Pareto-optimal if there exists no other experiment which has a better result on one criterion without having a worse result on another. There are usually several Pareto-optimal experiments and the advice of an expert will be necessary to decide which of the points

is preferable. Software for this application has been published [20] and a commercial version of the software is available [21].

In summary, the multi-criterion nature of chromatographic evaluation and optimization has been studied in three different ways, namely the weighted or unweighted summation of criteria, the threshold approach of finding a region acceptable from the point of view of one criterion and then optimizing the other, and the Pareto-optimality method.

As far as is known, all such methods have been limited to the simultaneous optimization of two types of criteria, and it is not difficult to think of additional criteria such as the detection limit and asymmetry of the peaks. It was investigated whether methods could be developed that included more than two different types of criteria. Operations research has for a long time studied the problem of MCDM and a literature search revealed that several such methods could be applied to optimization in chromatography. The approaches which seemed to be the most promising were the already described Pareto methodology, PROMETHEE, a method developed by Brans and Vincke [22] for finding optimal locations, and the desirability function approach of Derringer and Suich [2]. The application of PROMETHEE to a chemical experimental design method has already been described [23]. The Derringer method does not seem to have been studied at all and this work investigated whether it could be of use in the optimization of HPLC. This mathematical model, first presented by Harrington [24], but put into a more general form by Derringer, was used originally to optimize quality in product development (Derringer's application is about the multi-criterion optimization of a tyre tread compound) and is probably the most widely used approach to MCDM in that field. It is based on the transformation of the measured properties to a dimensionless desirability scale for each criterion, so that values of several properties, obtained from different scales of measurement, may be combined. The desirability scale ranges between $d = 0$, corresponding to a completely undesirable level of quality, to $d = 1$, which indicates an ultimate level of quality beyond which further improvements would have no value.

To transform the individual criteria into desirability values, two types of transformation are possible,

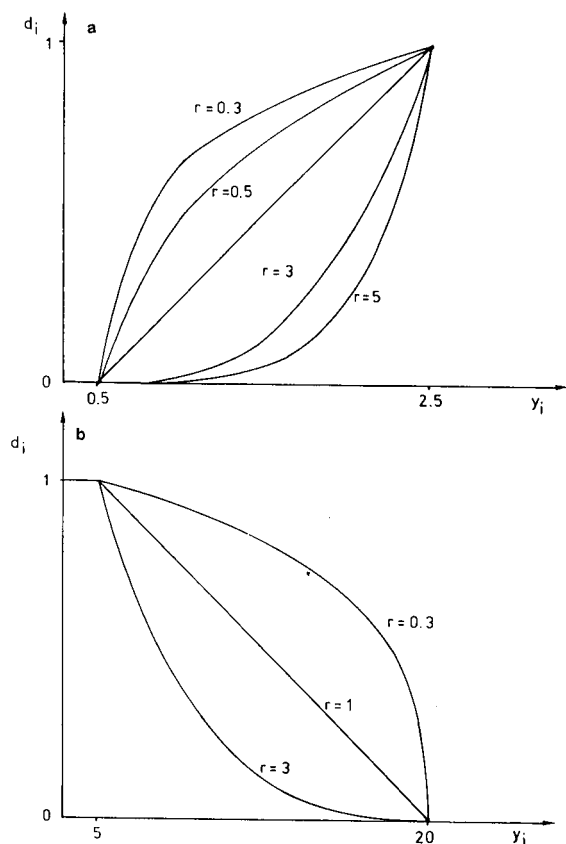


Fig. 1. Possible one-sided transformations of response variables Y_i into desirability values d_i . (a) Resolution; (b) retention times and asymmetry factors.

a one-sided and a two-sided transformation. In the one-sided transformation, the response variables Y_i ($i = 1, 2, \dots, k$, where k is the number of response variables), are transformed to the d -scale with the following equations (see also Fig. 1):

$$\begin{aligned}
 d_i &= 0 && \text{if } Y_i \leq Y_i^{(-)} \\
 d_i &= \left(\frac{Y_i - Y_i^{(-)}}{Y_i^{(+)} - Y_i^{(-)}} \right)^r && \text{if } Y_i^{(-)} < Y_i < Y_i^{(+)} \quad (4) \\
 d_i &= 1 && \text{if } Y_i \geq Y_i^{(+)}
 \end{aligned}$$

where $Y_i^{(-)}$ is the minimum acceptable value of criterion Y_i and $Y_i^{(+)}$ is the value beyond which improvements would serve no useful purpose. Both values have to be selected by the user. When separating two substances, for instance, it might be

decided that $R_s < 0.5$ is of no use, whereas increasing R_s beyond 2.0 would bring no further gain. Therefore, $d = 0$ for $R_s < 0.5 = Y_i^{(-)}$, $d = 1$ for $R_s > 2.0 = Y_i^{(+)}$ and a value in between is given for $0.5 < R_s < 2.0$ (Fig. 1a). The selection of a suitable value of r offers the user flexibility in the definition of desirability functions. Consider Fig. 1b. Suppose the highest acceptable retention time is 20 and it is not considered of interest that the time required should be less than 5. The most obvious way of giving a desirability value to times between 5 and 20 is by drawing a straight line between those two points. This is equivalent with $r = 1$ in eqn. 5. It may be reasoned that all times higher than 5 make the separation much less desirable and this would lead to a curve such as that obtained with $r = 3$. On the other hand, it might be reasoned that anything less than 20 becomes rapidly more desirable and this would then require a desirability function such as that with $r = 0.3$. It is up to the user to decide. In practice, the user is asked to estimate how desirable certain responses are (for instance, $t = 8, 12, 15$), and then to decide on r , so that the resulting desirability function fits the given desirabilities as well as possible.

It is possible that the most desired values are not beyond a certain limit, but are in between. In that instance a two-sided transformation is required, which is given by:

$$\begin{aligned}
 d_i &= \left(\frac{Y_i - Y_i^{(-)}}{c_i - Y_i^{(-)}} \right)^s && \text{if } Y_i^{(-)} \leq Y_i \leq c_i \\
 d_i &= \left(\frac{Y_i - Y_i^{(+)}}{c_i - Y_i^{(+)}} \right)^t && \text{if } c_i < Y_i \leq Y_i^{(+)} \quad (5) \\
 d_i &= 0 && \text{if } Y_i < Y_i^{(-)} \text{ or } Y_i > Y_i^{(+)}
 \end{aligned}$$

where c_i is a target value that can be selected anywhere between $Y_i^{(-)}$ and $Y_i^{(+)}$. Consider Fig. 2. Suppose the highest acceptable retention time again is 20, but retention times should not be less than 5 (for instance, in a separation with a large solvent peak) and that, preferably, they should be around 10. If retention times smaller than c_i make the separation less desirable, this would lead to a curve such as that obtained with $s = 3$. If any time above c_i but below $Y_i^{(+)}$ is almost as desirable as any other time between c_i and $Y_i^{(+)}$, a desirability function is required such as that with $t = 0.3$; s and t thus play

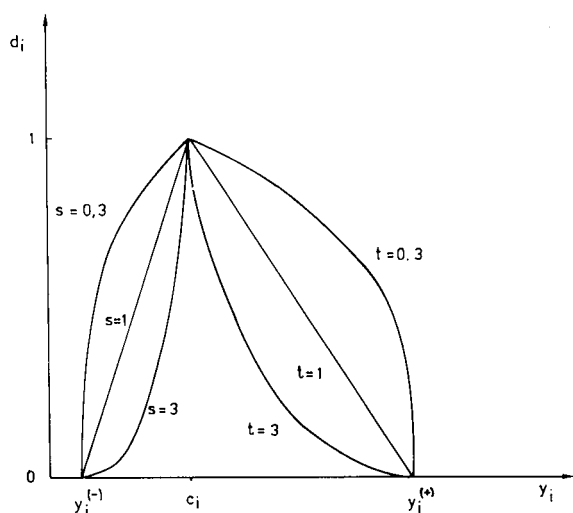


Fig. 2. Possible two-sided transformations of response variables Y_i into desirability values d_i .

the same role as r and allow a compromise to be found between two extremes.

In a second step the overall quality D is calculated by combining the desirability values obtained for the different criteria by using the geometric mean:

$$D = (d_1 \cdot d_2 \cdots d_k)^{1/k}$$

If one of the properties has an unacceptable value (that is, if $d = 0$), the overall product will also be unacceptable (resulting in $D = 0$), regardless of the value of the remaining properties. On the other hand, if all the properties are acceptable, the value of D will fall in the interval $[0, 1]$ and will increase with increasing d -values. It should be noted that the last step is similar to the solution proposed by Drouen *et al.* [3] to obtain global separation criteria.

RESULTS

To study the application of the desirability function in chromatography, it was applied to the selection of a chromatogram with the most desirable combination of three types of response, namely separation quality, analysis time and peak asymmetry.

The resolution between peaks (R_s) is used as the measure of separation. This means that $(n - 1)$ resolution values are determined between successive

pairs of n substances. Alternatively, $R_{s,\min}$, the lowest resolution value observed in the chromatogram, and r^* are also used. This does not mean that the resolution parameters are considered to be better parameters to quantify separation than, for instance, α -values or peak-to-valley ratios. The object of the study is to demonstrate the feasibility of the desirability function approach.

The retention time of the last peak is used as a measure of the analysis time and a maximum acceptable value has to be specified above which any result would be considered unacceptable.

Asymmetry factors (A_s) are taken into consideration because severe band tailing and broad peaks may cause inferior chromatograms. In the optimization of a reversed-phase separation of a mixture containing basic drugs, asymmetry often occurs. A_s is calculated as the ratio of the leading half of the peak to the trailing half, measured at a peak height of 0.1. Values of asymmetry factors have to approach as closely as possible the optimum value of 1. In theory, the opposite phenomenon of tailing is possible and could lead to values below 1. In practice, this does not often happen and it was not so in this application. If it were to occur, a two-sided transformation of A_s to d -values would be needed.

As an application, the optimization of an artificial mixture containing diazepam, papaverine, phenobarbital, amitriptyline, triamterene and flufenamic acid was studied. The mobile phase compositions, mixtures of methanol and phosphate buffer, are given in Table I. Two variables, the pH and the

TABLE I

MOBILE PHASE COMPOSITIONS AND NUMBER OF OBSERVED PEAKS IN THE CHROMATOGRAMS

The numbers refer to Fig. 3.

Chromatogram No.	Fraction of methanol (%)	pH of buffer	Number of peaks
3a	30	3.0	5
3b	39	3.0	5
3c	21	3.0	5
3d	30	2.0	4
3e	39	5.0	5
3f	30	6.0	5
3g	30	4.0	6
3h	21	5.0	6
3i	27	5.4	6

volume percentage methanol of the mobile phase, were optimized. The upper pH limit was set at 6 because, for amitryptiline, the retention time becomes too high at higher pH values. The lower pH limit was set at the limit of stability of the stationary phase, namely at pH 2 [25]. The volume percentage of organic modifier was varied between 20 and 40%. To scan the factor space defined in this manner, the solutes were chromatographed under conditions determined by seven points located in the factor space according to a two-factorial Doehlert design [26,27]. The results are shown in Fig. 3b-h. From those results and an initial "first guess" run (Fig. 3a), a ninth set of experimental conditions was derived. The result is shown in Fig. 3i. The values of the response variables are given in Tables II-VI.

The minimum [$Y_i^{(-)}$] and maximum [$Y_i^{(+)}$] acceptable values of the response variables, Y_i , are given in Table VII.

In general, a good separation between peaks is considered to correspond to a resolution of 1.5. For the one-sided transformation, $Y_i^{(-)}$ was set at 0.5 and $Y_i^{(+)}$ at 2.5. It might be argued that this is

a rather wide interval and, in fact, this is true. However, as this is a first application, it was considered more important to demonstrate the feasibility and principle of the method than to define carefully the different boundaries for practical work. For r^* -values, which range between 0 and 1, $Y_i^{(+)}$ was set equal to 0.95, because, in practice, ideal chromatograms showing $r^* = 1$ will be rare, and 0.95 would be completely acceptable. Minimum acceptable values of 0.05 and 0.005 were selected in the comparison of chromatograms with five or six peaks, respectively.

For demonstration purposes it was necessary to study a situation where A_s factors are of importance to the quality of the chromatogram and the separation conditions were chosen so that a high asymmetry occurs in some of the chromatograms. For that reason, the normal chromatographic requirements were relaxed and the A_s value for which $d = 0$ was set to 3.

For retention times, as has been explained, a linear function seems the most obvious to transform the response values into desirability values. For

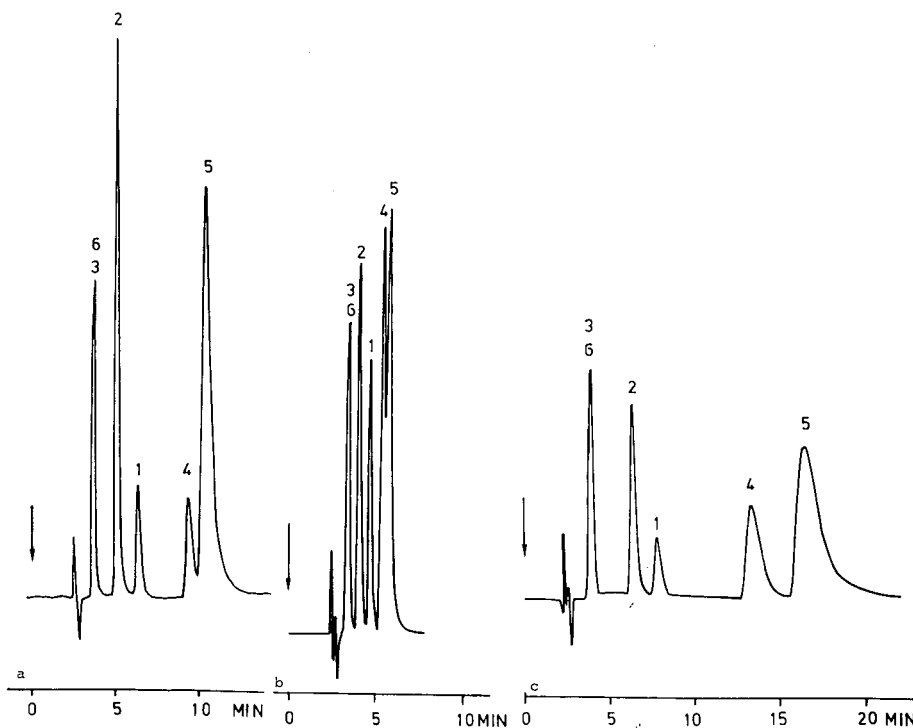


Fig. 3.

(Continued on p. 16)

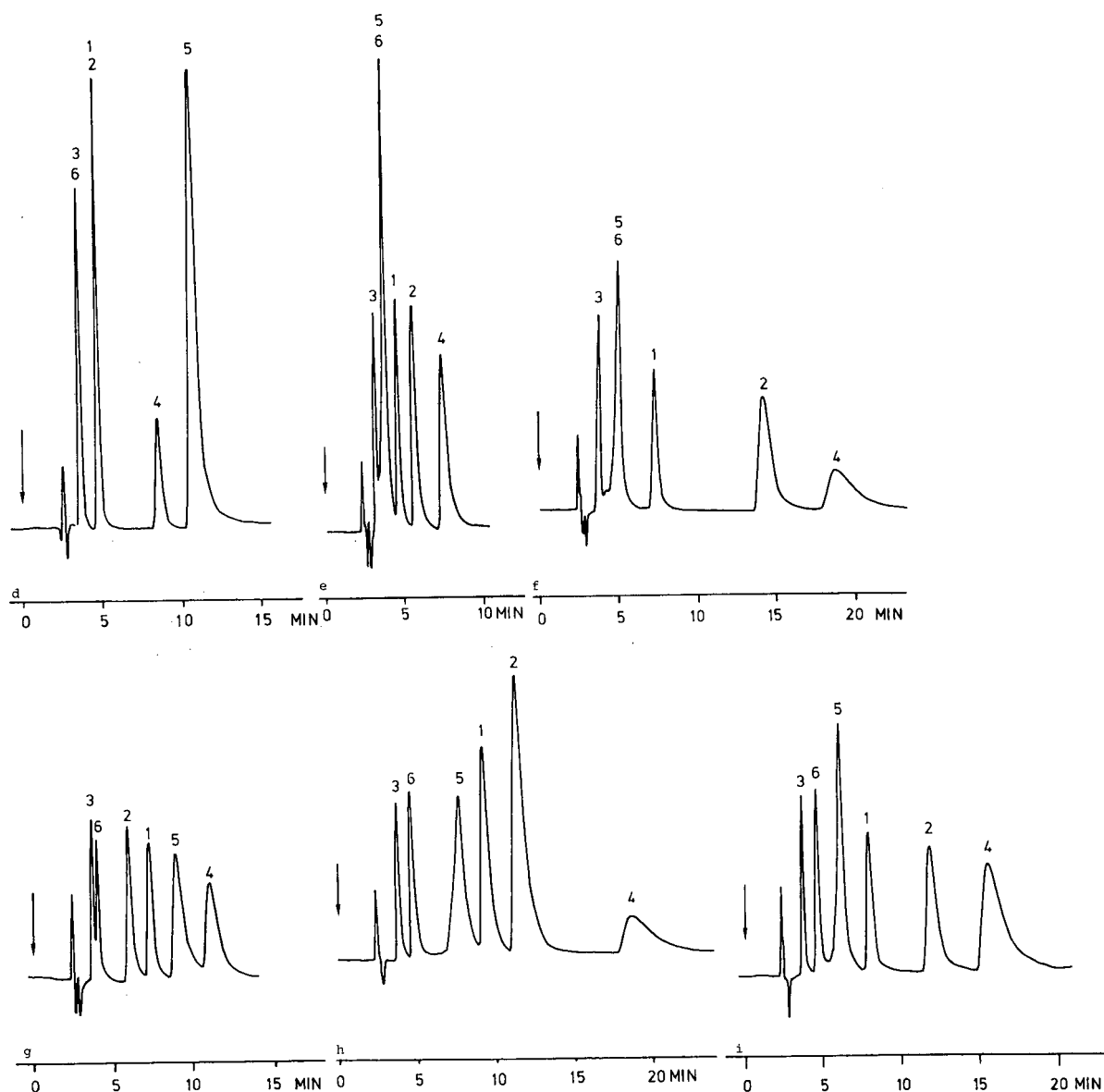


Fig. 3. Chromatograms following the Doehlert design (b-h), the expected "optimum" chromatogram (i) and a "first guess" run (a) of a sample containing six solutes. Peaks: 1 = diazepam; 2 = papaverine; 3 = phenobarbital; 4 = amitriptyline; 5 = flufenamic acid; 6 = triamterene.

separation criteria and asymmetry factors it is not so obvious whether a linear function should be applied and r -values have to be selected depending on the problem. If, for instance, a good separation is considered very important, large values of r have to be selected. This means that any resolution that is

a little less than the target value $Y_i^{(+)}$ will lead to a rapid decrease in d -values. In this work r was set equal to several values to demonstrate its effect (Tables VIII and IX).

For chromatograms containing less than six peaks, D -values equal zero because at least one

TABLE II

ASYMMETRY FACTORS OF CHROMATOGRAMS WITH SIX PEAKS

Peak	3g	3h	3i
1	1.20	1.17	0.86
2	0.83	1.00	1.60
3	1.00	0.67	1.00
4	2.50	3.30	2.92
5	2.25	0.73	0.64
6	1.25	0.75	0.89

TABLE III

RESOLUTIONS OF CHROMATOGRAMS WITH SIX PEAKS

Peak pair	3g	Peak pair	3h	3i
3-6	0.744	3-6	2.22	2.35
6-2	4.08	6-5	3.99	2.47
2-1	1.97	5-1	1.62	2.34
1-5	1.40	1-2	1.71	3.58
5-4	1.71	2-4	2.30	1.61

TABLE IV

RETENTION TIME OF THE LAST PEAK (t_L) AND CALIBRATED NORMALIZED RESOLUTION PRODUCT (r^*)

Y_i	t_L	r^*
3a	10.3	0.287
3b	5.75	0.014
3c	16.0	0.242
3e	7.52	0.196
3f	18.5	0.083
3g	11.6	0.010
3h	19.3	0.025
3i	15.6	0.0418

TABLE V

ASYMMETRY FACTORS OF CHROMATOGRAMS WITH FIVE PEAKS

Peak	3a	3c	Peak	3e	3f
1	1.25	1.67	1	1.70	1.00
2	1.33	1.00	2	1.20	2.71
3-6	1.00	0.75	3	0.75	0.83
4	0.75	2.17	4	1.50	4.66
5	0.75	2.54	5-6	0.80	1.00

TABLE VI

RESOLUTIONS OF CHROMATOGRAMS WITH FIVE PEAKS

Peak pair	3a	3b	3c	Peak pair	3e	3f
3, 6-2	2.10	1.25	3.56	3-5, 6	1.08	1.76
2-1	3.18	1.69	2.09	5, 6-1	1.37	2.70
1-4	4.41	2.31	4.47	1-2	2.20	5.84
4-5	0.893	0.655	1.15	2-4	2.54	2.39

TABLE VII

MINIMUM [$Y_i^{(-)}$] AND MAXIMUM [$Y_i^{(+)}$] ACCEPTABLE VALUES OF THE RESPONSE VARIABLE Y_i FOR ASYMMETRY FACTORS (A_s), RESOLUTION (R_s), MINIMUM RESOLUTION ($R_{s\min}$), CALIBRATED NORMALIZED RESOLUTION PRODUCT (r^*) AND RETENTION TIME OF THE LAST PEAK (t_L)

Response variable	A_s	R_s	$R_{s\min}$	r^*	t_L
$Y_i^{(+)}$	3.00	2.50	2.50	0.95	20.00
$Y_i^{(-)}$	1.20	0.50	0.50	0.05 or 0.005	5.00

resolution is unacceptable. The chromatogram in Fig. 3h has $D = 0$ and is ruled out because of the excess tailing of amitriptyline. Treating the three types of responses in the same way with $r = 1$ in the one-sided transformation, the chromatogram of Fig. 3g is marginally better than that of Fig. 3i (Table VIII). Emphasizing departures from target values for the analysis time compared with separation criteria and asymmetry factors, by setting $r = 3$ for the retention time of the last eluted peak, results in a preference for Fig. 3g, where the six components are separated in an analysis time 4 min shorter. If, however, larger values of r are applied for the resolution or for resolution-based criteria, the chromatogram in Fig. 3i is clearly preferred to that in Fig. 3g.

Although chromatograms exhibiting six peaks represent better experimental conditions, the five chromatograms with five peaks were also compared. Purely as a further exercise, it was supposed that they were chromatograms of only five substances and Derringer's method was applied to decide which of the chromatograms with five peaks was the best. Five such chromatograms were obtained. The chro-

TABLE VIII

VALUES OF r FOR RESPONSE CRITERIA AND CALCULATED D -VALUES OF CHROMATOGRAMS WITH SIX PEAKS

r					D	
A_s	R_s	$R_{s_{\min}}$	r^*	t_L	3i	3g
1.0	1.0	—	—	1.0	0.63	0.58
1.0	1.0	—	—	3.0	0.52	0.53
1.0	3.0	—	—	1.0	0.56	0.31
1.0	0.5	—	—	1.0	0.66	0.65
1.0	0.3	—	—	1.0	0.65	0.66
1.0	—	1.0	—	1.0	0.52	0.54
1.0	—	1.0	—	3.0	0.38	0.47
1.0	—	3.0	—	1.0	0.45	0.32
1.0	—	0.5	—	1.0	0.54	0.59
1.0	—	0.3	—	1.0	0.54	0.65
1.0	—	—	1.0	1.0	0.37	0.37
1.0	—	—	1.0	3.0	0.27	0.32
1.0	—	—	3.0	1.0	0.17	0.10
1.0	—	—	0.5	1.0	0.46	0.51
1.0	—	—	0.3	1.0	0.49	0.58

matogram in Fig. 3f shows $A_s > 3$, leading to $D = 0$. The chromatogram in Fig. 3b also leads to $D = 0$ as a result of the very poor resolution between peaks 4 and 5.

If all r values are set equal to 1, the chromato-

TABLE IX

VALUES OF r FOR RESPONSE CRITERIA AND CALCULATED D -VALUES OF SOME CHROMATOGRAMS WITH FIVE PEAKS

r					D		
A_s	R_s	$R_{s_{\min}}$	r^*	t_L	3a	3c	3e
1.0	1.0	—	—	1.0	0.79	0.60	0.77
1.0	1.0	—	—	3.0	0.72	0.46	0.74
1.0	5.0	—	—	1.0	0.38	0.35	0.31
1.0	0.3	—	—	1.0	0.90	0.66	0.90
1.0	0.5	—	—	1.0	0.86	0.64	0.86
1.0	—	1.0	—	1.0	0.73	0.50	0.79
1.0	—	1.0	—	3.0	0.65	0.34	0.75
1.0	—	5.0	—	1.0	0.29	0.26	0.39
1.0	—	0.3	—	1.0	0.86	0.56	0.90
1.0	—	0.5	—	1.0	0.82	0.54	0.87
1.0	—	—	1.0	1.0	0.77	0.47	0.73
1.0	—	—	1.0	3.0	0.68	0.32	0.69
1.0	—	—	5.0	1.0	0.36	0.19	0.25
1.0	—	—	0.3	1.0	0.88	0.55	0.87
1.0	—	—	0.5	1.0	0.83	0.52	0.84

grams in Fig. 3a and e best fulfil the postulated requirements (see Table IX). If, however, a short analysis time is the most important and a large value of r is selected for the retention time, the resulting D -values lead to a preference for the chromatogram in Fig. 3e, with a 2-min shorter run, over that in Fig. 3a, although the peaks are better separated in the latter chromatogram.

If large values of r are selected for the resolution, the D -value for Fig. 3a is clearly better than that for Fig. 3c, and both are more desirable than Fig. 3e. If the value of $R_{s_{\min}}$ is used to quantify the separation, Fig. 3e is preferred to Fig. 3a. The fact that $R_{s_{\min}}$ has the highest value reveals nothing about the remainder of the chromatogram: except for the minimum resolution nearly all the other resolution values of Fig. 3a are higher than for Fig. 3e. If r^* is used as the separation criterion, Fig. 3a has the highest value of the overall quality. Further research is needed to decide with more certainty, but it seems that using the separate R_s -values is more indicated, as $R_{s_{\min}}$ loses some information and to a large extent achieves the same as D with the separate R_s -values.

DISCUSSION

Derringer's desirability function has been introduced to chromatography to compare several chromatograms and select that with the most desirable combination of properties. This MCDM model has been shown to be convenient for the simultaneous optimization of three chromatographic performance goals and it should be possible to also apply it to the optimization of a still larger set of varying and opposing properties. The overall desirability function should also offer the possibility of using response surface methods to search for an optimum set of experimental conditions, or to restrict the factor space to one or more regions where a desirable combination of different aspects is achieved.

It is difficult to conclude at this stage which of the MCDM methods is to be preferred. More work with the different approaches is needed to achieve this.

For practical separations where it is justified to use only $R_{s_{\min}}$ and time as the criteria, the threshold approach seems the easiest to perform. The comparison does not include subjective elements, as is also true in all other evaluation methods. It might be argued that this completely eliminates the experi-

ence of the user and, certainly, it is not easily feasible to include additional criteria.

The essential difference between the Pareto-optimal method and the CRF/COF and Derringer approaches is that the former does not need *a priori* decisions about weighting one criterion against the other, whereas the latter do. The Pareto-optimal method is easy to understand and should be better known by the chromatographic community. This procedure offers the important advantage that the pay-off between the two criteria can be seen, allowing the analyst to evaluate quantitatively the loss in resolution against the gain in analysis time. In situations where the goals are not known, this seems to be the better method. It can be applied with a few more than two variables, but it then loses much of its appealing simplicity. It is not an objective method, as the final selection is made subjectively by an expert and not mathematically. As long as a real expert is available this is not a disadvantage and the method is a good tool for an expert who wants to know what are the best options available, before making a selection.

The CRF/COF method and the Derringer method are both subjective methods in the sense that weighting factors have to be selected for the former and a desirability function for the latter. The fact that a desirability function needs to be established does have advantages: it is necessary to formulate clearly a target and how departures from that target will be evaluated. The fact of doing this is in itself a very useful exercise. This way of thinking fits in well with the total quality concept, which has become so important in many applied laboratories. If the desirability function is well designed, then the Derringer approach should function well. It is much less clear what the exact meaning of the weighting factors in the first approach is, and it is concluded that of the two the Derringer method is to be preferred. The Derringer method is also the only method for which it is easy to incorporate more than two variables.

The Derringer method is not affected by peak cross-overs, because the identity of the peaks need not be known, at least in those situations where it is considered necessary to separate all substances. When new peaks may emerge during the optimization process, this means that for the chromatograms with a smaller number of peaks the desirability

function will be updated to zero, because one resolution was below the threshold, where it begins to have a non-zero desirability.

In summary, it is concluded that the threshold method, the Pareto-optimal method and the Derringer approach, as introduced here, all have their advantages and that the decision on which method to use depends on the problem and the availability of chromatographic expertise.

ACKNOWLEDGEMENTS

The authors thank NFWO and FGWO for financial assistance.

REFERENCES

- 1 A. Peeters, L. Buydens, D. L. Massart and P. J. Schoenmakers, *Chromatographia*, 26 (1988) 101.
- 2 G. Derringer and R. Suich, *J. Quality Technol.*, 12 (1980) 214–219.
- 3 A. C. J. H. Drouen, P. J. Schoenmakers, H. A. H. Billiet and L. de Galan, *Chromatographia*, 16 (1982) 48–52.
- 4 G. Mazerolles, D. Mathieu, R. Pahn-Tan-Luu and A. M. Siouffi, *J. Chromatogr.*, 485 (1989) 433–451.
- 5 S. L. Morgan and S. N. Deming, *Chromatographia*, 112 (1975) 267–285.
- 6 H. J. G. Debets, B. L. Bajema and D. A. Doornbos, *Anal. Chim. Acta*, 151 (1983) 131–141.
- 7 H. J. G. Debets, J. W. Weyland and D. A. Doornbos, *Anal. Chim. Acta*, 150 (1983) 259–265.
- 8 M. W. Watson and P. W. Carr, *Anal. Chem.*, 51 (1979) 1835–1842.
- 9 J. L. Glajch, J. J. Kirkland, K. M. Squire and J. M. Minor, *J. Chromatogr.*, 199 (1980) 57–79.
- 10 A. G. Wright, A. F. Fell and J. C. Berridge, *Chromatographia*, 24 (1987) 533–590.
- 11 J. C. Berridge, *J. Chromatogr.*, 244 (1982) 1–14.
- 12 P. R. Haddad, A. C. J. H. Drouen, H. A. H. Billiet and L. de Galan, *J. Chromatogr.*, 282 (1983) 71–81.
- 13 P. J. Schoenmakers, *Optimization of Chromatographic Selectivity*, Elsevier, Amsterdam, 1986.
- 14 P. J. Schoenmakers, *J. Liq. Chromatogr.*, 10 (1987) 1865–1886.
- 15 J. S. Kiel, S. L. Morgan and R. K. Abramson, *J. Chromatogr.*, 485 (1989) 585–596.
- 16 J. W. Weyland, *Anal. Chim. Acta*, 153 (1983) 93–101.
- 17 J. H. de Boer, A. K. Smilde and D. A. Doornbos, *Acta Pharm. Technol.*, 34 (1988) 140–143.
- 18 A. K. Smilde, C. H. P. Bruins and D. A. Doornbos, *J. Chromatogr.*, 400 (1987) 1–12.
- 19 A. K. Smilde, A. Knevelman and P. M. J. Coenegracht, *J. Chromatogr.*, 369 (1986) 1–10.
- 20 H. R. Keller and D. L. Massart, *Trends Anal. Chem.*, 9 (1990) 251–253.
- 21 *Optochron*, Betron Scientific International Rotterdam, 1990.

- 22 J. P. Brans and P. Vincke, *Management Sci.*, 31 (1985) 647-656.
- 23 H. R. Keller, D. L. Massart and J. P. Brans, *Chemom. Intell. Lab. Syst.*, 11 (1991) 175-189.
- 24 E. C. Harrington, *Ind. Quality Control*, 21 (1965) 494-498.
- 25 J. W. Dolan, *LC · GC*, 7 (1989) 476.
- 26 Hu Yuzhu and D. L. Massart, *J. Chromatogr.*, 485 (1989) 311-323.
- 27 Hu Yuzhu, *Trends Anal. Chem.*, 8 (1989) 126-128.

Continuous beds for standard and micro high-performance liquid chromatography

Jia-Li Liao, Rong Zhang and Stellan Hjertén*

Department of Biochemistry, University of Uppsala, Biomedical Center, P.O. Box 576, S-751 23 Uppsala (Sweden)

(First received April 24th, 1991; revised manuscript received May 27th, 1991)

ABSTRACT

Conventional high-performance liquid chromatographic columns are built up of small, uniform beads. The preparation of the columns involves many expensive and cumbersome steps. This paper describes a simpler method, which is not based on the use of preformed beads. The chromatographic bed consists of a compressed gel plug with intercommunicating "channels", the "walls" of which are impermeable to proteins. The gel bed is formed in one step: a monomer solution, including ligands, is polymerized in the chromatographic tube under such conditions that the polymer chains aggregate into bundles, for instance, by hydrophobic interaction [the voids ("channels") thus created between the polymer bundles, are large enough to permit passage of eluent]. The gel plug is then compressed 10–15 fold, which decreases the average diameter of the "channels". The gel bed formed shows a resolution that, at constant gradient volume, is independent of or increases with an increase in flow-rate, a property that it shares with a compressed, non-porous agarose bed. The potential of a continuous gel bed has been previously illustrated by a cation-exchange chromatography experiment. This paper gives details of the preparation of this cation-exchanger, as well as of beds for anion-exchange and hydrophobic-interaction chromatography. The usefulness of the beds is demonstrated by the separation of model proteins on columns with the diameters of 6 and 0.3 mm. For the micro column both on- and off-tube detection were used. In the latter procedure the protein zones were transferred by a buffer flow to a conventional UV detector as they leave the gel bed, and then to a fraction collector. This detection technique has the advantage that any detector and any flow-cell for high-performance liquid chromatography can be used. The sample becomes diluted, but the resolution and the sensitivity are about the same as those obtained with standard micro-flow-cells (the same technique has been used successfully for micro-preparative high-performance capillary electrophoresis). A new method of preparing salt gradients for micro columns is presented.

INTRODUCTION

The preparation of a chromatographic bed involves many steps: the preparation of the beads; washing to remove the suspension medium; sieving or elutriation of the beads to a uniform size (if they are not made monodisperse in the first step); derivatization; packing the column; and testing for bed homogeneity by measurement of plate numbers. This procedure is time-consuming and expensive.

We have recently described a considerably simplified method, which also has the potential to give a more homogeneous bed than do conventional packing procedures and, consequently, higher resolution [1]. The new method is based on polymerization of the monomers (including ligands) directly in the

chromatographic tube under such conditions that "channels" are created in the polymer plug formed. Following compression of the bed it is ready for use. In a note on this new technique we described a separation of proteins on a cation-exchanger [1]. The present paper deals with an extension of this earlier study to anion-exchange and hydrophobic-interaction chromatography (HIC), including experiments on micro-columns with on- and off-line detection.

EXPERIMENTAL

Materials and apparatus

Electrophoresis-purity reagents [N,N'-methylenebisacrylamide (BIS), ammonium persulphate,

N,N,N',N'-tetramethylethylenediamine (TEMED)] and ammonium sulphate (HPLC grade) were obtained from Bio-Rad Labs (Richmond, CA, USA); N-allyldimethylamine from Fluka (Buchs, Switzerland); acrylic acid from Merck (Schuchardt, Germany); and butyl acrylate from Aldrich (Steinheim, Germany).

The HPLC pump (Model 2150), the LC controller (Model 2152), and the recorder (Model 2210) were from Pharmacia LKB Biotechnology (Bromma, Sweden); and the UV monitor (Model 1306) from Bio-Rad-Labs. The syringe pump for off-tube detection of proteins separated on the micro HIC column (0.3 mm I.D.) was constructed by Mr. Per-Axel Lidström and Mr. Hans Pettersson of this institute. The stainless-steel tees were from Upchurch Scientific (Oak Harbor, WA, USA) and the PTFE tubing (0.3 mm I.D.) from Alltech (Deerfield, IL, USA).

The column tubes with 6 mm I.D. were made of Plexiglas [2]. A fused-silica tubing with 0.3 mm I.D. was purchased from SGE (Ringwood, Australia) and employed as the micro column tube. The same company supplied the 0.15-mm fused-silica tubing attached to the micro-column for on-tube detection of proteins in the eluate, and a 0.075-mm fused-silica tubing for the introduction of buffer gradient and sample. The design of the micro-column set-up is outlined in Fig. 1. The devices for on- and off-tube detection were the same as those we use routinely for high-performance capillary electrophoresis (see refs. 3 and 4, respectively).

Column preparation

Preparation of continuous beds for anion- and cation-exchange chromatography. N,N'-Methylenebisacrylamide (0.24 g) and N-allyldimethylamine (0.12 ml) were dissolved, with stirring, in 9.5 ml of 0.01 M sodium phosphate (pH 6.4). The pH was adjusted to 7 with 2 M HCl (ca. 400 μ l). Ammonium sulphate (0.5 g) and 100 μ l of a 10% (w/v) aqueous solution of ammonium persulphate were added. Following deaeration and addition of 100 μ l of the catalyst [a 5% (v/v) solution of TEMED] the reaction mixture was poured into a 350 \times 6 mm I.D. column tube [the final concentration of N,N'-methylenebisacrylamide was thus ca. 2.4% (w/v)]. After polymerization for 5 h, 0.01 M Tris-HCl (pH 8.5) was pumped into the column tube at a flow-rate

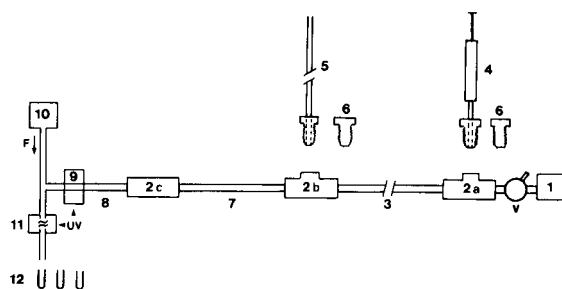


Fig. 1. Block diagram of the micro-column set-up. 1 = HPLC pump; 2a and 2b = zero dead-volume stainless-steel tees; 2c = union (ref. 5); 3 = gradient PTFE tubing (500 \times 0.3 mm I.D.); 4 = 50- μ l syringe; 5 = fused-silica tubing (150 \times 0.075 mm I.D., volume 0.64 μ l) for the introduction of buffer gradient and sample; 6 = stainless-steel nut (without bore); 7 = micro-column (fused-silica tubing, 70 \times 0.3 mm I.D., containing the compressed bed); 8 = post column (fused-silica tubing, 30 \times 0.15 mm I.D.) for on-line detection; 9 = on-tube detector; 10 = syringe pump; 11 = off-tube detector; 12 = fraction collector; v = valve.

of 0.5 ml/min. During this step the height of the gel plug decreased continuously. The pumping was not interrupted until the height became constant (ca 60 mm). The gel plug was then manually compressed further with the aid of the upper piston. The final height of the gel plug was 35 mm. The piston was fixed at this position to prevent the gel plug from expanding on elution at lower flow-rates. The compression thus decreased the height of the gel plug 10-fold.

We have previously shown the usefulness of continuous beds for the separation of proteins on a cation exchanger [1]. The method for the preparation of the bed was similar to that described above. The details were as follows. With stirring, 0.24 g of N,N'-methylenebisacrylamide was dissolved in 10 ml of 0.05 M sodium phosphate (pH 6.8), which was then supplemented with acrylic acid (0.005 ml), ammonium sulphate (0.45 g) and 0.1 ml of a 10% (w/v) aqueous solution of ammonium persulphate. The polymerization was initiated by adding 0.1 ml of a 5% (w/v) aqueous solution of TEMED to the deaerated solution. This monomer solution was poured into the column tube. Following polymerization, the bed was compressed as described for the anion exchanger.

Preparation of a continuous bed for hydrophobic-interaction chromatography. With stirring, 0.48 g of

N,N'-methylenebisacrylamide was dissolved in 20 ml of water. Following addition of 0.08 ml of butylacrylate, 0.3 g of ammonium sulphate and 200 μ l of a 10% (w/v) solution of ammonium persulphate, the mixture was deaerated and supplemented with 200 μ l of a 5% (w/v) solution of TEMED. Both the 450 \times 6 mm I.D. tube and the 600 \times 0.3 mm I.D. tube were filled with this catalysed monomer solution, which was allowed to polymerize for 5 h.

The 6-mm diameter bed was compressed to a height of 38 mm by pumping with a 0.01 M sodium phosphate solution (pH 7.0) containing 2.5 M ammonium sulphate, followed by manual pressing down of the piston as described above for the anion-exchange column.

The micro-column bed was prepared as follows. A union (2c in Fig. 1) containing a metal frit (pore diameter 2 μ m) was attached to the fused-silica tubing containing the HIC bed (0.3 mm I.D.) [5]. With the aid of the HPLC pump 1, the bed was compressed at a flow-rate of 0.01 ml/min from a height of 600 mm to 120 mm, and then further to 70 mm by increasing the pressure to 100 bar for 5 min. At this stage the nuts 6 were screwed into the tees 2a and 2b. The column tubing above the compressed gel bed was cut off. The lower segment containing the gel was coupled to the PTFE tubing 3 via the tee 2b.

The formation of small-volume salt gradients for elution of the microcolumn

A 8.5-ml linear salt gradient was generated in a 10-ml cylinder (13 mm I.D.) with the aid of the HPLC pump. The gradient was formed from 2.25 M ammonium sulphate in 0.01 M sodium phosphate buffer (pH 7.0) (at the bottom) to 0.25 M ammonium sulphate in the same buffer (at the top). Using a marking pen, the cylinder was graduated from the bottom into 17 equal sections. The distance between two divisions thus corresponded to 0.5 ml. After equilibration of the column bed by the pump 1 with 0.01 M sodium phosphate (pH 7.0) containing 2.25 M ammonium sulphate, the stainless-steel nuts (6 in Fig. 1) in the tees 2a and 2b were replaced by a 50- μ l syringe 4 and a 0.6- μ l tubing 5. Sodium phosphate (0.01 M, pH 7.0) containing 0.25 M ammonium sulphate was pressed into the gradient tubing 3 and the tubing 5 with the aid of the HPLC pump 1. The

valve v was then closed. The free end of the tubing 5 was immersed into the gradient, and 2 μ l of the solution at the centre of each section were taken up with the 50- μ l syringe 4 (starting with the top section). The final volume of the gradient in tubing 3 was thus $2 \times 17 = 34 \mu$ l (the volume of tubing 5 was only 0.64 μ l).

The free end of the tubing 5, now filled with 0.01 M sodium phosphate (pH 7.0) containing 2.25 M ammonium sulphate, was dipped into the sample solution, and 1 μ l of the sample was taken up into the tubing with the aid of the syringe 4. The tubing 5 was then immersed into the equilibration buffer, and 2 μ l were taken up with the syringe 4 (the sample was in this way introduced into the gradient tubing 3). The syringe 4 and tubing 5 (with connecting nuts) were replaced by the nuts 6. Valve v was opened and pump 1 turned on. Since the minimum flow-rate of the pump was 0.01 ml/min, the connection until the pump 1 and the tee 2a was loosened until the flow-rate in the column 7 was 0.001 ml/min.

The pore size in the "walls" of the "channels" in the gel bed

The porosity was studied by molecular-sieve chromatography on the beds for both HIC and anion-exchange chromatography (AEC) with standard proteins of different molecular weights dextran 2000 ($M 2 \cdot 10^6$) and sucrose as described for compressed beds of nonporous agarose beads [6,7]. A plot of elution volume against molecular weight showed that the proteins and the dextran did not penetrate the channel walls (sucrose probably penetrates only a thin surface layer, to judge from the observation in Fig. 2 that its elution volume differs only slightly from that of macromolecules).

Scanning electron microscopy of the continuous polymer beds

Compressed continuous polymer beds for HIC, AEC and cation-exchange chromatography (CEC) were removed from the column tubes and frozen immediately. Following freeze-drying, aliquots of the beds were examined by scanning electron microscopy. A micrograph of the HIC bed is shown in Fig. 3 (similar pictures were obtained for the AEC and CEC columns).

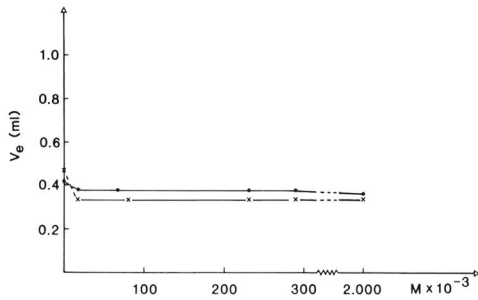


Fig. 2. Plot of elution volume (V_e) against the molecular weight (M) of some standard solutes chromatographed on a continuous bed. The figure illustrates that the "walls" of the "channels" in the continuous bed are impermeable to proteins. (●) AEC column (total volume 1.08 ml); (×) HIC column (total volume 1.11 ml).

The influence of the flow-rate on the resolution of the AEC column at constant gradient volume

The bed (35×6 mm I.D.) was equilibrated with 0.01 M Tris-HCl (pH 8.5). The sample consisted of 20 μ g of each of the proteins myoglobin (M), haemoglobin (H), ovalbumin (O), bovine serum albumin (A) and *R*-phycoerythrin (P), dissolved in

40 μ l of the equilibration buffer. The desorption was accomplished at the flow-rates 0.12, 0.25 and 0.50 ml/min by a 5.0-ml linear salt gradient generated from the equilibration buffer and the same buffer supplemented with 0.43 M sodium acetate (pH 8.5). Similar experiments were performed during 3 months on the same column without any change in the appearance of the chromatograms, indicating a good reproducibility and stability of the column. The last run during this test period is presented in Fig. 4.

A comparison between on-tube and off-tube detection of proteins separated on the micro-column

The sample consisted of ca. 0.4 μ g of each of the following proteins dissolved in 1 μ l of the equilibration buffer: myoglobin (M), ribonuclease (R), ovalbumin (O), α -chymotrypsinogen A (C) and *R*-phycoerythrin (P). The separation of the proteins was accomplished with a 35- μ l negative, linear gradient formed from 2.25 M ammonium sulphate in 0.01 M sodium phosphate (pH 7.0) (the equilibration buffer), and 0.25 M ammonium sulphate in the same phosphate buffer. The flow-rate was 1 μ l/min.

For on-tube monitoring, the "flow cuvette" of the

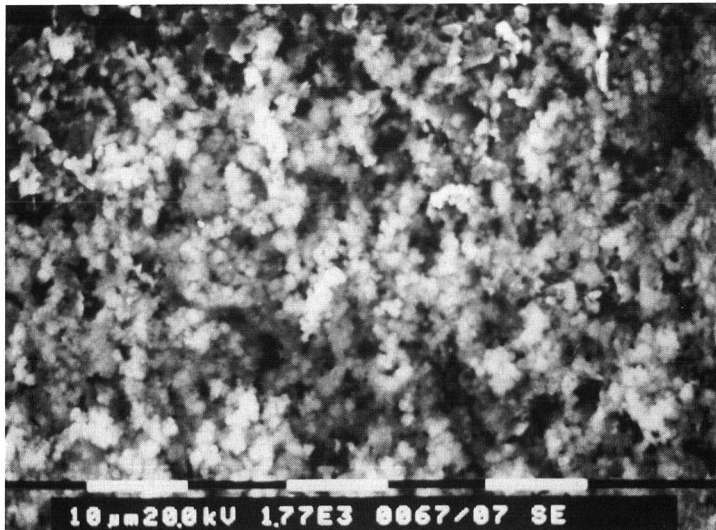


Fig. 3. Scanning electron micrograph of the continuous HIC polymer bed. The white bars represent a length of 10 μ m. If the micrograph gives a true picture of the bed it is composed of "walls" of aggregated particles and "channels" between the aggregates in which buffer can flow. (Preparation and photo: Leif Ljung, Department of Anatomy, University of Uppsala, Uppsala, Sweden).

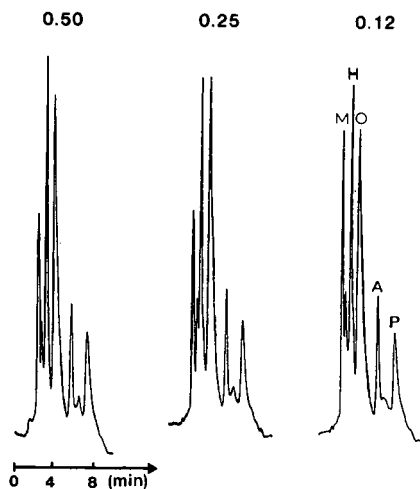


Fig. 4. Influence of flow-rate at constant gradient volume on the appearance of the chromatograms obtained by AEC on a continuous bed. The sample ($40 \mu\text{l}$) contained $20 \mu\text{g}$ each of the proteins myoglobin (M), haemoglobin (H), ovalbumin (O), albumin (A) and phycoerythrin (P). Bed dimensions, $38 \times 6 \text{ mm}$ I.D.; gradient, from 0 to 0.43 M sodium acetate in 0.01 M Tris-HCl (pH 8.5). A 5-ml gradient was used at the flow-rates 0.50, 0.25 and 0.12 ml/min . The figure shows that the resolution is independent of the flow-rate.

detector 9 consisted of a $30 \times 0.15 \text{ mm}$ I.D. fused-silica tubing 8 attached to the outlet of the micro-column 7 (see Figs. 1 and 5a). For off-tube monitoring, the flow-through cell (volume $8 \mu\text{l}$; light path 10 mm) in the Bio-Rad Model 1306 HPLC UV detector (11 in Fig. 1) was used (Fig. 5b). The cross-flow solution, 0.01 M sodium phosphate (pH 7.0), was delivered from the syringe pump 10 at 0.06 ml/min .

RESULTS AND DISCUSSION

A comparison of Fig. 4 with Fig. 7a in ref. 11 indicates that the resolution of proteins on compressed continuous beds is about the same as that on compressed beds of the high-resolving non-porous agarose beads [2,6,7,11]. In view of this high resolution of the continuous beds, in combination with the very low cost and ease of preparation (which also makes them attractive for fractionation on a large scale), some readers may be interested in using such beds. Therefore, we have described in detail both the preparation and the handling of the columns.

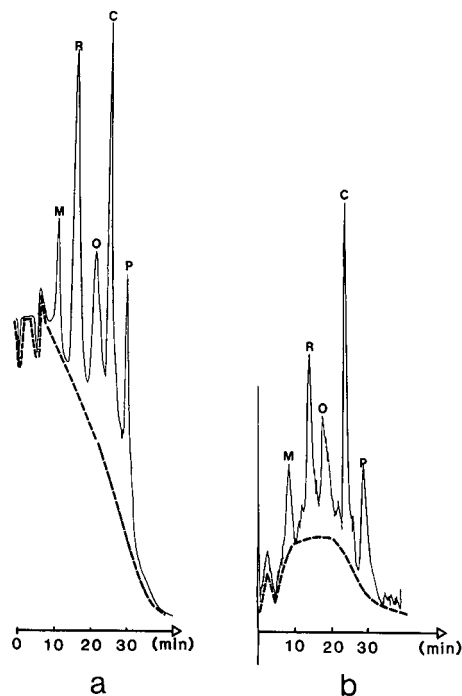


Fig. 5. Micro-column HIC with on-tube (a) and off-tube (b) detection. Bed dimensions, $70 \times 0.3 \text{ mm}$ I.D. The sample contained $0.4 \mu\text{g}$ each of the proteins myoglobin (M), ribonuclease (R), ovalbumin (O), α -chymotrypsinogen A (C) and phycoerythrin (P). Sample volume, $1 \mu\text{l}$. A linear $35\text{-}\mu\text{l}$ gradient from 0.01 M sodium phosphate (pH 7.0), containing 2.25 M ammonium sulphate, to 0.01 M sodium phosphate (pH 7.0), containing 0.25 M ammonium sulphate, was used at a flow-rate of $1 \mu\text{l/min}$. The principle of the on- and off-tube detection is given in Fig. 1. The syringe pump 10 (see Fig. 1) delivered 0.01 M sodium phosphate buffer (pH 7.0) at a flow-rate of $60 \mu\text{l/min}$.

Studies in progress are aimed at further improvement of the chromatographic properties.

Fig. 3 indicates that the continuous beds are built up of "walls" of aggregated polymer particles (diameter *ca.* $0.5 \mu\text{m}$) and "channels" (diameter $3\text{--}4 \mu\text{m}$) between the aggregates. However, some caution is warranted in deducing the structure of the bed from the photo, since the preparation of the bed for microscopy may have changed its appearance. For instance, the observed "channel" diameter may be larger than the actual one [9,10].

Since the "walls" of the "channels" do not permit passage of proteins (Fig. 2) it is not surprising that the beds, after compression, resemble the compressed non-porous agarose beds [6-8] in the sense

that the resolution at constant gradient volume is independent of the flow-rate or even increase with an increase in flow-rate (see Fig. 4 in this paper and Fig. 1 in ref. 1). This characteristic and highly desirable feature will be discussed in a forthcoming paper.

The addition of ammonium sulphate to the monomer solution served to increase the hydrophobic interaction between the polymer chains formed and thus to create "channels" between them (the monomer should not be too hydrophilic). There are, however, other possible ways to design continuous beds, involving, for instance, the use of (mixtures of) organic solvents to fit the polarity (hydrophobicity) of the monomers and the polymers formed. By carefully tuning the experimental conditions it is undoubtedly possible to prepare more rigid and homogeneous continuous beds than those described herein and in ref. 1, thus increasing the efficiency of a column.

ACKNOWLEDGEMENTS

This study was financially supported by the Swedish Natural Science Research Council, and the

Carl Trygger and the Knut and Alice Wallenberg Foundations.

REFERENCES

- 1 S. Hjertén, J.-L. Liao and R. Zhang, *J. Chromatogr.*, 473 (1989) 273.
- 2 S. Hjertén, in M. T. W. Hearn (Editor), *HPLC of Proteins, Peptides and Polynucleotides*, VCH Publishers, in press.
- 3 S. Hjertén, in H. Hirai (Editor), *Electrophoresis '83*, Walter de Gruyter, Berlin, 1984, pp. 71–79.
- 4 S. Hjertén and M.-D. Zhu, in B. Rånby (Editor), *Physical Chemistry of Colloids and Macromolecules, Proceedings of the Svedberg Symposium, Uppsala, August 22–24, 1984*, Blackwell, London 1987, pp. 133–136.
- 5 T. Takeuchi, T. Saito and D. Ishii, *J. Chromatogr.*, 351 (1986) 295.
- 6 S. Hjertén and J.-L. Liao, *J. Chromatogr.*, 457 (1988) 165.
- 7 J.-L. Liao and S. Hjertén, *J. Chromatogr.*, 457 (1988) 175.
- 8 S. Hjertén, K. Yao and J.-L. Liao, *Makromol. Chem., Macromol. Symp.*, 17 (1988) 349.
- 9 J. Gressel and A. W. Robards, *J. Chromatogr.*, 114 (1975) 455.
- 10 R. Röchel and M. D. Brager, *Anal. Chem.*, 681 (1975) 415.
- 11 S. Hjertén, J. Mohammad, K.-O. Eriksson and J.-L. Liao, *Chromatographia*, 31 (1991) 85.

Protein adsorption capacity of a porous phenylalanine-containing membrane based on a polyethylene matrix

Min Kim, Kyoichi Saito* and Shintaro Furusaki

Department of Chemical Engineering, Faculty of Engineering, University of Tokyo, Hongo, Tokyo 113 (Japan)

Takanobu Sugo and Isao Ishigaki

Japan Atomic Energy Research Institute, Takasaki Radiation Chemistry Research Establishment, Takasaki, Gunma 370-12 (Japan)

(First received July 30th, 1990; revised manuscript received June 17th, 1991)

ABSTRACT

A porous hollow-fibre membrane containing L-phenylalanine as a pseudo-biospecific ligand has been prepared by radiation-induced grafting of glycidyl methacrylate onto polyethylene microfiltration hollow fibre, followed by coupling of the produced epoxide group with L-phenylalanine. The remaining epoxide group was hydrolysed into a diol group with sulphuric acid. The L-phenylalanine and the diol group acted in a complementary way as a pseudo-biospecific ligand and a hydrophilic group, respectively. The adsorption capacity of bovine gamma globulin on the resulting porous adsorbent could be determined by the specific surface area of the adsorbent when the ligand was in excess over the protein.

INTRODUCTION

When one molecule of an affinity pair is immobilized on a solid support, the resulting material is called an affinity adsorbent capable of separating the other molecule specifically from a complex solution. The separation technique using the affinity adsorbents has been applied to the purification and concentration of diluted and valuable proteins from bioprocess fluids [1], and to the removal of undesirable proteins from human plasma [2]. Of various kinds of affinity adsorbent, those based on agarose gel beads have been widely used on a laboratory scale. Since agarose retains water at the ratio of 40 g of water per gram of dry agarose, wet agarose gel is highly hydrophilic. Thus, agarose gel has the advantage that proteins will not adsorb on it non-selectively. A great number of studies have been reported concerning agarose-based affinity chromatography [3,4]. However, the relationship between protein adsorption capacity and the ligand density

or specific surface area of the agarose-based affinity adsorbents is not defined, because of the difficulties of varying the ligand density over a wide range and determining the specific surface area in the wet state for the agarose gel.

We have suggested a novel method of introducing functional groups into a porous polyethylene hollow-fibre membrane [5,6]. This method is effective in that the functionality can be easily introduced into the porous matrix at a given density by selecting the reaction conditions of preparation.

The objectives of our study are two-fold: (1) to prepare the porous adsorbent containing a hydrophobic amino acid as a pseudo-biospecific ligand, and (2) to correlate the protein adsorption capacity of the porous adsorbent with its ligand density and specific surface area. In this study, L-phenylalanine and bovine gamma globulin were selected as ligand and protein, respectively. L-Phenylalanine has been used as a ligand for the isolation of tRNA ligase [7] and chorismate mutase/prephenate dehydratase [8]

from *E. coli*, and for the purification of human IgA from serum [9].

EXPERIMENTAL

Preparation of L-phenylalanine-containing membrane

Fig. 1 shows the preparation process for the adsorbent containing L-phenylalanine as a pseudo-biospecific ligand. Commercially available porous polyethylene hollow fibre (Asahi Chemical Industry) was used as the trunk polymer for grafting. The inner and outer diameters of the hollow fibre were 0.62 and 1.24 mm, respectively. Reagent-grade glycidyl methacrylate (GMA) was purchased from Tokyo Kasei Industry and was used without further purification. L-Phenylalanine (L-Phe) was purchased from Wako Pure Chemical Industry.

The hollow fibre was irradiated by an electron beam at ambient temperature in a nitrogen atmosphere. Immediately after irradiation, the hollow fibre was exposed to a vapour of deaerated GMA, which reacted with the trapped radicals in the trunk polymer. Details of GMA grafting have been described in previous publications [5,6]. The amount of GMA introduced into the starting hollow fibre was defined as the degree of GMA grafting:

$$\text{degree of GMA grafting (d.g.)} = \frac{100[(W_1 - W_0)/W_0]}{100} \quad (1)$$

where W_0 and W_1 are the weights of starting and GMA-grafted hollow fibre, respectively.

The epoxide group of the grafted branches was coupled with L-Phe. L-Phe was dissolved in deionized water, and the pH was adjusted to 13 with sodi-

um hydroxide. The GMA-grafted hollow fibre was immersed in the L-Phe solution at 353 K. After a predetermined time, the hollow fibre was removed and washed repeatedly with water. Subsequently, the remaining epoxide group in the hollow fibre was converted into a diol group by immersing the hollow fibre in 1 M sulphuric acid at 353 K for 2 h. The fibre was washed several times with water and then dried under reduced pressure. The coupling efficiency of epoxide group with L-Phe, X_c , and the ligand density were defined as follows:

$$W_2 = W_0 + (W_1 - W_0)[(142 + 165)X_c/100 + (142 + 18)(1 - X_c/100)]/142$$

$$\text{coupling efficiency } (X_c) = \frac{100[142(W_2 - W_0)]}{(W_1 - W_0) - 160}/147 \quad (2)$$

$$\text{ligand density} = [(W_1 - W_0)/142]X_c/100/W_2 \quad (3)$$

where W_2 is the weight of L-Phe-containing hollow fibre, and the factors 165, 142 and 18 are the molecular masses of L-Phe, GMA and water, respectively. The resulting hollow fibre was designated as a Phe-C fibre, where C denotes capillary.

To evaluate the amount of protein adsorbed non-selectively on the Phe-C fibre, a diol-group-containing hollow fibre was prepared by hydrolysing the GMA-grafted hollow fibre with sulphuric acid. The resulting hollow fibre is referred to as a GMA-H-C fibre.

Properties of the Phe-C fibre

After the Phe-C fibre had been dried, its specific surface area was determined according to the BET method. Two drying methods for the fibres were compared: drying under reduced pressure and freeze-drying.

Because a microfiltration hollow-fibre membrane is used as the trunk polymer, the Phe-C fibre is still permeable to water. The water flux was determined using the apparatus described in ref. 10. To prevent a decrease in permeability caused by particle accumulation, water prepared by passage through an ultrafiltration (UF) module was used as the feed solution. The UF water permeated through the membrane from the inside to the outside. The pure water flux (PWF) was calculated by dividing the flow-rate by the inner surface area of the hollow fibre. The PWFs of the hollow fibres with and without methanol treatment were determined. Metha-

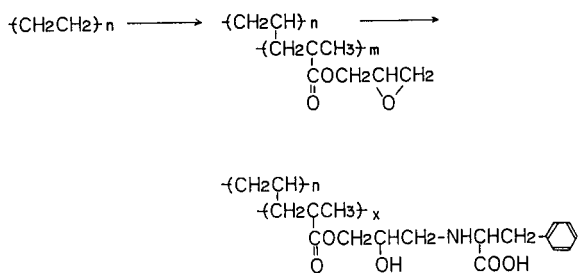


Fig. 1. Preparation of the adsorbent with L-Phe as a pseudo-biospecific ligand. The epoxide group in the GMA-grafted hollow fibre was coupled with L-Phe.

nol treatment indicates that, before the flux measurement, the fibre was immersed for 10 min in methanol, which was then replaced with water. The filtration pressure was kept at $1.0 \cdot 10^5$ Pa. The feed solution was kept at 303 K.

Adsorption and elution of bovine gamma globulin

Bovine gamma globulin (BGG) was purchased from Sigma (No. G5009, Cohn Fraction II, III) and used as received. BGG was dissolved in a buffer (3.3 M NaCl, 0.01 M Tris-HCl, pH 8.0). This buffer can facilitate the hydrophobic interaction and inversely depress the electrostatic binding between the protein and the polymer surface [11]. Adsorption isotherms were determined in a batchwise method. A fixed amount of the Phe-C fibre was immersed in the BGG solution. The mixture was incubated at 303 K for 24 h to allow the system to reach equilibrium. The amount of protein adsorbed on the fibre was calculated from the decrease in BGG concentration in the solution. The Langmuir isotherm closely fitted the adsorption data, and then the saturation capacity was determined. BGG was determined by UV spectroscopy.

Next, the BGG adsorbed onto the Phe-C fibre was eluted by immersing the fibre in 0.01 M Tris-HCl buffer containing 1–2 M NaCl, and in a mixture of 50% v/v ethylene glycol and 1 M NaCl for 24 h. Elution was done at the same volume ratio of fibre to eluate. The amount of BGG in each eluate was determined. The elution ratio, *i.e.* the ratio of the eluted amount to the initially adsorbed amount was calculated.

RESULTS AND DISCUSSION

Preparation of the Phe-C fibre

L-Phe was introduced into the hollow fibre by reaction of the epoxide group in the GMA-grafted hollow fibre with the amino group of L-Phe. Fig. 2 shows the coupling efficiency as a function of the reaction time. The coupling efficiency levelled off after 24 h. By varying the degree of GMA grafting between 10% and 200%, the final coupling efficiency and ligand density were measured. Fig. 3 shows that the final coupling efficiency was *ca.* 13%, irrespective of the degree of GMA grafting. The corresponding ligand density ranged from 0.15 to 0.6 mmol per dry gram of the Phe-C fibre. Moreover,

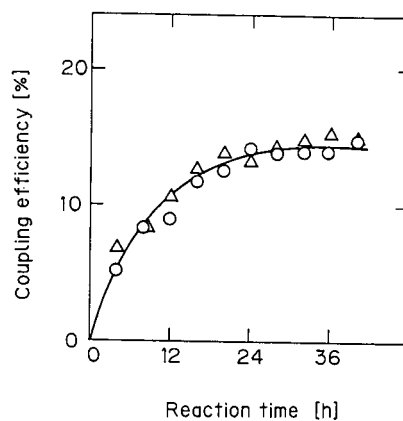


Fig. 2. Coupling efficiency as a function of reaction time. The GMA-grafted hollow fibres with 80% (○) and 130% (△) degree of GMA grafting were immersed in the L-Phe solution with pH initially adjusted to 13. Temperature: 353 K.

the ligand density per wet volume of the fibre, 0.05–0.28 mmol/ml, was calculated by multiplying each apparent density of the fibre. The ligand density of the Phe-C fibre was an order of magnitude higher than that of commercial affinity beads based on agarose, *e.g.* 0.01 mmol/ml [12]. The method suggested in this study can provide the polymeric support with a desired ligand density by selecting either the degree of GMA grafting or the coupling efficiency in preparation.

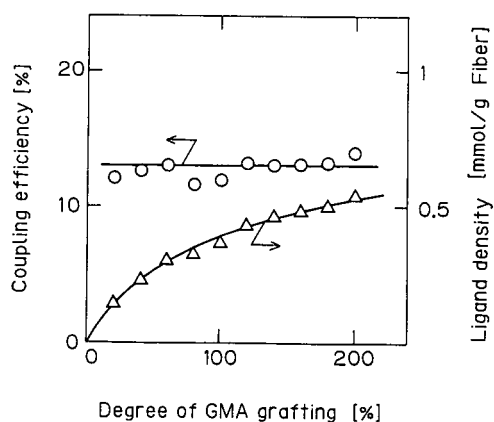


Fig. 3. Coupling efficiency as a function of degree of GMA grafting. The coupling efficiency and ligand density were calculated from eqns. 2 and 3, respectively.

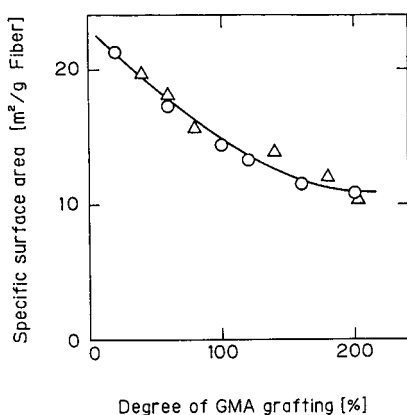


Fig. 4. Specific surface area of Phe-C fibre as a function of degree of GMA grafting. The GMA-grafted hollow fibres were coupled with L-Phe at a coupling efficiency of 13%. After the Phe-C fibre was vacuum-dried (○) or freeze-dried (△), its specific surface area was determined.

Properties of the Phe-C fibre

Fig. 4 shows the specific surface area of the hollow fibres. The specific surface area of the starting hollow fibre was $23 \text{ m}^2/\text{g}$. The specific surface area of the Phe-C fibre decreased as the degree of GMA grafting increased. This decrease is due to the formation of the grafted branches on the surface of the pores with relatively smaller diameters [13].

The pure water flux is shown in Fig. 5 as a function of the degree of GMA grafting, where the sym-

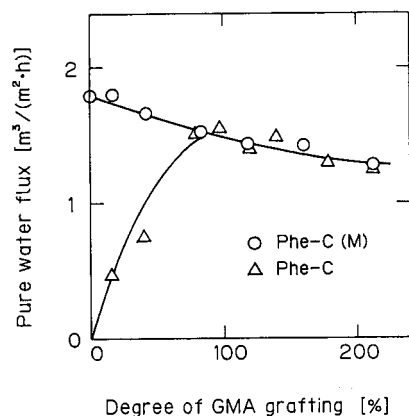


Fig. 5. Pure water flux as a function of degree of GMA grafting. Pure water flux was compared between the Phe-C fibres with and without methanol treatment. The symbol (M) indicates that the dried Phe-C fibre was immersed in methanol for 10 min and then replaced with water.

bol (M) indicates the hollow fibre pretreated with methanol. Methanol filled the pores of the fibres and then was replaced with water. The PWF of the Phe-C fibre decreased gradually with an increasing degree of GMA grafting. When the degree of GMA grafting reached *ca.* 100%, the PWFs of the fibre with and without methanol treatment coincided. The epoxide group of the GMA-grafted fibre was coupled with L-Phe to reach the final coupling efficiency of 13%. Some of the uncoupled epoxide group were hydrolysed into a diol group during coupling, and some remained as epoxide. Since the remaining epoxide was hydrolysed to the diol group with sulphuric acid quantitatively, the density of the diol group increased with an increase in the degree of GMA grafting (d.g.) under a constant coupling efficiency:

$$\begin{aligned} \text{density of diol group} &= [(W_1 - W_0)(1 - X_c/100)/142]/W_2 \quad (4) \\ &= \frac{(\text{d.g.})(1 - X_c/100)/100}{142 + (\text{d.g.})(147X_c/100 + 160)/100} \end{aligned}$$

As a result, a degree of GMA grafting of *ca.* 100% was regarded as the point at which the polyethylene-based hollow fibre was satisfactorily hydrophilised from the standpoint of the water flux.

Non-selective adsorption of BGG

A negligible amount of protein adsorbed non-selectively on the adsorbents is one of the important

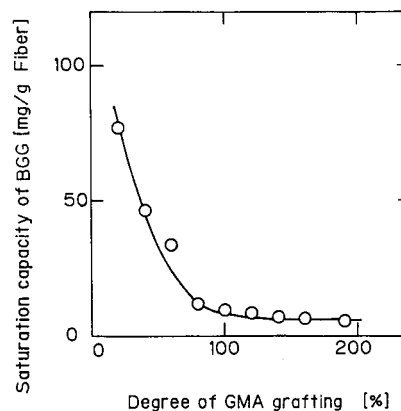


Fig. 6. Saturation capacity of BGG on the diol-group-containing fibre. The GMA-H-C fibre was prepared by hydrolysis of the GMA-grafted fibre then equilibrated with the BGG solution buffered with 0.01 M Tris-HCl and 3.3 M NaCl (pH 8).

requisites. Using exclusively diol-group-containing hollow fibre (GMA-H-C fibre), which was prepared by hydrolysing the GMA-grafted hollow fibre with sulphuric acid, non-selective adsorption isotherms of BGG were measured. The saturation capacities of GMA-H-C fibres with different degrees of GMA grafting can be obtained from the Langmuir plot of the corresponding isotherm, and they are plotted in Fig. 6 as a function of the degree of GMA grafting. The saturation capacity of BGG on the GMA-H-C fibre decreased as the degree of GMA grafting increased. When the degree of GMA grafting exceeded *ca.* 100%, it decreased to a constant value. The dependence of non-selective saturation capacity on the degree of GMA grafting was in excellent accordance with that of the water flux. Satisfactory hydrophilization of the hollow fibre suggests that the diol-group-containing grafted branches cover the polyethylene matrix entirely and retain water on themselves. Hydrated water on the polymer surface will reduce the hydrophobic interaction between the protein and the polymer surface. This effect has also been observed during the design of a biocompatible film modified with hydrophilic monomers, such as 2-hydroxyethyl methacrylate (HEMA) [14,15].

Specific adsorption of BGG

The amount of L-Phe immobilized on the hollow fibre could be varied by changing the reaction time during the coupling of the GMA-grafted hollow fibre with a constant degree of GMA grafting (d.g. = 70%, 110% and 150%). Fig. 7 shows an example of adsorption isotherms for Phe-C fibres containing an identical amount of the grafted branches and different ligand densities. Fig. 8 indicates that the saturation capacity exhibited a constant value irrespective of the density of the Phe ligand. In this range of the ligand density, the molar ratio, R_a , of the L-Phe ligand to BGG (assumed molecular mass 156 000) adsorbed specifically on it was of the order of 10^3 ; in other words, the ligand was far in excess of what is required to bind BGG.

$$R_a = \frac{\text{(ligand density)}}{\text{(molar conc. of protein adsorbed at saturation)}} \quad (5)$$

However, the density of the diol group obtained from the degree of GMA grafting of at least 100% is necessary to minimize the amount of BGG adsorbed non-selectively, as discussed above. Al-

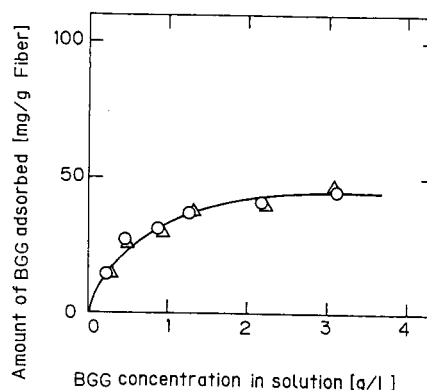


Fig. 7. Adsorption isotherms of Phe-C fibres with different ligand densities. The Phe-C fibres, which contained an identical amount of graft branches (110%) and different ligand densities of 0.2 (Δ) and 0.55 (\circ) mmol/g fibre, were equilibrated with the BGG solution.

though an excess ligand density is reported to interfere with the affinity interaction [4], this phenomenon was not observed in this affinity system.

In order to examine the possibility and extent of protein multi-point attachment on the Phe-C fibre with increasing ligand density, BGG was eluted from the Phe-C fibre with the Tris-HCl buffer containing various concentrations of NaCl. Decreasing salt concentration weakens the hydrophobic interaction between the Phe-C fibre and BGG [16]. As

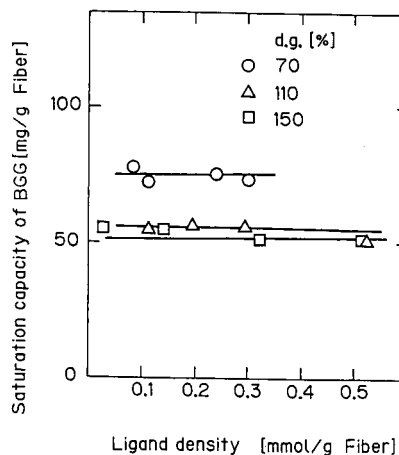


Fig. 8. Saturation capacity of BGG on Phe-C fibre as a function of ligand density. The ligand density ranged from 0.02 to 0.52 mmol/g for GMA grafting varying from 70% to 150%, and coupling efficiency ranging from 3% to 13%.

TABLE I
ELUTION RATIO FOR DIFFERENT ELUENTS AT VARIOUS LIGAND DENSITIES

Ligand density (mmol/g fibre)	Eluent		
	0.01 M Tris-HCl + 1 M NaCl	0.01 M Tris-HCl + 2 M NaCl	50 v/v% EG ^a + 1 M NaCl
0.101	79%	79%	100%
0.185	81%	80%	100%
0.463	82%	73%	94%

^a Ethylene glycol.

shown in Table I, no significant difference in the elution ratio was observed in the range of the ligand density of 0.101–0.463 mmol/g. The mixture of 50 v/v% ethylene glycol and 1 M NaCl eluted BGG quantitatively. This indicates that the bond energy is almost constant, irrespective of the ligand density. However, it is difficult to explain the absence of multi-point attachment to the ligand.

The amount of BGG adsorbed non-selectively on the Phe-C fibre was *ca.* 10% of the amount adsorbed specifically (Fig. 6). Fig. 9 shows that the saturation capacity of BGG can be determined from the specific surface area of the porous hollow fibre when the ligand is in excess of BGG. The gamma globulin is a mixture of IgG and IgA. The pre-

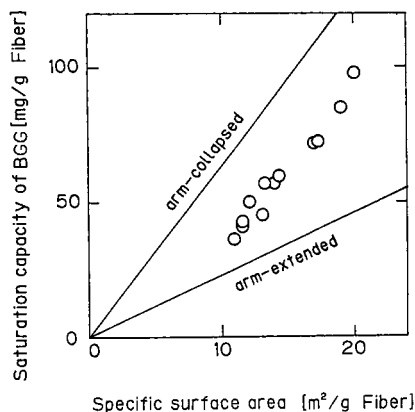


Fig. 9. Saturation capacity of BGG on Phe-C fibre as a function of specific surface area. The theoretical lines were determined from eqn. 6 for two extreme orientations: arm-collapsed and arm-extended adsorptions.

dominant component, IgG, has a molecular mass of 150 000 and consists of four peptide chains: two identical heavy chains and two identical light chains. These chains are linked by strong disulphide bonds into a Y- or T-shaped structure with hinge-like flexible arms. Thus an IgG molecule would expand and contract significantly with the variation of the ionization of the ionizable groups in the molecule. When the molecule is fully charged, either at low pH or high pH, the arms can be completely extended because of charge repulsion. Where there is no intermolecular charge interaction, the arms would probably collapse, owing to an intermolecular attractive hydrophobic interaction [17]. Since the bottom end of the Y or T (the Fc portion) is much more hydrophobic than the tips of the Y or T (the F(ab')₂ portions) of the IgG molecules, end-on adsorption of IgG on the Phe-C is certainly favoured. There are thus two possible extreme conformations: arm-collapsed with end-on adsorption, and arm-extended with end-on adsorption. The theoretical saturation capacity, q_s , can be calculated from the following:

$$q_s = a_v M / (a N_A) \quad (6)$$

where a_v and a are the specific surface area and the cross-sectional area occupied by an IgG molecule, and M and N_A are the molecular mass of BGG and the Avogadro number. Theoretical lines for arm-collapsed and arm-extended adsorption are depicted in Fig. 9 by inserting the corresponding estimated projection area per molecule, 3900 and 10 700 Å². Our experimental results were situated between the two extreme conformations.

CONCLUSION

A porous hollow-fibre membrane containing L-Phe as a pseudo-biospecific ligand has been prepared by radiation-induced grafting of GMA onto a polyethylene microfiltration hollow-fibre membrane, and thereafter by coupling of the produced epoxide group with L-Phe. The remaining epoxide group was hydrolysed to a diol group with sulphuric acid.

The density of the diol group obtained from the degree of GMA grafting of at least 100% was necessary to minimize the non-selective adsorption of BGG onto the Phe-containing adsorbent based on polyethylene.

The molar ratio of the Phe ligand to BGG ranged up to 10^3 . The excess ligand did not interfere with the ordinary adsorption.

The adsorption capacity for BGG of the resulting porous adsorbent could be determined by the specific surface area of the adsorbent when the ligand was in excess of BGG.

ACKNOWLEDGEMENT

The authors thank Kazuo Toyomoto of the Industrial Membrane Division of Asahi Chemical Industry Co., Ltd. for his help in providing the starting hollow fibre.

REFERENCES

- 1 E. Hochuli, *J. Chromatogr.*, 444 (1988) 293.
- 2 Z. Yamazaki, F. Kanai, Y. Idezuki, N. Yamawaki, K. Inagaki and N. Tsuda, *Jpn. J. Artif. Organs*, 16(1987) 1203.
- 3 P. D. G. Dean, W. S. Johnson and F. A. Middle (Editors), *Affinity Chromatography*, IRL Press, Oxford, 1985.
- 4 W. H. Scouten, *Affinity Chromatography*, Wiley, New York, 1981, p. 89.
- 5 K. Saito, T. Kaga, H. Yamagishi, S. Furusaki, T. Sugo and J. Okamoto, *J. Membrane Sci.*, 43 (1989) 131.
- 6 K. Saito, M. Ito, H. Yamagishi, S. Furusaki, T. Sugo and J. Okamoto, *Ind. Eng. Chem. Res.*, 28 (1989) 1808.
- 7 P. I. Forrester and R. L. Hancock, *Can. J. Biochem.*, 51 (1973) 231.
- 8 M. H. Gething, B. E. Davidson and T. A. A. Dopheide, *Eur. J. Biochem.*, 71 (1976) 317.
- 9 G. J. Doellgast and A. G. Plaut, *Immunochemistry*, 13 (1976) 135.
- 10 M. Kim, K. Saito, S. Furusaki, T. Sugo and J. Okamoto, *J. Membrane Sci.*, 56 (1991) 289.
- 11 B. H. J. Hofstee, *Biochem. Biophys. Res. Com.*, 63 (1975) 618.
- 12 Sigma Chemical Co., *Catalogue*, St. Louis, 1990, p. 1453.
- 13 H. Yamagishi, K. Saito, S. Furusaki, T. Sugo and J. Okamoto, *Nippon Kagaku Kaishi*, (1988) 212.
- 14 D. Cohn, A. S. Hoffman and B. D. Ratner, *J. Appl. Polym. Sci.*, 29 (1984) 2645.
- 15 B. Jansen and G. Ellinghorst, *J. Biomed. Mater. Res.*, 19 (1985) 1085.
- 16 J. Porath, L. Sundberg, N. Fornstedt and I. Olsson, *Nature (London)*, 245 (1973) 465.
- 17 B. Bagchi and S. M. Birnbaum, *J. Colloid Interface Sci.*, 83 (1981) 460.

Two-dimensional mapping by high-performance liquid chromatography of pyridylamino oligosaccharides from various glycosphingolipids

Kanako Ohara*, Mutsumi Sano, Akihiro Kondo and Ikunoshin Kato

Biotechnology Research Laboratories, Takara Shuzo Co., Ltd., 3-4-1 Seta, Otsu, Shiga 520-21 (Japan)

(First received March 18th, 1991; revised manuscript received June 3rd, 1991)

ABSTRACT

A method to map sugars two-dimensionally for the analysis of the structures of oligosaccharides from glycosphingolipids is described. Nine neutral and ten acidic oligosaccharides were obtained from glycosphingolipids by endoglycoceramidase digestion and labelled with 2-aminopyridine. The pyridylamino oligosaccharides were clearly separated by high-performance liquid chromatography on commercially available C₁₈-silica and amide-silica column. All compounds tested were mapped without any overlapping. The separation of the pyridylamino oligosaccharides on the C₁₈-silica column depended on the numbers and positions of sialic acid and N-acetylhexosamine residues; on the amide-silica column, the separation depended on the total number of sugar residues.

INTRODUCTION

The oligosaccharides on cell surfaces change in type and amount when the cells differentiate or become malignant, so the involvement of oligosaccharides in cell recognition is of much interest [1]. A glycosphingolipid consists of a hydrophobic ceramide moiety and a hydrophilic oligosaccharide moiety, making it amphipathic. Many ceramides are only slightly different from other ceramides, so analysis of the structures of the oligosaccharides in glycosphingolipids can be difficult, especially when chromatography is used. Analytical methods for the identification of the structures of glycosphingolipids involve thin-layer chromatography, mass spectrometry, and nuclear magnetic resonance (NMR). However, more than a trace amount of purified sample is needed in these methods, and only certain structures can be identified [2-5].

Hase *et al.* [6] developed a method for a kind of pyridylation in which there is fluorescence labelling of oligosaccharides with 2-aminopyridine. The combination of pyridylation with high-

performance liquid chromatography (HPLC) makes it possible to analyse oligosaccharides sensitively, with a detection limit of 50 fmol of pyridylamino (PA) oligosaccharides. PA-oligosaccharides from glycoproteins have been analysed by HPLC on reversed-phase and normal-phase columns, and each elution position has been plotted two-dimensionally by Hase *et al.* [7] and Tomiya *et al.* [8]. Higashi *et al.* [9] have reported a method for analysis in which oligosaccharides from glycosphingolipids are labelled with UV-absorbing reagent, *p*-aminobenzoic acid ethyl ester (ABEE), and analysed by HPLC. The sensitivity of detection of the ABEE derivatives was inadequate, and at least 500 pmol of oligosaccharides were needed for a typical analysis. Large ABEE-oligosaccharides, such as ABEE-G_{T1b}, were not mapped with the reversed-phase column, since they were eluted in the void volume.

Kondo *et al.* [10] reported an improved method in which sialic acid residues are not released by pyridylation. We used this method for the analysis of the structures of oligosaccharides obtained from glycosphingolipids. PA-oligosaccharides were ana-

TABLE I

ELUTION POSITIONS OF PA-OLIGOSACCHARIDES FROM PALPAK TYPE R AND S COLUMNS

Elution positions on HPLC columns are expressed as the numbers of glucose units of the corresponding standard glucose oligomers. The conditions for HPLC are described in Experimental. The abbreviations of Svennerholm [16] for gangliosides are used for the oligosaccharides of the corresponding gangliosides. The other oligosaccharides are abbreviated as recommended by the IUPAC-IUB Commission on Biochemical Nomenclature [17]. Glc = glucose; Gal = galactose; GlcNAc = N-acetylglucosamine; GalNAc = N-acetylgalactosamine; SA = N-acetylneuraminic acid; NeuGc = N-glycolylneuraminic acid.

Abbreviation	Structure of oligosaccharides	No. of Glc units	
		Type R	Type S
Lac	Gal β 1-4Glc	0.9	2.1
Gg ₃	GalNAc β 1-4Gal β 1-4Glc	1.1	2.6
Gg ₄	Gal β 1-3GalNAc β 1-4Gal β 1-4Glc	0.9	3.8
G _{M3} -A	SA α 2-3Gal β 1-4Glc	3.2	2.1
G _{M3} -G	NeuGc α 2-3Gal β 1-4Glc	2.9	2.5
G _{M2}	GalNAc β 1-4Gal β 1-4Glc	3.3	2.6
	3 SA α 2		
G _{M1}	Gal β 1-3GalNAc β 1-4Gal β 1-4Glc	3.3	3.4
	3 SA α 2		
G _{D3}	SA α 2-8SA α 2-3Gal β 1-4Glc	4.5	2.7
G _{D2}	GalNAc β 1-4Gal β 1-4Glc	4.5	3.2
	3 SA α 2-8SA α 2		
G _{D1a}	Gal β 1-3GalNAc β 1-4Gal β 1-4Glc	5.2	3.5
	3 3 SA α 2 SA α 2		
G _{D1b}	Gal β 1-3GalNAc β 1-4Gal β 1-4Glc	4.3	4.0
	3 SA α 2-8SA α 2		
G _{T1b}	Gal β 1-3GalNAc β 1-4Gal β 1-4Glc	6.3	4.0
	3 3 SA α 2 SA α 2-8SA α 2		
G _{Q1b}	Gal β 1-3GalNAc β 1-4Gal β 1-4Glc	10.0	4.3
	3 3 SA α 2-8SA α 2 SA α 2-8SA α 2		
Gb ₃	Gal α 1-4Gal β 1-4Glc	1.2	2.8
Gb ₄	GalNAc β 1-3Gal α 1-4Gal β 1-4Glc	2.6	3.4
Gb ₅	GalNAc α 1-3GalNAc β 1-3Gal α 1-4Gal β 1-4Glc	3.6	4.0
Lc ₃	GlcNAc β 1-3Gal β 1-4Glc	2.2	2.7
Lc ₄	Gal β 1-3GlcNAc β 1-3Gal β 1-4Glc	2.7	3.5
nLc ₄	Gal β 1-4GlcNAc β 1-3Gal β 1-4Glc	2.4	3.6

lysed by HPLC on a C_{18} silica column and also on an amide-silica column. We plotted the elution positions of the PA-oligosaccharides on a two-dimensional sugar map. This mapping is useful for the analysis of the structures of the oligosaccharides in glycosphingolipids.

EXPERIMENTAL

Oligosaccharides and glycosphingolipids

The structure of and abbreviations for the oligosaccharides used are listed in Table I. The oligosaccharides were released from the various glycosphingolipids by digestion with endoglycoceramidase from *Rhodococcus* sp. strain G-74-2 (Seikagaku Kogyo, Tokyo, Japan). Glycosphingolipids G_{M1} , G_{M2} , G_{M3-A} , G_{D1a} , G_{D1b} , G_{T1b} , and G_{Q1b} were purchased from Bachem Feinchemikalien (Bubendorf, Switzerland). Glycosphingolipids G_{b3} , G_{b4} , G_{b5} , G_{g4} , G_{M3-G} , and G_{D3} were purchased from BioCarb Chemicals (Lund, Sweden). Oligosaccharides Lc_4 and nLc_4 were purchased from Seikagaku Kogyo. PA- G_3 was prepared by acid hydrolysis of PA- G_{M2} in 20 mM HCl for 1 h at 90°C. PA- Lc_3 and PA- G_{D2} were prepared from PA- Lc_4 and PA- G_{D1b} , respectively, by digestion with β -galactosidase from an *Aspergillus* sp. as described below.

Enzyme reaction

The glycosphingolipids (10–300 nmol) were digested at 37°C for 15 h with endoglycoceramidase (0.5–10 mU) in 10–300 μ l of 50 mM sodium acetate buffer (pH 6.0) containing 5–150 μ g of sodium taurodeoxycholate [11]. The oligosaccharides released were detected by thin-layer chromatography (HPTLC aluminium sheets, Silica Gel 60, E. Merck, Darmstadt, Germany) developed in 1-butanol–acetic acid–water (2:1:1), and made visible with orcinol– H_2SO_4 reagent [12].

Pyridylamino derivatization

PA-oligosaccharides were obtained by the method of Kondo *et al.* [10] with use of a Palstation apparatus (Takara Shuzo, Kyoto, Japan). Then 100 nmol of the oligosaccharide obtained were aminated with 20 mg of the fluorescent reagent 2-aminopyridine in 10 μ l of acetic acid at 90°C for 1 h. To the reaction mixture, 10 μ l of acetic acid containing 1.95 mg of dimethylamine borane was

added, and a reductive reaction was allowed to proceed at 80°C for 1 h. The reaction mixture was evaporated at reduced pressure with a stream of N_2 gas, and the residue was put on a Sephadex G-15 column (200 \times 8 mm I.D.; Pharmacia, Uppsala, Sweden) to remove excess reagents [7]. The fractions in each peak were hydrolysed in 4 M trifluoroacetic acid at 100°C for 3 h, and the hydrolysate was analysed with a Beckman Ultrasphere ODS column (250 \times 4.6 mm I.D.; 5 μ m particle size) by the method of Takemoto *et al.* [13]. The fractions in which the residue of the reduced end was PA-glucose were regarded as containing PA-oligosaccharides.

The purified PA-oligosaccharides were checked by 1H NMR measurements, digestion with various exoglycosidases, and gas chromatography by the method of Mega and Ikenaka [14].

Exoglycosidase digestion

To prepare PA- Lc_3 or PA- G_{D2} , 10 pmol of PA- Lc_4 or PA- G_{D1b} were digested with 0.2 U of β -galactosidase (E.C. 3.2.1.23) from an *Aspergillus* sp. (Toyobo, Osaka, Japan) in 0.1 M acetate buffer (pH 5.0) at 37°C for 15 h. The structures of PA- G_{D2} and PA- Lc_3 were checked by exoglycosidase digestion and HPLC analysis only, because the amounts of the purified samples were small. By HPLC with the two columns described below, an acid hydrolysate of PA- G_{D2} was eluted at the same position as PA- G_{g3} . Next, 10 pmol of PA- nLc_4 were digested at 37°C for 15 h with 2 mU of β -galactosidase from bovine testes (Seikagaku Kogyo) in 0.1 M sodium citrate–phosphate buffer (pH 4.3) containing 1% bovine serum albumin and 10% glycerol. PA- Lc_3 was eluted at the same position as PA- nLc_4 digested with β -galactosidase from bovine testes. Then, 10 pmol of PA- Lc_3 were digested at 37°C for 15 h with 2 mU of β -N-acetylhexosaminidase (E.C. 3.2.1.52) from jack beans (Seikagaku Kogyo) in 0.1 M citrate–phosphate buffer (pH 5.0), and the digest was eluted at the same position as PA-Lac during HPLC.

Analysis of PA-oligosaccharides by HPLC

PA-oligosaccharides were separated with a Shimadzu LC-6A HPLC system with the two kinds of columns.

Column I was a C_{18} silica column, Palpak Type R column (250 \times 4.6 mm I.D.; 5 μ m particle size;

Takara Shuzo), used in reversed-phase HPLC. The flow-rate was 1.0 ml/min at 40°C. Solvent A was 50 mM acetic acid, adjusted to pH 5.0 with triethylamine, and solvent B was solvent A containing 0.5% 1-butanol. After injection of a sample into the column equilibrated with solvent A, the ratio of solvent B was increased on a linear gradient to 50% over a 50-min period. PA-oligosaccharides were detected by their fluorescence, with excitation and emission wavelengths of 320 and 400 nm, respectively.

Column II was an amide-silica column, Palpak Type S column (250 × 4.6 mm I.D.; 5 µm particle size; Takara Shuzo), used in size-fractionation HPLC. The flow-rate was 1.0 ml/min at 40°C. Solvent C was a 25:75 mixture of 200 mM acetic acid, adjusted to pH 7.3 with triethylamine, and acetonitrile, and solvent D was a 50:50 mixture of the same two components. After injection of a sample into the column equilibrated with solvent C, the ratio of solvent D was increased, on a linear gradient to 50% over a 25-min period. PA-oligosaccharides were detected by their fluorescence, with excitation and emission wavelengths of 310 and 380 nm, respectively.

Construction of two-dimensional maps

To standardize the elution positions of PA-oligosaccharides on HPLC columns, PA-isomaltooligosaccharides (Takara Shuzo) prepared from a dextran hydrolysate were analysed on the same columns and with the same solvents and conditions. Glucose units were defined by comparison of the elution position of each PA-oligosaccharide with that of the standard glucose oligomers. Glucose unit numbers obtained by reversed-phase HPLC (Palpak Type R column) were expressed on the abscissa, and those obtained by size-fractionation HPLC (Palpak Type S column) were expressed on the ordinate, when two-dimensional maps were plotted.

Preparation of PA-oligosaccharides from bovine brain acetone powder

The gangliosides were extracted from 50 mg of bovine brain acetone powder by the method of Folch *et al.* [15]. The extract containing gangliosides was digested at 37°C for 24 h with 2.5 mU of endoglycosamidase in 100 µl of 50 mM sodium acetate buffer (pH 6.0) containing 50 µg of sodium

taurodeoxycholate. Then two 1 mU amounts of endoglycosamidase were added, 24 h apart, and digestion was continued for 24 h after the second addition. The reaction mixture was evaporated, and the residue was directly labelled with 2-aminopyridine as described above. The reaction mixture was evaporated with a stream of N₂ gas under reduced pressure. The PA derivatives of the oligosaccharides were purified by gel filtration on a Sephadex G-15 column. Some of the fractions from HPLC were lyophilized and dissolved in 50 µl of 0.1 M sodium acetate buffer (pH 4.5). The solution was incubated with 50 mU of sialidase (E.C. 3.2.1.18) from *Arthrobacter ureafaciens* (Nacalai Tesque, Kyoto, Japan) at 37°C for 15 h.

RESULTS AND DISCUSSION

HPLC of standard glucose oligomers

When a single variety of PA-oligosaccharide is analysed by HPLC, it may elute at different times if the column is from different lots, or if the column contents have degraded, or if there are small differences in the preparation of the solvents, so it is necessary to standardize the elution position. The results of standardization are shown in Fig. 1. On both columns, the smaller oligomers were eluted sooner, and each oligomer was eluted separately.

HPLC analysis of PA-oligosaccharides

Nineteen kinds of PA-oligosaccharide prepared from glycosphingolipids were analysed by HPLC with the two types of column. Glucose units were defined by comparison of the elution position of each PA-oligosaccharide with that of the standard glucose oligomers (Table I). To check for reproducibility of the results, and for possible effects of differences in the lot or the number of times the column was used, three runs were done. Different columns were used for each run, with two new columns of different lots and one used column (several to dozens of hours of use) of the same lot as one of the new columns. For each PA-oligosaccharide, except PA-G_{Q1b}, the numbers of glucose units obtained from HPLC were exactly the same when rounded off from two to one decimal places. Thus, column degeneration did not affect the results, except for PA-G_{Q1b}. The numbers of glucose units of PA-G_{Q1b} were the same on the amide-silica column

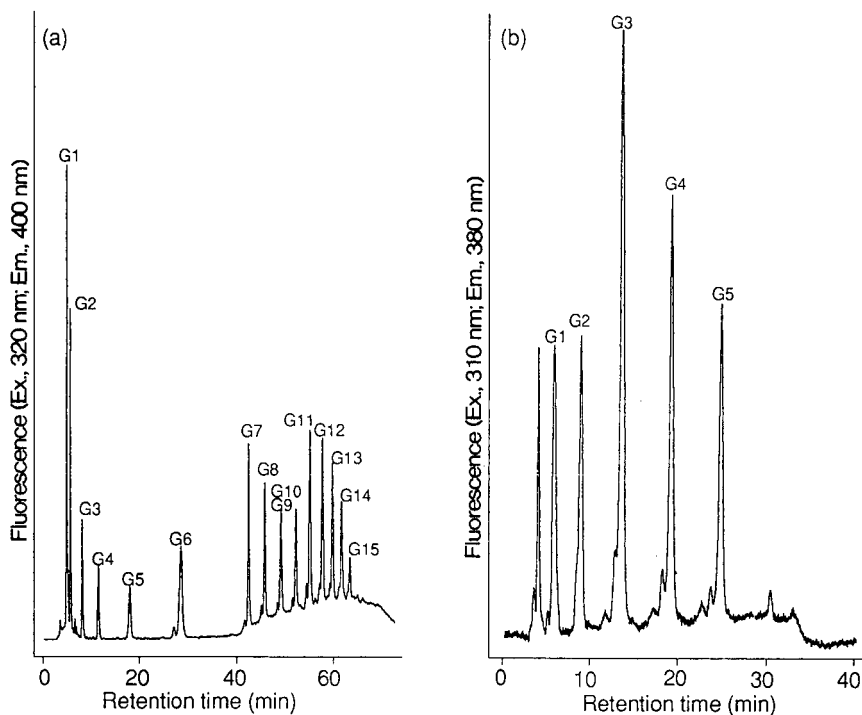


Fig. 1. HPLC profiles of pyridylaminoglucose oligomers (a) on a C_{18} silica column and (b) on an amide-silica column. The gradient starts at time 0. Glucose unit numbers are indicated.

in the three runs, but those on the C_{18} silica column became smaller as the column contents gradually degraded.

On the C_{18} silica column, HPLC of the nineteen kinds of PA-oligosaccharides took 50 min; on the amide-silica column, it took 25 min.

Two-dimensional mapping of PA-oligosaccharides

The glucose units obtained were plotted on a two-dimensional map (Fig. 2).

An NeuAc residue bonded to a galactose residue by an α 2-3 linkage retarded elution from the C_{18} silica column by two glucose units, but did not retard elution from the amide-silica column. The following four pairs gave such results, with the second of each pair eluted later: PA-Lac and PA- G_{M3-A} ; PA- G_{G3} and PA- G_{M2} ; PA- G_{M1} and PA- G_{D1a} ; and PA- G_{D1b} and PA- G_{T1b} .

An NeuAc residue bonded to an NeuAc residue by an α 2-8 linkage retarded elution from the C_{18} silica column by one glucose unit, and it retarded elution from the amide-silica column by 0.5 glucose

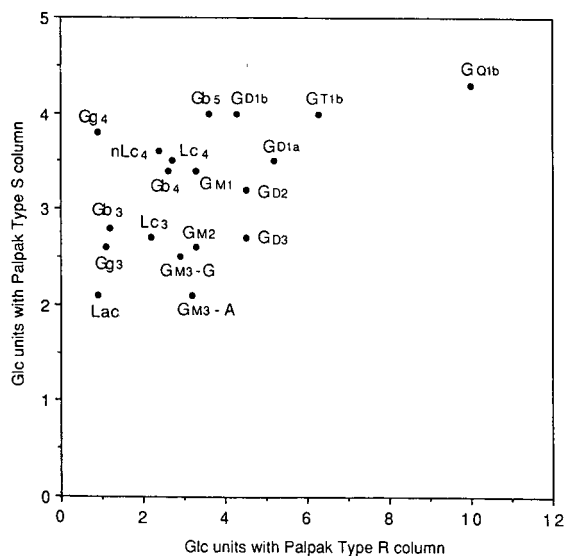


Fig. 2. Two-dimensional sugar map of PA-oligosaccharides. The numbers on the abscissa and ordinate indicate the glucose unit numbers obtained on the Palpak Type R and S columns, respectively.

units. The pairs giving such results were: PA-G_{M3}-A and PA-G_{D3}; PA-G_{M2} and PA-G_{D2}; PA-G_{M1} and PA-G_{D1b}; and PA-G_{D1a} and PA-G_{T1b}.

PA-G_{M3}-A was separated from PA-G_{M3}-G.

A GalNAc residue bonded by a β 1-4 linkage did not retard elution from the C₁₈ silica column, but it retarded elution from the amide-silica column by 0.5 glucose units. The pairs giving such results were: PA-Lac and PA-Gg₃; PA-G_{M3}-A and PA-G_{M2}; and PA-G_{D3} and PA-G_{D2}.

A galactose residue did not retard elution from the C₁₈ silica column, but it retarded elution from the amide-silica column by one glucose unit. The pairs giving such results were: PA-G_{M2} and PA-G_{M1}; and PA-G_{D2} and PA-G_{D1b}.

PA-Gg₄, PA-Gg₃, PA-Lac, and PA-Gb₃ were eluted from the C₁₈ silica column at a position close to the void volume, and they were not separated well. On the amide-silica column, their separation was satisfactory.

The elution positions of the PA-oligosaccharides did not overlap, and were as predicted, except for the number of glucose units of PA-Gg₄ on the amide-silica column (Fig. 2). To judge from the results with PA-Gg₃ and PA-G_{M2}, PA-G_{M1} and PA-G_{D1a}, and PA-Lac and PA-G_{M3}-A, PA-Gg₄ should have eluted at the same position as PA-G_{M1} on the amide-silica column; all of these pairs are different by the presence or absence of a NeuAc residue bonded to a galactose residue by an α 2-3 linkage. The elution position suggested that the structure of PA-Gg₄ shown in Table I might be different from the correct one, so the structure was checked as follows: (i) the elution position of PA-Gg₄ was the same as that of the acid hydrolysate of PA-G_{M1}; (ii) the digests of PA-Gg₄ with β -galactosidase from the *Aspergillus* sp. were eluted at the same position as PA-Gg₃ on a two-dimensional map; (iii) ¹H NMR measurements were consistent with the structure in Table I. Therefore, the structure in Table I was correct. We do not know why PA-Gg₄ was retarded on the amide-silica column. Perhaps PA-Gg₄ interacted with the amide substituents or silica gel of the amide-silica column.

Application of the two-dimensional map for characterization of PA-oligosaccharides from bovine brain acetone powder

PA-oligosaccharides prepared from bovine brain

acetone powder were analysed by HPLC with the C₁₈ silica column (Fig. 3a). Portions of the fractions of peaks A to E were treated by acid hydrolysis, followed by HPLC with a Beckman Ultrasphere ODS column by the method of Takemoto *et al.* [13]. The peaks B to E, in which the residue of the reduced end was PA-glucose, were then analysed on the amide-silica column (Fig. 3b). Each fraction gave

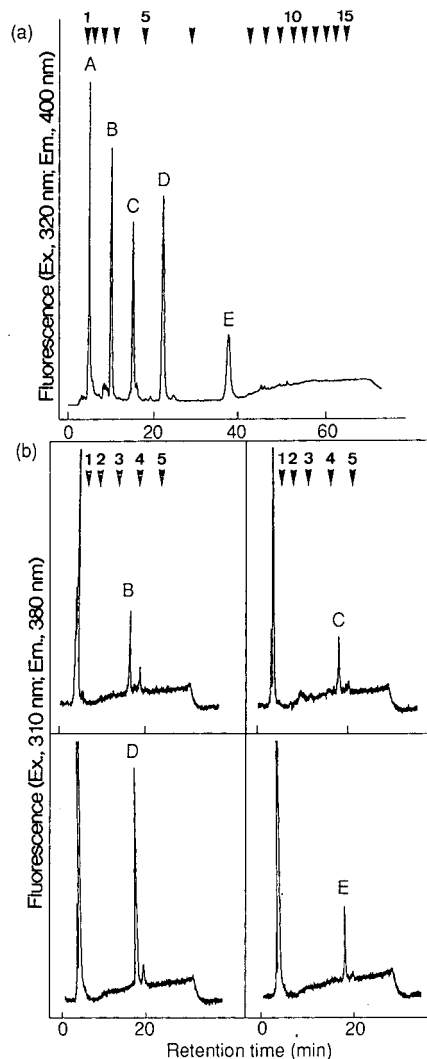


Fig. 3. HPLC profiles of PA-oligosaccharides released from bovine brain acetone powder. (a) PA-oligosaccharides obtained from 160 μ g of bovine brain acetone powder were injected into a Palpak Type R column. The gradient starts at time 0. Glucose unit numbers are indicated. (b) Each peak B-E was chromatographed again on a Palpak Type S column.

a single peak, and each elution position on two HPLC columns was plotted on a two-dimensional map. The elution position of each fraction coincided with one of the four standard oligosaccharides, as follows: B and G_{M1}; C and G_{D1b}; D and G_{D1a}; and E and G_{T1b}. To check these results, the fractions of the peaks were digested with exoglycosidases, and the digests were analysed by HPLC. Then the elution positions were plotted on a two-dimensional map. We found that peak B was converted into PA-G_{M2} by β -galactosidase from an *Aspergillus* sp., and that peak C was converted into PA-G_{D2}. Both peaks D and E were converted into PA-G_{g4} by sialidase, but part remained as PA-G_{M1}. These results of exoglycosidase digestion are consistent with the structures we propose for the compounds corresponding to peaks B to E.

In this use of two-dimensional mapping, all of the major peaks correspond to points on the map. If new oligosaccharides that correspond to nothing on the map are found in a sample, the sample should be digested with exoglycosidases and then analysed by HPLC. The use of pyridylation, together with two-dimensional mapping and ¹H NMR analysis, should make structural analysis of complicated sugar chains from small amounts of glycosphingolipids easier than before.

REFERENCES

- 1 S. Hakomori, *Annu. Rev. Biochem.*, 50 (1981) 733.
- 2 J. L. Magnani, D. F. Smith and V. Ginsburg, *Anal. Biochem.*, 109 (1980) 399.
- 3 H. Higashi, Y. Fukui, S. Ueda, S. Kato, Y. Hirabayashi, M. Matsumoto and M. Naiki, *J. Biochem.*, 95 (1984) 1517.
- 4 Y. Hirabayashi, K. Koketsu, H. Higashi, Y. Suzuki, M. Matsumoto, M. Sugimoto and T. Ogawa, *Biochim. Biophys. Acta*, 876 (1986) 178.
- 5 H. Higashi, T. Sugii and S. Kato, *Biochim. Biophys. Acta*, 963 (1988) 333.
- 6 S. Hase, T. Ibuki and T. Ikenaka, *J. Biochem.*, 95 (1984) 197.
- 7 S. Hase, K. Ikenaka, K. Mikoshiba and T. Ikenaka, *J. Chromatogr.*, 434 (1988) 15.
- 8 N. Tomiya, J. Awaya, M. Kurono, S. Endo, Y. Arata and N. Takahashi, *Anal. Biochem.*, 171 (1988) 73.
- 9 H. Higashi, M. Ito, N. Fukaya, S. Yamagata and T. Yamagata, *Anal. Biochem.*, 186 (1990) 355.
- 10 A. Kondo, J. Suzuki, N. Kuraya, S. Hase, I. Kato and T. Ikenaka, *Agric. Biol. Chem.*, 54 (1990) 2169.
- 11 M. Ito and T. Yamagata, *J. Biol. Chem.*, 261 (1986) 14 278.
- 12 C. François, R. D. Marshall and A. Neuberger, *Biochem. J.*, 83 (1962) 335.
- 13 H. Takemoto, S. Hase and T. Ikenaka, *Anal. Biochem.*, 145 (1985) 245.
- 14 T. Mega and T. Ikenaka, *Anal. Biochem.*, 119 (1982) 17.
- 15 J. Folch, M. Lees and G. H. S. Stanley, *J. Biol. Chem.*, 226 (1957) 497.
- 16 L. Svennerholm, *J. Neurochem.*, 10 (1963) 613.
- 17 IUPAC-IUB Commission on Biochemical Nomenclature, *Eur. J. Biochem.*, 79 (1977) 11.

Retention behaviour of a template-assembled synthetic protein and its amphiphilic building blocks on reversed-phase columns

Verena Steiner*

Pharmaceuticals Research, Ciba-Geigy Ltd., CH-4002 Basel (Switzerland)

Martin Schär and K. Olaf Börnsen

Analytical Research, Ciba-Geigy Ltd., CH-4002 Basel (Switzerland)

Manfred Mutter

Institut de Chimie Organique, Université de Lausanne, CH-1005 Lausanne (Switzerland)

(First received March 6th, 1991; revised manuscript received June 24th, 1991)

ABSTRACT

The retention behaviour of a six-helix bundle template-assembled synthetic protein (TASP) molecule and its amphiphilic building blocks was investigated. The TASP consists of a circular template, *cyclo*(1–12)[KG]₆, and six identical potentially α -helical peptides of the sequence KLALKLALKALKLALKLA. As an α -helix, this peptide is amphiphilic along the axis of its helix. Based on this sequence, the retention times of a set of acetylated peptides containing from seven to twenty amino acids on a Nucleosil C₁₈ column were compared with another set of peptides with the same amino acid composition but a non-amphiphilic structure. Peptide elution was effected with linear trifluoroacetic acid (TFA)–water to TFA–acetonitrile gradients. The difference in retention times increased with peptide length; the 9-mers eluted at the same time, but there was a difference of 3.5 min for the 13-mers and 22.3 min for the 20-mer, indicating the induction of secondary structure on binding to the stationary phase. The same pair of 20-mers on Vydac C₁₈, C₄ and biphenyl columns gave differences in retention times of 23.2, 16.7 and 12.3 min, respectively. The TASP molecule was irreversibly adsorbed to C₁₈ stationary phases, whereas it was eluted from C₄ and biphenyl columns as a single sharp peak. Several side-products resulting from the synthesis of the TASP molecule were identified by matrix-assisted laser desorption ionization mass spectroscopy. A comparison of the retention times of these side-products and the results of pre-column denaturation experiments indicated that the tertiary structure of the TASP molecule is maintained on binding to biphenyl and C₄ columns.

INTRODUCTION

The *de novo* design of proteins with a predetermined three-dimensional structure is impeded by the limited knowledge of the rules governing protein folding. A promising approach to overcome this problem is the concept of template-assembled synthetic proteins (TASP) [1]. This approach combines the prediction of secondary structure with the power of synthetic chemistry: TASP molecules are

built by coupling peptides with potentially amphiphilic secondary structures to a template. The self-association of the building blocks leads to compact structures.

The TASP molecule under investigation was designed to form a six-helix bundle with the lysine side-chains exposed to the exterior. The inner surface of the hollow bundle is lined with alanines forming a hydrophobic cavity of about 0.7 nm diameter.

The TASP molecule displays several features which make it prone to irreversible binding on hydrocarbonaceous matrices. First, the molecule has an unusually high content of hydrophobic residues. The membrane protein bacteriorhodopsin [2], for example, contains 60% hydrophobic amino acids, whereas the TASP molecule described here contains 67%. Secondly, the highly basic TASP molecule has 36 amino groups but lacks carboxy groups. Interactions of the amino groups with surface silanol groups of the stationary phase could lead to irreversible adsorption, but they can be suppressed by end-capping and by using trifluoroacetic acid (TFA) in the mobile phase to prevent ionization of the remaining silanols [3].

Finally, as has been reported elsewhere [4–8], the binding of potentially amphiphilic helices to C₈ and C₁₈ matrices induces a secondary structure and leads to a considerably stronger retention. As the TASP molecule contains six potentially amphiphilic helices, strong adsorption is expected.

The tertiary structures of most proteins are stabilized by hydrophobic interactions. On binding to a reversed-phase (RP) matrix, these interactions were ruptured. Various reports on the disruption of the tertiary structure on binding to RP columns exist. Mant *et al.* [9] investigated the denaturation of nineteen proteins on C₁₈, C₈, C₄ and phenyl columns. On C₁₈, C₈ and C₄ sorbents, all the proteins were denatured. On the phenyl column, all the proteins except lysozyme and avidin were denatured, whereas the latter showed only partial unfolding. Similar findings were reported by Ingraham *et al.* [10], for the rigidity of the 129-amino acid lysozyme with four intrachain cystine cross-links. A comprehensive study of the RP chromatographic behaviour of proteins in different unfolded states has been made by Lin and Karger [11]. By using only mildly destabilizing conditions, such as low temperature (4°C), a C₄-bonded stationary phase and propan-1-ol as an organic modifier, a number of proteins yielded two well separated peaks corresponding to the folded and an unfolded conformation. In addition, they distinguished between different states of denaturation and found that the degree of unfolding was as follows: folded \ll RP surface-unfolded $<$ pre-column urea-unfolded $<$ pre-column reduced and urea-unfolded.

There are no reports of the induction of an α -hel-

ical conformation on binding to biphenyl columns. In this work, the retention times of the potentially amphiphilic twenty-amino acid α -helix acLAK-LALKLALKLALKLAKLA on C₄, C₁₈ and biphenyl columns was compared with the non-amphiphilic helical sequence acLAKALKLKLALAL-LAKLKLAKLA, where the charged side-chains are distributed all around the helix cylinder. The helix-inducing effect was investigated as a function of peptide length using the same peptide and shorter fragments thereof. In addition, the retention behaviour of the TASP molecule was studied using C₁₈, C₄ and biphenyl columns. It was investigated whether the tertiary structure of the molecule is disrupted on binding to the stationary phase.

EXPERIMENTAL

High-performance liquid chromatography

A Spectra Physics SP 8700 solvent delivery system was used coupled to a Shimadzu UV-120-02 spectrophotometer and a Shimadzu C-R1B integrator-printer. The columns used were Vydac (The Separations Group, Hesperia, CA, USA) 214TP 5415 C₄, 218TP 5415 C₁₈ and 219TP 5415 biphenyl (15 cm \times 4.6 mm I.D., 5 μ m particle size, 30 nm pore size, from Macherey-Nagel, Düren, Germany). The flow-rate was 1 ml/min. Eluent A was 0.1% TFA; eluent B was acetonitrile + 0.1% TFA. The absorbance units full scale (a.u.f.s.) values were between 0.2 and 1. All chromatograms were obtained at room temperature.

Peptide identification

The peptides were identified by directly analyzing the collected peak fractions with a laboratory-built laser desorption ionization mass spectrometer [12]. Typically, 5 μ l of 10⁻⁵ M analyte solution were mixed with 5 μ l of 10⁻¹ M sinapinic acid and 1 μ l of this mixture was applied to the probe tip.

Reagents

All reagents were of at least analytical-reagent grade. Acetonitrile (spectroscopy grade) and guanidine hydrochloride (GuHCl) were from Fluka (Buchs, Switzerland) and sodium dodecyl sulphate (SDS) from Behring Diagnostics (La Jolla, CA,

USA). The water was of MilliQ quality (Millipore, Bedford, MA, USA). The eluents were degassed by continuous sparging with helium.

Peptides

The design, synthesis and purification of the TASP molecule and its building blocks has been described in detail elsewhere [13]. Briefly, the potentially α -helical 20-mers and their shorter derivatives from four to nineteen amino acids were synthesized by solid-phase peptide synthesis using standard protocols for 9-fluorenylmethyloxycarbonyl protection of the N-terminus. After each coupling step, an aliquot of resin was removed to obtain the shorter fragments.

The TASP molecule was assembled in solution by coupling the protected potentially amphiphilic 18-mers via their free C-termini to the six ϵ -amino groups of the template. For reasons of simplification, the potentially amphiphilic α -helical peptide KLALKLALKALKLALKLA is denoted HELIX (H), the TASP molecule TH₆ and the incomplete coupling products TH₃, TH₄ and TH₅.

Pre-column denaturation

Unless otherwise stated, 10 μ l of oligopeptide in 95% TFA (containing 10 μ g peptide/ μ l) were mixed with 90 μ l of 6 M GuHCl solution of 2% SDS solution and heated to 96°C for 10 min. After cooling to room temperature, 50 μ l were injected onto the column.

RESULTS AND DISCUSSION

Retention behaviour of amphiphilic building blocks

Induction of secondary structure as a function of peptide length. Two sets of peptides from seven to twenty residues in length with the same amino acid composition, but differing in their sequence, were constructed; they are listed in Table I. The sequence of the first set gives an amphiphilic structure on α -helix formation, whereas the sequence of the second set is non-amphiphilic (see helical wheel diagrams in Fig. 1).

The peptides were chromatographed on a 5 μ m, 10 nm Nucleosil C₁₈ column (25 cm \times 4 mm I.D.). Eluent A was 0.1% TFA; eluent B was 0.1% TFA in acetonitrile. A linear gradient from 0 to 80% B in 80 min was used. The retention times (t_R) are listed in Table I. The 22.3 min difference in retention time between the 20-mers decreases gradually with shorter sequences. The 9-mers elute at the same time. The retention times as a function of peptide length are shown in Fig. 2; only the sequences with strongly hydrophobic N- and C-termini were considered. Fig. 2 implies that the minimum length for secondary structure effects is between 9 and 13 residues. Thus, the high accuracy in the prediction of retention times for peptides up to sixteen residues reported by Guo *et al.* [14] cannot be obtained with the amphiphilic set of peptides. In this set, as shown by Houghten and DeGraw [15], the sequence domains must be taken into account.

TABLE I

RETENTION TIMES OF AMPHIPHILIC AND NON-AMPHIPHILIC SEQUENCES

Sequences with strongly hydrophobic residues at either end are printed in bold. The peptides were chromatographed on a 5 μ m, 10 nm Nucleosil C₁₈ column (25 cm \times 4 mm I.D.). Eluent A was 0.1% TFA and eluent B 0.1% TFA in acetonitrile. A linear gradient from 0 to 80% B in 80 min was used.

Residue	Amphiphilic sequence	t_R (min)	Non-amphiphilic sequence	t_R (min)
20	acLAKLALKLALKALKLALKLA	69.1	acLAKALKLKLALALLAKLKLA	46.8
19	acAKLALKLALKALKLALKLA	60.1	acAKALKLKLALALLAKLKLA	48.2
18	acKLALKLALKALKLALKLA	57.8	acKALKLKLALALLAKLKLA	48.7
17	acLALKLALKALKLALKLA	62.1	acALKLKLALALLAKLKLA	47.8
15	acLKLALKALKLALKLA	56.7	acLKLALALLAKLKLA	47.5
13	acLALKALKLALKLA	49.8	acKLALALLAKLKLA	46.3
9	acALKLALKLA	41.2	acALLAKLKLA	41.2
8	acLKLALKLA	40.7	acLLAKLKLA	40.5
7	acKLALKLA	33.4	acLAKLKLA	35.0

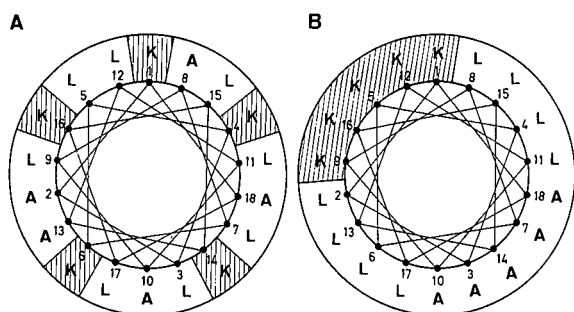


Fig. 1. Helical wheel diagrams of (A) the non-amphiphilic and (B) the amphiphilic 18-mer of Table I, looking from the C-terminal end (residue 18) down the helix axis.

Induction of secondary structure as a function of the matrix. The retention times of the 20-mers in Table I were evaluated using C_{18} , C_4 and biphenyl columns of the same dimensions. The results are given in Table II and Fig. 3. The biphenyl stationary phase shows the weakest retention, whereas the C_{18} column exhibits the strongest interaction. As expected, the amphiphilic peptide is retained more strongly.

The results may suggest that C_{18} ligands have the strongest and biphenyl ligands the weakest effect on the induction of secondary structure. However, when the 4- to 20-mers were compared on C_{18} and biphenyl columns, there was no significant difference between short peptides without secondary structure effects and the longer sequences with putative ligand-induced conformational stabilization (Fig. 4). Note that the columns used for the two sets

TABLE II

RETENTION TIMES OF THE AMPHIPHILIC AND NON-AMPHIPHILIC 20-MER

Sequences are given in Table I. The peptides were chromatographed on Vydac 5 μm , 30 nm columns (15 cm \times 4.6 mm I.D.). Eluent A was 0.1% TFA; eluent B 0.1% TFA in acetonitrile. A linear gradient from 0 to 80% B in 80 min was used.

Matrix	t_R (min)		Δt_R
	Non-amphiphilic 20-mer	Amphiphilic 20-mer	
C_{18}	42.9	66.1	23.2
C_4	41.3	58.0	16.7
Biphenyl	37.5	49.8	12.3

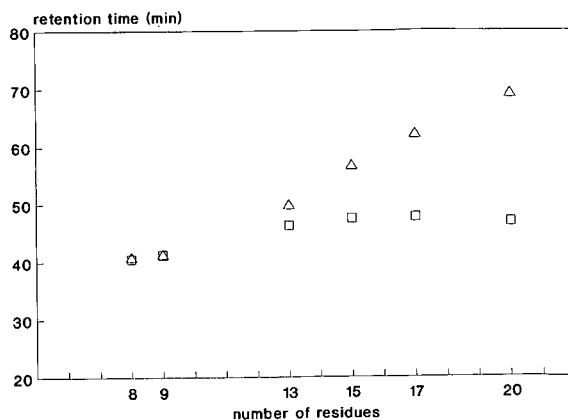


Fig. 2. Retention times of amphiphilic and non-amphiphilic peptides as a function of length. (Δ) Potentially amphiphilic; (\square) non-amphiphilic peptide. Sequences and conditions as in Table I.

of separations have different dimensions. It seems that the interaction with biphenyl-bonded phases is in general weaker.

Retention behaviour of TASP

TASP on C_{18} , C_4 and biphenyl columns. Fig. 5 shows the chromatograms of TASP (TH₆) and its building block peptide KLALKLALKALKLALKLA (denoted as HELIX) on C_{18} , C_4 and biphenyl columns. As predicted, TASP interacts strongly with the C_{18} matrix, leading to a small broad peak indicating denaturation and partly irreversible binding. In contrast, on the C_4 and biphenyl columns, the TASP molecule elutes much earlier and as a sharp peak. This result raises the question of whether the tertiary structure of the TASP molecule, in which predominantly lysine side-chains are exposed at the surface, is maintained on binding to C_4 and biphenyl phases.

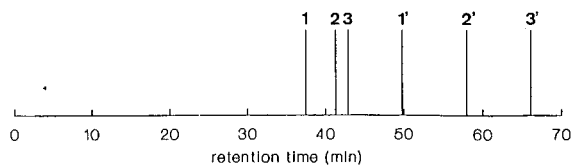


Fig. 3. Effect of matrix on retention time. 1, 2, 3 = Non-amphiphilic 20-mer peptide on biphenyl, C_4 and C_{18} columns, respectively; 1', 2', 3' = amphiphilic 20-mer peptide on biphenyl, C_4 and C_{18} columns, respectively. Sequences are given in Table I; conditions as in Table II.

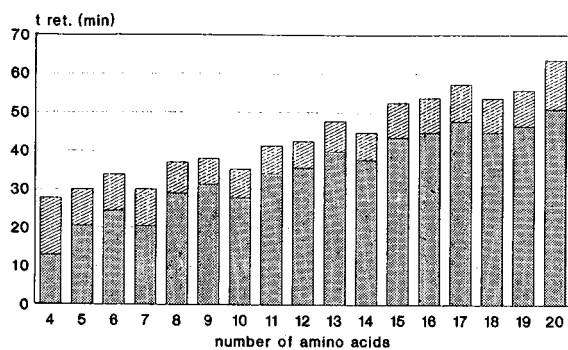


Fig. 4. Retention times of acetylated peptides a from four to twenty residues on C_{18} and biphenyl columns. Dotted areas, retention time on biphenyl column; hatched areas, retention time on C_{18} column minus retention time on biphenyl column. The sequences of the peptides are listed in Table I, or can be derived from this table. Columns: $5 \mu\text{m}$, 10 nm Nucleosil C_{18} ($250 \text{ cm} \times 4 \text{ mm I.D.}$) and $5 \mu\text{m}$, 30 nm Vydac biphenyl $15 \text{ cm} \times 4.6 \text{ mm I.D.}$.

Conformation of TASP on RP matrices. It is generally known that most proteins are denatured on binding to a RP matrix [16]. For the TASP molecule, however, there were hints that this is not so.

First, as can be seen in Fig. 5, the elution times of TASP and HELIX are very similar. On the biphenyl column, for example, the retention time of HELIX was 15.0 min, whereas the TASP molecule eluted at 18.4 min. As has been reported for peptide oligomers, there is a linear relationship between the natural logarithm of the number [17] or the molecular mass [16] of monomers and the retention time. Based on this assumption, regression analysis was performed using t_R values of the 11- to 20-mers on the biphenyl column (data not shown). Under the conditions where the single HELIX elutes at 15.0 min and TASP at 18.4 min, it was estimated that a di-HELIX would elute at 21.9 min and a hexa-HELIX at 34.3 min. Hence, despite the rough estimation, it seems unlikely that the TASP molecule interacts with the phenyl matrix by fully exposing the hydrophobic faces of the six HELICES to it.

A second indication that the tertiary structure is maintained on binding to biphenyl columns is the retention behaviour of the intermediate condensation product TH_4 and TH_5 . Interestingly, they co-eluted from the biphenyl columns with TH_6 in the same peak, although C_4 columns could partially separate them.

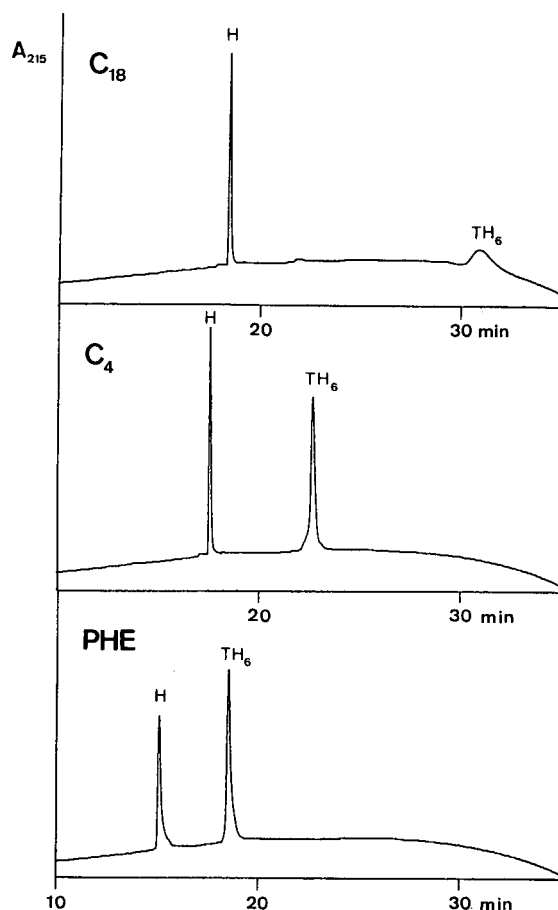


Fig. 5. Elution profiles of HELIX (H) and TASP (TH_6) on C_{18} , C_4 and biphenyl columns. Injection, $60 \mu\text{l}$; a.u.f.s., 0.5; columns, Vydac $5 \mu\text{m}$ 30 nm $15 \text{ cm} \times 4.6 \text{ mm I.D.}$; solvent A, 0.1% TFA; solvent B, 0.1% TFA in acetonitrile. Linear gradient from 10 to 90% B in 30 min.

A fragment condensation with $\approx 5\%$ incompletely protected HELIX fragments and the identification of side-products by matrix-assisted laser desorption ionization mass spectroscopy gave further information. During the reaction, a small amount of di-HELICES, which were also partly condensed on the template, leading to TH_7 appeared as side-products. Fig. 6 shows the laser desorption ionization mass spectrum of the reaction mixture. In Table III, the experimentally determined masses are compared with the calculated masses.

The biphenyl chromatogram of the reaction mix-

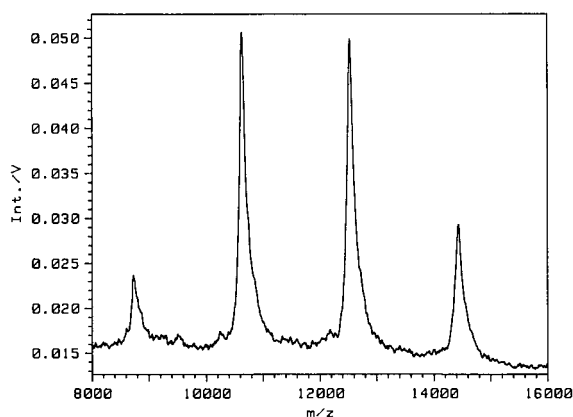


Fig. 6. Laser desorption/ionization mass spectrum (measured in positive-ion mode) of TH_x , the products from coupling HELIX (H) to the template (T). For mass assignments, see Table III.

ture (Fig. 7) shows that three different di-HELICES (H_2) appear. As a HELIX contains five ϵ -amino groups, the three peaks may be ascribed to the three possible isomers. As has been reported by Buettner and Houghten [7], amphiphilic helices are bound to the RP stationary phase by exposing their hydrophobic side to the matrix. As with the HELIX, the di-HELICES are also assumed to expose their hydrophobic sides to the matrix. Since the putative hydrophobic contact areas are different for the three di-HELIX isomers, they are eluted as three distinct peaks. Another by-product is TH_7 , a TASP molecule with an additional HELIX coupled to an ϵ -amino group of one of the six regular HELICES. The main peak contains TH_4 , TH_5 and TH_6 . Two details deserve closer examination: (1) H_2 elutes later than TH_x ; (2) although TH_4 , TH_5 and TH_6 elute

TABLE III

ASSIGNMENT OF MASS FOR THE PEPTIDES IN THE REACTION MIXTURE (SEE ALSO FIG. 6)

Peptide	Calculated molecular mass	m/z	δ
H	1919.6	1921.4	1.8
H_2	3821.2	3825.1	4.0
TH_4	8717.7	8729.9	12.2
TH_5	10619.2	10632.4	13.2
TH_6	12520.8	12532.0	11.2
TH_7	14422.4	14433.0	10.6

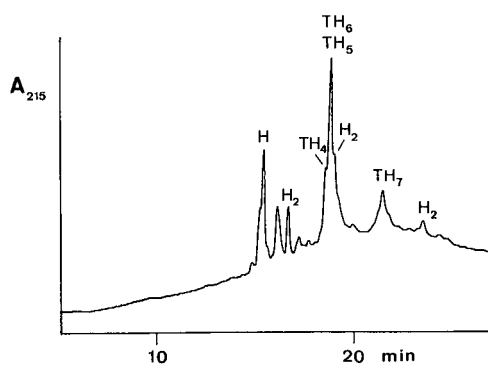


Fig. 7. Elution profile of crude product from a condensation fragment with incompletely protected HELIX. (H) HELIX; (H_2) di-HELIX; (TH_4 , TH_5) incomplete TASP molecules; (TH_6) TASP molecule; (TH_7) TASP with an additional HELIX. Column, Vydac biphenyl 5 μ m, 30 nm, 15 cm \times 4.6 mm I.D. Solvent A, 0.1% TFA; solvent B, 0.1% TFA in acetonitrile. Linear gradient from 10 to 90% B in 30 min.

at the same time, TH_7 the TASP molecule with an extra HELIX, is considerably more retained. From these characteristics it can be assumed that TH_4 , TH_5 and TH_6 bind in their folded form as parallel helix bundles with most of the hydrophobic side-chains exposed to the interior. In contrast, the surplus HELIX in TH_7 is not integrated in the parallel α -helix bundle and therefore seems to be able to expose its hydrophobic face to the matrix, leading to the stronger retention of TH_7 .

Pre-column denaturation of HELIX and TASP

Lin and Karger [11] distinguished between RP surface-unfolded, urea-unfolded and reduced-unfolded forms of proteins. Pre-column urea-unfolding was achieved by heating the protein in 8 M urea to 90°C for 2–5 min and cooling before injection. Similarly, the reaction mixture used here (dissolved in 95% TFA and containing H, H_2 , TH_3 , TH_4 , TH_5 , TH_6 and TH_7) was mixed with a nine-fold excess of 6 M GuHCl (v/v). No disruption of the structure could be observed after 15 min at room temperature prior to injection onto a biphenyl column. Therefore, the samples were stored for 10 min at 96°C. Fig. 8 shows the chromatograms of pure HELIX with and without 6 M GuHCl and heat treatment. It demonstrates that this harsh treatment has only a minor effect.

Pre-column denaturation of the reaction mixture

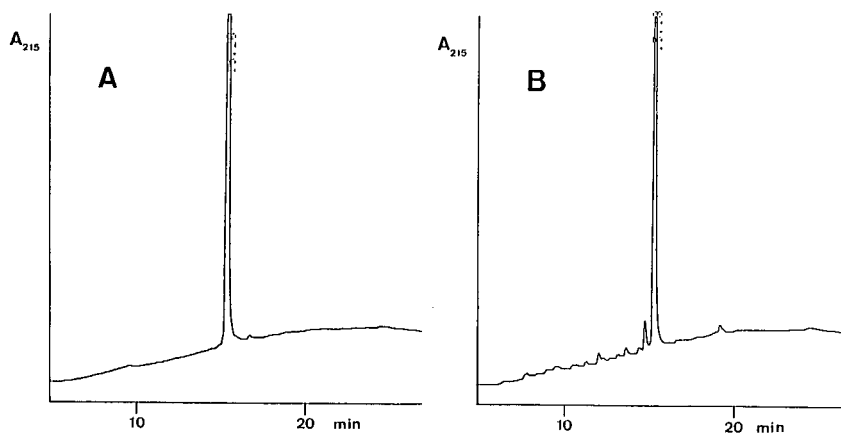


Fig. 8. Pre-column denaturation of HELIX with 6 M GuHCl and heat. (A) HELIX before, (B) HELIX after treatment. Column, Vydac biphenyl 5 μ m, 30 nm, 15 cm \times 4.6 mm I.D. Solvent A, 0.1% TFA; solvent B, 0.1% TFA in acetonitrile. Linear gradient from 10 to 90% B in 30 min.

shown in Fig. 7 indicates the breakdown of the tertiary structure followed by irreversible adsorption, whereas secondary structures of HELIX and the three H₂ isomers seem more resistant (Fig. 9). SDS is obviously not able to dissociate the tertiary struc-

ture, as can be seen in Fig. 10, which shows the chromatogram after treatment with 2% SDS and heat. This suggests that SDS renders the peptides more hydrophobic, but leaves the secondary and tertiary structures intact.

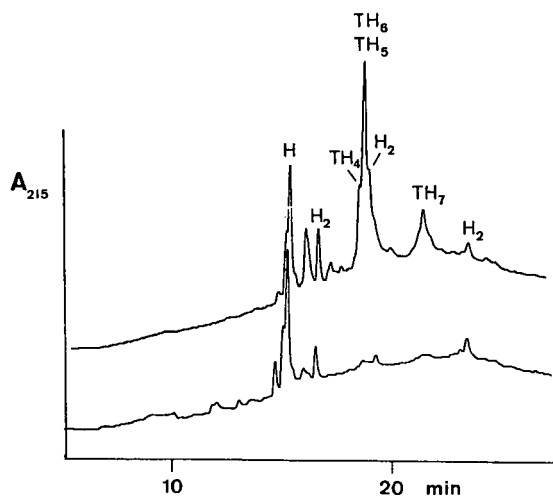


Fig. 9. Pre-column denaturation of the reaction mixture from Fig. 7 with GuHCl and heat. Upper profile, before denaturation. Column, Vydac biphenyl 5 μ m, 30 nm, 15 cm \times 4.6 mm I.D. Solvent A, 0.1% TFA; solvent B, 0.1% TFA in acetonitrile. Linear gradient from 10 to 90% B in 30 min.

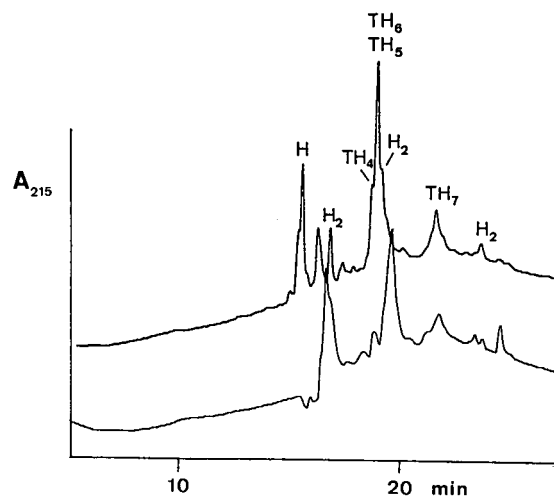


Fig. 10. Chromatogram of the reaction mixture from Fig. 7 after treatment with 2% SDS and heat. Upper profile, before treatment. Column, Vydac biphenyl 5 μ m, 30 nm, 15 cm \times 4.6 mm I.D. Solvent A, 0.1% TFA; solvent B, 0.1% TFA in acetonitrile. Linear gradient from 10 to 90% B in 30 min.

ACKNOWLEDGEMENTS

The authors thank Dr. Robert Carey for careful editing of this manuscript and H. Rink, Dr. H. H. Peter and Dr. W. Märki for their support.

REFERENCES

- 1 M. Mutter, *Trends Biochem. Sci.*, 13 (1988) 260.
- 2 G. E. Gerber and H. G. Khorana, *Methods Enzymol.*, 88 (1982) 56.
- 3 L. R. Gurley, D. A. Prentice, J. G. Valdez and W. D. Spall, *J. Chromatogr.*, 266 (1983) 609.
- 4 W. S. Hancock, D. R. Knighton and D. R. K. Harding, *Peptides 1984*, Almquist and Wiksell, Stockholm, 1984, p. 145.
- 5 T. R. A. Houghten and J. M. Ostresh, in T. Shiba and S. Sakakibara (Editors), *Peptide Chemistry 1987, Proceedings of the Japanese Peptide Symposium, Osaka, 1988*, Protein Research Foundation, Osaka, 1988, p. 101.
- 6 N. E. Zhou, C. T. Mant and R. S. Hodges, *Peptide Res.*, 3 (1990) 8.
- 7 K. Buettner and R. A. Houghten, in E. Giralt and D. Andreu (Editors), *Peptides 1990, Proceedings of the 21st European Peptide Symposium 1990, Platja d'Oro*, Escom, Leiden, 1990, p. 478.
- 8 M. T. W. Hearn, *Life Sci.*, 41 (1987) 987.
- 9 C. T. Mant, N. E. Zhou and R. S. Hodges, *J. Chromatogr.*, 476 (1989) 363.
- 10 R. H. Ingraham, S. Y. M. Lau, A. K. Taneja and R. S. Hodges, *J. Chromatogr.*, 327 (1985) 77.
- 11 S. Lin and B. L. Karger, *J. Chromatogr.*, 499 (1990) 89.
- 12 O. Börnsen, M. Schär, V. Steiner and E. Gassmann, *Biol. Mass Spectrom.*, 20 (1991) 471.
- 13 V. Steiner, K. Gubernator, O. Börnsen, M. Schär, H. Rink and M. Mutter, *Peptide Res.*, in press.
- 14 D. Guo, C. T. Mant, A. K. Taneja and R. S. Hodges, *J. Chromatogr.*, 359 (1986) 519.
- 15 R. A. Houghten and S. T. DeGraw, *J. Chromatogr.*, 386 (1987) 223.
- 16 S. J. M. Lau, A. K. Taneja and R. S. Hodges, *J. Chromatogr.*, 317 (1984) 129.
- 17 C. T. Mant, T. W. L. Burke, J. A. Black and R. S. Hodges, *J. Chromatogr.*, 458 (1988) 193.

High-performance affinity chromatography of NADP⁺ dehydrogenases from cell-free extracts using a nucleotide analogue as general ligand

J. Alhama, J. López-Barea and F. Toribio*

Departamento de Bioquímica y Biología Molecular, Facultad de Veterinaria, Universidad de Córdoba, Avda. Medina Azahara s/n., 14071 Córdoba (Spain)

(First received March 8th, 1991; revised manuscript received June 10th, 1991)

ABSTRACT

An epoxy-activated silica column (50 cm × 0.45 cm I.D.) was derivatized with 8-[(6-aminohexyl)amino]-2'-phosphoadenosine-5'-diphosphoribose; the bound ligand concentration was 11.4 μmol/g of dry silica, and the useful loading capacity was 2.3 mg of glutathione reductase. The new high-performance liquid chromatographic column specifically retained NADP⁺-dependent enzymes, which were quantitatively eluted specifically by NADP⁺ or, with better resolution, by potassium chloride. The new high-performance liquid chromatographic support was applied to the purification of glutathione reductase and glucose-6-phosphate dehydrogenase from cell-free extracts of baker's yeast, fish liver and rabbit hemolysates, with high recoveries and excellent purification factors.

INTRODUCTION

High-performance liquid affinity chromatography (HPLAC) combines the biospecificity of conventional affinity chromatography with the speed of operation, resolution and sensitive detection of high-performance liquid chromatography (HPLC) [1]. Adenine nucleotide derivatives have been used for many years as general ligands for conventional affinity chromatography [2,3], covalently attached to insoluble supports through either the N-6 [4] or the C-8 [5] adenine ring position, the hydroxyl groups of the ribose ring [6] or the phosphate groups [7]. Their ability to retain a certain enzyme depends on whether the geometrical orientations of the modified nucleotide properly fit the enzyme-binding site [8,9]. The type of immobilized adenine nucleotide also selects the kind of enzymes retained: ATP, ADP and AMP bind mainly kinases [10]; NAD⁺, NADP⁺, 2'-phosphoadenosine, 5'-diphosphoribose (ATPR) and 2',5'-ADP retain NAD(P)⁺-dependent dehydrogenases [11,12]; and 3',5'-ADP is specific for coenzyme A-related enzymes [13].

Epoxy-silica has been successfully used in the field of HPLAC [14–16] as a carrier for biological ligands, since its mechanical rigidity and porosity allows high pressures and flow-rates, resulting in a fast technique for purifying biologically active molecules. Epoxy groups on the support react in the pH range 3–7.5 with nucleophiles such as primary amine, sulfhydryl or hydroxyl. The presence of such groups in a wide range of biomolecules allows their binding to the epoxy-activated silica. Other alternative chemical modifications of silica-based supports, with reactive groups such as tresyl [17], isothiocyanate [18], or primary hydroxyl [19], have also been used to link covalently several ligands containing primary or secondary amino groups.

Alcohol dehydrogenase [17] and lactate dehydrogenase [20,21] have been purified using AMP and NAD⁺ bound to silica-based supports. Dyes structurally related to pyridine nucleotides have also been used for purification by HPLAC of several enzymes [2,22–25]. In this paper, we report the development of a new support with an NADP⁺ analogue, 8-[(6-aminohexyl)amino]-2'-phosphoadeno-

sine-5'-diphosphoribose (AHC8-ATPR), attached through the C-8 position of the adenine ring to epoxy-activated silica, as a specific group ligand for purification by HPLAC of several NADP⁺-dependent dehydrogenases. The new support shows very high specificity, excellent yields of the retained enzymes and short operation times, and has been used with several cell-free extracts, from which glutathione reductase and glucose-6-phosphate dehydrogenase have been highly purified.

EXPERIMENTAL

Chemicals

Bromine, Dowex 1-X8 resin, bovine serum albumin, ovalbumin, baker's yeast alcohol: NAD⁺ dehydrogenase (EC 1.1.1.1), glucose-6-phosphate dehydrogenase (EC 1.1.1.49), glutathione reductase (EC 1.6.4.2) and hexokinase (EC 2.7.1.1), *Thermotoga maritima* alcohol: NADP⁺ dehydrogenase (EC 1.1.1.2), rabbit muscle lactate dehydrogenase (EC 1.1.1.27) and pyruvate kinase (EC 2.7.1.40), pig heart isocitrate dehydrogenase (EC 1.1.1.42) and citrate synthase (EC 4.1.3.7), and NAD(P)⁺, NAD(P)H and 3-[N-morpholine]propane sulfonic acid (MOPS) were purchased from Sigma. Bacto peptone was from Difco. Salts for the mobile phases were from Merck. All other chemicals used were of the highest purity.

Equipment

HPLC was performed using a Beckman apparatus equipped with two 110B pumps, an Altex 210A injection valve, a 163 UV detector and a 406 analog interface module. Integration was performed by an AT computer with the System Gold software from Beckman. Affinity chromatography was carried out with Beckman Ultrafinity-EP (5.0 cm × 0.45 cm I.D.) columns, packed with epoxy-activated silica. An LKB 2112 Redirac collector was used to fractionate the column eluate for monitoring enzymatic activities. A Spherisorb amino-propyl silica column (5 μm, 25 cm × 0.4 cm I.D.) from Tracer Analytica was used for chromatographic control throughout the synthesis of the nucleotide analogue. Cell-free extracts were filtered through 0.45-μm filters before application to the HPLC affinity columns.

Centrifugations were carried out on J2-21 and L8-80M Beckman centrifuges. High-purity water

was obtained from a Milli-Q water purifier (Millipore). The eluting solvents were degassed under vacuum for 30 min in an ultrasonic bath and filtered through 0.2-μm membrane filters. Spectrophotometric measurements and enzyme kinetics were carried out in a Beckman DU-7 spectrophotometer. A Braun Labsonic apparatus was used for sonic disintegration of yeast cells, and an IKA Ultraturrax T-25 homogenizer for preparation of fish-liver extracts.

Enzyme assays

The enzymatic activities were assayed as previously published at the temperatures indicated: alcohol: NAD⁺ dehydrogenase [26] 25°C, alcohol: NADP⁺ dehydrogenase [27] 40°C, lactate dehydrogenase [28] 37°C, isocitrate dehydrogenase [29] 37°C, glucose-6-phosphate dehydrogenase [30] 25°C, glutathione reductase [12] 30°C, hexokinase [31] 25°C, pyruvate kinase [32] 37°C and citrate synthase [33] 37°C. One unit of activity is defined as the amount of enzyme catalyzing the transformation of 1 μmol of substrate into product per minute.

Cell-free extract preparations

Baker's yeast. Cells grown with 1% bacto peptone and 2% glucose as carbon source were harvested by centrifugation at 15 000 g for 10 min, washed with 250 mM MOPS buffer, pH 7.5, containing 1 mM EDTA and centrifuged at 48 400 g for 10 min. The pellet was resuspended with four volumes of buffer and sonicated four times for 15 s at 1-min intervals. Cellular debris was removed by centrifugation at 48 400 g for 10 min, and the supernatant was dialyzed overnight against extraction buffer. The cell-free extract contained 0.62 U/ml glutathione reductase (0.09 U/mg specific activity) and 0.42 U/ml glucose-6-phosphate dehydrogenase (0.06 U/mg specific activity).

Rabbit hemolysate. Cells from freshly drawn rabbit arterial blood were collected by centrifugation and lysed by osmotic shock with 5 mM MOPS buffer, pH 7.0, containing 1 mM EDTA (2 ml per ml of packed cells). Cellular debris was removed by centrifugation at 48 400 g for 10 min and the supernatant was again centrifuged at 184 000 g for 1.5 h; the hemolysate was dialyzed overnight against a suitable MOPS buffer (25–250 mM, pH 7.0–7.5). The extract contained 0.31 U/ml glutathione reduc-

tase (0.003 U/mg) and 0.61 U/ml glucose-6-phosphate dehydrogenase (0.005 U/mg).

Fish liver. Frozen *Mugil cephalus* liver was minced and ground in liquid nitrogen. The powder was extracted with a similar volume of 5 mM Tris-HCl buffer, pH 7.4, containing 250 mM sucrose and 10 mM reduced glutathione (GSH). The slurry was diluted three-fold with 1.15% (w/v) potassium chloride solution and centrifuged at 9000 g for 10 min. The supernatant was ultracentrifuged at 105 000 g for 1 h, and dialyzed overnight against an appropriate MOPS buffer (25–250 mM, pH 7.0–7.5). The glutathione reductase activity in this extract was 0.28 U/ml (0.052 U/mg) and that of glucose-6-phosphate dehydrogenase 0.96 U/ml (0.158 U/mg).

Protein determination. Protein concentrations were estimated by the bicinchoninic acid protein assay [34] using bovine serum albumin as standard.

Synthesis of the ligand

The synthesis of 8-[(6-aminohexyl)amino]-2'-phosphoadenosine-5'-diphosphoribose (AHC8-ATPR, Fig. 1) was carried out as a modification of the procedure described by López-Barea and Lee [12]: NADP⁺ (4 g, 3.945 mmol), was dissolved in 15

ml of 1 M sodium acetate buffer, pH 4.5. Liquid bromine (2.5 ml, 48.56 mmol) was then added dropwise to the solution with vigorous stirring; during this process the pH was maintained between 3.9 and 4.5 by adding 1 M sodium hydroxide. After 70 min at room temperature the unreacted bromine was extracted seven times, with 30 ml of carbon tetrachloride each time. To the aqueous phase which contained 8-bromo-NADP⁺ (C8-BrNADP⁺), 350 ml of cold acetone (−80°C) were added and stored overnight at −80°C. The yellow precipitate was washed with 60 ml of cold acetone and redissolved in 20 ml of water. Then, 1,6-diaminohexane (12.0 g, 103 mmol) in 5.0 ml of water was added to the C8-BrNADP⁺ solution and heated at 60°C for 3 h. The coupling of the spacer arm was monitored spectrophotometrically by following the shift in absorbance maximum from 267 nm (C8-BrNADP⁺, $\epsilon = 20.7 \text{ mM}^{-1} \text{ cm}^{-1}$) to 279 nm (AHC8-ATPR, $\epsilon = 18.0 \text{ mM}^{-1} \text{ cm}^{-1}$): the A_{279}/A_{267} ratio changed from 0.71 to 1.11 within 4.5 h of coupling. The reaction mixture was diluted to 2 l with HPLC-grade water and loaded at a flow-rate of 100 ml/h into a Dowex 1-X8 column (180-ml bed), previously equilibrated with 1 M ammonium carbonate and extensively washed with water. The elution was performed by a linear ammonium carbonate gradient (0–1.5 M). The fractions (15 ml) with an absorbance maximum at 279 nm were pooled and lyophilized. Ion-exchange HPLC was performed to follow the synthesis of the ligand (Fig. 1).

Coupling of the ligand to the epoxy silica column

Optimization of the coupling reaction was performed in a batchwise mode using the Beckman Ultrafinity-EP column capacity kit, which contains 100 mg of the same support as the prepacked column. For coupling to the column, the purified AHC8-ATPR (0.813 g) was dissolved in 10 ml of 0.85 M potassium phosphate buffer, pH 8.4, containing 0.3 M sodium hydrogencarbonate. The epoxy-silica prepacked column was attached to an HPLC pump primed with the same loading buffer; column flow was adjusted to 1 ml/min until liquid eluted from column end, then it was shifted to 0.2 ml/min and recycled overnight at 45°C. To remove ionically bound ligand, the column was washed with 1 M potassium chloride for 30 min at 1 ml/min. Hydrophobically bound ligand was removed

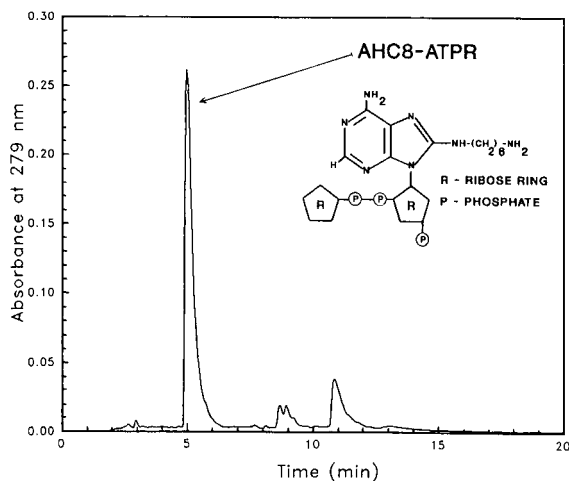


Fig. 1. Monitoring of AHC8-ATPR synthesis. Column, Spherisorb APS (25 × 0.4 cm I.D.); back-pressure, 135 bar; flow-rate, 1.0 ml/min; temperature, ambient; irrigant buffer, 0.04 M phosphate, pH 2.8; applied sample, 20 μ l of a 0.75 mg/ml solution of AHC8-ATPR lyophilized after Dowex 1-X8 chromatography dissolved in irrigant buffer. Elution was effected with a linear gradient of potassium chloride (0–0.8 M in irrigant buffer, pH 2.7) lasting 15 min after sample injection.

by washing the column with 20 mM potassium chloride under identical conditions. The unreacted epoxy groups were converted into the corresponding diol structures by a mild acid hydrolysis with 10 mM hydrochloric acid, pH 2.2, pumped at 0.5 ml/min for 2 h at 50°C. After washing with equilibration buffer the column was ready for use.

Ligand density was determined as follows: ligand-substituted epoxy silica (100 mg) was heated at 60°C for 30 min in 1 ml of 1 M sodium hydroxide. To the solubilized support 4 ml of 100 mM sodium phosphate buffer, pH 7.0, 1 ml of 1 M hydrochloric acid and distilled water were added to 10 ml final volume. A reference solution was prepared similarly with underivatized epoxy-silica. Ligand concentration was calculated from the molar absorptivity of the AHC8-ATPR at 279 nm.

The breakthrough capacity of the affinity column was determined as follows: a solution of glutathione reductase (0.182 mg/ml) in 100 mM MOPS buffer, pH 7.0, containing 1 mM EDTA was passed through the column at a flow-rate of 1 ml/min until the detector indicated an increasing baseline at 280 nm. At that point the enzyme was just beginning to break through, and if the loading process continued the curve would reach a maximum; the amount of enzyme retained up to this point represented the maximum dynamic capacity [35].

Chromatographic procedures

Ion-exchange high-performance liquid chromatography. The Spherisorb column was equilibrated with 40 mM potassium phosphate, pH 2.8 (buffer A), at a flow-rate of 1 ml/min. After sample injection (20 μ l), elution was carried out with a linear gradient of buffer B (buffer A + 0.8 M potassium chloride, pH 2.7) lasting 15 min. Detection was performed in each case at the maximum absorption wavelength.

Affinity chromatography. Unless otherwise stated the Ultrafinity column derivatized with AHC8-ATPR was equilibrated with loading buffer C (250 mM MOPS buffer, pH 7.5, containing 1 mM EDTA) at 1 ml/min. Samples of 500 μ l containing a mixture of nine commercial enzymes shown in Table III (0.1–0.2 mg of each enzyme per ml of buffer C) were injected into the column. The column was extensively washed with buffer C until the A_{280} returned to zero. The retained enzymes were eluted

either non-specifically by a linear potassium chloride gradient (0–1.25 M in buffer C) lasting 10 min, or specifically with a linear NADP⁺ gradient (0–1.5 mM in buffer C) lasting 15 min. Fractions of 400 μ l were collected and assayed for enzymatic activities. All chromatographic procedures were performed at room temperature.

RESULTS AND DISCUSSION

The nucleotide analogue AHC8-ATPR bound to Sepharose 4B has been used previously to purify mouse liver glutathione reductase [12]: the enzyme was purified 35-fold in 36 h with 86% overall yield. The use of agarose for preparative affinity chromatography is limited by its low flow-rates, diminished peak resolution and bacterial degradation, resulting in ligand leakage. The HPLC methodology would be essentially free of such problems and highly valuable for unstable proteins requiring rapid isolation procedures. For this reason we decided to use the same ligand to purify by HPLAC several NADP⁺-dependent enzymes.

The different steps throughout the synthesis of AHC8-ATPR were controlled by ion-exchange HPLC. Fig. 1 shows the chromatogram obtained with a sample of the Dowex I-X8 column eluate: the main peak, corresponding to AHC8-ATPR (retention time 5.0 min), represented at least 82% of the total peaks area.

The ligand concentration on the support was 11.4 μ mol/g of dry silica, corresponding to 16% of the initial epoxy groups of the underivatized silica, a value higher than the usual 10% previously described for epoxy-activated silica [20]. A standard measurement of the useful loading capacity of the columns is the 1% breakthrough capacity [35]: using glutathione reductase as the reference NADP⁺ dehydrogenase, this was determined to be 2.3 mg of enzyme for a 5.0 cm x 0.45 cm I.D. analytical column.

The suitability of AHC8-ATPR for affinity chromatography was studied by measuring the inhibition constants [36] of the soluble uncoupled ligand against different enzymes. Table I summarizes the results obtained: with the exception of isocitrate dehydrogenase, the NADP⁺-dependent enzymes showed low inhibition constant (K_i) values for AHC8-ATPR. The other enzymes tested, NAD⁺-,

TABLE I
INHIBITION CONSTANTS OF DIFFERENT ENZYMES
TOWARD AHC8-ATPR IN SOLUTION

Enzyme	Specificity	Inhibition constant ^a (K_i in μM)
Glucose-6-phosphate dehydrogenase	NADP ⁺	7
Glutathione reductase	NADP ⁺	58
Alcohol dehydrogenase	NADP ⁺	83
Isocitrate dehydrogenase	NADP ⁺	— ^b
Alcohol dehydrogenase	NAD ⁺	— ^b
Lactate dehydrogenase	NAD ⁺	639
Citrate synthase	Coenzyme A	409
Pyruvate kinase	ATP	2614
Hexokinase	ATP	7615

^a Determined by Dixon plot [36] using at least two substrate and six AHC8-ATPR concentrations.

^b No inhibition observed under our experimental conditions.

ATP- and coenzyme A-dependent enzymes, displayed much higher K_i values or were not inhibited. Thus, as expected, AHC8-ATPR could be selectively used for affinity chromatography of NADP⁺-dependent dehydrogenases.

The effect of different factors, namely ionic strength, type of buffer and pH, on the binding of different classes of enzymes was studied in a batch-wise mode using the Ultrafinity-EP column capacity kits. The kit was derivatized under the conditions stated above, although conveniently scaled down. The results obtained with four commercial enzymes are shown in Table II. MOPS buffer was the most effective for specific binding of NADP⁺-dependent dehydrogenases: ionic strengths higher than 100 mM quantitatively retained glutathione reductase and glucose-6-phosphate dehydrogenase, which were eluted by potassium chloride with recoveries close to 100%; the other two enzymes were not retained under identical conditions. The bind-

TABLE II
EFFECT OF TYPE OF BUFFER, IONIC STRENGTH AND pH ON THE BINDING OF DIFFERENT ENZYMES TO THE AFFINITY SUPPORT

	Phosphate buffer, pH 7.0				MOPS buffer, pH 7.0				100 mM MOPS buffer		
	15 ^a	30	60	150	20 ^a	50	100	150	6.5 ^b	7.0	7.5
<i>Glutathione reductase</i>											
Loaded ^c	8.9	9.2	8.9	8.9	11.9	10.6	10.5	11.5	11.0	10.5	10.0
Washed ^d	0.4	0.7	1.5	4.1	0.8	0.2	0.7	2.0	2.5	0.7	2.1
Eluted ^e	7.9	8.2	6.9	4.0	10.9	8.9	8.6	9.4	7.9	8.6	6.6
<i>Glucose-6-phosphate dehydrogenase</i>											
Loaded ^c	8.7	11.9	8.8	8.9	9.9	9.9	9.9	11.1	11.3	9.9	11.3
Washed ^d	1.0	3.2	5.3	6.3	0.8	0.0	0.2	0.1	0.7	0.2	0.1
Eluted ^e	5.9	5.9	2.6	0.4	8.3	9.1	9.9	11.6	12.0	10.0	10.6
<i>Lactate dehydrogenase</i>											
Loaded ^c	10.1	9.3	9.1	9.3	12.2	9.2	11.9	10.9	11.8	11.9	11.5
Washed ^d	0.5	3.6	7.5	7.2	0.2	1.9	9.3	8.5	0.4	9.3	8.3
Eluted ^e	3.6	2.1	0.2	0.0	7.9	3.2	0.1	0.1	6.1	0.0	0.0
<i>Pyruvate kinase</i>											
Loaded ^c	3.7	3.5	4.5	4.2	8.5	13.8	6.0	8.9	8.5	6.0	10.2
Washed ^d	1.4	1.4	2.6	3.7	0.5	4.3	5.1	5.5	0.1	5.1	9.8
Eluted ^e	0.9	1.5	0.6	0.2	8.6	10.8	1.1	0.4	6.9	1.2	0.7

^a Ionic strength of loading buffer expressed in mM.

^b pH value of loading buffer.

^c Total units present in 1.0 ml of loading buffer.

^d Total units washed with 6.0 ml of each loading buffer.

^e Total units eluted with 6.0 ml of 10 mM potassium phosphate buffer, pH 7.0, containing 1 mM EDTA and 0.5 M potassium chloride.

ing of the model enzymes was less effective and specific using phosphate buffer: while at low ionic strength glutathione reductase and glucose-6-phosphate dehydrogenase were mostly bound to the support, an increase in ionic strength significantly lowered their binding, especially that of the second enzyme. With both buffers, at low ionic strengths, the support indiscriminately retained all four enzymes tested, probably because of unspecific ionic interactions with the immobilized ligand, avoided at higher ionic strengths [20]. Even at low ionic strengths, the recoveries obtained using MOPS buffer were much higher than with phosphate buffer. The poorer results with phosphate buffer could be due to competition of free phosphate ions and the 2'-phosphate of C8-ATPR for the phosphate-binding site present in NADP⁺-dependent dehydrogenases [37]. The effect of different pH values on the binding of the model enzymes was studied with 100 mM MOPS buffer. At pH 7.0 and 7.5 the support almost completely retained both NADP⁺-dependent enzymes, while mostly excluding the other two enzymes. Consequently, MOPS buffer of at least 100 mM and pH 7.0–7.5 was selected for the standard operation with the new affinity support.

The chromatographic behavior of the new affinity column was studied using a mixture of nine different commercially available enzymes. Fig. 2A and B shows the chromatograms obtained with two mixtures of enzymes using non-specific potassium chloride elution and specific elution by NADP⁺, respectively, while Table III shows quantitative data about the total units loaded, washed and eluted. Glutathione reductase and glucose-6-phosphate dehydrogenase were fully retained and eluted out of the column with recoveries close to 100%. Of the NADP⁺-dependent alcohol dehydrogenase loaded, 60–75% was also retained and recovered from the column, as well as a small amount of pyruvate kinase, in agreement with the previous results shown in Table II. All other enzymes tested were completely unretained by the column under such conditions. The NADP⁺-dependent isocitrate dehydrogenase was not retained at all by the affinity column, in agreement with the lack of inhibition shown by AHC8-ATPR in Table I, and its lack of binding to a NADP⁺-type support in conventional affinity chromatography [11,13]. As shown in Fig. 2A, elution with potassium chloride yielded a better resolution

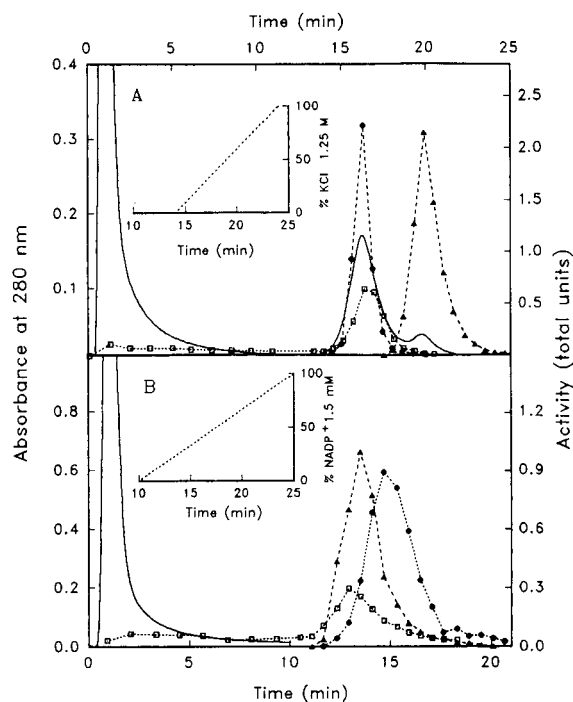


Fig. 2. HPLAC of mixtures of commercially available enzymes. Conditions were as described in the *Chromatographic procedures* section and sample compositions are shown in Table III. Temperature, ambient; back-pressure, 28 bar; flow-rate, 1.0 ml/min. (A) Unspecific elution by potassium chloride gradient: — = absorbance at 280 nm; ● = glutathione reductase activity; ▲ = glucose-6-phosphate dehydrogenase activity; □ = NADP⁺-dependent alcohol dehydrogenase (U × 4). (B) Specific elution by NADP⁺ gradient: — = absorbance at 280 nm; ● = glutathione reductase activity; ▲ = glucose-6-phosphate dehydrogenase activity (U × 0.5); □ = NADP⁺-dependent alcohol dehydrogenase (U × 2).

of glutathione reductase and glucose-6-phosphate dehydrogenase, while with NADP⁺ (Fig. 2B) glucose-6-phosphate dehydrogenase was eluted before glutathione reductase, in agreement with their K_i values for AHC8-ATPR (Table I). In addition, NADP⁺ elution did not improve the peak shapes, thus leading to significant overlapping.

The real test of excellent performance of an HPLAC support should be the efficient purification of enzymes from cell-free extracts. Thus after the results obtained with model mixtures of enzymes, we initiated the purification of glutathione reductase and glucose-6-phosphate dehydrogenase from three different cell-free extracts. The following

TABLE III
CHROMATOGRAPHIC BEHAVIOR OF THE AFFINITY COLUMN TOWARDS A MIXTURE OF MODEL ENZYMES

Enzyme	Unspecific elution			Specific elution		
	Loaded ^a	Washed ^b	Eluted ^c	Loaded ^a	Washed ^b	Eluted ^c
Hexokinase	2.6	2.3	0.0	4.5	4.0	0.0
Pyruvate kinase	3.4	2.8	0.1	3.4	2.7	0.0
Citrate synthase	3.5	3.5	0.0	3.3	3.5	0.0
Lactate dehydrogenase	7.5	7.8	0.0	6.4	6.7	0.0
Isocitrate hydrogenase	3.5	3.5	0.0	2.2	2.2	0.0
Alcohol: NAD ⁺ dehydrogenase	6.3	6.7	0.0	5.3	5.7	0.0
Alcohol: NADP ⁺ dehydrogenase	1.0	0.3	0.6	1.2	0.3	0.9
Glutathione reductase	5.0	0.0	4.7	4.3	0.0	4.4
Glucose-6-phosphate dehydrogenase	7.3	0.0	7.3	6.4	0.0	7.6

^a Total units of each enzyme contained in 500 μ l of a mixture injected into the column.

^b Non-retained enzymatic activities expressed as total units.

^c Activity of the enzymes retained by the column, expressed as total units.

chromatographic conditions were used: 2.0 ml of each cell-free extract were loaded into the column at a flow-rate of 1 ml/min; an extensive washing with the loading buffer was carried out until the A_{280} returned to a stable baseline; elution of the bound enzymes was carried out with a linear potassium chloride gradient (0–1.25 M) in loading buffer lasting 10 min. Fractions (0.4 ml) were collected and analyzed for enzymatic activities and protein concentrations.

Table IV summarizes the results obtained with several extracts under different conditions. In yeast cell-free extract, both enzymes were retained and recovered from the column with yields near to 100% and high purification factors. With fish liver extracts, glutathione reductase was not bound in 250 mM MOPS buffer, although glucose-6-phosphate dehydrogenase was partially retained and recovered with a 57-fold purification factor, probably because of the lower amount of proteins retained under such conditions. As previously shown in Table II, a lowered ionic strength improved the binding and recovery of both enzymes, although the purification factors decreased in parallel as more proteins were retained. With the rabbit hemolysate, glutathione reductase was not retained at 250 mM MOPS buffer, but it did bind at 25 mM loading buffer, with a 77% recovery and a 142-fold purification factor. On the other hand, glucose-6-phos-

phate dehydrogenase was retained under both conditions with similar recoveries and very high purification factors, 502- and 440-fold, respectively.

Fig. 3 shows the chromatogram obtained with the yeast cell-free extract: an excellent resolution was observed between both enzymes with the potassium chloride gradient, in close analogy with the reconstruction experiment of Fig. 2A. These results were obtained with an analytical column at a flow-rate of only 1 ml/min; nevertheless even under such limited conditions the chromatographic procedure was completed in less than 45 min, with quite good purification factors (Table IV).

Modified nucleotides have been employed to purify NAD⁺-dependent dehydrogenases using HPLAC [17,21]. Nilsson and Mosbach [17] reported an 80% recovery after chromatography of pure lactate and alcohol dehydrogenases using N⁶-(6-aminoethyl)-NAD⁺ coupled to tressyl-activated porous silica. Wikström and Larsson [21] purified lactate dehydrogenase from ox heart cell-free extract using an NAD⁺ analogue coupled to dextran-coated porous quartz fibres with a 90% recovery and a 35-fold purification factor. As far as we know, our work reports for the first time the purification of NADP⁺-dependent dehydrogenases by HPLAC, using an NADP⁺ analogue as specific group ligand, coupled through the C-8 position of the adenine ring to an epoxy-activated porous silica matrix.

TABLE IV

PURIFICATION OF GLUTATHIONE REDUCTASE AND GLUCOSE-6-PHOSPHATE DEHYDROGENASE FROM DIFFERENT CELL-FREE EXTRACTS^a

Cell-free extracts (loading buffer)	Glutathione reductase		Glucose-6-phosphate dehydrogenase	
	Recovery (%)	Purification (fold)	Recovery (%)	Purification (fold)
<i>Baker's yeast</i>				
MOPS 250 mM, pH 7.5	90	104	118	35
<i>Fish liver</i>				
MOPS 250 mM, pH 7.5	Unbound	Unbound	59	57
MOPS 50 mM, pH 7.5	62	28	63	22
MOPS 25 mM, pH 7.0	70	19	69	19
<i>Rabbit hemolysate</i>				
MOPS 250 mM, pH 7.5	Unbound	Unbound	66	502
MOPS 25 mM, pH 7.0	77	142	67	440

^a A sample of 2.0 ml of each cell-free extract was loaded into the column. The recovery is expressed as a percentage of the initial activity loaded. The purification is expressed as the ratio of specific activity of the peak fraction to specific activity of the cell-free extract.

The results summarized in Table IV and Fig. 3 show that AHC8-ATPR is an excellent specific group ligand for purification of NADP⁺-related enzymes by HPLAC in crude extracts from different sources. Three arguments validate such a statement:

(1) Experiments with model enzymes and those carried out with cell-free extracts show that the new affinity support is highly specific for NADP⁺-dehydrogenases.

(2) The recoveries of the retained enzymatic activities, at least 70%, are similar to those previously obtained in the purification of NADP⁺-dependent dehydrogenases by HPLAC [17,21–24].

(3) The specificity and resolving power of our support yield higher purification factors (19- to 502-fold) than those previously reported for NADP⁺-dependent enzymes [17,23–25].

Our results also significantly improve those obtained using the same ligand, AHC8-ATPR, in conventional affinity chromatography, with a 50-fold decrease in chromatographic run time.

In conclusion, we propose the new support, with AHC8-ATPR covalently attached to epoxy-activated porous silica, as a very convenient affinity matrix for separation of NADP⁺-dependent enzymes.

The chromatographic procedure described in this work can also be easily scaled up for laboratory semipreparative purposes, by using a commercially available prepacked column instead of an analytical one.

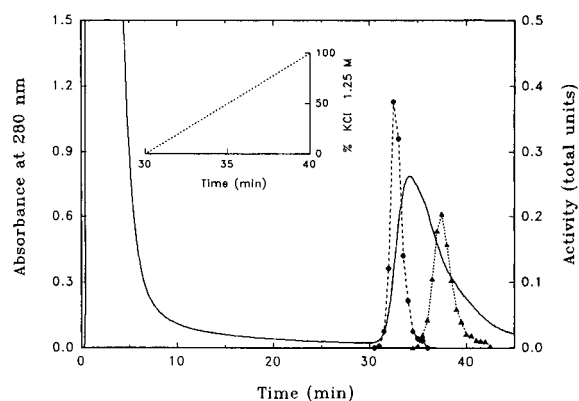


Fig. 3. HPLAC of a cell-free extract of baker's yeast. A 2-ml sample of baker's yeast cell-free extract was injected into the column at a flow-rate of 1 ml/min. Starting solvent: 250 mM MOPS buffer, pH 7.5, 1 mM EDTA. Elution: linear potassium chloride gradient (0–1.25 M) in starting solvent. — = Absorbance at 280 nm; ● = glutathione reductase activity; ▲ = glucose-6-phosphate dehydrogenase activity.

REFERENCES

- 1 S. Ohlson, L. Hansson, P. O. Larsson and K. Mosbach, *FEBS Lett.*, 93 (1978) 5.
- 2 C. R. Lowe, *An Introduction to Affinity Chromatography*, Elsevier Biomedical, Amsterdam, 1985, p. 430.
- 3 P. P. G. Dean, W. S. Johnson and F. A. Middle, *Affinity Chromatography: A Practical Approach*, IRL Press, Oxford, 1985, p. 136.
- 4 S. Barry and P. O'Carra, *FEBS Lett.*, 37 (1973) 134.
- 5 C. Y. Lee, D. A. Lappi, B. Wermuth, J. Everse and N. O. Kaplan, *Arch. Biochem. Biophys.*, 163 (1974) 561.
- 6 R. Lamed, Y. Levin and M. Wilchek, *Biochim. Biophys. Acta*, 304 (1973) 231.
- 7 M. J. Harvey, C. R. Lowe, D. B. Graven and D. G. Dean, *Eur. J. Biochem.*, 41 (1974) 335.
- 8 I. M. Chaiken, *J. Chromatogr.*, 376 (1986) 11.
- 9 P. Mohr and K. Pommerening, *Affinity Chromatography: Practical and Theoretical Aspects (Chromatographic Science Series, Vol. 33)*, Marcel Dekker, New York, 1986 p. 67.
- 10 C. Y. Lee, L. H. Lazarus, D. S. Kabakoff, P. J. Russel, M. Laver and N. O. Kaplan, *Arch. Biochem. Biophys.*, 178 (1977) 8.
- 11 C. Y. Lee and N. O. Kaplan, *Arch. Biochem. Biophys.*, 168 (1975) 665.
- 12 J. Lopez-Barea and C. Y. Lee, *Eur. J. Biochem.*, 98 (1979) 487.
- 13 P. Brodelius, P. O. Larsson and K. Mosbach, *Eur. J. Biochem.*, 47 (1974) 81.
- 14 Y. D. Clonis, in R. W. A. Oliver (Editor), *HPLC of Macromolecules: A Practical Approach*, IRL Press, Oxford, 1989 p. 157.
- 15 P. O. Larsson, *Methods Enzymol.*, 104 (1984) 212.
- 16 A. Fallon, R. F. G. Booth and L. D. Bell, in R. H. Burdon and P. H. Knippenberg (Editors), *Applications of HPLC in Biochemistry. Laboratory Techniques in Biochemistry and Molecular Biology*, Elsevier, Amsterdam, 1987 p. 106.
- 17 K. Nilsson and K. Mosbach, *Biochem. Biophys. Res. Commun.*, 102 (1981) 449.
- 18 F. B. Anspach, H. J. Wirth, K. K. Unger, P. Stanton and J. R. Davies, *Anal. Biochem.*, 179 (1989) 171.
- 19 K. Ernst-Cabrera and M. Wilchek, *Anal. Biochem.*, 159 (1986) 267.
- 20 P. O. Larsson, M. Glad, L. Hansson, M. O. Mansson, S. Ohlsson and K. Mosbach, *Adv. Chromatogr.*, 21 (1983) 41.
- 21 P. Wikström and P. O. Larsson, *J. Chromatogr.*, 388 (1987) 123.
- 22 B. Anspack, K. K. Unger, J. Davies and M. T. W. Hearn, *J. Chromatogr.*, 450 (1988) 195.
- 23 Y. D. Clonis, *J. Chromatogr.*, 407 (1987) 179.
- 24 D. A. P. Small, T. Atkinson and C. R. Lowe, *J. Chromatogr.*, 266 (1983) 151.
- 25 Y. D. Clonis, K. Jones and C. R. Lowe, *J. Chromatogr.*, 363 (1986) 31.
- 26 L. A. Decker (Editor), *Worthington Enzyme Manual*, Worthington Biochemical, Freehold, NJ, 1977 p. 9.
- 27 R. J. Lamed and J. G. Zeicus, *Biochem. J.*, 195 (1981) 183.
- 28 H. U. Bergmeyer, *Methods of Enzymatic Analysis*, Vol. 2, Academic Press, New York, 1974 p. 575.
- 29 H. U. Bergmeyer, *Methods of Enzymatic Analysis*, Vol. 2, Academic Press, New York, 1974 p. 624.
- 30 L. A. Decker, (Editor), *Worthington Enzyme Manual*, Worthington Biochemical, Freehold, NJ, 1977 p. 27.
- 31 W. Gruber, H. Höllering and H. U. Bergmeyer, *Enzymol. Biol. Clin.*, 7 (1966) 115.
- 32 H. U. Bergmeyer, *Methods of Enzymatic Analysis*, Vol. 1, Academic Press, New York, 1974 p. 510.
- 33 H. U. Bergmeyer, *Methods of Enzymatic Analysis*, Vol. 1, Academic Press, New York, 1974 p. 443.
- 34 P. K. Smith, R. I. Krohn, G. T. Hermanson, A. K. Mallia, F. H. Gartner, M. D. Provenzano, E. K. Fujimoto, N. M. Goeke, B. J. Olson and D. C. Klenk, *Anal. Biochem.*, 150 (1985) 76.
- 35 D. F. Hollis, S. Ralston, E. Suen, N. Cooke and R. G. Shorr, *J. Liq. Chromatogr.*, 10 (1987) 2349.
- 36 M. Dixon, *Biochem. J.*, 55 (1953) 170.
- 37 N. S. Scrutton, A. Berry and R. N. Perham, *Nature*, 343 (1990) 38.

Determination of metacycline and related substances by column liquid chromatography on poly(styrene–divinylbenzene)

Weng Naidong, K. Verresen, E. Roets and J. Hoogmartens*

Katholieke Universiteit Leuven, Laboratorium voor Farmaceutische Chemie, Instituut voor Farmaceutische Wetenschappen, Van Evenstraat 4, B-3000 Leuven (Belgium)

(First received April 2nd, 1991; revised manuscript received June 13th, 1991)

ABSTRACT

Isocratic column liquid chromatography on poly(styrene–divinylbenzene) copolymer allowed complete separation of metacycline, 4-epimetacycline, oxytetracycline, doxycycline and 6-epidoxycycline. 2-Acetyl-2-decarboxamidometacycline was eluted on the tail of metacycline. The mobile phase was 2-methyl-2-propanol–0.2 M phosphate buffer (pH 9.0)–0.01 M sodium ethylenediaminetetraacetate (pH 9.0)–water (2.5:10:10:77.5, m/v/v/v). The flow-rate was 1.0 ml/min and detection was performed at 254 nm. Official standards were compared and a number of commercial bulk samples and specialties were analysed. 2-Acetyl-2-decarboxamidometacycline, 6-epidoxycycline and doxycycline were the main impurities, while 4-epimetacycline and oxytetracycline were minor impurities.

INTRODUCTION

Metacycline (MTC) (Fig. 1) is a broad-spectrum, semi-synthetic antibiotic prepared from oxytetracycline (OTC) [1]. Although column liquid chromatography (LC) of several tetracyclines and their degradation products has been discussed extensively, the separation of metacycline and potential impurities which may be formed during synthesis has not been reported. Perhaps this is because information about the related substances of MTC has not been available. Microbiological assay is still the official

method for determining MTC in the United States Pharmacopeia XXII [2]. In a companion paper we report on the isolation of 2-acetyl-2-decarboxamidometacycline (ADMTC), 6-epidoxycycline (6-EDOX) and doxycycline (DOX) from commercial MTC [3]. Analogues of ADMTC, such as 2-acetyl-2-decarboxamidooxytetracycline (ADOTC) or 2-acetyl-2-decarboxamidotetracycline (ADTC), only possess about 10% of the activity of the corresponding tetracycline [4,5]. DOX is an active antibiotic while 6-EDOX has only little activity [6,7].

In this paper, an isocratic method is described, using poly(styrene–divinylbenzene) (PSDVB) copolymer as the stationary phase. It enables the complete separation of 4-epimetacycline (EMTC), OTC, MTC, 6-EDOX and DOX. ADMTC is eluted on the tail of MTC. The method is based upon LC methods previously elaborated in this laboratory for the analysis of DOX [8–10], TC [11,12], OTC [13,14] and demeclocycline (DMCTC) [15]. The method has been used to compare official standards and to analyse a number of commercial samples.

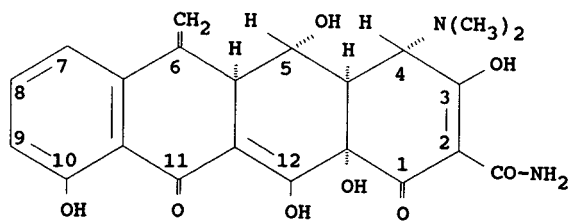


Fig. 1. Structure of metacycline.

EXPERIMENTAL

Reference substances and samples

The United States Pharmacopeia Reference Standard (U.S.P. - RS) Lot F (930 $\mu\text{g}/\text{mg}$) and Lot G, The European Pharmacopoeia Chemical Reference Substance (Ph. Eur. - CRS), which is not used for quantitative work, and the W.H.O. Second International Standard (W.H.O.-IS) were compared. House standards of MTC \cdot HCl (95.3%, m/m) and DOX \cdot HCl (93.1%, m/m) were available in the laboratory. 6-EDOX \cdot HCl (96.5%, m/m) was obtained from the European Pharmacopoeia (Strasbourg, France). The content of DOX \cdot HCl and 6-EDOX \cdot HCl in the last two reference substances has been reported previously [8,10]. A reference sample of OTC (99.0%, m/m) was obtained from Janssen Chimica (Beerse, Belgium). Percentages are expressed as the hydrochloride salt. A small amount of EMTC \cdot HCl was also prepared but its purity was not determined exactly since it is only a minor impurity of MTC. This sample was not used for quantitative work.

Bulk samples of MTC \cdot HCl were obtained from different plants of one manufacturer. Capsules produced by the same manufacturer were obtained from the Belgium market.

Solvents and reagents

2-Methyl-2-propanol was from Janssen Chimica and was distilled before use. Other reagents were of *pro analysi* quality (Merck, Darmstadt, Germany). Water was freshly distilled twice from a glass apparatus.

LC equipment and operating conditions

The LC apparatus consisted of an L-6200 pump (Merck-Hitachi, Darmstadt, Germany), a Marathon autosampler equipped with a 20- μl loop (Spark Holland, Emmen, Netherlands), a Waters Model 440 detector set at 254 nm (Waters Assoc., Milford, MA, USA) and a Model 3393 A integrator (Hewlett-Packard, Avondale, PA, USA). The PSDVB copolymers PLRP-S, 8 μm , 100 \AA (Polymer Labs, Church Stretton, UK) and RoGel, 7-9 μm (RSL - BioRad, Eke, Belgium) were packed in 250 mm \times 4.6 mm I.D. columns following a previously described method [16]. The column was maintained at 60°C in an oven. The flow-rate was 1.0

ml/min. The back-pressure was between 45 and 70 bar, depending on the brand of packing material. For some experiments, a Waters 990 photodiode array detector was used. The mobile phases finally used contained 2% (m/v) and 2.5% (m/v) 2-methyl-2-propanol as the organic modifier for PLRP-S and RoGel, respectively. The required amounts were weighed and rinsed into a volumetric flask. All mobile phases contained 10% (v/v) 0.2 M potassium hydrogenphosphate buffer (pH 9.0) and 10% (v/v) 0.01 M sodium ethylenediaminetetraacetate (EDTA). During preparation of the latter solution, the pH was adjusted to 9.0 with sodium hydroxide solution. The volume was made up with water. The mobile phase was degassed by sonication.

Sample preparation and stability

About 25.0 mg of bulk samples were precisely weighed, dissolved in 0.01 M hydrochloric acid and diluted to 50.0 ml with the same solvent. For capsules, the sample was weighed to obtain the equivalent of about 25.0 mg of MTC \cdot HCl and diluted to 50.0 ml with 0.01 M hydrochloric acid. The mixture was sonicated for 5 min at room temperature and then centrifuged at 2500 g for 5 min. The supernatant liquid was filtered through a membrane filter with 1.5- μm pores. The solutions were stable for at least 2 days at 6°C.

RESULTS AND DISCUSSION

Development of the chromatographic method

Experience obtained with previous LC analysis [8-16] on PSDVB stationary phases was used for the present studies. In preliminary experiments, it was observed that tetrabutylammonium (TBA) hydrogensulphate, used in the mobile phases for analysis of DOX, TC, OTC and DMCTC, had to be omitted in the mobile phase for analysis of MTC, otherwise poor separation of ADMTC and 6-EDOX was obtained. In the former methods, TBA was needed to obtain satisfactory separation of the corresponding 4-epimer or 6-epimer (for DOX).

As for the other tetracyclines, 2-methyl-2-propanol was chosen as the organic modifier. The influence of the mobile phase pH and the amount of organic modifier on the separation is shown in Fig. 2. At pH 7.0, ADMTC is eluted after 6-EDOX, while at higher pH this order is reversed. At pH 9.0, not only

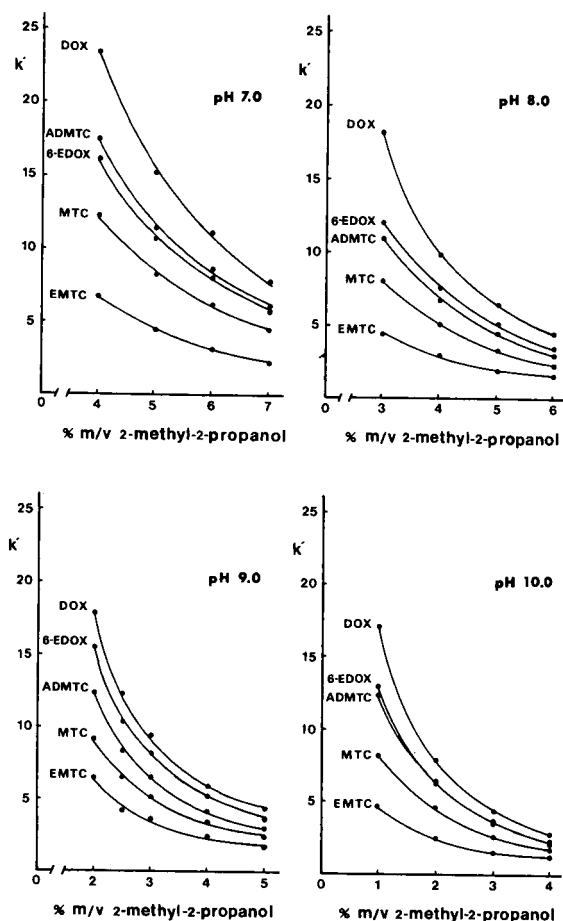


Fig. 2. Influence of the concentration of the organic modifier and the pH of the mobile phase on the separation of metacycline and related substances. Column: RoGel. Mobile phase: 2-methyl-2-propanol (x g)–0.2 M phosphate buffer of the pH indicated (10.0 ml)–0.01 M EDTA (10.0 ml), the pH of which was brought to the pH indicated with a solution of sodium hydroxide–water (up to 100.0 ml). See Experimental section for other conditions, EMTC = 4-epimetacycline; MTC = metacycline; ADMTC = 2-acetyl-2-decarboxamidometacycline; 6-EDOX = 6-epidoxycycline; DOX = doxycycline.

was the selectivity better than that at pH 8.0, but also the symmetry improved and the plate number increased. Detailed results for OTC were not added since preliminary tests revealed that OTC was always eluted well before EMTC. The influence of the phosphate buffer concentration was also investigated. Retention increased with increasing concentration. The separation of ADMTC and 6-EDOX decreased when more than 15% (v/v) 0.2 M phos-

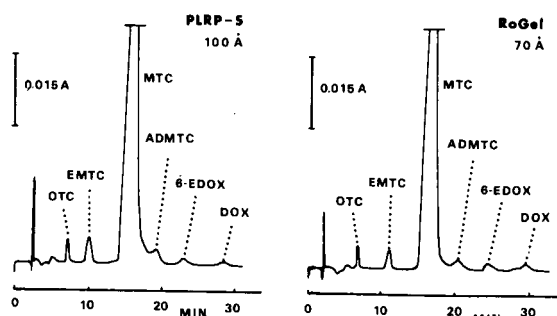


Fig. 3. Typical chromatogram of metacycline hydrochloride spiked with OTC and EMTC. Mobile phase: 2-methyl-2-propanol (x g per 100 ml)–0.2 M phosphate buffer pH 9.0 (10.0 ml)–0.01 M EDTA pH 9.0 (10.0 ml)–water (up to 100.0 ml). PLRP-S, 100 Å (8 μ m): $x = 2.0$; RoGel, 70 Å (7–9 μ m): $x = 2.5$. Amount injected: 10 μ g. Flow-rate: 1.0 ml/min. Detection: UV at 254 nm. Temperature: 60°C. Content (% m/m): OTC, 0.9; EMTC, 0.8; ADMTC, 0.4; 6-EDOX, 0.5; DOX, 0.2.

phate buffer was used. In order to have sufficient buffer capacity, a content of 10% (v/v) was chosen. The presence of EDTA in the mobile phase is necessary, otherwise the separation of MTC and ADMTC rapidly deteriorates. A concentration of 10% (v/v) 0.01 M EDTA was used throughout.

A column temperature of 60°C was maintained throughout the study. This temperature was also found to be suitable for the analysis of other tetracyclines [8–16]. The stability of MTC during analysis was checked by repeated analysis of MTC · HCl house standard at 50 or 60°C. The areas of the MTC peak were not found to differ significantly. The good repeatability of the method (see below) was also an indication of MTC stability. Peak homogeneity was determined by on-line photodiode array detection.

Fig. 3 shows chromatograms obtained on PLRP-S, 100 Å and RoGel. The physical properties of the packing materials and chromatographic characteristics are indicated in Table I. All further analyses were performed on a RoGel column.

Calibration curves, repeatability and limits of quantitation

Calibration curves were constructed with the house standards MTC · HCl and DOX · HCl and with the reference substance 6-EDOX · HCl. The following relationships were found, where y = peak area, x = mass (μ g), corrected for its content of

TABLE I
CHROMATOGRAPHIC CHARACTERISTICS OF THE
STATIONARY PHASES

See Fig. 2 for chromatographic conditions.

	Column	
	PLRP-S, 8 μm , 100 \AA	RoGel 7–9 μm , 70 \AA
Amount (% m/v) of 2-methyl-2-propanol in mobile phase	2.0	2.5
Plate number per per column (MTC)	2340	2950
Peak symmetry (MTC), $b_{0.05}/2a^a$	1.09	1.03
<i>Resolution</i>		
OTC-EMTC	4.6	5.6
EMTC-MTC	5.4	5.1
MTC-ADMTC	2.5	2.8
ADMTC-6-EDOX	2.1	2.3
6-EDOX-DOX	2.0	1.9
<i>Capacity factor (k')</i>		
OTC	2.20	2.21
EMTC	3.39	4.07
MTC	5.70	6.50
ADMTC	7.30	8.35
6-EDOX	8.89	10.27
DOX	11.00	12.34

^a $b_{0.05}$ = Width of the peak at one-twentieth of the peak height.
 a = Distance between the perpendicular dropped from the peak maximum and the leading edge of the peak at one-twentieth of the peak height.

hydrochloride salt injected, r = correlation coefficient, $S_{y,x}$ = standard error of estimate, R = range of injected mass examined, n = number of analyses. MTC · HCl: $y = 96913 + 194907x$; $r = 0.9979$; $S_{y,x} = 21566$; $R = 8\text{--}12 \mu\text{g}$; $n = 12$. DOX · HCl: $y = 1767 + 162902x$; $r = 0.9997$; $S_{y,x} = 680$; $R = 0.05\text{--}0.4 \mu\text{g}$; $n = 15$. 6-EDOX · HCl: $y = -500 + 168447x$; $r = 0.9970$; $S_{y,x} = 2053$; $R = 0.05\text{--}0.4 \mu\text{g}$; $n = 15$. MTC · HCl: $y = 625 + 197631x$; $r = 0.9999$; $S_{y,x} = 356$; $R = 0.05\text{--}0.4 \mu\text{g}$; $n = 15$. The calibration curves were not used to calculate the content of the samples but only to check the linearity. The calculations for the content of the main component were based on the results obtained for the MTC · HCl house standard in each series of analyses. The limits of quantitation (LOQ) were 0.02% (m/m) for OTC and EMTC and 0.1% (m/m)

for ADMTC, 6-EDOX and DOX. The house standard was analysed 54 times over a period of 7 days. The relative standard deviation (R.S.D.) for MTC was 1.0%.

Comparison of metacycline hydrochloride standards

The MTC · HCl house standard was titrated with perchloric acid in non-aqueous conditions. A total of five titrations gave a mean of 95.5% (m/m) MTC · HCl (R.S.D. = 0.5%). A total of three Karl Fischer titrations gave a mean of 0.9% (m/m) water (R.S.D. = 5.6%). The standard contained also 2.8% (m/m) acetone ($n = 5$, R.S.D. = 1.1%) and 0.7% (m/m) *n*-butanol ($n = 4$, R.S.D. = 8%), as determined by gas chromatography (GC). The total content of MTC · HCl house standard was therefore accepted to be 95.5% (m/m), and this figure was corrected by means of chromatography. The total concentration of chromatographic impurities corresponded to 0.2% (m/m). Therefore, the MTC · HCl house standard was assigned a purity of 95.3% (m/m).

Using the MTC · HCl house standard, the content of the official standards was compared by LC. Table II summarizes the results obtained. The MTC · HCl content was determined by comparison with the chromatograms for the MTC · HCl house standard, obtained on the same day. Reference solutions of MTC · HCl, 6-EDOX · HCl and DOX · HCl prepared at a concentration of 0.005 mg/ml, corresponding to 0.5% (m/m), were used to determine the content of ADMTC · HCl, 6-EDOX · HCl and DOX · HCl, respectively. Since an ADMTC · HCl reference sample was not available, it was expressed in terms of MTC · HCl. The R.S.D. values given in parentheses are within acceptable limits for all the determinations. The declared content for the U.S.P. Lot F of 930 $\mu\text{g}/\text{mg}$ activity, determined by microbiological assay, is very close to the content of 92.0% (m/m), expressed as MTC base, and determined by the LC method.

Analysis of commercial samples

The commercial samples were analysed as described above for the standards. Table III shows results for the bulk samples of MTC · HCl. The repeatability of the assay is good. The content of OTC · HCl and EMTC · HCl is lower than the LOQ for all the samples. Since MTC carries a hydroxyl

TABLE II

COMPOSITION OF METACYCLINE HYDROCHLORIDE STANDARDS

Values (% , m/m) are expressed in terms of the hydrochloride salt; *n* = number of analyses; R.S.D. values (%) are given in parentheses; ND = not determined owing to the limited amount of sample.

Chromatography	House standard ^a	Ph. Eur.-CRS	U.S.P.-RS, Lot F, 930 µg/mg	U.S.P.-RS, Lot G	W.H.O.-IS
Number of solutions	54	4	4	3	2
Number of analyses	54	8	6	6	4
Number of days	7	2	2	2	1
OTC	<0.02	<0.02	<0.02	<0.02	<0.02
EMTC ^b	<0.02	<0.02	<0.02	<0.02	<0.02
ADMTC ^b	<0.1	0.5 (9)	0.4 (3)	<0.1	0.5 (3)
DOX	0.1 (28)	0.2 (18)	<0.1	<0.1	<0.1
6-EDOX	0.1 (26)	0.2 (9)	<0.1	<0.1	<0.1
MTC	95.3 (1.0)	97.7 (0.9)	99.3 (0.9)	99.9 (0.9)	99.2 (0.9)
Subtotal	95.5	98.6	99.7	99.9	99.7
Titration	95.5	ND	ND	ND	ND
<i>n</i> (R.S.D., %)	5 (0.5)				
Water determined	0.9	ND	ND	ND	ND
<i>n</i> (R.S.D., %)	3 (5.6)				
Water declared		0.9	0.6	0.2	0.5
		Ref. 17	Ref. 18	Ref. 18	Ref. 19
Total	99.9	99.5	100.3	100.1	100.2

^a This sample also contains 2.8% (m/m) acetone (*n* = 5, R.S.D. = 1%) and 0.7% (m/m) *n*-butanol (*n* = 4, R.S.D. = 8%).

^b Expressed in terms of MTC · HCl.

group at C-5 it is, like OTC and DOX, more stable to epimerization in C-4. This is probably because of hydrogen bonding of the C-5 hydroxyl with the C-4 dimethylamino group [20]. The absence of a hydroxyl at C-6 excludes the possibility of acid degradation to the corresponding anhydro derivative

[21]. The ADMTC · HCl or 6-EDOX · HCl contents are always lower than 1% (m/m); the DOX · HCl content is always lower than 0.5% (m/m). The water content for all the bulk samples is well within the U.S.P. limit of 2% (m/m) [2].

Table IV gives the results obtained for capsules.

TABLE III

COMPOSITION OF BULK SAMPLES OF METACYCLINE HYDROCHLORIDE

Values (% , m/m) are expressed in terms of the hydrochloride; four independent chromatographic analyses and four Karl Fischer titrations were performed for each sample within one day; R.S.D. values (%) are given in parentheses.

Sample	OTC	EMTC ^a	MTC	ADMTC ^a	6-EDOX	DOX	Water content	Total
31256701	<0.02	<0.02	98.2 (0.3)	0.8 (5)	0.3 (4)	0.1 (10)	0.6 (4)	100.0
088-0672	<0.02	<0.02	98.8 (0.9)	0.3 (8)	0.3 (6)	0.1 (5)	0.6 (7)	100.1
21256707	<0.02	<0.02	97.5 (0.5)	0.5 (4)	0.6 (3)	0.2 (21)	0.6 (5)	99.4
836-56007	<0.02	<0.02	97.8 (0.9)	0.3 (8)	0.4 (7)	0.2 (3)	0.6 (7)	99.3
21256705	<0.02	<0.02	99.2 (0.6)	0.4 (2)	0.5 (2)	0.2 (5)	0.6 (9)	100.9
21256708	<0.02	<0.02	97.1 (1.0)	0.6 (1)	0.4 (5)	0.3 (5)	0.6 (5)	99.0
31256702	<0.02	<0.02	98.4 (0.7)	0.5 (1)	0.2 (8)	0.2 (4)	0.5 (11)	99.8
51256004	<0.02	<0.02	98.4 (0.7)	0.4 (2)	0.4 (2)	0.2 (31)	0.2 (20)	99.6

^a Expressed in terms of MTC · HCl.

TABLE IV

COMPOSITION OF CAPSULES

Values (% m/m) are expressed in terms of the hydrochloride salt as claimed on the label; four independent analyses were performed for each sample within one day; R.S.D. values (%) are given in parentheses.

Sample	Sample age in months	OTC	EMTC ^a	MTC	ADMTc ^a	6-EDOX	DOX
A	60	<0.02	0.05 (12)	97.8 (1.2)	0.2 (2)	1.1 (1)	0.4 (11)
B	60	<0.02	0.05 (23)	99.7 (0.8)	0.2 (3)	1.1 (0.5)	0.4 (15)
C	60	<0.02	0.05 (30)	100.1 (1.4)	0.1 (5)	0.8 (1)	0.2 (19)

^a Expressed in terms of MTC · HCl.

MTC · HCl in capsules is quite stable. Only trace amounts of EMTC · HCl (0.05%, m/m) were measured for all the capsules. The contents of DOX and 6-EDOX seem to be somewhat higher than those in bulk samples. However, these impurities, which are obtained by reduction of the methylene group, are formed during the semi-synthesis rather than upon storage.

CONCLUSION

The results show that the described LC method is suitable for the determination of MTC in bulk samples and in preparations. An important advantage of the method is its applicability to the different polymer stationary phases available on the market. This is not often obtained with silica-based reversed-phase materials, for which it is known that important differences in selectivity can exist between brands.

ACKNOWLEDGEMENTS

The National Fund for Scientific Research (Belgium) is acknowledged for financial support. The authors thank A. Decoux for skillful secretarial assistance. The gift of samples by Dr. Melamed of Pfizer France is gratefully acknowledged.

REFERENCES

- 1 L. A. Mitscher, *The Chemistry of the Tetracycline Antibiotics*, Marcel Dekker, New York, 1978.
- 2 *The United States Pharmacopeia XXII*, United States Pharmacopeial Convention, Rockville, MD, 1990.
- 3 W. Naidong, K. Verresen, R. Busson, E. Roets and J. Hoogmartens, *J. Chromatogr.*, 586 (1991) 67.
- 4 F. A. Hochstein, M. Schach von Wittenau, F. W. Tanner, Jr. and K. Murai, *J. Am. Chem. Soc.*, 82 (1960) 5934.
- 5 M. W. Miller and F. A. Hochstein, *J. Org. Chem.*, 27 (1962) 2525.
- 6 M. Schach von Wittenau, J. J. Beereboom, R. K. Blackwood and C. R. Stephens, *J. Am. Chem. Soc.*, 84 (1962) 2645.
- 7 C. R. Stephens, J. J. Beereboom, H. H. Rennhard, P. N. Gordon, K. Murai, R. K. Blackwood and M. Schach von Wittenau, *J. Am. Chem. Soc.*, 85 (1963) 2643.
- 8 K. Dihuidi, M. J. Kucharski, E. Roets, J. Hoogmartens and H. Vanderhaeghe, *J. Chromatogr.*, 325 (1985) 413.
- 9 J. Hoogmartens, R. Melamed, J. Miller, C. van der Vlies and H. Vanderhaeghe, *Pharmeuropa*, 1 (1988) 39.
- 10 J. Hoogmartens, N. H. Khan, H. Vanderhaeghe, A. L. van der Leeden, M. Oosterbaan, G. L. Veld-Tulp, W. Plugge, C. van der Vlies, D. Mialanne, R. Melamed and J. H. McB. Miller, *J. Pharm. Biomed. Anal.*, 7 (1989) 601.
- 11 K. Wolfs, E. Roets, J. Hoogmartens and H. Vanderhaeghe, *J. Chromatogr.*, 358 (1986) 444.
- 12 N. H. Khan, P. Wera, E. Roets and J. Hoogmartens, *J. Liq. Chromatogr.*, 13 (1990) 1351.
- 13 N. H. Khan, E. Roets, J. Hoogmartens and H. Vanderhaeghe, *J. Chromatogr.*, 405 (1987) 229.
- 14 J. Hoogmartens, Weng Naidong, N. H. Khan, A. Malley, U. Hearty, R. Melamed, J. P. Gousset, P. Creed, C. Wooliam, J. H. McB. Miller, J. Fuchs and H. Vanderhaeghe, *Pharmeuropa*, 2 (1990) 77.
- 15 Weng Naidong, E. Roets and J. Hoogmartens, *J. Pharm. Biomed. Anal.*, 7 (1989) 1691.
- 16 Weng Naidong, E. Roets and J. Hoogmartens, *Chromatographia*, 30 (1990) 105.
- 17 *European Pharmacopoeia*, Document PA/PH/SG (84) 46.
- 18 W. W. Wright, *United States Pharmacopeia*, Rockville, MD, personal communication.
- 19 J. W. Lightbown, P. De Rossi and P. Isaacson, *Bull. W.H.O.*, 47 (1972) 343.
- 20 D. A. Hussar, P. J. Niebergall, E. T. Sugita and J. T. Doluisio, *J. Pharm. Pharmacol.*, 20 (1968) 539.
- 21 J. R. D. McCormick, E. R. Jensen, P. A. Miller and A. P. Doerschuk, *J. Am. Chem. Soc.*, 82 (1960) 3381.

Isolation of doxycycline, 6-epidoxycycline and 2-acetyl-2-decarboxamidometacycline from commercial metacycline by preparative column liquid chromatography on silica gel

Weng Naidong, K. Verresen, R. Busson, E. Roets and J. Hoogmartens*

Katholieke Universiteit Leuven, Laboratorium voor Farmaceutische Chemie, Instituut voor Farmaceutische Wetenschappen, Van Evenstraat 4, B-3000 Leuven (Belgium)

(First received April 2nd, 1991; revised manuscript received June 13th, 1991)

ABSTRACT

Isolation of doxycycline, 6-epidoxycycline and 2-acetyl-2-decarboxamidometacycline from commercial metacycline was achieved by preparative column liquid chromatography on silica gel, previously impregnated with edetate (EDTA). Careful control of the pH of EDTA allowed fine tuning of the separation. The mobile phases were composed of dichloromethane, methanol and 0.1 mM EDTA at pH 9.0 or 6.0. Structures were confirmed with nuclear magnetic resonance spectroscopy. The presence of doxycycline and its 6-epimer in commercial metacycline has not previously been described. The presence of the 2-acetyl derivative was not surprising since analogous 2-acetyl derivatives have been identified in other tetracyclines.

INTRODUCTION

In the companion paper we reported on a column liquid chromatographic (LC) method for the assay and purity control of the tetracycline antibiotic metacycline hydrochloride (MTC · HCl) [1]. Using this analytical method, three substances of unknown identity (UNK1, UNK2 and UNK3) were separated. In commercial MTC · HCl samples, UNK1 and UNK3 were each found to be present up to about 1% (m/m) and UNK2 up to about 0.5% (m/m), all expressed as MTC · HCl. On the other hand, oxytetracycline (OTC), the starting material for the semi-synthesis of MTC and 4-epimetacycline (EMTC), a potential degradation product of MTC, were almost absent in commercial MTC samples. UNK1, UNK2 and UNK3 were isolated by LC on silica gel buffered with edetate (EDTA) of definite pH, and identified as 2-acetyl-2-decarboxamidometacycline (ADMTC), doxycycline (DOX) and 6-epidoxycycline (6-EDOX). The structures of

MTC and its related substances are shown in Fig. 1. DOX and 6-EDOX are obtained from MTC by reduction. This is also the pathway for the semi-synthesis of the clinically used DOX. Thus, these impurities could be formed by accidental reduction during the preparation of MTC. ADMTC is formed from the corresponding 2-acetyl-2-decarboxamidooxytetracycline (ADOTC), which is present in the starting material as an impurity.

EXPERIMENTAL

Reagents and solvents

Methanol (Belgolabo, Overijse, Belgium) was distilled from a glass apparatus. Dichloromethane (Janssen Chimica, Beerse, Belgium) was distilled over diphosphorus pentoxide to remove the alcohol added as a stabilizer. Water was twice distilled from a glass apparatus. Disodium EDTA was of *pro analysi* quality (Baker Chemicals, Deventer, Netherlands).

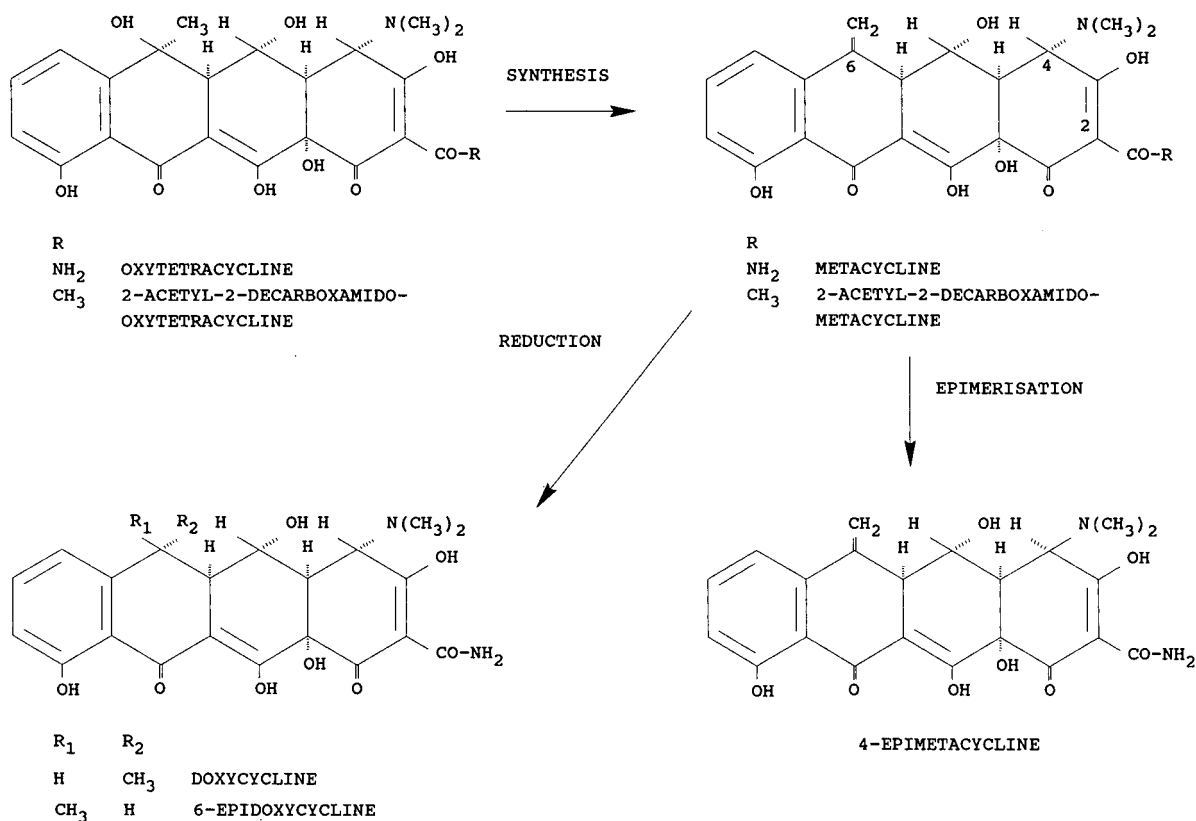


Fig. 1. Structures of metacycline and its related substances.

Commercial MTC · HCl (Pfizer, France) containing 0.5% UNK1, 0.3% UNK2 and 0.7% UNK3 as determined by the analytical LC method, was used for preparative isolation. Reference DOX · HCl and 6-EDOX · HCl were obtained from the European Pharmacopoeia (Strasbourg, France). Reference OTC was obtained from Janssen Chimica. EMTC was prepared from MTC by storing a solution of MTC at pH 3, and the EMTC formed was isolated from the mixture by open-column chromatography on silica gel as described below.

Open-column chromatography on silica gel

This technique was used for a rough separation of the impurities from MTC. The glass column (5 cm I.D.) was packed with 150 g of silica gel 60 H, 40–63 μm (Merck, Darmstadt, Germany). Before use the silica gel was suspended in EDTA (10%, m/v), previously adjusted to pH 9.0 with sodium

hydroxide, sonicated for 5 min, filtered off and dried at 110°C overnight. The treated silica gel was slurred in dichloromethane for column packing. The sample was dissolved in methanol and diluted with dichloromethane. The mobile phase was dichloromethane–methanol–0.1 mM EDTA at pH 9.0 (74:23:3, v/v/v), with a flow-rate of 18 ml/min. Fractions of 20 ml were collected.

Open-column chromatography on XAD

This technique was used for removing inorganic salts from purified substances. The glass column (1 cm I.D.) was packed with a suspension of 5 g of XAD2, 50–100 μm (Serva, Heidelberg, Germany) in methanol and washed with water. The sample was loaded on the column in aqueous solution, and after flushing the column with water the product of interest was washed out with methanol.

Preparative column liquid chromatography

The laboratory-assembled chromatograph consisted of two Milton Roy minipumps (Laboratory Data Control, Riviera Beach, FL, USA), assembled as described before [2]. A 4.5-ml loop was fitted on the Model CV-6-UHPa-N60 Valco injector (Houston, TX, USA). The Model 150 Altex Biochemical UV detector (Berkeley, CA, USA) was equipped with a preparative cell.

The preparative columns, A (25 cm × 2.2 cm I.D.) or B (25 cm × 1.0 cm I.D.), were packed in the laboratory with silica gel 60 H, 15 μm (Merck). Fine particles were removed by flotation in water as previously described [3]. Before use the silica gel was suspended in EDTA (10%, m/v), previously adjusted to pH 9.0 (for column A) or pH 6.0 (for column B), by sonication for 5 min, filtered off and dried at 110°C overnight. The packing procedure was the same as previously described [3]. Guard columns A (25 cm × 2.2 cm I.D.) or B (25 cm × 1.0 cm I.D.) were packed by hand with silica gel from the same batch at pH 9.0 or 6.0. These columns were used to saturate the mobile phase with EDTA. Guard columns were replaced after 40 h. The separation columns were used throughout the study without loss of performance. Mobile phases for columns A and B were dichloromethane-methanol-0.1 mM EDTA, pH 9.0 (59:35:6, v/v/v), and dichloromethane-methanol-0.1 mM EDTA, pH 6.0 (55:42:3, v/v/v), respectively.

Samples were dissolved in the mobile phase at a concentration of not more than 30 mg/ml. The flow-rate was set at 14 ml/min for column A and 7 ml/min for column B.

Thin-layer chromatography (TLC)

Precoated silica gel layers on aluminium were used, *i.e.* silica gel 60 F₂₅₄ (Merck) and Alugram SIL G/UV₂₅₄ (Macherey-Nagel, Düren, Germany). Before use, the plates were evenly sprayed with a 10% (m/v) solution of EDTA, the pH of which was adjusted to 9.0 with sodium hydroxide. About 10 ml were used for plates of 10 cm × 20 cm. The plates were dried in a horizontal position for at least 30 min at room temperature and then in an oven at 100–110°C for at least 30 min shortly before use. From each fraction collected from the open column, 2 μl were applied on the plate to evaluate its composition. The chromatographic chamber was

lined with paper and equilibrated with the mobile phase, dichloromethane-methanol-water (59:35:6, v/v/v), for at least 1 h prior to use. The plate was developed at room temperature over a distance of 7.5 cm (about 15 min) and dried with a stream of hot air. The plates were examined in ultraviolet light at 365 nm. A more thorough discussion of the TLC method for identification of tetracyclines has been published previously [4,5].

Nuclear magnetic resonance (NMR)

¹H and ¹³C Fourier transform (FT) spectra were taken with a Jeol FX 90 Q Nuclear magnetic resonance (NMR) spectrometer (Tokyo, Japan), operating at 89.60 MHz (¹H) or 22.53 MHz (¹³C), in 5-mm tubes and at a probe temperature of 30°C. Samples were prepared in deuterated dimethylsulphoxide (DMSO-d₆) with tetramethylsilane (TMS) as reference.

RESULTS AND DISCUSSION

For the validation of an analytical LC method for MTC, it was decided to identify the impurities of commercial samples of MTC. Preliminary experiments indicated that the impurities detected (UNK1, UNK2 and UNK3) were not degradation-products. These substances had to be separated by chromatography from commercial MTC containing only small amount of impurities. Attempts to prepare samples enriched in impurities by recrystallization were unsuccessful.

In 1967, Ascione *et al.* [6] described column chromatography on kieselguhr treated with EDTA and benzene-chloroform (40:60 or 30:70, v/v) and *n*-butanol-chloroform (50:50, v/v) as mobile phases to separate tetracyclines. The inherent low capacity of kieselguhr makes this material less suitable for the isolation of small amount of impurities from MTC samples. In 1989, Oka *et al.* [7] isolated photodecomposition products of tetracycline by using silica gel and benzene-ethyl acetate (19:1, v/v) or mixtures of chloroform-methanol-water as mobile phases. We were unable to separate the impurities of interest from MTC with this method because of severe streaking, probably due to complex formation with the metal ions in the silica gel. In 1990, Drexel *et al.* [8] isolated lumitetracycline from photodecomposed tetracycline by using a LiChorsorb

RP-8 LoBar column with a mobile phase of ethanol-0.05 M oxalic acid (pH 3.0) (30:70, v/v). However, on reversed-phase packings, separation of UNK1 and MTC was not achieved in our laboratory.

The column chromatographic method for isolation of UNK1, UNK2 and UNK3 was developed on the basis of experience with TLC of tetracyclines [4,5]. TLC of a commercial sample was performed on silica gel layers sprayed with 10% EDTA solutions of various pH. The results are shown in Fig. 2. At pH 6.0, UNK1, UNK2 and UNK3 were well separated from each other, but no separation was achieved between UNK3 and MTC. At pH 9.0, UNK2, UNK3 and MTC were well separated from each other, but the separation between UNK1 and UNK2 was insufficient. It was therefore decided to separate a mixture of UNK1 + UNK2 from UNK3 by column chromatography on silica gel pretreated with EDTA at pH 9.0, followed by further separation of UNK1 and UNK2 at pH 6.0. The separation of polar compounds by LC on buffered silica gel has been described previously [9].

A rough separation of the MTC impurities from 10 g of a commercial sample was performed by open-column chromatography on silica gel at pH 9.0, as described in the Experimental section. TLC was used to monitor the separation. Fractions 15–

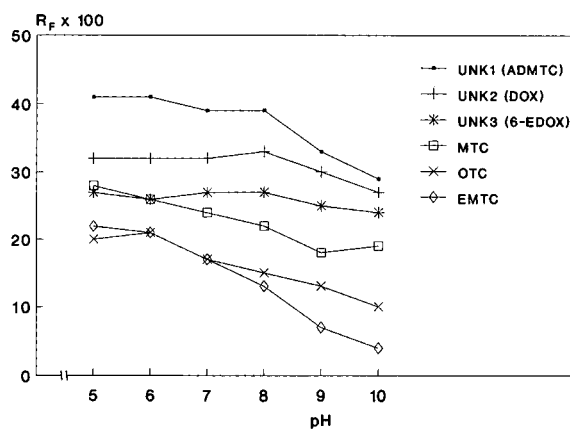


Fig. 2. Influence of the stationary phase pH on the separations obtained by TLC. Stationary phase: silica gel (Alugram), sprayed with 10% EDTA solutions at different pH. See Experimental section for other conditions. Mobile phase: dichloromethane-methanol-water (59:35:6, v/v/v). The values used to construct the graph are the means of several experiments.

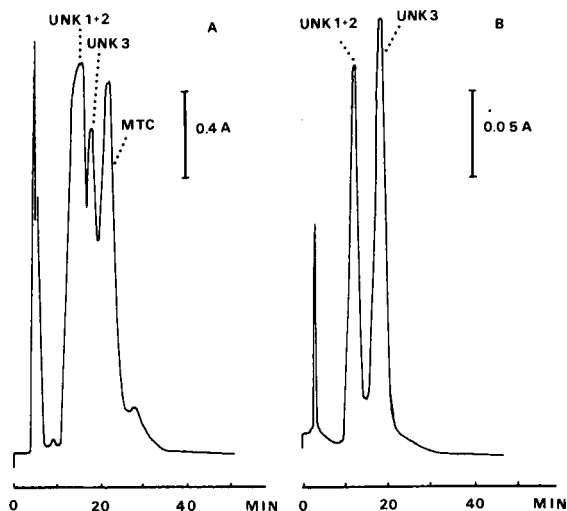


Fig. 3. Isolation of UNK3 (6-EDOX) by preparative column liquid chromatography. (A) Separation of a mixture of UNK1 + UNK2 from UNK3 and metacycline. (B) Further purification of UNK3. Stationary phase: silica gel, 15 μ m, treated with EDTA at pH 9.0 (25 cm \times 2.2 cm I.D.). Mobile phase: dichloromethane-methanol-0.1 mM EDTA, pH 9.0 (59:35:6, v/v/v). Flow-rate: 14 ml/min. Detection: UV 254 nm. Sample load: 120 mg. MTC = metacycline.

24 (fraction I) contained UNK1 and UNK2 while fractions 25–34 (fraction II) contained UNK1, UNK2 and UNK3 and some MTC.

Further purification was carried out by preparative column liquid chromatography on silica gel treated with EDTA at pH 9.0. Fraction II was separated into UNK1 + UNK2, UNK3 and MTC, as shown in Fig. 3. UNK3 was purified further using the same method to yield about 20 mg of chromatographically pure UNK3. The mixture UNK1 + UNK2 was added to fraction I, obtained by open-column chromatography. Fraction I was separated into UNK1 and UNK2 by LC on silica gel pretreated with EDTA at pH 6.0, as shown in Fig. 4. This procedure gave chromatographically pure UNK1 (25 mg) and UNK2 (20 mg). The substances thus obtained were washed free of inorganic salts by open-column chromatography on XAD2 as described in the Experimental section. The resultant samples of UNK1 (20 mg), UNK2 (10 mg) and UNK3 (12 mg) had purities greater than 90%, as determined by analytical LC [1].

The structures UNK1, UNK2 and UNK3 were

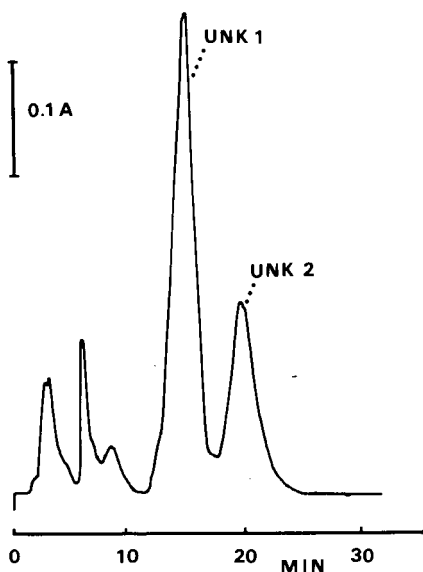


Fig. 4. Isolation of UNK1 (ADMTC) and UNK2 (DOX) by preparative column liquid chromatography from a mixture of UNK1 and UNK2. Stationary phase: silica gel, 15 μ m, treated with EDTA at pH 6.0 (25 cm \times 1 cm I.D.). Mobile phase: dichloromethane-methanol-0.1 mM EDTA, pH 6.0 (55:42:3, v/v/v). Flow-rate: 7 ml/min. Detection: UV 254 nm. Sample load: 20 mg.

elucidated by a combination of chromatographic and spectroscopic methods. UNK2 and UNK3 showed the same behaviour in TLC and analytical LC as reference substances of DOX and 6-EDOX, respectively. Their identity was further confirmed by photodiode array detection (Waters Assoc., Milford, MA, USA) and ^1H and ^{13}C NMR. On the basis of its chromatographic behaviour, UNK1 was assumed to be 2-acetyl-2-decarboxamidometacycline (ADMTC). Corresponding derivatives were observed to elute immediately after the main compound in comparable LC systems developed for doxycycline, oxytetracycline, tetracycline and demeclocycline [10–13]. The UV spectra obtained by photodiode array detection showed that, for the 2-acetyl-2-decarboxamido derivatives, the ratio of the absorbance at 270 nm to that at 380 nm was larger than the ratio for the corresponding tetracycline; the 2-acetyl-2-decarboxamido derivatives showed a pronounced minimum at about 240 nm, which was absent for the corresponding tetracycline. Such behaviour was also observed for the spectra of UNK1 and MTC.

The structure of ADMTC (UNK1) was confirmed by NMR. The ^1H NMR spectrum data were: δ 2.15 (3H, s, $\text{C}_2\text{-COCH}_3$), 2.71 [6H, s, $\text{C}_4\text{-N}(\text{CH}_3)_2$], 3.30–3.80 (br, C_{4a}H , C_5H and C_{5a}H), 3.99 (1H, s, C_4H), 5.38 and 5.51 (2H, AB pattern, $\text{C}_6 = \text{CH}_2$), 6.98 (1H, d, $J = 8$ Hz, C_9H), 7.17 (1H, d, $J = 8$ Hz, C_7H), 7.60 (1H, t, $J = 8$ Hz, C_8H). Comparing the spectrum with that of MTC, reported by Casy and Yasin in 1983 [14], an additional three-proton signal at δ 2.15 and disappearance of signals between δ 9 and 10 from the carboxamido group at C-2 are the most important differences. The ^{13}C NMR spectral data were: 192.8 ppm (s, C_{11}), 191.5 ppm (s, C_1), 190.4 (s, $\text{C}_2\text{-COCH}_3$), 183.2 (s, C_3), 179.1 (s, C_{12}), 160.7 (s, C_{10}), 142.8 (s, C_{6a}), 141.4 (s, C_6), 136.7 (d, C_8), 117.2 (d, C_7), 116.3 (d, C_9), 114.6 (s, C_{10a}), 113.2 (t, $\text{C}_6 = \text{CH}_2$), 109.5 (s, C_2), 104.8 (s, C_{11a}), 76.3 (s, C_{12a}), 66.4 (d, C_4), 66.2 (d, C_5), 44.6 (d, C_{5a}), 41.6 [q, $\text{N}(\text{CH}_3)_2$], 40.6 (d, C_{4a}) and 31.1 (q, $\text{C}_2\text{-COCH}_3$). The multiplicity mentioned in parentheses was that observed in an off-resonance spectrum (OFR). The assignment for close-lying peaks with the same multiplicity may be interchanged. In comparison with the ^{13}C NMR results for MTC, reported by Casy and Yasin in 1984 [15], the presence of an acetyl instead of an amido group at C-2 was evident by the additional signal at 31.1 ppm (quartet, OFR). This is the characteristic downfield movement of about 19 ppm of the acetyl group carbonyl compared with that of the amido group. A downfield shift of about 15 ppm for C-2 is observed.

ADMTC has not been previously described, but 2-acetyl-2-decarboxamido derivatives of tetracycline, chlortetracycline and oxytetracycline have been isolated from special fermentation cultures [16,17]. It is assumed that 2-acetyl-2-decarboxamidooxytetracycline, known to be present at up to 2% in commercial OTC samples, was transformed into ADMTC during the semisynthesis of MTC from OTC. DOX and 6-EDOX were unexpected MTC impurities. Accidental contamination was excluded, since more 6-EDOX than DOX was found in commercial MTC samples, while 6-EDOX constitutes only a small impurity (< 1%, m/m) in commercial DOX samples. Moreover, 6-EDOX and DOX were present in all the samples examined. Careful examination of several commercial samples of OTC, the starting material for semisynthesis of MTC, showed

the absence of DOX and 6-EDOX. It is therefore suggested that DOX and 6-EDOX are formed by partial reduction of MTC during the semisynthesis of the latter.

ACKNOWLEDGEMENTS

The authors thank Dr. Melamed (Pfizer, France) for the gift of a metacycline samples and Mrs. A. Decoux for skilful secretarial assistance. The National Fund for Scientific Research (Belgium) is acknowledged for financial support.

REFERENCES

- 1 W. Naidong, K. Verresen, E. Roets and J. Hoogmartens, *J. Chromatogr.*, 586 (1991) 61.
- 2 I. Wouters, S. Hendrickx, E. Roets, J. Hoogmartens and H. Vanderhaeghe, *J. Chromatogr.*, 291 (1984) 59.
- 3 I. O. Kibwage, G. Janssen, E. Roets, J. Hoogmartens and H. Vanderhaeghe, *J. Chromatogr.*, 346 (1985) 309.
- 4 W. Naidong, Th. Cachet, E. Roets and J. Hoogmartens, *J. Planar Chromatogr.*, 2 (1989) 424.
- 5 W. Naidong, E. Roets and J. Hoogmartens, *Pharmeuropa*, 2 (1990) 212.
- 6 P. P. Ascione, J. B. Zagar and G. P. Chrekian, *J. Pharm. Sci.*, 56 (1967) 1396.
- 7 H. Oka, Y. Ikai, N. Kawamura, M. Yamada, K. Harada, S. Ito and M. Suzuki, *J. Agric. Food Chem.*, 37 (1989) 226.
- 8 R. E. Drexel, G. Olack, C. Jones, G. N. Chmurny, R. Santini and H. Morrison, *J. Org. Chem.*, 55 (1990) 2471.
- 9 R. Schwarzenbach, *J. Liq. Chromatogr.*, 2 (1979) 205.
- 10 J. Hoogmartens, N. H. Khan, H. Vanderhaeghe, A. L. van der Leeden, M. Oosterbaan, G. L. Veld-Tulp, W. Plugge, C. van der Vlies, D. Mialanne, R. Melamed and J. H. McB. Miller, *J. Pharm. Biomed. Anal.*, 7 (1989) 601.
- 11 N. H. Khan, E. Roets, J. Hoogmartens and H. Vanderhaeghe, *J. Chromatogr.*, 405 (1987) 229.
- 12 N. H. Khan, P. Wera, E. Roets and J. Hoogmartens, *J. Liq. Chromatogr.*, 13 (1990) 1351.
- 13 W. Naidong, E. Roets and J. Hoogmartens, *J. Pharm. Biomed. Anal.*, 7 (1989) 1691.
- 14 A. F. Casy and A. Yasin, *J. Pharm. Biomed. Anal.*, 1 (1983) 281.
- 15 A. F. Casy and A. Yasin, *J. Pharm. Biomed. Anal.*, 2 (1984) 19.
- 16 M. W. Miller and F. A. Hochstein, *J. Org. Chem.*, 27 (1962) 2525.
- 17 F. A. Hochstein, M. Schach von Wittenau, F. W. Tanner, Jr. and K. Murai, *J. Am. Chem. Soc.*, 82 (1960) 5934.

Analysis of dyes extracted from textile fibers by thermospray high-performance liquid chromatography–mass spectrometry[☆]

Jehuda Yinon*

Department of Environmental Sciences and Energy Research, Weizmann Institute of Science, 76100 Rehovot (Israel)

Jacob Saar^{☆☆}

Department of Research and Development, Mahteshim Chemical Works Ltd., P.O. Box 60, 84100 Beer Sheva (Israel)

(First received May 14th, 1991; revised manuscript received June 28th, 1991)

ABSTRACT

Thermospray high-performance liquid chromatography was used to analyze a series of disperse dyes extracted from polyester and cellulose acetate fibers, a basic dye from orlon fiber and a vat dye from denim. Molecular characterization of each dye was obtained from the extract of a single fiber, 5–10 mm long. This was achieved by high-performance liquid chromatographic separation followed by thermospray mass spectrometry of the separated dye.

INTRODUCTION

Textile fibers found at a crime scene can be used as physical evidence in a wide range of crimes, such as crimes that involve personal contact in which cross-transfers may occur between the clothing of suspect and victim.

The value of fibers as evidence will depend on the forensic scientist's ability to narrow their origin to a limited number of sources, or even to a single source. The mass production of textiles makes this a difficult task. It is therefore of major importance to be able to define all the possible characteristics of fibers found at the scene of the crime, in order to compare them with fibers found on the suspect.

An important part of forensic fiber examination involves the characterization of textile dyestuffs. Three techniques are commonly used for this purpose: thin-layer chromatography (TLC) [1–4], visible microspectrophotometry [1,3,5] and high-performance liquid chromatography (HPLC) [2,6–8].

There are several limitations in the use of these techniques. Microspectrophotometry is applicable to small fibers, but considers only the spectral characteristics of the dyes, which show considerable variation. In this method chemical and structural differences between dyes are not taken into consideration. TLC requires a relatively large amount of extracted dye, which may not always be available on a single short fiber. Also, the reproducibility of dye separation by TLC is not satisfactory [7]. HPLC has a much better sensitivity and reproducibility than TLC for analysis of dyes, but characterization of a dye is based on retention time only. As hundreds of dyes are used in the textile dyeing industry, ambigu-

* Contribution No. 18, Department of Environmental Sciences and Energy Research, The Weizmann Institute of Science.

** Present address: Chemagis Ltd., P.O. Box 3593, 84135 Beer Sheva, Israel.

ous results might be obtained because of overlapping of HPLC peaks and similar retention times for different dyes. Also, some dyes are complex mixtures and most dyes are not chemically pure, resulting in additional chromatographic peaks. Even multi-wavelength detection does not provide an absolute answer to this problem.

Thermospray high-performance liquid chromatography-mass spectrometry (HPLC-TSP-MS) has been found to be a selective technique for separation, identification and quantification of dyes in various matrices [9-15].

Disperse dyes, based on anthraquinone and azo compounds, are the major coloring agents in use with polyester and cellulose acetate fabrics. As synthetic fibers are of major importance in the textile industry, mainly disperse dyes were selected to study the application of HPLC-TSP-MS in the identification of dyes extracted from textile fibers.

EXPERIMENTAL

Samples

Most dyed fibers were taken from pattern cards

TABLE I
INVESTIGATED SAMPLES

C.I. = Color Index.

Commercial name of dye	C.I. name	C.I. number	M.W.	Structure ^a	Type of fiber	Manufacturer
1.5% Serisol Fast Yellow GD	Disperse Yellow 3	11855	269	1	Diacetate	Yorkshire
2.0% Serisol Fast Yellow PL 150	Disperse Yellow 9	10375	274	2	Diacetate	Yorkshire
1.2% Resolin Yellow 5GS	Disperse Yellow 5	12790	324	3	Polyester	Bayer
0.72% Dispersol Orange B-A Grains	Disperse Orange 1	11080	318	4	Polyester	ICI
0.6% Serilene Orange 5R300	Disperse Orange 1	11080	318	4	Polyester	Yorkshire
0.6% Serilene Orange 2RL200	Disperse Orange 25	11227	323	5	Polyester	Yorkshire
0.72% Dispersol Orange B-2R 200 Grains	Disperse Orange 25	11227	323	5	Polyester	ICI
1% Resolin Orange F3R 200%	Disperse Orange 25	11227	323	5	Polyester	Bayer
2.2% Resolin Orange RL	Disperse Orange 13	26080	352	6	Polyester	Bayer
0.6% Serilene Yellow Brown 2RL 150	Disperse Orange 37	—	391	7	Polyester	Yorkshire
1.5% Serisol Brilliant Red X3B 200	Disperse Red 11	62015	268	8	Diacetate	Yorkshire
0.6% Serisol Fast Scarlet BD 200	Disperse Red 1	11110	314	9	Diacetate	Yorkshire
0.6% Serisol Fast Crimson BD 150	Disperse Red 13	11115	348	10	Diacetate	Yorkshire
0.6% Serilene Red Brown R-FS 150	Disperse Brown 1	11152	432	11	Diacetate	Yorkshire
1.5% Serisol Brilliant Blue BGN 300	Disperse Blue 3	61505	296	12	Diacetate	Yorkshire
1.0% Resolin Blue BBL5	Disperse Blue 165	—	405	13	Polyester	Bayer
1.0% Yoracryl Yellow RL	Basic Yellow 28	—	309	14	Orlon	Yorkshire
Indigo	Vat Blue 1	73000	262	15	Denim	Levi Strauss

^a See Fig. 1.

supplied by the manufacturers. The blue denim fibers were taken from an old pair of blue jeans. Details of the studied samples and structures are given in Table I and Fig. 1. A single fiber, 5-10 mm long, was pushed to the bottom of a 5-cm-long glass capillary tube of 2 mm O.D. and 0.8 mm I.D., previously sealed at one end by heating. For the disperse dyes, 5 μ l of chlorobenzene were added, and the tube sealed and heated at 100°C for 15 min [6]. After cooling, the tube was opened and the extract was injected into the HPLC-MS system. For the basic dye, formic acid at room temperature was used, and for the vat dye formic acid with heating at 80°C for 1 min was used. Standards of Indigo (Vat Blue 1) (dye content ~99%) and Disperse Orange 13 (dye content ~15%) were purchased from Aldrich (Milwaukee, WI, USA). They were dissolved in acetone, and 5 μ l of each were injected into the HPLC-MS system.

Equipment

The instrument used was a 4510B Finnigan-MAT (San Jose, CA, USA) HPLC-MS system with a thermospray interface and ion source. The HPLC

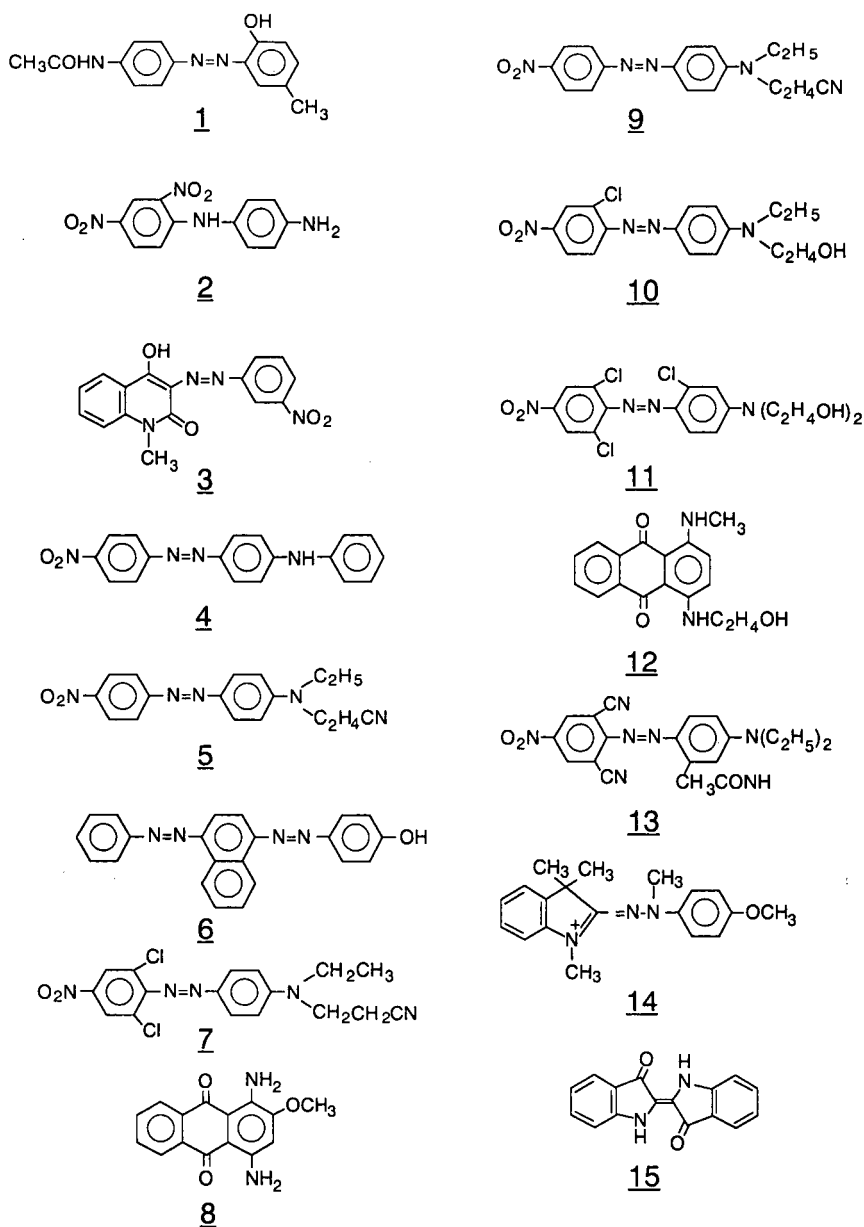


Fig. 1. Structures of compounds 1–15.

system consisted of a CM4000 LDC Milton Roy solvent-delivery system with a Rheodyne 7125 injector valve fitted with a 5- μ l sample loop. The column was a Merck C₁₈ column (15 cm \times 4 mm I.D.). The chromatograph was operated in the gradient mode, starting at a mobile phase of methanol–water

(50:50), changing within 5 min to 100% methanol and staying at that level for 20 min. The flow-rate was 0.9 ml/min. The buffer, 0.1 M ammonium acetate, was delivered post-column via the TSP interface into the ion source by a Constametric Bio 3000 Milton Roy delivery pump.

TABLE II
THERMOSPRAY MASS SPECTRAL IONS OF DYES

Dye	M.W.	Structure ^a	Ions observed (percentage relative abundance)
Dispersive Yellow 3	269	1	271(17); 270(100)
Disperse Yellow 9	274	2	297(32); 292(24); 276(9); 275(100); 245(15)
Disperse Yellow 5	324	3	347(15); 326(17); 325(100)
Disperse Orange 1	318	4	320(15); 319(100); 289(11)
Disperse Orange 25	323	5	346(7); 325(15); 324(100)
Disperse Orange 13	352	6	354(21); 353(100)
Disperse Orange 37	391	7	396(8); 394(41); 392(100)
Disperse Red 11	268	8	270(11); 269(100)
Disperse Red 1	314	9	316(15); 315(100)
Disperse Red 13	348	10	351(20); 350(11); 349(100)
Disperse Brown 1	432	11	437(8); 435(23); 433(20); 301(42); 280(12); 279(100); 231(12)
Disperse Blue 3	296	12	298(13); 297(100); 242(11); 241(12); 234(10)
Disperse Blue 165	405	13	406(17); 405(31); 404(21); 331(100)
Basic Yellow 28	309	14	311(84); 310(100)
Vat Blue 1	262	15	264(11); 263(100); 257(13) 245(14); 237(14); 235(16); 234(83); 230(13)

^a See Fig. 1.

Typical operating temperatures of the thermo-spray interface were vaporizer, 105–115°C; jet, 250°C; source, 250°C. Repeller was operated at a voltage of 100 V. Scan time was 2.0 s.

RESULTS AND DISCUSSION

In HPLC–MS, in addition to recording exact chromatographic retention times, one is looking at mass chromatograms of characteristic ions, representing the dyes eluted through the column which are ionized in the TSP interface and detected by the mass spectrometer.

Table II represents the positive ions of the investigated dyes and their relative abundance. These TSP mass spectral ions were found to agree with published data [9–11,13,14] and with TSP mass spectra of standard dyes. Mainly MH⁺ ions were produced, but sometimes also some fragment or adduct ions. The TSP mass spectrum of Disperse Yellow 9 (Fig. 2) contains two adduct ions: [M + NH₄]⁺ at *m/z* 292 and [M + Na]⁺ at *m/z* 297. The sodium is an impurity in the ammonium acetate. An [M + Na]⁺ ion is also observed in the TSP mass spectrum of Disperse Yellow 5, at *m/z* 347. The TSP mass spectrum of Disperse Orange 1 contains a fragment ion, [MH – NO]⁺, at *m/z* 289. The TSP mass spectrum of Disperse Brown 1 contains several ions,

including the ion forming the base peak at *m/z* 279, which probably originate from dibutyl phthalate, which coeluted with the dye. These ions were not observed in the TSP mass spectrum or in the mass spectrometry–mass spectrometry–collision-activated dissociation (MS–MS–CAD) spectrum of Disperse Brown 1 [11].

The ion at *m/z* 279 also appeared in the mass chromatograms of other dyes (Disperse Blue 3 and Basic Yellow 28), although not coeluting with them. The phthalate eluted at 15.30 min, which was also the eluting time of Disperse Brown 1. Also, in the mass spectrum of Disperse Blue 3 (see Fig. 6), some ions could not be attributed to the dye; they are probably due to impurities. In the TSP mass spectrum of Disperse Blue 165 the base peak is at *m/z* 331, which can be attributed to the fragment ion [MH – NO₂ – C₂H₅]⁺. This has to be substantiated by MS–MS–CAD. The ions at *m/z* 405 and 404 are probably due to an impurity coeluting with the dye. The TSP mass spectrum of the Indigo extract (Vat Blue 1) (see Fig. 8) contains some ions due to impurities or other components. Many dyes are blends of several components.

At this stage only the identification of the major dye in each extract was of interest, and not the additives or other components of the fiber which might have been extracted together with the dye. In

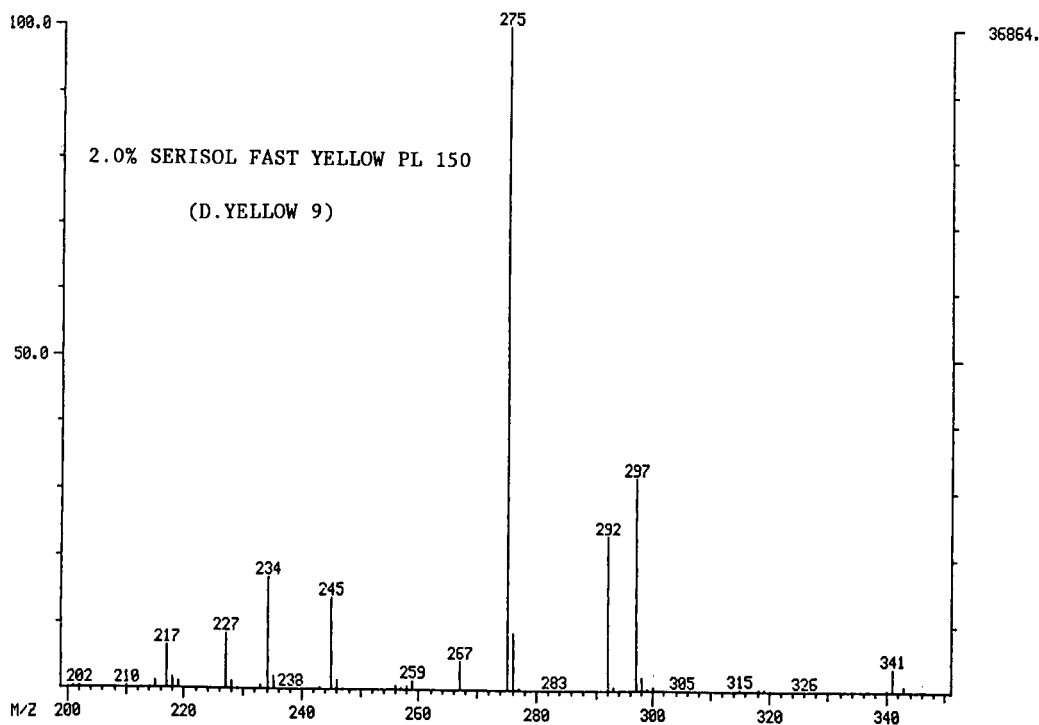
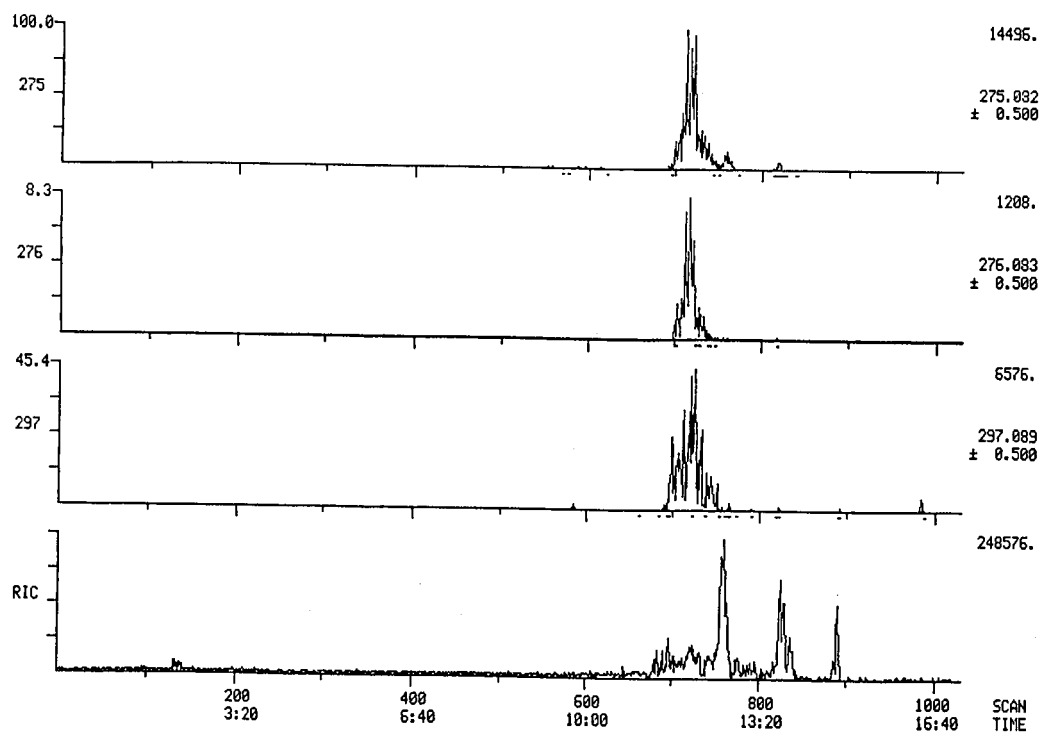


Fig. 2. HPLC mass chromatogram and TSP mass spectrum of 2.0% Serisol Fast Yellow PL 150.

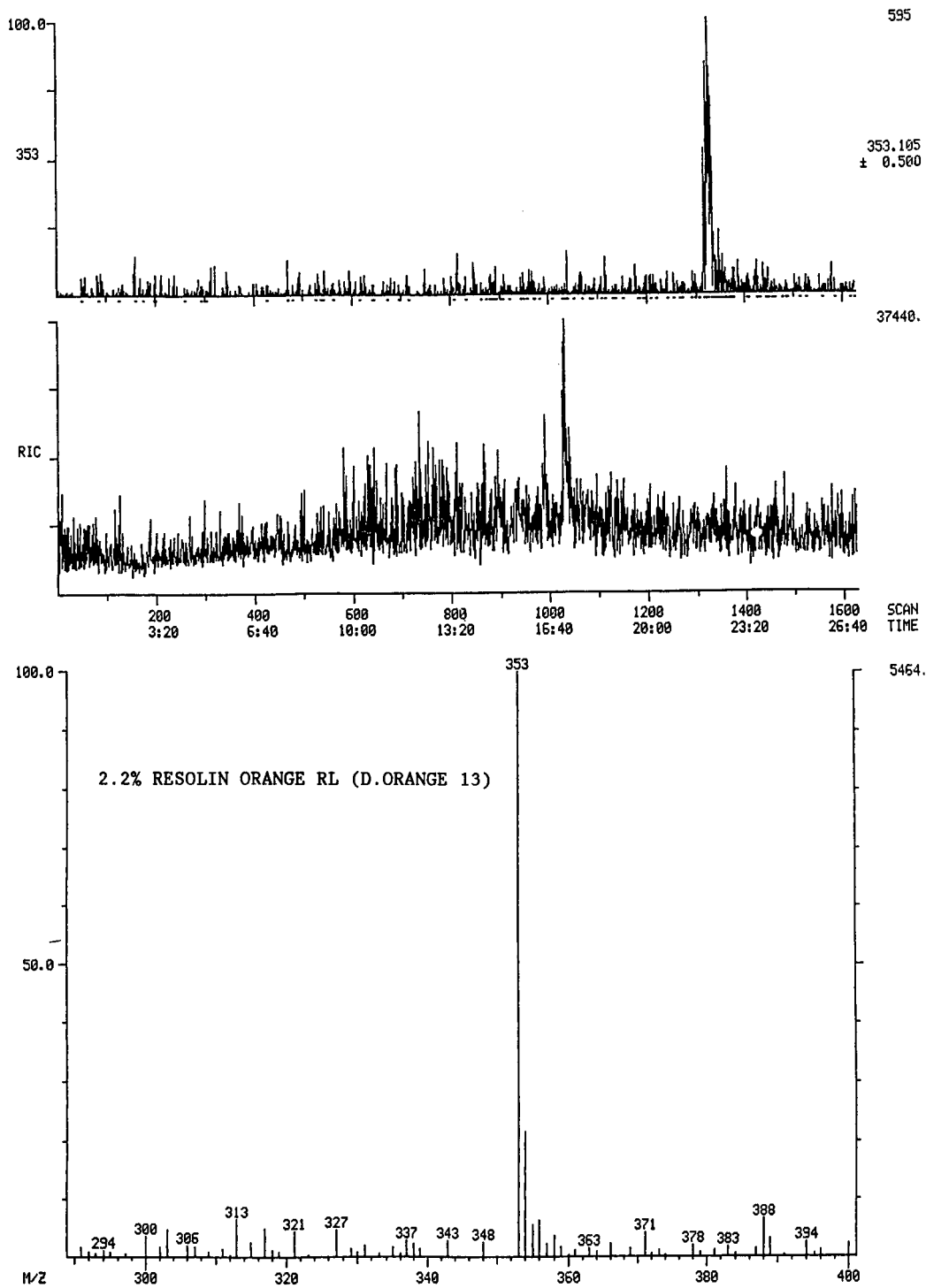


Fig. 3. HPLC mass chromatogram and TSP mass spectrum of 2.2% Resolin Orange RL.

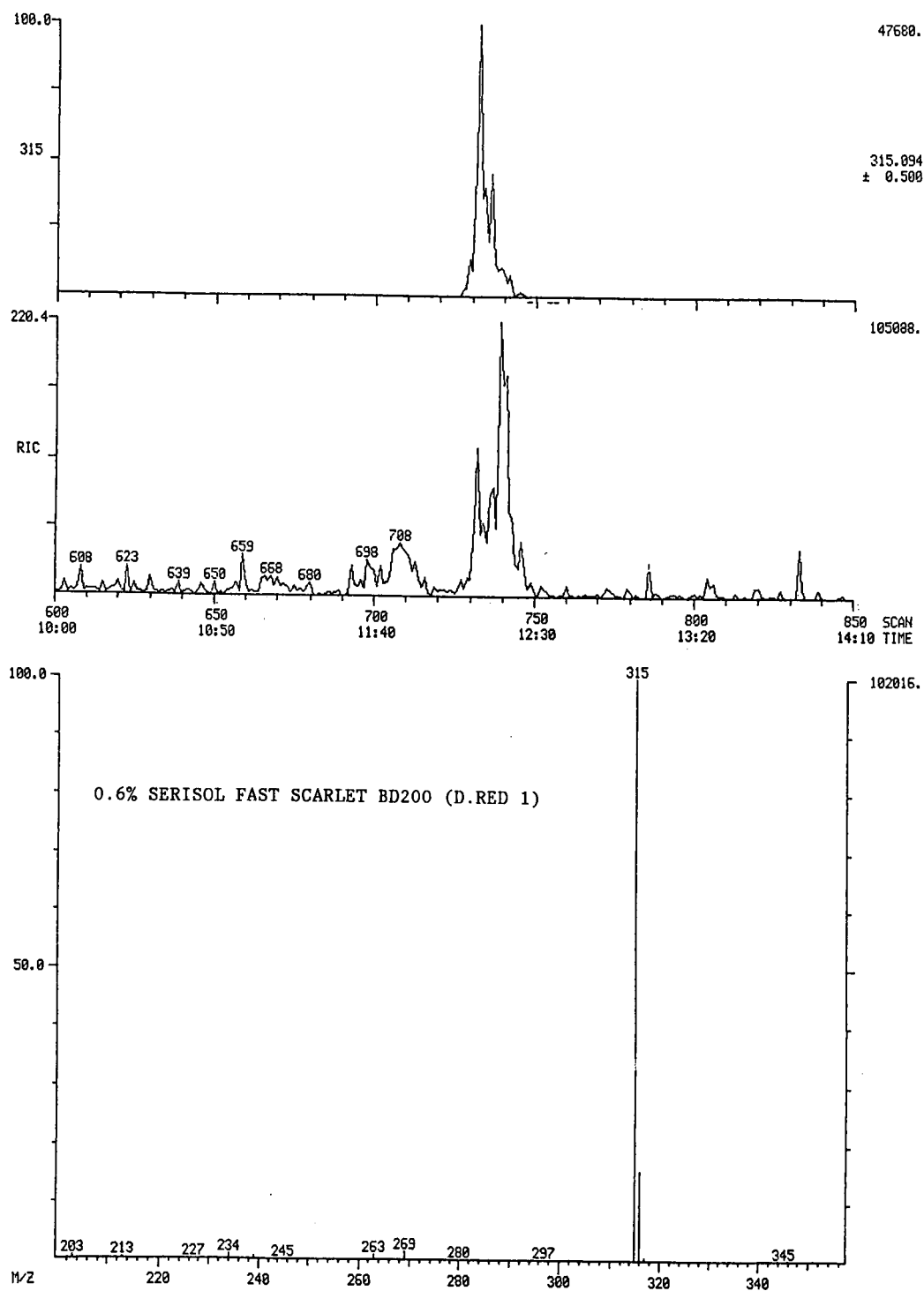


Fig. 4. HPLC mass chromatogram and TSP mass spectrum of 0.6% Serisol Fast Scarlet BD200.

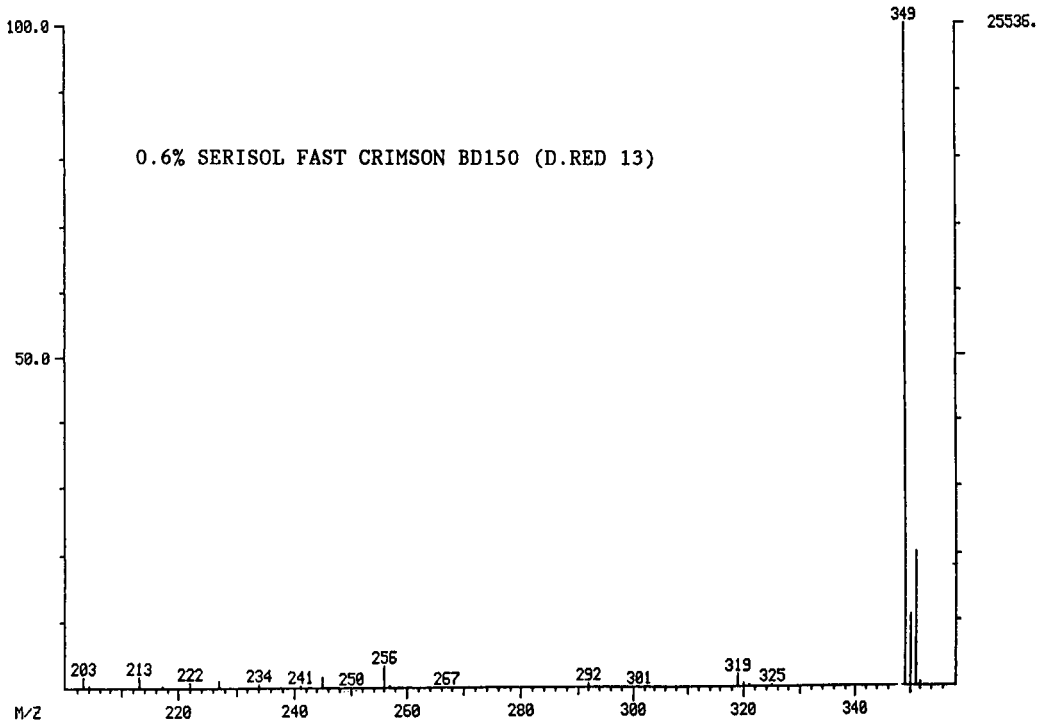
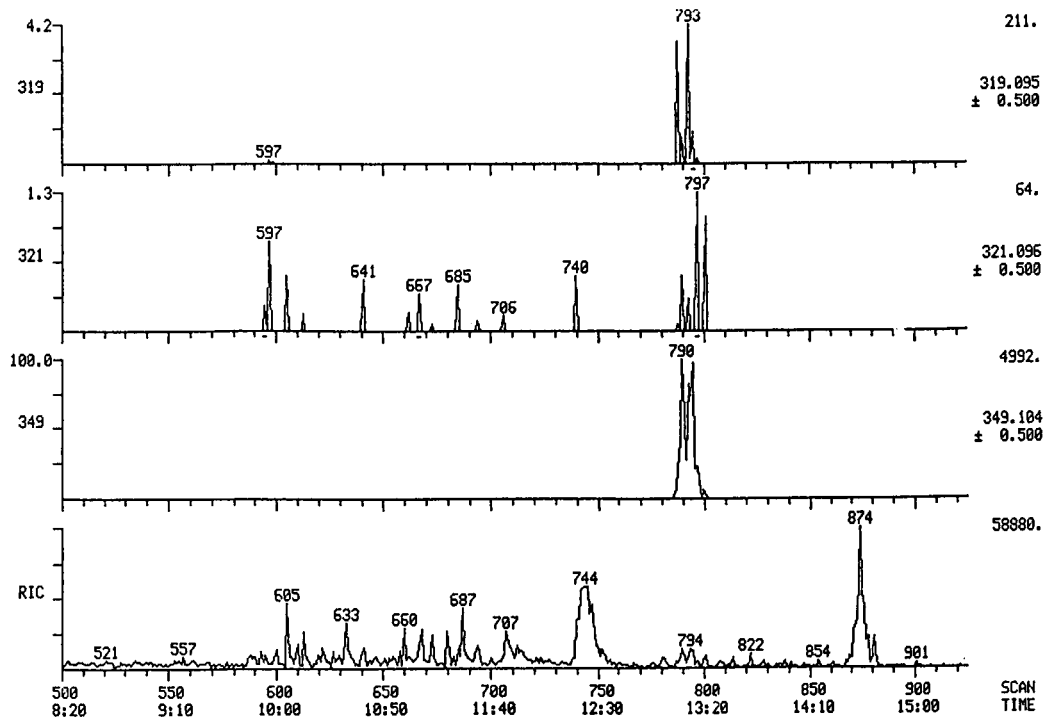


Fig. 5. HPLC mass chromatogram and TSP mass spectrum of 0.6% Serisol Fast Crimson BD 150.

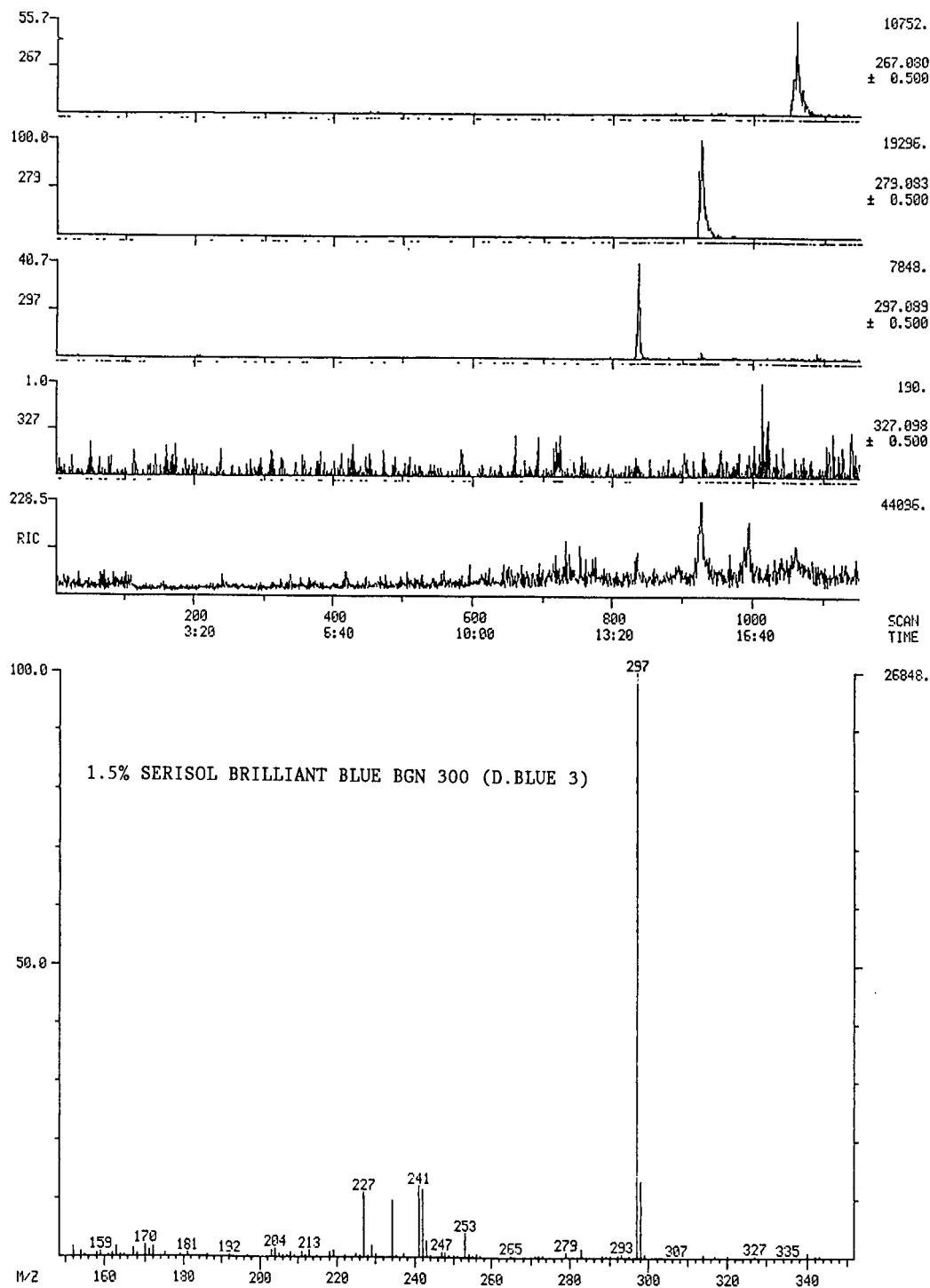


Fig. 6. HPLC mass chromatogram and TSP mass spectrum of 1.5% Serisol Brilliant Blue BGN 300.

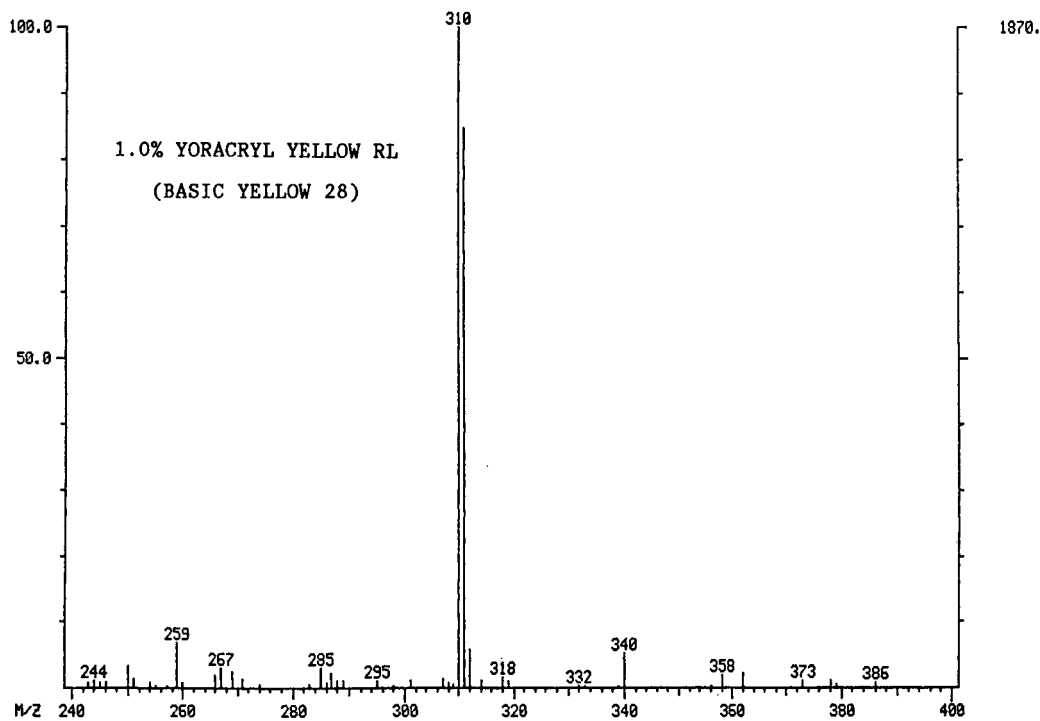
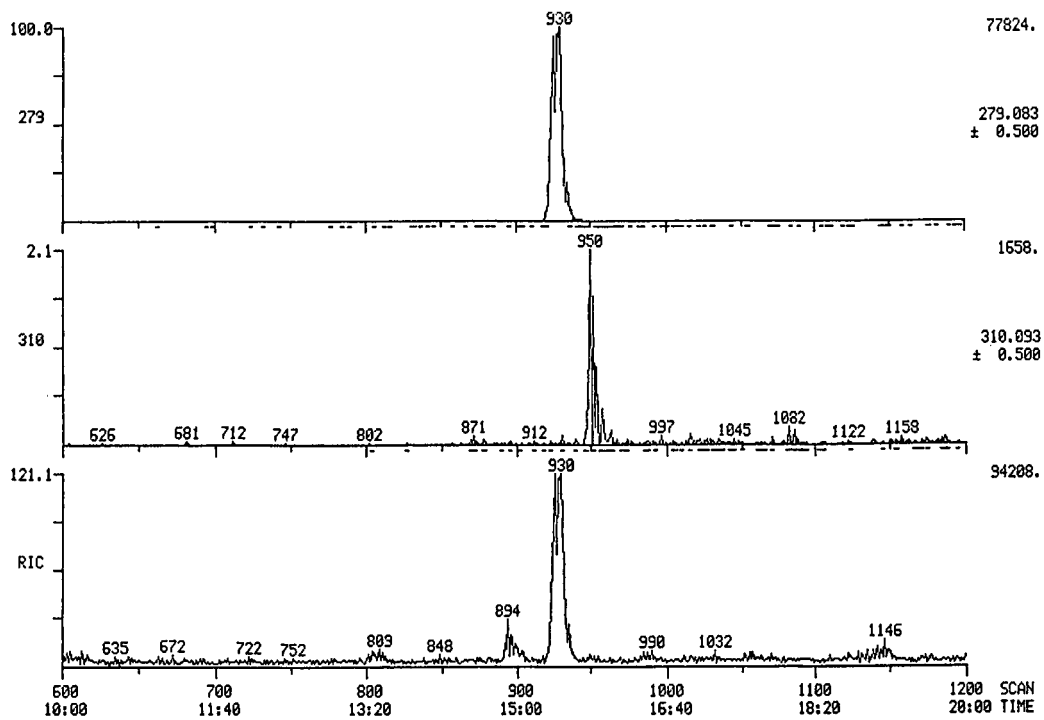


Fig. 7. HPLC mass chromatogram and TSP mass spectrum of 1.0% Yoracryl Yellow RL.

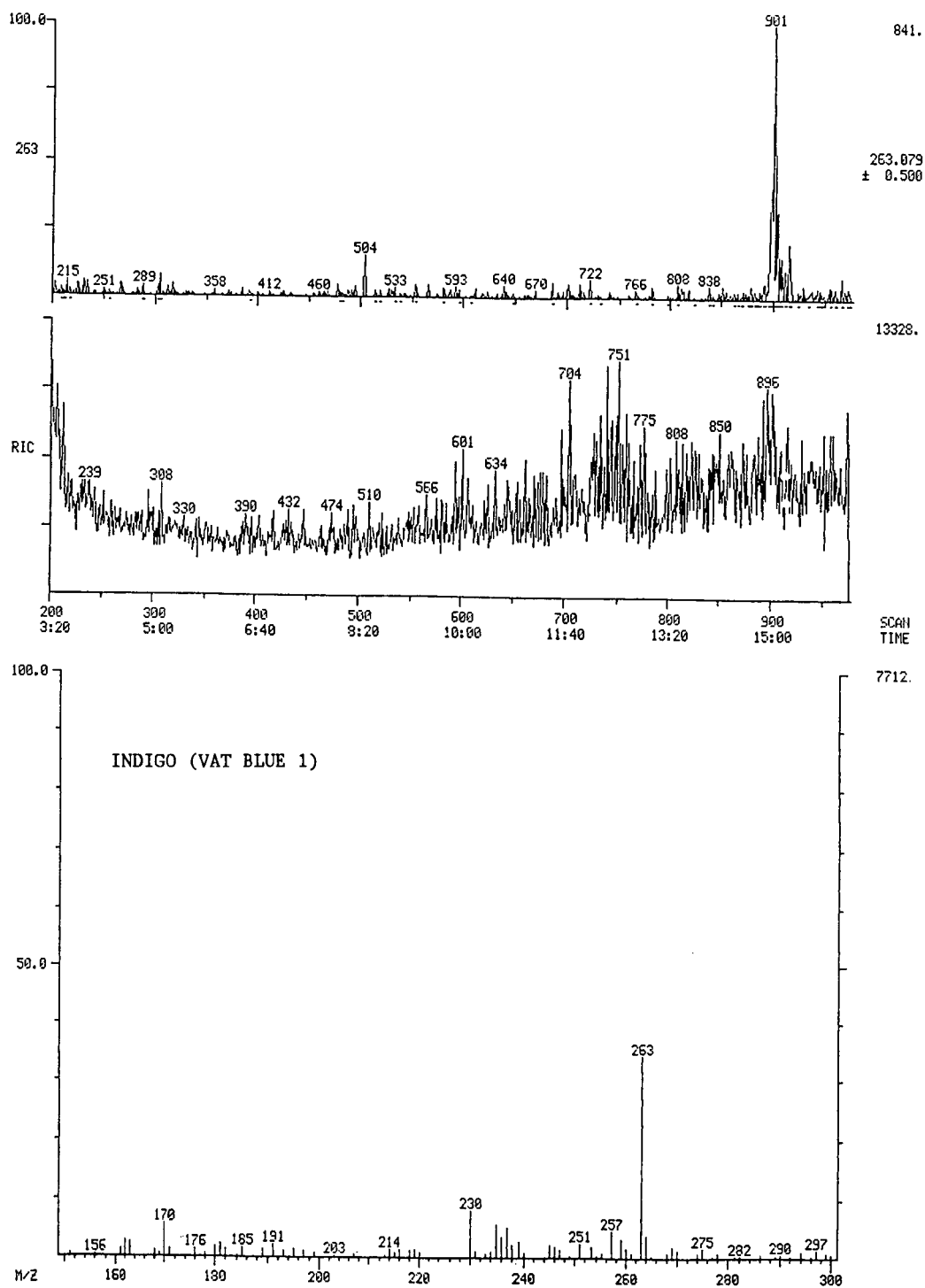


Fig. 8. HPLC mass chromatogram and TSP mass spectrum of Indigo.

order to separate those components from the dye of interest, one has to improve the HPLC separation characteristics.

Figs. 2–8 represent examples of reconstructed total ion current (RIC) and mass chromatograms and TSP mass spectra of seven of the investigated dyes. In most of the chromatograms it can be seen that the dye component is very small relative to the other components present in the fiber extract. Only by using HPLC–MS is it possible to identify characteristic ions of the dye. The chromatogram of 2.2% Resolin Orange RL (D. Orange 13) in Fig. 3 is a typical example which shows how the mass chromatogram of the MH^+ ion of the dye at m/z 353 is singled out from a noisy RIC chromatogram. Such a peak would have been hard to observe in a HPLC chromatogram with a UV detector because of lack of specificity. The amount of dye is very small, as fibers having a length of 2–10 mm contain 2–200 ng of dye, depending on the depth of the dyeing [16]. The amount of dye also depends on the shade percentage. The lightest shades of the investigated dyes were 0.6% (*i.e.* 600 g of the dye had been used to color 100 kg of fiber).

It is, of course, essential that the dyestuff be efficiently extracted from the fibers, and that the dye remains unchanged during the extraction procedure. The solvents chosen were found to be most suitable from a whole range of solvents suggested [2–4,6].

CONCLUSIONS

From our preliminary study it was found that TSP–HPLC–MS is a method having enough selectivity and sensitivity for identification of dyes extracted from single textile fibers. A library of TSP

mass spectra of textile dyes will have to be created to serve as reference library.

Further work is in progress to examine the various components present in commercial dyes, by increasing the HPLC chromatographic separation, and to evaluate the possibility of differentiating between fibers of the same color but with different shades. The list of dyes and type of fibers investigated will be expanded.

REFERENCES

- 1 R. Macrea, R. J. Dudley and K. W. Smalldon, *J. Forensic Sci.*, 24 (1979) 117.
- 2 J. C. West, *J. Chromatogr.*, 208 (1981) 47.
- 3 K. G. Wiggins, R. Cook and Y. J. Turner, *J. Forensic Sci.*, 33 (1988) 998.
- 4 G. M. Golding and S. Kokot, *J. Forensic Sci.*, 34 (1989) 1156.
- 5 M. C. Grieve, J. Dunlop and P. Haddock, *J. Forensic Sci.*, 33 (1988) 1332.
- 6 B. B. Wheals, P. C. White and M. D. Paterson, *J. Chromatogr.*, 350 (1985) 205.
- 7 D. K. Laing, R. Gill, C. Blacklaws and H. M. Bickley, *J. Chromatogr.*, 442 (1988) 187.
- 8 R. M. E. Griffin, T. G. Kee and R. W. Adams, *J. Chromatogr.*, 445 (1988) 441.
- 9 L. D. Betowski and J. M. Ballard, *Anal. Chem.*, 56 (1984) 2604.
- 10 R. D. Voyksner, *Anal. Chem.*, 57 (1985) 2600.
- 11 J. M. Ballard and L. D. Betowski, *Org. Mass Spectrom.*, 21 (1986) 575.
- 12 A. P. Bruins, L. O. G. Weidolf, J. D. Henion and W. L. Budde, *Anal. Chem.*, 59 (1987) 2647.
- 13 J. Yinon, T. L. Jones and L. D. Betowski, *Rapid Commun. Mass Spectrom.*, 3 (1989) 38.
- 14 J. Yinon, T. L. Jones and L. D. Betowski, *Biomed Environ. Mass Spectrom.*, 18 (1989) 445.
- 15 M. A. McLean and R. B. Freas, *Anal. Chem.*, 61 (1989) 2054.
- 16 R. Macrae and K. W. Smalldon, *J. Forensic Sci.*, 24 (1979) 109.

Prediction of retention indexes

II. Structure–retention index relationship on polar columns

C. T. Peng* and Z. C. Yang

Department of Pharmaceutical Chemistry, School of Pharmacy, University of California, San Francisco, CA 94143-0446 (USA)

S. F. Ding

Department of Chemistry, Beijing Normal University, Beijing (China)

(First received September 17th, 1990; revised manuscript received June 4th, 1991)

ABSTRACT

A method is described for the prediction of the retention index (I) from chemical structure, using the number of atoms in the molecule (Z), the I increment for atom addition (A) and the group retention factors ($GRFs$) of the functional groups and substituents. This method can predict the retention indexes of a wide range of compounds, such as acids, alcohols, amines, acid esters, aldehydes, ketones, ethers, aromatic hydrocarbons, alicyclics, heterocyclics, etc. on polar as well as non-polar columns to within 3% error. Accurate A and GRF values are essential to the prediction. These values can be obtained from homologous series, but a system of arbitrarily assigned A value and adjusted $GRFs$ are also used. The $GRFs$ of the substituents and functional groups depend on the polarity and polarizability of the analyte and the stationary phase and also on the molecular connectivity of the atoms, namely, primary, secondary and tertiary carbon atoms or hydrogen atoms, to which these groups are attached. Highly polar and polarizable groups can alter the A value. When the functionality of a group is masked by substitution, the analyte molecule will tend to behave chromatographically like hydrocarbons. The difficulty in predicting the I values of compounds of multi-functionality by the rule of additivity is the unknown intramolecular interaction that can alter both A and GRF values.

INTRODUCTION

In tritium labeling by radiation-induced reactions, the desired product is often formed together with some labeled by-products. To understand the mechanism of labeling, these by-products must be identified. The by-products are formed in no-carrier-added state and have negligible mass; even if all the material formed in a single run is collected, the amount will still be insufficient to establish their identity by conventional analytical techniques. The volatile by-products can be separated by gas chromatography and detected by radioactivity. On non-polar and polar columns, the radioactive peaks have

characteristic retention indexes (I), from which one may gain preliminary structural information.

We reported earlier [1] a structure–retention index relationship for predicting the retention index of a compound on non-polar columns (SE-30, DB-1), based on (i) the number of carbon and carbon equivalent atoms (Z) in the molecule, (ii) the retention index increment (A) for atom addition and (iii) the group retention factors ($GRFs$) for substituents and functional groups. This report shows that this same approach can be applied to predict I on polar columns using GRF constants derived for substituents and functional groups on polar columns.

EXPERIMENTAL

The materials and methods are essentially those described in the previous paper [1]. A stainless-steel column, 3.05 m \times 3.175 mm I.D., packed with 10% Carbowax 20M (CW-20M) on 80–100 mesh Supelcoport (Supelco, Bellefonte, PA, USA) and a fused-silica capillary column DB-Wax (15 m \times 0.53 mm I.D., film thickness 1.0 μ m) (J & W Scientific, Folsom, CA, USA) were used. A linear temperature program was adopted, beginning at 40°C isothermally for 4 min, after which the temperature was increased to 200°C at the rate of 8°C/min and maintained for 60 min or longer as required. The injection port was kept at 250°C and the detector at 300°C. A mixture of *n*-alkanes, from pentane (C₅) to hexacosane (C₂₆) or to dotriacontane (C₃₂), was used as markers; when necessary the standard were injected together with the analyte. Retention index measurements were preferably made on small mass peaks. For large mass peaks that are truncated at the full-scale height, the truncated width, expressed in time, is subtracted from the retention time reported by the electronic integrator for *I* calculation. *I* was computed using the equation of Van den Dool and Kratz [2], thus:

$$I = 100i \cdot \frac{X - M_{(n)}}{M_{(n+i)} - M_{(n)}} + 100n \quad (1)$$

where *n* is the number of carbon atoms in *n*-alkanes used as markers; *X*, *M*_(*n*), and *M*_(*n*+*i*) are the adjusted retention times of the analyte, the normal alkane marker with *n* carbon atoms eluting before and that with (*n* + *i*) carbon atoms eluting after the analyte, respectively; *i* is the interval and usually has the value of 1 or 2.

Linear regression analysis of *I* vs. the number of atoms in homologous series was performed on a 486 personal computer, using SAS statistical program for the PC, from the SAS Institute (Cary, NC, USA). Statistical data listed for the regression equations include (i) the number of data values in the set (*n*), (ii) the standard errors (S.E.) for the regression coefficient and the intercept, (iii) the coefficient of determination (*R*²) and (iv) significance probability (*p*), *i.e.*, the probability of getting a greater *F* statistic than that obtained if the hypothesis is true. The meaning of these terms is given in ref. 3.

RESULTS AND DISCUSSION

The prediction of *I* is based on the fact that the *I* value of a monofunctional molecule is invariably higher than that of a *n*-alkane molecule of equal atom number. This leads to the use of *GRF*s for *I* contributions from substituents and functional groups. The Kováts convention for calculating *I* is adopted [4]. According to this convention, *n*-hexane will be assigned a *I* of 600 on both non-polar and polar columns, irrespective of their different retention times.

The *I* values of *n*-alkanes increase with the number of carbon atoms (*n*) in the molecule and can be expressed as:

$$I = 100n \quad (2)$$

This value is also known as the base value [1] when *n* is replaced with *Z*, the total number of atoms in the molecule. *Z* includes carbon atoms and carbon equivalent atoms, such as oxygen, nitrogen, sulfur, chlorine, bromine and iodine, which may be found in the molecule. Compounds containing substituents, functional groups and other structural features will have higher *I* values than the base values. The *I* values of a homologous series will increase smoothly with increasing numbers of the carbon atoms or methylene groups in the homologues. A plot of the observed *I* values against *n* or *Z* values will yield a straight line which may be represented by the following linear regression equations:

$$I = An + (GRF)_n \quad (3)$$

$$= AZ + (GRF)_Z \quad (4)$$

where *A* is the regression coefficient, representing the *I* increment for atom addition, and *GRF* the intercept, representing the group retention factor or functionality constant. The subscript differentiates between the *GRF*s based on *n* or *Z*. In eqns. 3 and 4 shown above, *Z* is greater than *n* but (*GRF*)_{*Z*} is smaller than (*GRF*)_{*n*}. The term (*GRF*)_{*n*} may also contain the atom contribution of the substituent. Table I lists the *GRF* and *A* values for a number of homologues of monofunctionality on DB-Wax and CW-20M columns.

The magnitude of the *GRF* is dependent not only upon the polarity and polarizability of the substituent and functional group but also on the stationary

TABLE I
GROUP RETENTION FACTORS (GRFs) AND THE ATOM INCREMENTS (*A* VALUES)

Substituent and functional group	Formula	GRF	
		Calculated by eqn. 7 (<i>A</i> = 100)	By linear regression equation
<i>(A) Aliphatic series</i>			
(1) Alkanoic acids Analabs data ^a	R-COOH		997.15 ± 2.61 (107.69 ± 0.27) ^b (<i>n</i> = 6, <i>R</i> ² = 1.0000, <i>p</i> = 0.0001)
Our data		1029	994.09 ± 9.85 (103.72 ± 0.99) (<i>n</i> = 11, <i>R</i> ² = 0.9992, <i>p</i> = 0.0001)
(2) Primary alcohols Analabs data ^a	R-CH ₂ -OH		648.79 ± 0.65 (102.65 ± 0.066) (<i>n</i> = 5, <i>R</i> ² = 1.000, <i>p</i> = 0.0001)
Our data		647	632.86 ± 5.97 (100.92 ± 0.49) (<i>n</i> = 11, <i>R</i> ² = 0.9998, <i>p</i> = 0.0001)
(3) Secondary alcohols	>CH-OH	530	
(4) Tertiary alcohols (2-methyl-2-alkanols)	$\begin{array}{c} \\ -C-OH \\ \end{array}$	410	394.90 ± 2.73 (98.53 ± 0.73) (<i>n</i> = 5, <i>R</i> ² = 1.0000, <i>p</i> = 0.0001)
(5) Primary amines, 1°	R-CH ₂ -NH ₂	417	407.29 ± 3.35 (101.06 ± 0.35) (<i>n</i> = 8, <i>R</i> ² = 0.9999, <i>p</i> = 0.0001)
2°	R-CH-NH ₂	350	
3°	R-C-NH ₂	229	
(6) Secondary amines	R-CH ₂ -NH-R'	180	
(7) Tertiary amines	R'R''NR'''	(See text)	(See text)
(8) Aldehydes	R-CH ₂ -CHO	388	375.50 ± 3.11 (102.50 ± 0.34) (<i>n</i> = 5, <i>R</i> ² = 1.0000, <i>p</i> = 0.0001)
(9) Ketones, "peripheral"	R-CH ₂ -CO-CH ₃	388	
"inner"	R-CH ₂ -CO-CH ₂ -R'	355	
(10) Fatty acid esters (our data)			
methyl esters	R-CH ₂ -COOCH ₃	294	302.88 ± 4.71 (99.91 ± 0.45) (<i>n</i> = 9, <i>R</i> ² = 0.9999, <i>p</i> = 0.0001)
ethyl esters	R-CH ₂ -COOC ₂ H ₅	270	288.85 ± 16.55 (96.79 ± 1.50) (<i>n</i> = 10, <i>R</i> ² = 0.9981, <i>p</i> = 0.0001)
propyl esters	R-CH ₂ -COOC ₃ H ₇	259	288.70 ± 16.09 (95.93 ± 1.34) (<i>n</i> = 10, <i>R</i> ² = 0.9984, <i>p</i> = 0.0001)
butyl esters	R-CH ₂ -COOC ₄ H ₇	256	276.50 ± 25.48 (96.34 ± 2.15) (<i>n</i> = 6, <i>R</i> ² = 0.9980, <i>p</i> = 0.0001)
(11) Ether linkage	C-CH ₂ -O-CH ₂ -C	70	
(12) Alkyl thiol	R-SH	370	
(13) Sulfide linkage	R-S-R'	256	
(14) Disulfide linkage	R-S-S-R'	377	
(15) Terminal carbon-carbon double bond	R-CH ₂ -CH=CH ₂	40	
(16) Terminal carbon-carbon triple bond	R-CH ₂ -C≡CH	300	
(17) Non-terminal carbon-carbon double bond	R-CH=CH-R'	60	
(18) Quaternary carbon atom	$\begin{array}{c} C \\ \\ C-C-C \\ \\ C \end{array}$	(-)100	

(Continued on p. 88)

TABLE I (continued)

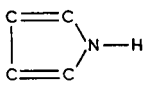
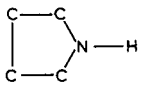
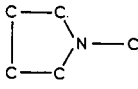
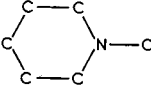
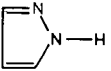
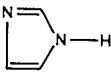
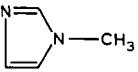
Substituent and functional group	Formula	GRF	
		Calculated by eqn. 7 ($A = 100$)	By linear regression equation
(19) Tertiary carbon atom	$\begin{array}{c} \text{C} \\ \\ \text{C}-\text{C}-\text{X} \\ \\ \text{C} \end{array}$	(-) 75	
(20) Iso carbon/chain branching	R-CH(CH ₃) ₂ or R-CHR ₁ R ₂	(-) 50	
(21) Adjacent carbon-carbon double bond and carbonyl bond	R-C=C-C=O	53	
(22) N-Ethylamine group	R-NH-C ₂ H ₅	(-) 50	
(23) Acid amide group	R-CO-NH ₂	1600 ($A = 45$)	
(24) Monosubstituted acid amido group	R-CO-NHR'	1430 ($A = 45$)	
(25) Disubstituted acid amido group	R-CO-NR' ₂	1016 ($A = 64$)	
(26) Chlorine atom connected to methylene group	R-CH ₂ -Cl	464	426.91 ± 2.42 (104.11 ± 0.24) ($n = 11, R^2 = 1.0000, p = 0.0001$)
(27) Bromine atom connected to methylene carbon	R-CH ₂ -Br	592	515.33 ± 8.75 (107.89 ± 0.81) ($n = 12, R^2 = 0.9994, p = 0.0001$)
(28) Bromine atom connected to tertiary carbon	R-CH-Br	492	486.05 ± 18.18 (100.72 ± 2.22) ($n = 5, R^2 = 0.9985, p = 0.0001$)
(29) Bromine atom in 2-bromoalkanoic acids, ethyl ester	R-CHBr-COOC ₂ H ₅	386	
(30) Iodine atom connected to methylene atom	R-CH ₂ -I	710	633.85 ± 5.71 (109.88 ± 0.66) ($n = 12, R^2 = 0.9996, p = 0.0001$)
(31) Difference between <i>cis</i> and <i>trans</i> isomers		60	
<i>(B) Alicyclic series</i>			
(1) Cyclopropane ring	C ₃ H ₆	105	
(2) Cyclobutane ring	C ₄ H ₈	110	
(3) Cyclopentane ring	C ₅ H ₁₀	122	
(4) Cyclopentene ring	C ₅ H ₈	163	
(5) Cyclopentadiene ring	C ₅ H ₆	210	
(6) Cyclohexane ring	C ₆ H ₁₂	123	
(7) Cyclohexene ring	C ₆ H ₁₀	208	
(8) Cycloheptane ring	C ₇ H ₁₄	183	
(9) Cycloheptene ring	C ₇ H ₁₂	217	
(10) Difference between <i>cis</i> and <i>trans</i> isomers		30	
(11) Alicyclic -OH group	>CH-OH	580	
(12) Alicyclic C=O group	>C=O	465	
(13) C=C-C=O group in cyclopentene ring	C=C-C=O	106	
(14) C=C-C=O group in cyclohexene ring	C=C-C=O	40	
(15) Oxygen atom in the 5-membered ring	-O-	80	
(16) Oxygen atom in the 6-membered ring	-O-	160	
(17) Alicyclic amino group	>CH-NH ₂	350	
(18) Sulfur atom in 5-membered ring	>S	200	
(19) Imino group in cyclopentadiene ring		800	
(20) Imino group in cyclopentane ring		380	

TABLE I (continued)

Substituent and functional group	Formula	GRF	
		Calculated by eqn. 7 (A = 100)	By linear regression equation
(21) Tertiary nitrogen atom in azole ring		140	
(22) Tertiary nitrogen atom in azine ring		200	
(23) 1,2-Diaza group in azole ring		300	
(24) 1,3-Diaza group in azole ring		800	
(25) 1,3-Diaza group in N-methylated azole ring		550	
(26) One C=C bond in azole ring, additional contribution		40	
(27) Two C=C bonds in azole ring, additional contribution		190	
(28) Imino -NH- group connected to 2 double bonds in 5-membered ring	C=C-NH-C=C	800	
(29) Methyl group ortho to ring N		(-) 70	
(30) Imino -NH- group in azine ring		325	
(31) 1,4-Diaza group in azine ring		30	
(32) 1,3-Diaza group in azine ring		80	
(33) 1,2-Diaza group in azine ring		520	
(34) Cl atom attached to cyclohexane ring	R'-Cl	440	
(35) Cl atom attached to 1-cyclohexene ring		369	
(36) Br atom attached to cyclohexane ring	R'-Br	580	
(37) Br atom attached to 1-cyclohexene ring		516	
(38) I atom attached to cyclohexane ring	R'-I	726	
(39) I atom connected to 1-cyclohexene ring		676	
(C) Aromatic series			
(1) Benzene ring		350	
(2) 1,3-Cyclohexadiene ring		264	
(3) 1,4-Cyclohexadiene ring		314	
(4) Ethynyl group connected to phenyl ring	Ar-C≡CH	210	
(5) Carbon-carbon double bond connected to phenyl ring	Ar-CH=CH ₂	80	
(6) Fusion between two phenyl rings		60	
(7) Link between two phenyl rings		80	
(4) Phenolic -OH	Ar-OH	900	
(5) Aryl ether -O- linkage	Ar-O-R	190	
(6) Aryl aldehyde/ketone	Ar-CHO or Ar-CO-R(Ar')	388	
(7) Aryl thiol	Ar-SH	340	
(8) Aryl -NH ₂ group	Ar-NH ₂	667	

(Continued on p. 90)

TABLE I (continued)

Substituent and functional group	Formula	GRF	
		Calculated by eqn. 7 ($A = 100$)	By linear regression equation
(9) Aryl aryl imino -NH- group	Ar-NH-Ar'	586	
(10) Aryl alkyl imino -NH- group	Ar-NH-R	523	
(11) Additional -NH- group to N-methyl piperidine ring		240	
(12) Phenyl dimethylamino group	Ar-N(CH ₃) ₂	260	
(13) Tertiary nitrogen in 6-membered ring	C-N=C	240	
(14) Additional nitrogen to form 1,4-diaza ring	C-N=C-C=N	30	
(15) Additional nitrogen to form 1,3-diaza ring	C-N=C-N=C	80	
(16) Additional nitrogen to form 1,2-diaza ring	C-N=N-C or C=N-N=C	520	
(17) Nitrogen in the iso position of the quinoline ring		40	
(18) Methyl group in the <i>ortho</i> position to ring N		(-) 70	
(19) Methyl group in the <i>para</i> position to ring N		70	
(20) Methyl group in the <i>peri</i> position to ring N		(-)100	
(21) Aryl chlorine atom	Ar-Cl	276	
(22) Aryl bromine atom	Ar-Br	426	
(23) Aryl iodine atom	Ar-I	604	
(24) Size factor		120	
(D) <i>Ortho</i> effects			
(1) Adjacent groups in benzene ring			<i>Ortho</i> effect <i>a/b</i>
CH ₃ + CH ₃		(+) 50	
CH ₃ + COOH		(-) 40	
CH ₃ + N(C ₂ H ₅) ₂		(-)300	
C ₆ H ₅ + C ₆ H ₅		(-)400	
NH ₂ + C ₂ H ₅		(-) 70	
NH ₂ + Cl		(-) 70	
NH ₂ + OCH ₃		(-)160	
NH ₂ + OC ₂ H ₅		(-)227	
NH ₂ + COOCH ₃		(-)200	
NH ₂ + CHO		(-)220	
OH + CH ₃		(-)100	
OH + C ₂ H ₅		(-)100	
OH + CH ₂ CH=CH ₂		(-)150	
OH + <i>tert.</i> -butyl		(-) 90	
OH + OCH ₃		(-)500	
OH + OC ₂ H ₅		(-)610	
OH + CHO		(-)870	
OH + CO-CH ₃		(-)870	
OH + CO-OC ₂ H ₅		(-)925	
Cl + OH		(-)390	
Br + OH		(-)242	
Br + CHO		(-)126	
CO-OC ₂ H ₅ + CO-OC ₂ H ₅		(-) 90	
(2) Conjugate substituents in 1,4 positions of phenyl ring			<i>Para</i> effect
CHO + OCH ₃		(+) 60	
CHO + N(CH ₃) ₂		(+)360	

^a Data from ref. 15.

^b The GRF values calculated by linear regression equations are given in the form of $GRF \pm S.E.$ ($A \pm S.E.$) where A is the regression coefficient and S.E. the standard errors. The statistics given are the number of data points (n), standard errors for the regression coefficient and the intercept (S.E.), the coefficient of determination (R^2) and the significance probability (p), *i.e.*, the probability of getting a greater F statistic than that obtained if the hypothesis is true. It should be pointed out that all regression analysis can be seriously distorted by a single incorrect data value (see ref. 3).

phase. The highly polar carboxyl, hydroxyl and amino groups interact strongly with the polar stationary phase and are retained longer than the less polar substituents. The difference between the I values of the analyte on polar and non-polar columns is known as the column difference (ΔI), expressed as follows:

$$\Delta I = (I)_{\text{CB-20M}} - (I)_{\text{SE-30}} \quad (5)$$

or

$$\Delta I = (GRF)_{\text{polar}} - (GRF)_{\text{non-polar}} \quad (6)$$

Eqn. 6 is based on the assumption that the analyte has similar A values on both polar and non-polar columns. The column difference is characteristic of the analyte molecule and is determined by aromaticity, unsaturation, conjugation, electron density and polarizability of the molecule [5].

It may be pointed out that the use of n -alkanes as markers for I calculation is preferred. Other markers such as methyl esters of fatty acids [6,7], 1-nitroalkanes [8], n -alkyl trichloroacetates [9], etc. [10,11] containing polar and polarizable groups that are not inert, may render the calculation of $GRFs$ difficult. The GRF can be a good index for ranking the polarity and polarizability of the stationary phases; this ability will be lost when polar and polarizable substances are used as markers. Research activities in the field of retention index, especially regarding the use of n -alkanes, have been comprehensively reviewed [12,13]. Contributions to I by primary, secondary, and tertiary alcohol functionalities were first discussed by Kováts in 1965 [14].

In the absence of known A and GRF values, the I value (I_p) may be predicted using the following expression [1]:

$$I_p = 100Z + \sum m_i - \sum n_i \quad (7)$$

where Z is the total number of carbon atoms and carbon equivalent atoms. The terms m_i and n_i represent the $GRFs$ of i th functional group and substituent. Acid, alcohol, aldehyde, amine, ether, ketone, phenol, single and fused phenyl rings, isolated and conjugated double bonds, *ortho* effect a , *para* effect, etc. give positive $GRFs$, and chain branching, quaternary carbon, *ortho* effect b , etc. give negative $GRFs$.

The A in eqn. 7 is arbitrarily assigned a value of

100 with the m_i and n_i adjusted accordingly to match the I_p with the observed value (I_{obs}). The I_p from eqn. 7 and the I from eqns. 3 and 4 should be within 3% error of the I_{obs} . On polar columns the I values for small molecules may show large fluctuations, and many polar compounds do not emerge from the column. Linear regression equations for all the homologous series studied have regression coefficients near 100, with only a few exceptions. This justifies the use of eqn. 7 as a predictor of I . $GRFs$ of substituents and functional groups for CW-20M and DB-Wax columns are given in Table I. Groups of the compounds studied are given below. I data from other sources are also included for comparison [15,16].

Cycloalkanes, cycloalkenes and aromatic hydrocarbons

Ring formation and the presence of double bonds increase I . For 6-membered carbocyclic ring compounds, the increase in I progresses from cyclohexane to cyclohexene to benzene. Cyclohexane, cyclohexene and benzene show GRF values of 123, 208 and 350 on polar column, and 62, 64 and 58 on non-polar column [1], respectively. The column difference (ΔI) is small for cyclohexane, moderate for cyclohexene and large for benzene. The GRF value for ring formation increases with increasing ring size from cyclopropane to cyclodecane. Other structural features, such as ring fusion, ring linkage, chain branching, etc. alter bond connectivity [17,18] and show only small column differences.

Table II lists the GRF and the functionality constants (Δm_f) of different hydrocarbon rings. Derivation of GRF and Δm_f is given by eqns. 4 and 5 in ref. 1. These terms are used interchangeably here. The I of cyclopentadiene is unavailable but can be extrapolated from those of cyclopentane and cyclopentene; the extrapolated value is used for predicting the I values of polynuclear aromatics and heterocyclics containing the cyclopentadiene ring.

The terminal double bonds in aliphatic hydrocarbons contribute less to I than the non-terminal double bonds; chain branching and the presence of tertiary and quaternary carbon atoms in the molecule reduce the I by 50, 75 and 100 on polar column, respectively. Substitution of a H atom in alicyclic hydrocarbons by a methyl or an alkyl group decreases the I by 50, due to chain branching. Chain

TABLE II
GRFs (Δm_f VALUES) FOR THE FORMATION OF ALICYCLIC HYDROCARBONS FROM THEIR LINEAR ANALOGUES

Compound	Formula	I_{obs}^a	100Z	Δm_f^a
Cyclopropane	C ₃ H ₆	405	300	105
Cyclopentane	C ₅ H ₁₀	622	500	122
Cyclopentene	C ₅ H ₈	663	500	163
Cyclohexane	C ₆ H ₁₂	723	600	123
Cyclohexene	C ₆ H ₁₀	808	600	208
1,3-Cyclohexadiene	C ₆ H ₈	864	600	264
1,4-Cyclohexadiene	C ₆ H ₈	914	600	314
Benzene	C ₆ H ₆	950	600	350
Cycloheptane	C ₇ H ₁₄	883	700	183
Cycloheptene	C ₇ H ₁₂	917	700	217
1,3-Cycloheptadiene	C ₇ H ₁₀	1060	700	360
1,3,5-Cycloheptatriene	C ₇ H ₈	1089	700	389
Cyclooctane	C ₈ H ₁₆	1014	800	214
Cyclooctene	C ₈ H ₁₄	1035	800	235
1,3-Cyclooctadiene	C ₈ H ₁₂	1100 ^b	800	300
1,5-Cyclooctadiene	C ₈ H ₁₂	1164	800	364
1,3,5,7-Cyclooctatetraene	C ₈ H ₈	1199	800	399
Cyclodecane	C ₁₀ H ₂₀	1361	1000	361

^a I_{obs} is the observed I ; Δm_f is the functionality constant.

^b Value taken from ref. 16.

branching alters the molecular connectivity. The fusion and bond linking of two alicyclic rings in decahydrodronaphthalene and bicyclohexyl exert no influence on their I values. A comparison of the observed and predicted I values of some aliphatic and aromatic hydrocarbons is given in Tables III and IV.

The I values of polynuclear aromatic hydrocarbons may require the inclusion of a size factor. The co-planarity resulting from two or more phenyl rings fusing together may increase the I of the molecule beyond the usually predicted value. Extended conjugated systems may also cause an increase in I .

Aliphatic carboxylic acids

The carboxylic acid group is highly polar; the lower homologues of the aliphatic acids can be chromatographed underivatized on polar and non-polar columns. The GRF for the aliphatic carboxyl group is 1029 for the A value equal to 100. In comparison, the GRF for the carboxyl group on non-polar DB-1 column is 257.09 with an associated

A value of 93.38 [1]. The column difference (ΔI) for the carboxyl group is about 770 units. Plotting the I_{obs} of a series of aliphatic carboxylic acid homologues against Z yields a straight line, as shown in Fig. 1. The regression coefficient (A) and the intercept (GRF) of the linear regression equation are given in Table I. The Δm_f for the aliphatic carboxyl group and the comparison of observed and predicted I of aliphatic carboxylic acids are given in Table V.

Carboxylic acid esters

On non-polar SE-30 column the esters of the fatty acids were found to behave chromatographically in the same way as aliphatic hydrocarbons [1]. The residual polarity and polarizability of the acid ester group may cause additional retention on CW-20M column. The GRF on polar column for this molecular moiety is equal to the column difference (ΔI). The methyl, ethyl, propyl and butyl acid esters have column differences of +294, +270, +259 and +256 units, respectively. This value must be added to the base value to yield the predicted I of the ester

TABLE III

COMPARISON OF OBSERVED AND PREDICTED I VALUES OF ALKANES^a

The $GRFs$ (m_i and n_i) have the following values: (1) quaternary carbon atom = -100, (2) non-terminal C=C double bond = +60, (3) chain branching = -50, (4) cyclohexane ring = +123, (5) cyclohexene ring = +208, (6) phenyl ring = +350, (7) ethynyl group connected to phenyl ring = +210, (8) cycloheptane ring = +183, (9) cycloheptene ring = +217, (10) terminal C=C bond = +40, (11) aryl ether -O- linkage = +190, (12) 1,3-cyclohexadiene = +264, (13) 1,4-cyclohexadiene ring = +314.

Compound	Formula	I_{obs}	Lit. [16]	$100Z + \Sigma m_i - \Sigma n_i$	I_p	Difference (%)
Neohexane	C ₆ H ₁₄	500		600 - 100	500	0
<i>n</i> -Hexane	C ₆ H ₁₄	619		600	600	3.07
2,2,4-Trimethylpentane	C ₈ H ₁₈	711		800 - 50 - 100	650	8.58
<i>n</i> -Heptane	C ₇ H ₁₆	712		700	700	1.69
2,4,4-Trimethyl-1-pentene	C ₈ H ₁₆	750		800 + 50 - 100 - 50	700	6.67
2-Heptene	C ₇ H ₁₄	753		700 + 60	760	0.92
Methylcyclohexane	C ₇ H ₁₄	784		700 + 123 - 50	773	1.4
1-Octene	C ₈ H ₁₆	831		800 + 50	850	2.23
3-Methyl-1-cyclohexene	C ₇ H ₁₂	852		700 + 208 - 50	858	0.7
4-Methyl-1-cyclohexene	C ₇ H ₁₂	859		700 + 208 - 50	858	1.16
1,3-Dimethylcyclohexane	C ₈ H ₁₆	860		800 + 123 - 2 × 50	823	4.3
2-Octene	C ₈ H ₁₆	875		800 + 60	860	1.71
1-Methyl-1-cyclohexene	C ₇ H ₁₂	900		700 + 208	908	0.88
Methylcycloheptane	C ₈ H ₁₆	935		800 + 183 - 50	933	0.21
Methylcycloheptene	C ₈ H ₁₄	1000		800 + 217 - 50	967	3.3
4-Vinyl-1-cyclohexene	C ₈ H ₁₂	1039		800 + 208 - 50 + 50	1008	2.98
1-Decene	C ₁₀ H ₂₀		1039	1000 + 40	1040	0.1
Dipentene (<i>p</i> -Mentha-1,8-diene)	C ₁₀ H ₁₆	1204		1000 + 203 + 50 - 50	1203	0.08
1-Methoxy-1,3-cyclohexadiene	C ₇ H ₁₀ O	1250		800 + 264 + 190	1254	0.32
1-Methoxy-1,4-cyclohexadiene	C ₇ H ₁₀ O	1268		800 + 314 + 190	1304	2.76
1-Dodecene	C ₁₂ H ₂₄		1241	1200 + 50	1250	0.72
Phenylacetylene	C ₈ H ₆		1361	800 + 350 + 210	1360	0.07
Tricyclo[6,4,0,0(2,7)]dodecane	C ₁₂ H ₂₀	1502		1200 + 2 × 123 + 80	1526	1.57
1-Hexadecene	C ₁₆ H ₃₂		1654	1600 + 50	1650	0.06
2,6,10,14-Tetramethylpentadecane	C ₁₉ H ₄₀		1668	1900 - 4 × 50	1700	1.88

^a The $GRFs$ are listed in the order of their appearance in the table. I_{obs} = observed I ; I_p = predicted I ; Difference % = (Difference between I_{obs} and I_p) × 100/(I_{obs} or I_p).

on polar column. Tables VI and VII show a comparison of the observed and predicted I values of some fatty acid esters and aromatic acid esters. Substituents and functional groups in the *ortho* positions of the aromatic ring tend to interact and form hydrogen bonding to decrease I substantially. These are known as *ortho* effects b with negative GRF values.

Acid amides

The acid amide group contains both N and O

atoms and is probably the most polar and polarizable substituent encountered in our study. The acid amido group can drastically alter the A value of the molecule. Since only a small number of the lower members of the acid amide series were studied, the A and the GRF values obtained for the lower members may deviate somewhat from the linear relationship for the series. Our study shows that the free, the N-substituted and the N,N-disubstituted acid amides have A values of 45, 45 and 64, and GRF values of 1600, 1430 and 1016, respectively. The

TABLE IV

COMPARISON OF OBSERVED AND PREDICTED I VALUES OF AROMATIC HYDROCARBONS^a

The $GRFs$ (m_i and n_i) have the following values: (1) phenyl ring = +350, (2) chain branching = -50, (3) cyclohexane ring = +123, (4) *trans* isomer-*cis* isomer = -60, (5) *ortho* effect a between two *ortho* methyl groups in the phenyl ring = +“50”, (6) aryl Cl atom = +276, (7) cyclopentene ring = +163, (8) cyclopropyl ring = +105, (9) cyclohexene ring = +208, (10) cyclopentadiene ring = +210, (11) fusion of two phenyl rings = +60, (12) aryl ether -O- linkage = +190, (13) link between two phenyl rings = +80, (14) double bond conjugated with phenyl ring = +80, (15) aryl Br atom = +426, (16) *ortho* effect b between two phenyl rings = -“400”, (17) size factor = +120. The quotation marks indicate that these values were arbitrarily selected.

Compound	Formula	I_{obs}	Lit. [16]	$100Z + \Sigma m_i - \Sigma n_i$	I_p	Difference (%)
Benzene	C ₆ H ₆	947		600 + 350	950	0.32
Toluene	C ₇ H ₈	1051	1043	700 + 350	1050	0.1
Ethyl benzene	C ₈ H ₁₀	1129		800 + 350	1150	1.93
<i>p</i> -Xylene	<i>p</i> -C ₈ H ₁₀	1155	1138	800 + 350	1150	0.43
<i>m</i> -Xylene	<i>m</i> -C ₈ H ₁₀	1164		800 + 350	1150	1.2
Cumene (isopropyl benzene)	C ₉ H ₁₂	1182		900 + 350 - 50	1200	1.5
Decahydronaphthalene, <i>trans</i>	C ₁₀ H ₁₈	1156	1163	1000 + 2 × 123 - 60	1186	2.53
<i>cis</i>		1216		1000 + 2 × 123	1246	2.41
Decahydronaphthalene, <i>cis</i>	C ₁₀ H ₁₈	1227	1232	1000 + 2 × 123	1246	1.52
<i>n</i> -Propylbenzene	C ₉ H ₁₂	1228		900 + 350	1250	1.76
<i>o</i> -Xylene	<i>o</i> -C ₈ H ₁₀	1232		800 + 350 + “50”	1200	2.6
1,3,5-Trimethyl benzene	C ₉ H ₁₂	1271		900 + 350	1250	1.65
<i>p</i> -Cymene (4-isopropyltoluene)	C ₁₀ H ₁₄	1272		1000 + 350 - 50	1300	2.15
1,2,4-Trimethyl benzene	C ₉ H ₁₂	1311		900 + 350 + 50	1300	0.84
<i>n</i> -Butylbenzene	C ₁₀ H ₁₄	1312	1316	1000 + 350	1350	2.81
<i>m</i> -Chlorotoluene	C ₇ H ₇ Cl		1313	700 + 350 + 276	1326	0.98
Indan	C ₉ H ₁₀	1377	1365	900 + 350 + 163	1413	2.55
Cyclopropyl benzene	C ₉ H ₁₂	1414		900 + 350 + 105	1355	4.17
Bicyclohexyl	C ₁₂ H ₂₂	1420	1431	1200 + 2 × 123	1446	1.79
1,2,4,5-Tetramethylbenzene	C ₁₀ H ₁₄	1459		1000 + 350 + 2 × 50	1450	0.62
Tetralin	C ₁₀ H ₁₂	1525	1525	1000 + 350 + 208	1558	2.31
Indene	C ₉ H ₈	1526	1479	900 + 350 + 208 + 60	1518	0.52
Perhydrofluorene	C ₁₃ H ₂₂		1632	1300 + 2 × 123 + 122	1668	2.16
Cyclohexyl benzene	C ₁₂ H ₁₆	1660	1662	1200 + 350 + 123	1673	0.66
1-Fluoronaphthalene	C ₁₀ H ₇ F		1715	1000 + 2 × 350 + 60	1760	2.56
Naphthalene	C ₁₀ H ₈	1739	1722	1000 + 2 × 350 + 60	1760	1.19
<i>o</i> -Dimethoxybenzene	C ₈ H ₁₀ O ₂		1715	1000 + 350 + 2 × 190	1730	0.87
2-Methyl naphthalene	C ₁₁ H ₁₀	1852		1100 + 2 × 350 + 60	1860	0.43
1-Methyl naphthalene	C ₁₁ H ₁₀	1855		1100 + 2 × 350 + 60	1860	0.27
1-Ethyl naphthalene	C ₁₂ H ₁₂		1943	1200 + 2 × 350 + 60	1960	0.87
Biphenyl	C ₁₂ H ₁₀	1974		1200 + 2 × 350 + 80	1980	0.3
Diphenylmethane	C ₁₃ H ₁₂		1994	1300 + 2 × 350	2000	0.3
2-Chloronaphthalene	C ₁₀ H ₇ Cl		2006	1000 + 2 × 350 + 276	2036	1.47
3,4-Dimethoxystyrene	C ₁₀ H ₁₂ O ₂	2039		1200 + 350 + 2 × 190 + 80	2010	1.42
Bibenzyl	C ₁₄ H ₁₄	2061		1400 + 2 × 350	2100	0.8
Acenaphthene	C ₁₂ H ₁₀	2133	2108	1200 + 2 × 350 + 163 + 60	2123	0.47
1-Methoxynaphthalene	C ₁₁ H ₁₀ O		2143	1200 + 2 × 350 + 60 + 190	2150	0.32
1-Phenyldodecane	C ₁₈ H ₃₀		2155	1800 + 350	2150	0.23
1-Bromonaphthalene	C ₁₀ H ₇ Br		2157	1000 + 2 × 350 + 60 + 426	2186	1.33
1,2,3,4,5,6,7,8-Octahydroanthracene	C ₁₄ H ₁₈	2153		1400 + 350 + 2 × 208	2166	0.6

TABLE IV (continued)

Compound	Formula	I_{obs}	Lit. [16]	$100Z + \Sigma m_i - \Sigma n_i$	I_p	Difference (%)
Fluorene	$C_{13}H_{10}$	2264	2311	$1300 + 2 \times 350 + 208 + 2 \times 60$	2328	2.75
<i>o</i> -Terphenyl	$C_{18}H_{14}$	2649		$1800 + 3 \times 350 + 2 \times 80 - "400"$	2610	1.47
Anthracene	$C_{14}H_{10}$	2630		$1400 + 3 \times 350 + 2 \times 60 + 120$	2690	0.81
Phenanthrene	$C_{14}H_{10}$	2712		$1400 + 3 \times 350 + 2 \times 60 + 120$	2690	0.03
<i>p</i> -Terphenyl	$C_{18}H_{14}$	3129		$1800 + 3 \times 350 + 2 \times 80 + 120$	3130	0.03
Pyrene	$C_{16}H_{10}$	3135		$1600 + 4 \times 350 + 120$	3120	0.48
2,3-Benzanthracene	$C_{18}H_{12}$	9999				
Triphenylene	$C_{18}H_{12}$	9999				

^a See footnote in Table III.

magnitude and trend of these A and GRF values suggest that substitution in highly polar and polarizable functional groups not only reduces the GRF but also alters the A value. Table VIII shows the comparison of observed and predicted I values of some free and substituted acid amides.

In Table VIII, formamide appears to have a higher I than acetamide, even though the latter has one more carbon atom than the former. In formamide the acid amido group is connected to a H

atom but not to a C atom. The atom to which the functional group is connected can strongly influence the GRF value. Other examples are amino $-NH_2$ and alcoholic $-OH$ groups which give different $GRFs$ when connected to secondary and tertiary C atoms.

Aliphatic alcohols

The primary alcohol ($-CH_2-OH$) group has a GRF value of +162 on non-polar column [1] and +641 on polar column, with a column difference of approximately 480. The hydroxyl group is one of the most polar functional groups. The linear plot of Z vs. I for the alkanols is given in Fig. 1 and the corresponding coefficient and intercept for the linear regression equation are listed in Table I.

Hydroxyl groups connected to secondary and tertiary carbon atoms form secondary and tertiary aliphatic alcohols and have GRF values of +530 and +410, respectively, on polar column. On non-polar column, the secondary and tertiary alcoholic $-OH$ groups have GRF values of +85 and +15, respectively [1], yielding a column difference slightly smaller than the primary alcoholic $-OH$ group. Table IX shows the Δm_f for the hydroxyl group in n -alkanols, and Table X compares the observed and predicted I values of other alcohols.

Phenols

The phenolic $-OH$ group can undergo conjugation with the ring to yield a co-planar structure which gives a higher GRF than the alcoholic $-OH$ group. The I values of the phenols listed in Table XI are taken from ref. 14. Substituents at the *ortho*

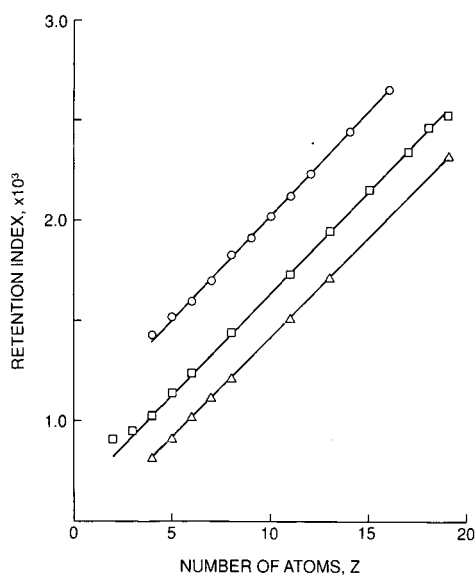


Fig. 1. Linear plots of I vs. the number of atoms (Z) of the homologous series of alkanolic acids (\circ), alkanols (\square) and aminoalkanes (\triangle) on polar column.

TABLE V

THE Δm_f OF THE ALIPHATIC CARBOXYL GROUP AND COMPARISON OF OBSERVED AND PREDICTED I VALUES OF n -ALKANOIC ACIDS (ON CW-20M)^a

The $GRFs$ have the following values: (1) aliphatic carboxylic acid group, R-COOH = +1029, (2) chain branching = -50, (3) cyclobutane ring = +110, (4) cyclopentane ring = +122.

Compound	Formula	I_{obs}	Lit.	100Z	Δm_f	I_p	Difference (%)
Acetic acid	C ₂ H ₄ O ₂	1430	1430 [16]	400	1030	1429	0.07
<i>n</i> -Propionic acid	C ₃ H ₆ O ₂	1518	1523 [16]	500	1018	1529	0.72
<i>n</i> -Butanoic acid	C ₄ H ₈ O ₂	1600	1614 [16]	600	1000	1629	1.78
<i>n</i> -Pentanoic acid	C ₅ H ₁₀ O ₂	1706		700	1006	1729	1.33
2-Methylpentanoic acid	C ₆ H ₁₂ O ₂		1746 [16]			1779	1.86
<i>n</i> -Hexanoic acid	C ₆ H ₁₂ O ₂	1834	1822 [16]	800	1034	1829	0.27
<i>n</i> -Heptanoic acid	C ₇ H ₁₄ O ₂	1916	1962 [15] 1935 [16]	900	1016	1929	0.67
<i>n</i> -Octanoic acid	C ₈ H ₁₆ O ₂	2029	2072 [15]	1000	1029	2029	0
<i>n</i> -Nonanoic acid	C ₉ H ₁₈ O ₂	2132	2182 [15]	1100	1032	2129	0.14
<i>n</i> -Decanoic acid	C ₁₀ H ₂₀ O ₂	2238	2290 [15]	1200	1038	2229	0.4
Lauric acid	C ₁₂ H ₂₄ O ₂	2451		1400	1051	2429	0.9
Myristic acid	C ₁₄ H ₂₈ O ₂	2660		1600	1060	2629	1.17
Average				1028.55 ± 17.94			
				(100Z + $\Sigma m_i - \Sigma n_i$)			
Cyclobutane carboxylic acid	C ₅ H ₈ O ₂		1831 [16]	700 + 110 + 1029		1839	0.44
Cyclopentane propionic acid	C ₈ H ₁₄ O ₂		2169 [16]	1000 + 122 + 1029		2151	0.83
Cyclopentane carboxylic acid	C ₆ H ₁₀ O ₂		1932 [16]	800 + 122 + 1029		1951	0.97

^a See footnote in Table III.

TABLE VI

COLUMN DIFFERENCES AND I VALUES OF METHYL ESTERS OF ALIPHATIC ACIDS ON NON-POLAR AND POLAR COLUMNS^a

The $GRFs$ (m_i and n_i) have the following values: (1) ethyl ester group = +270, (2) ether -O- linkage = +70.

Compound	Formula	I_{obs}		Column difference (ΔI)
		On SE-30	On CW-20M	
<i>Methyl esters</i>				
Methyl propionate	C ₄ H ₈ O ₂	613	900	287
Methyl butyrate	C ₅ H ₁₀ O ₂	711	1000	289
Methyl pentanoate	C ₆ H ₁₂ O ₂	808	1109	301
Methyl hexanoate	C ₇ H ₁₄ O ₂	908	1200	292
Methyl heptanoate	C ₈ H ₁₆ O ₂	1007	1302	295
Methyl octanoate	C ₉ H ₁₈ O ₂	1110	1400	290
Methyl nonanoate	C ₁₀ H ₂₀ O ₂	1200	1507	307
Methyl decanoate	C ₁₁ H ₂₂ O ₂	1309	1600	291
Methyl laurate	C ₁₃ H ₂₆ O ₂	1503	1800	297
Average				294.33 ± 6.42

TABLE VI (continued)

Compound	Formula	I_{obs}		Column difference (ΔI)	
		On SE-30	On CW-20M		
<i>Ethyl esters</i>					
Ethyl acetate	C ₄ H ₈ O ₂	600	900	300	
Ethyl propionate	C ₅ H ₁₀ O ₂		966		
Ethyl butyrate	C ₆ H ₁₂ O ₂	787	1046	262	
Ethyl pentanoate	C ₇ H ₁₄ O ₂	885	1149	264	
Ethyl hexanoate	C ₈ H ₁₆ O ₂	982	1246	264	
Ethyl heptanoate	C ₉ H ₁₈ O ₂	1084	1345	261	
Ethyl octanoate	C ₁₀ H ₂₀ O ₂	1180	1451	271	
Ethyl nonanoate	C ₁₁ H ₂₂ O ₂	1282	1552	270	
Ethyl decanoate	C ₁₂ H ₂₄ O ₂	1378	1645	267	
Ethyl laurate	C ₁₄ H ₂₈ O ₂	1537	1848	275	
			Average	274.44 ± 11.99	
<i>Propyl esters</i>					
Propyl acetate	C ₅ H ₁₀ O ₂		986		
Propyl propionate	C ₆ H ₁₂ O ₂	794	1059	265	
Propyl butyrate	C ₇ H ₁₄ O ₂	882	1137	255	
Propyl pentanoate	C ₈ H ₁₆ O ₂	980	1233	253	
Propyl hexanoate	C ₉ H ₁₈ O ₂	1080	1337	257	
Propyl heptanoate	C ₁₀ H ₂₀ O ₂	1177	1434	257	
Propyl octanoate	C ₁₁ H ₂₂ O ₂	1277	1539	262	
Propyl nonanoate	C ₁₂ H ₂₄ O ₂	1376	1631	255	
Propyl decanoate	C ₁₃ H ₂₆ O ₂	1471	1729	258	
Propyl laurate	C ₁₅ H ₃₀ O ₂	1661	1930	269	
			Average	259.00 ± 5.27	
<i>Butyl esters</i>					
Butyl formate	C ₅ H ₁₀ O ₂	712	1033	321	
Butyl propionate	C ₇ H ₁₄ O ₂	891	1157	266	
Butyl butyrate	C ₈ H ₁₆ O ₂	979	1227	248	
Butyl valerate	C ₉ H ₁₈ O ₂	1078	1336	258	
Butyl hexanoate	C ₁₀ H ₂₀ O ₂	1175	1427	252	
Butyl heptanoate	C ₁₁ H ₂₂ O ₂	1278	1533	255	
Butyl nonanoate	C ₁₃ H ₂₆ O ₂	1470	1725	255	
			Average	255.67 ± 6.09	
		Lit. [16]	(100Z + Σm_i and Σn_i)	I_p	Difference (%)
2-Ethoxyethanol, acetate	C ₆ H ₁₂ O ₃	1290	900 + 270 + 70	1240	3.88
Ethylene glycol diacetate	C ₆ H ₁₁ O ₄	1539	1000 + 2 × 270	1540	0.06
2-(2-Butoxyethoxy)ethanol, acetate	C ₁₀ H ₂₀ O ₄	1838	1400 + 270 + 2 × 70	1810	1.52
Triethylene glycol, diacetate	C ₁₀ H ₁₈ O ₆	2337	1600 + 2 × 270 + 2 × 70	2337	2.44

^a See footnote in Table III.

position of the phenol can interact and hydrogen bond with the adjacent phenolic -OH group to mask its functionality and reduce I . The decrease in I of the o -isomers is attributed to $ortho$ effect b and is

obtained as the difference between the I values of the o -isomer and the m -isomer. In the absence of $para$ effect, the I values of the p -isomer may be used for that of the m -isomer.

TABLE VII

COMPARISON OF OBSERVED AND PREDICTED I VALUES OF SOME MIXED ACID ESTERS^a

The $GRFs$ (m_i and n_i) have the following values: (1) non-terminal C=C double bond = +60, (2) methyl ester group = +295, (3) conjugation of the -C=C-O group in alkane chain = +53, (4) cyclohexane ring = +123, (5) cyclopentadiene ring = +210, (6) O atom in 5-membered ring = +80, (7) conjugation of -C=C-O group in 5-membered ring = +106, (8) phenyl ring = +350, (9) cyclopentane ring = +122, (10) *ortho* effect b between methyl and carboxy group = -"40", (11) carboxy group = +270, (12) butyl ester group = +256, (13) propyl ester group = +259, (14) *ortho* effect b between two carboxy groups = -"90".

Compound	Formula	I_{obs}	Lit. [16]	$100Z + \Sigma m_i$ and Σn_i	I_p	Difference (%)
Crotonic acid, methyl ester	C ₅ H ₈ O ₂		1108	700 + 60 + 295 + 53	1108	0
Methyl cyclohexane carboxylate	C ₈ H ₁₃ O ₂	1384		1000 + 123 + 295	1418	2.39
2-Furoic acid, methyl ester	C ₆ H ₆ O ₃		1570	900 + 210 + 80 + 295 + 106	1591	1.32
Methyl benzoate	C ₈ H ₈ O ₂	1678	1614	1000 + 350 + 295	1645	1.97
Tetrahydrofurfuryl alcohol propionate	C ₈ H ₁₄ O ₃	1635		1100 + 122 + 80 + 295	1597	2.32
Phenyl acetate	C ₈ H ₈ O ₂	1660		1000 + 350 + 295	1645	0.9
<i>o</i> -Tolyl acetate	C ₉ H ₁₀ O ₂	1716		1100 + 350 + 295 - "40"	1705	0.64
Ethyl benzoate	C ₉ H ₁₀ O ₂	1718	1659	1100 + 350 + 270	1720	0.12
<i>m</i> -Tolyl acetate	C ₉ H ₁₀ O ₂	1756		1100 + 350 + 295	1745	0.63
<i>p</i> -Tolyl acetate	C ₉ H ₁₀ O ₂	1769		1100 + 350 + 295	1745	1.36
Benzyl acetate	C ₉ H ₁₀ O ₂	1779		1100 + 350 + 295	1745	1.91
Ethyl phenylacetate	C ₁₀ H ₁₂ O ₂	1821		1200 + 350 + 270	1820	0.05
2-Phenylethyl acetate	C ₁₀ H ₁₂ O ₂	1854		1200 + 350 + 295	1845	0.49
<i>n</i> -Butyl benzoate	C ₁₁ H ₁₄ O ₂	1903		1300 + 350 + 256	1906	0.16
2-Furoic acid, propyl ester	C ₈ H ₁₀ O ₃		1696	1100 + 210 + 80 + 259	1649	2.77
2-Furoic acid, hexyl ester	C ₁₁ H ₁₆ O ₃		2000	1400 + 210 + 80 + 256	1946	2.7
<i>n</i> -Amyl benzoate	C ₁₂ H ₁₆ O ₂	2017		1400 + 350 + 256	2006	0.55
Methyl <i>p</i> -anisate	C ₉ H ₁₀ O ₃	2084		1200 + 350 + 295 + 190	2035	1.31
Ethyl cinnamate	C ₁₁ H ₁₂ O ₂	2173		1400 + 350 + 60 + 270 + 53	2133	1.84
<i>n</i> -Heptyl benzoate	C ₁₄ H ₂₀ O ₂	2217		1600 + 350 + 256	2206	0.5
<i>m</i> -Phenylene diacetate	C ₁₀ H ₁₀ O ₄	2301		1400 + 350 + 2 × 295	2340	1.67
Dimethyl phthalate	C ₁₀ H ₁₀ O ₄	2325		1400 + 350 + 2 × 295	2340	0.64
Diethyl phthalate	C ₁₂ H ₁₄ O ₄	2400		1600 + 350 + 2 × 270 - "90"	2400	0
<i>n</i> -Decyl benzoate	C ₁₇ H ₂₆ O ₂	2519		1900 + 350 + 256	2506	0.52
Benzyl benzoate	C ₁₄ H ₁₂ O ₂	2638		1600 + 2 × 350 + 295	2595	1.66

^a See footnote in Table III.

Ethers and sulfides

On non-polar columns the ethers behave chromatographically as hydrocarbons, but on polar columns the ethers are retained longer. The free electron pairs on the ether oxygen atom can interact with the polar stationary phase to prolong the retention of the ether. The straight chain aliphatic ether oxygen has a GRF value of +70.

Oxygen attached to the phenyl ring can assume a co-planar configuration with the ring and enhance retention. Aromatic ether -O- linkage has a GRF of

+190 in anisole. In diphenyl ether the bulky substituents can sterically hinder the interaction of the ether oxygen with the stationary phase to reduce the GRF value. A comparison of the observed and predicted I values of ethers is given in Table XII.

The GRF for the sulfide group is +256 and that for the disulfide group is +377. The sulfide group is similar to an ether in structure except that the ether oxygen is replaced with a sulfur atom. The sulfur atom is assigned an equivalency of two carbon atoms and contributes 200 units in I .

TABLE VIII

COMPARISON OF OBSERVED AND PREDICTED I VALUES OF ACID AMIDES^a

The $GRFs$ have the following values: (1) amido $-CO-NH_2$ group = +1600, (2) amido $-CO-NHR$ group = +1430, (3) amido $-CO-NR_2$ group = +1016, (4) for the value of A , the I increment for atom addition, see text, (5) $-NH-C_2H_5$ group = -50, (6) phenyl ring = +350, (7) tertiary N atom in aryl ring = +240.

Compound	Formula	I_{obs}	Lit. [16]	$AZ + \Sigma m_i$	I_p	Difference (%)
Formamide	CH ₃ NO	1791		$3 \times 45 + 1600$	1735	3.13
Acetamide	C ₂ H ₄ NO	1775	1725	$4 \times 45 + 1600$	1780	2.81
Propionamide	C ₃ H ₆ NO	1821	1801	$5 \times 45 + 1600$	1825	0.22
N-Methylformamide	C ₂ H ₅ NO		1615	$4 \times 45 + 1430$	1610	0.31
N-Methylacetamide	C ₃ H ₇ NO	1648	1609	$5 \times 45 + 1430$	1655	0.42
N-Ethylacetamide	C ₄ H ₉ NO		1608	$6 \times 45 + 1430 - 50$	1650	2.55
N-Methylpropionamide	C ₄ H ₈ NO	1690	1645	$6 \times 45 + 1430$	1700	0.59
N-Butylacetamide	C ₆ H ₁₃ NO		1793	$8 \times 45 + 1430$	1790	0.17
N-Allylacrylamide	C ₆ H ₉ NO		1871	$8 \times 45 + 1430 + 2 \times 40$	1870	0.05
N,N-Dimethylformamide	C ₃ H ₆ NO	1327	1312	$5 \times 64 + 1016^b$	1336	0.67
N,N-Dimethylacetamide	C ₄ H ₈ NO	1409	1384	$6 \times 64 + 1016$	1400	0.64
N,N-Diethylformamide	C ₅ H ₁₁ NO		1413	$7 \times 64 + 1016 - 50$	1414	0.07
N,N-Dimethylpropionamide	C ₅ H ₁₀ NO	1454		$7 \times 64 + 1016$	1464	0.68
N,N-Dibutylformamide	C ₉ H ₁₉ NO		1744	$11 \times 64 + 1016$	1720	1.38
N-Methylformanilide	C ₈ H ₉ NO		2027	$10 \times 64 + 1016 + 350$	2006	1.04
N,N-Diethylnicotinamide	C ₁₀ H ₁₄ N ₂ O		2353	$13 \times 64 + 1016 + 350 +$ $240 - 2 \times 50$	2338	0.64

^a See footnote in Table III.

^b Regression equation for N,N-disubstituted acid amides: $I = 63.50 Z \pm 1015.67$.

TABLE IX

GRF (Δm_i) OF ALCOHOL HYDROXYL GROUP AND COMPARISON OF OBSERVED AND PREDICTED I VALUES HOMOLOGOUS PRIMARY ALIPHATIC ALCOHOLS^a

Compound	Formula	I_{obs}	Lit.	100Z	Δm_i	I_p	Difference (%)
Methanol	CH ₄ O	909		200	709	847	6.82
Ethanol	C ₂ H ₆ O	944		300	644	947	0.32
1-Propanol	C ₃ H ₈ O	1025	1027 [16]	400	625	1047	2.1
1-Butanol	C ₄ H ₁₀ O	1141	1135 [16]	500	641	1147	0.52
1-Pentanol	C ₅ H ₁₂ O	1236	1200 [16]	600	636	1247	0.88
1-Hexanol	C ₆ H ₁₄ O		1367 [15]	700	667	1347	1.46
1-Heptanol	C ₇ H ₁₆ O	1440	1470 [15]	800	640	1447	0.48
1-Octanol	C ₈ H ₁₈ O		1573 [15]	900	673	1547	1.65
1-Decanol	C ₁₀ H ₂₂ O	1735	1778 [15] 1752 [16]	1100	635	1747	0.69
1-Dodecanol	C ₁₂ H ₂₆ O	1950	1983 [15]	1300	650	1947	0.15
1-Tetradecanol	C ₁₄ H ₃₀ O	2157		1500	657	2147	0.46
1-Hexadecanol	C ₁₆ H ₃₄ O	2352		1700	652	2347	0.21
1-Heptadecanol	C ₁₇ H ₃₆ O	2475		1800	657	2447	0.41
1-Octadecanol	C ₁₈ H ₃₈ O	2534		1900	634	2547	0.51
Average 647.00 ± 13.91							

^a See footnote in Table III. Regression equation for homologues of n -alkanols: $I = 100.54 Z + 641.34$.

TABLE X

COMPARISON OF OBSERVED AND PREDICTED I VALUES OF SOME ALCOHOLS (ON DB-WAX)^a

The $GRFs$ (m_i and n_i) have the following values: (1) aliphatic secondary alcohol $-OH = +530$, (2) aliphatic tertiary alcohol $-OH = +410$, (3) terminal $C=C$ double bond $= +40$, (4) chain branching $= -50$, (5) aliphatic primary alcohol $-OH = +647$, (6) terminal $C-C$ triple bond $= +300$, (7) quaternary C atom $= -100$, (8) 5-membered alicyclic ring $= +122$, (9) alicyclic $-OH = +580$, (10) alkyl ether $-O-$ link $= +70$, (11) alkyl $-Cl$ atom $= +464$, (12) 6-membered alicyclic ring $= +123$, (13) difference between *cis* and *trans* isomer $= +50$, (14) cyclohexene ring $= +208$, (15) alkyl $-Br$ atom $= +592$, (16) cycloheptane ring $= +183$, (17) aryl ether $-O-$ linkage $= +190$.

Compound	Formula	I_{obs}	Lit. [16]	$100Z + \Sigma m_i - \Sigma n_i$	I_p	Difference (%)
2-Propanol	C_3H_8O	942		400 + 530	930	0.96
<i>tert.</i> -Butyl alcohol	$C_4H_{10}O$	916		500 + 410	910	0.66
<i>tert.</i> -Amyl alcohol	$C_5H_{12}O$	1015		600 + 410	1010	0.49
2-Methyl-3-buten-2-ol	$C_5H_{10}O$		1023	600 + 410 + 40	1050	2.57
2-Butanol	$C_4H_{10}O$	1031	1082	500 + 530	1030	0.1
2,3-Dimethyl-2-butanol	$C_6H_{14}O$		1082	700 + 410 - 50	1060	2.03
2-Methyl-1-propanol	$C_4H_{10}O$	1092		500 + 647 - 50	1097	0.46
2-Pentanol	$C_5H_{12}O$		1110	600 + 530	1130	1.77
3-Pentanol	$C_5H_{12}O$		1110	600 + 530	1130	1.77
Allyl alcohol	C_3H_6O	1122	1110	400 + 647 + 40	1087	3.12
1-Methoxy-2-propanol	$C_4H_{10}O_2$	1135		600 + 530	1130	0.44
4-Methyl-2-pentanol	$C_6H_{14}O$	1181		700 + 530 - 50	1180	0.08
3-Ethyl-3-pentane	$C_7H_{16}O$		1196	800 + 410	1210	1.16
2-Methyl-3-butyn-2-ol	C_5H_8O	1230		600 + 410 + 300 - 100	1210	1.63
3-Methyl-1-butanol	$C_5H_{12}O$	1231		600 + 647 - 50	1197	3.09
3,3-Dimethyl-1-butanol	$C_6H_{14}O$		1249	700 + 647 - 100	1247	0.16
2-Methyl-2-heptanol	$C_8H_{18}O$		1280	900 + 410	1310	2.29
2-Ethyl-1-butanol	$C_6H_{14}O$	1312		700 + 647 - 50	1297	1.14
Cyclopentanol	$C_5H_{10}O$	1327	1297	600 + 122 + 580	1302	1.88
2-Propyn-1-ol	C_3H_4O	1357		400 + 647 + 300	1347	0.74
2-Methoxy-1-butanol	$C_5H_{12}O_2$		1359	700 + 647 + 70 - 50	1367	0.59
6-Methyl-2-heptanol	$C_8H_{18}O$		1365	900 + 530 - 50	1380	1.09
2-Chloroethanol	C_2H_5OCl	1379		300 + 647 + 464	1411	2.27
Cyclohexanol	$C_6H_{12}O$	1400	1392	700 + 123 + 580	1403	0.21
2-Methyl cyclohexanol <i>trans</i>	$C_7H_{14}O$	1438		800 + 123 + 580 - 50	1453	1.03
			1409			
3-Methyl cyclohexanol <i>trans</i> (32%)	$C_7H_{14}O$	1459				
<i>cis</i> (68%)		1482		800 + 123 + 580 - 50	1453	1.96
4-Methyl cyclohexanol <i>trans</i> (18%)	$C_7H_{14}O$	1456	1447			
<i>cis</i> (82%)		1476	1430	800 + 123 + 580 - 50	1453	1.56
2-Cyclohexen-1-ol	C_6H_8O	1479		700 + 208 + 580	1488	0.6
2-Bromoethanol	C_2H_5BrO		1492	300 + 647 + 592	1539	3.05
Tetrahydrofurfuryl alcohol	$C_5H_{10}O_2$	1496		700 + 122 + 647	1469	1.8
Cycloheptanol	$C_7H_{14}O$		1547	800 + 183 + 530	1513	2.2
1,3-Propanediol	$C_3H_8O_2$	1789		500 + 2 × 647	1794	0.28
Benzyl alcohol	C_7H_8O		1857	800 + 350 + 647	1797	3.23
Diethylene glycol	$C_4H_{10}O_3$		1953	700 + 2 × 647	1994	2.06
2[2-(2-Methoxyethoxy)-ethoxy]- ethanol	$C_7H_{16}O_4$		1963	1100 + 647 + 3 × 70	1957	0.31
α -Butyl benzyl alcohol	$C_{11}H_{16}O$		2050	1200 + 530 + 350	2080	1.44
2-(Benzoyloxy)ethanol	$C_9H_{12}O_2$	2129		1100 + 350 + 70 + 647	2167	1.75
2-Phenoxyethanol	$C_8H_{10}O_2$		2139	1000 + 350 + 190 + 647	2187	2.19

^a See footnote in Table III.

TABLE XI

COMPARISON OF OBSERVED AND PREDICTED *I* VALUES OF PHENOLS AND THIOLS^a

The *GRFs* (m_i and n_i) have the following values: (1) phenyl ring = +350, (2) aryl thiol -SH group = +340, (3) alkyl thiol -SH group = +370, (4) phenolic -OH group = +900, (5) aryl Cl atom = +276, (6) ortho effect b between -OH and -Cl = -"390", (7) aryl ether -O- linkage = +190, (8) ortho effect b between -OH and -OC₂H₅ groups = -"610", (9) ortho effect b between -OH and -OCH₃ groups = -"500", (10) ortho effect b between -OH and -CH₃ groups = -"100", (11) ortho effect b between -OH and -C₂H₅ groups = -"100", (12) ortho effect a between two adjacent methyl groups = + "50", (13) terminal C=C double bond = +40, (14) ortho effect b between -OH and allyl group = -"150", (15) aryl Br atom = +426, (16) ortho effect b between -OH and -Br atom = -"242", (17) quaternary C atom = -100, (18) ortho effect b between -OH and *tert.* butyl group = -"90".

Compound	Formula	<i>I</i> _{obs}	Lit. [16]	100Z + Σ <i>m</i> _{<i>i</i>} - Σ <i>n</i> _{<i>i</i>}	<i>I</i> _p	Difference (%)
Benzene thiol	C ₆ H ₆ S		1491	800 + 350 + 340	1490	0.07
Benzyl mercaptan	C ₇ H ₈ S		1618	900 + 350 + 370	1620	0.12
<i>o</i> -Chlorophenol	C ₆ H ₅ ClO		1830	700 + 350 + 900 + 276 - "390"	1836	0.33
<i>o</i> -Ethoxyphenol	C ₈ H ₁₀ O ₂		1831	1000 + 350 + 900 + 190 - "610"	1830	0.05
Guaiacol	C ₇ H ₈ O ₂		1840	900 + 350 + 900 + 190 - "500"	1840	0
2,6-Dimethylphenol	C ₈ H ₁₀ O		1889	900 + 350 + 900 - 2 × "100"	1950	3.13
<i>o</i> -Cresol	C ₇ H ₈ O		1979	800 + 350 + 900 - "100"	1950	1.47
Phenol	C ₆ H ₆ O	1954		700 + 350 + 900	1950	0.2
2-Ethylphenol	C ₈ H ₁₀ O		2044	900 + 350 + 900 - "100"	2050	0.29
<i>p</i> -Cresol	C ₇ H ₈ O		2055	800 + 350 + 900	2050	0.24
<i>m</i> -Cresol	C ₇ H ₈ O		2059	800 + 350 + 900	2050	0.44
2,3-Dimethylphenol	C ₈ H ₁₀ O		2120	900 + 350 + 900 + "50" - "100"	2100	0.94
2-Allylphenol	C ₉ H ₁₀ O		2132	1000 + 350 + 900 + 40 - "150"	2140	0.37
<i>o</i> -Bromophenol	C ₆ H ₅ BrO		2134	700 + 350 + 900 + 426 - "242"	2134	0
3,5-Dimethylphenol	C ₈ H ₁₀ O		2146	900 + 350 + 900	2150	0.19
3-Ethylphenol	C ₈ H ₁₀ O		2151	900 + 350 + 900	2150	0.05
<i>o-tert.</i> -Butyl phenol	C ₁₀ H ₁₄ O		2161	1100 + 350 + 900 - 100 - "90"	2160	0.05
3,4-Dimethylphenol	C ₈ H ₁₀ O		2189	900 + 350 + 900 + "50"	2200	0.5
<i>m</i> -Ethoxyphenol	C ₈ H ₁₀ O ₂		2427	1000 + 350 + 900 + 190	2440	0.53

^a See footnote in Table III.

Aldehydes and ketones

Aliphatic aldehyde and ketone groups are different in their attachment to C and H atoms but share the same *GRF* value. A similar situation also prevails for these groups on non-polar column. The keto group attached to a phenyl ring has the same *GRF* of +388 as for aliphatic ketones, but the keto group attached to an alicyclic ring has a higher *GRF* value of +465. Tables XIII and XIV show the comparison of observed and predicted *I* values of aliphatic, alicyclic and aromatic aldehydes and ketones.

In aromatic aldehydes and ketones, the 1,4 or *para* substituents can extend their conjugation through the phenyl ring to increase *I*; in contrast, the *ortho* substituents can mutually interact and hydrogen

bond to decrease *I*. *p*-Hydroxybenzaldehyde, *p*-dimethylaminobenzaldehyde and *p*-anisaldehyde belong to the first category and salicylaldehyde, 2'-hydroxyacetophenone and *o*-anisaldehyde to the second category. The effects of extended conjugation and hydrogen bonding are given, respectively, in terms of *GRF* values under the name of *para* effect and *ortho* effect *b* in Table I.

Aliphatic amines

The N and O atoms have electronegativity values of 3.0 and 3.5, respectively, as compared to 2.5 for the C atom [19]. This difference is reflected in the *GRFs* of the amino and hydroxyl groups. The aliphatic amino -NH₂ group is less polar than the

TABLE XII

COMPARISON OF OBSERVED AND PREDICTED I VALUES OF ETHERS AND SULFIDES^a

The $GRFs$ (m_i and n_i) have the following values: (1) aliphatic ether -O- linkage = +70, (2) sulfide -S- linkage = +256, (3) terminal C=C double bond = +40, (4) chain branching = -50, (5) aliphatic sulfide -S-S- linkage = +377, (6) tertiary C atom = -75, (7) phenyl ring = +350, (8) aryl ether -O- linkage = +190, (9) link between two phenyl rings = +80.

Compound	Formula	I_{obs}	Lit. [16]	$100Z + \Sigma m_i - \Sigma n_i$	I_p	Difference (%)
Ethyl ether	C ₄ H ₁₀ O	616	1842	500 + 70	570	7.47
Propyl ether	C ₆ H ₁₄ O	782		700 + 70	770	0.15
Butyl ether	C ₈ H ₁₈ O	971		900 + 70	970	0.1
Pentyl ether	C ₁₀ H ₂₂ O	1163	1161	1100 + 70	1170	0.6
Hexyl ether	C ₁₂ H ₂₆ O	1368	1359	1300 + 70	1370	0.15
Octyl ether	C ₁₆ H ₃₄ O	1763		1700 + 70	1770	0.39
Allyl sulfide	C ₆ H ₁₀ S		1151	800 + 256 + 2 × 40	1136	1.3
(2-Ethylhexyl) vinyl ether	C ₁₀ H ₂₀ O		1168	1100 + 70 + 40 - 50	1160	0.68
Butyl sulfide	C ₈ H ₁₈ S		1256	1000 + 256	1256	0
<i>tert.</i> -Butyl disulfide	C ₈ H ₁₈ S ₂		1323	1200 + 377 - 2 × 75	1727	0.23
Anisole	C ₇ H ₈ O	1340		800 + 350 + 190	1340	0
1,2-Dibutoxyethane	C ₁₀ H ₂₂ O ₂		1348	1200 + 2 × 70	1340	0.59
Isopentyl sulfide	C ₁₀ H ₂₂ S		1359	1200 + 256 - 2 × 50	1356	0.22
Propyl disulfide	C ₆ H ₁₄ S ₂	1377		1000 + 377	1377	0
Phenetole (ethoxybenzene)	C ₈ H ₁₀ O		1383	900 + 350 + 190 - 50	1390	0.5
Isobutyl disulfide	C ₈ H ₁₈ S ₂		1428	1200 + 377 - 2 × 50	1477	3.32
Benzyl ethyl ether	C ₉ H ₁₂ O		1438	1000 + 350 + 70	1420	1.25
<i>m</i> -Methylanisole	C ₈ H ₁₀ O		1441	900 + 350 + 190	1440	0.07
Butyl disulfide	C ₈ H ₁₈ S ₂		1567	1200 + 377	1577	0.63
<i>o</i> -Dimethoxybenzene	C ₈ H ₁₀ O ₂		1715	1000 + 350 + 2 × 190	1730	0.87
Bis(2-butoxyethyl)ether	C ₁₂ H ₂₆ O ₃		1727	1500 + 3 × 70	1710	0.98
1,3-Dimethoxybenzene	C ₈ H ₁₀ O ₂		1737	1000 + 350 + 2 × 190	1730	0.4
Pentyl disulfide	C ₁₀ H ₂₂ S ₂		1768	1400 + 377	1777	0.51
Phenyl ether	C ₁₂ H ₁₀ O	2055		1300 + 2 × 350 + 70	2070	0.72
Phenyl sulfide	C ₁₂ H ₁₀ S		2287	1400 + 2 × 350 + 256	2356	2.97
<i>o</i> -Phenylanisole	C ₁₃ H ₁₂ O		2246	1400 + 2 × 350 + 190		
Benzyl ether	C ₁₄ H ₁₄ O		2356	1500 + 2 × 350 + 70	2270	3.65
<i>p</i> -Phenoxyanisole	C ₁₃ H ₁₂ O ₂		2438	1500 + 2 × 350 + 190 + 80	2470	1.3

^a See footnote in Table III. Average GRF value for the alkyl ether linkage = 69.50 ± 7.01 .

alcoholic -OH group on polar column. The GRF for the aliphatic amino -NH₂ group is +416 as against +647 for the aliphatic primary alcoholic -OH group. Plotting the I values of the homologous primary amines against Z yields a straight line, as shown in Fig. 1. The A and GRF values for the aliphatic amines are given in Table I.

The aliphatic primary amino (-NH₂) group has a column difference of about +280. When the -NH₂

group is attached to a secondary or a tertiary carbon atom, the GRF is reduced to +350 or +229, respectively. The GRF value of the imino groups in the N,N-dialkyl-substituted secondary amines, such as dibutylamine, is about +180 but that for the N-alkyl-N-aralkyl substituted secondary amines is about +260. The GRF values for the tertiary N atom in N,N,N-trialkylsubstituted amines may vary with the size of the substituted alkyl groups.

TABLE XIII

COMPARISON OF OBSERVED AND PREDICTED I VALUES OF ALIPHATIC ALDEHYDES AND KETONES^a

The GRF s (m_i and n_i) have the following values: (1) "peripheral" aliphatic aldehyde or ketone group = +388, (2) "inner" keto group at 3 or 4 position of the carbon chain = +355, (3) chain branching = -50, (4) non-terminal C=C double bond = +60, (5) conjugation of -C=C=O group in alkane chain = +53.

Compound	Formula	I_{obs}	Lit.	$100Z + \sum m_i - \sum n_i$	I_p	Difference (%)
Acetone	C ₃ H ₆ O	816		400 + 388	788	3.43
Propanal	C ₃ H ₆ O	782		400 + 388	788	0.76
2-Methylpropanal	C ₄ H ₈ O		824 [15]	500 + 388 - 50	838	1.67
2-Butanal	C ₄ H ₈ O		910 [16]	500 + 388	888	2.42
3-Methyl butanal	C ₅ H ₁₀ O		928 [15]	600 + 388 - 50	938	1.07
3-Pentanone	C ₅ H ₁₀ O		977 [16]	600 + 388	988	1.11
2-Pentanone	C ₅ H ₁₀ O		992 [15]	600 + 388	988	0.4
2-Methyl-3-pentanone	C ₆ H ₁₂ O		1000 [16]	700 + 355 - 50	1005	0.5
4-Methyl-2-pentanone	C ₆ H ₁₂ O		1019 [15] 1012 [16]	700 + 388 - 50	1038	1.83
2-Butenal	C ₄ H ₆ O		1038 [16]	500 + 388 + 60 + 53	1001	3.56
3-Hexanone	C ₆ H ₁₂ O		1048 [16]	700 + 355	1055	0.66
2-Methyl-3-hexanone	C ₇ H ₁₄ O		1066 [16]	800 + 355 - 50	1105	3.53
2-Hexanone	C ₆ H ₁₂ O		1078 [16]	700 + 388	1088	0.92
Hexanal	C ₆ H ₁₂ O		1094 [15]	700 + 388	1088	0.54
Heptanal	C ₇ H ₁₄ O		1195 [15]	800 + 388	1188	0.59
2-Heptanone	C ₇ H ₁₄ O		1194 [15] 1180 [16]	800 + 388	1188	0.5
3-Heptanone	C ₇ H ₁₄ O		1124 [16]	800 + 355	1155	2.68
3-Octanone	C ₈ H ₁₆ O		1252 [16]	900 + 355	1255	0.24
Octanal	C ₈ H ₁₆ O		1297 [15]	900 + 388	1288	0.69
5-Nonanone	C ₉ H ₁₈ O		1325 [16]	1000 + 355	1355	2.21
Nonanal	C ₉ H ₁₈ O		1400 [15]	1000 + 388	1388	0.86
Decanal	C ₁₀ H ₂₀ O		1504 [15]	1100 + 388	1488	1.06
2-Heptadecanone	C ₁₇ H ₃₄ O		2148 [15]	1800 + 388	2188	1.83

^a See footnote in Table III. Average GRF value for the aldehyde group = 387.92 ± 17.55 .

The functionality of the tertiary amino groups in triethylamine, N,N-diethylbenzylamine, tributylamine, tripropylamine, tribenzylamine, etc. decreases with increasing size of the substituent groups. Plotting the GRF difference, namely ($I_{obs} - I_p$), of the tertiary amines against Z yields a linear relationship, as shown in Fig. 2. This means that bulky substituents tend to diminish I , and the GRF of the tertiary amino group decreases in proportion to the bulkiness of the substituents. This finding is in accord with an early observation that the highly substituted amines behave chromatographically as

n -alkanes [1]. Table XV shows the observed and predicted I values of some alkyl and alicyclic amines.

Aromatic amines

Aromatic amino groups in aniline, anisidine, toluidine, etc. have higher GRF values than the aliphatic amino groups, owing to co-planar configuration of the molecule as a result of conjugation with the phenyl ring. In the planar configuration the primary aromatic amino group is retained longer on the column and has a GRF of +667, considerably higher than that of the aliphatic primary amino

TABLE XIV

COMPARISON OF OBSERVED AND PREDICTED I VALUES OF ALICYCLIC AND AROMATIC ALDEHYDES AND KETONES^a

The $GRFs$ (m_i and n_i) have the following values: (1) 5-membered alicyclic ring = +122, (2) alicyclic carbonyl C=O group = +465, (3) 6-membered alicyclic ring = +123, (4) chain branching = -50, (5) cyclopentene ring = +163, (6) conjugation of -C=C=O group in 5-membered ring = +106, (7) cycloheptane ring = +183, (8) O atom in 5-membered ring = +80, (9) phenyl ring = +350, (10) aryl or alkyl C=O group = +388, (11) cyclohexene ring = +208, (12) quaternary C atom = -100, (13) conjugation of -C=C=O group in 6-membered ring = +40, (14) phenolic -OH group = +900, (15) *ortho* effect b between -OH and -COCH₃ groups = -"870", (16) aryl Br atom = +426, (17) *ortho* effect b between -Br and -CHO groups = -"126", (18) alkyl Br atom adjacent to C=O group = +386, (19) aryl ether -O—linkage = +190, (20) extended conjugation between -OCH₃ to -CHO groups in *para* positions of phenyl ring = +60, (20) alkyl -NH₂ group = +417, (21) ring fusion = +60, (22) tertiary amino Ar-N(CH₃)₂ group = +260, (23) *para* effect for the extended conjugation from -N(CH₃)₂ to -CHO = +360.

Compound	Formula	I_{obs}	Lit. [16]	100Z + Σm_i - Σn_i	I_p	Difference (%)
Cyclopentanone	C ₅ H ₈ O		1187	600 + 122 + 465	1187	0
Cyclohexanone	C ₆ H ₁₀ O		1289	700 + 123 + 465	1288	0.8
2-Methylcyclohexanone	C ₇ H ₁₂ O		1305	800 + 123 + 465 - 50	1338	2.47
3-Methylcyclohexanone	C ₇ H ₁₂ O		1324	800 + 123 + 465 - 50	1338	1.05
4-Methylcyclohexanone	C ₇ H ₁₂ O		1339	800 + 123 + 465 - 50	1338	0.07
2-Cyclopenten-1-one	C ₅ H ₆ O		1347	600 + 163 + 465 + 106	1334	0.97
Cycloheptanone	C ₇ H ₁₂ O		1417	800 + 183 + 465	1448	2.14
2-Furaldehyde	C ₅ H ₄ O ₂		1456	700 + 122 + 80 + 465	1455	0.07
Benzaldehyde	C ₇ H ₆ O	1517	1513	800 + 350 + 388	1538	1.36
3,5,5-Trimethyl-2-cyclohexen-1-one	C ₉ H ₁₄ O		1577	1000 + 208 + 465 + 40 - 100	1613	2.23
3,5-Dimethyl-2-cyclohexen-1-one	C ₈ H ₁₂ O		1597	900 + 208 + 465 + 40 - 50	1563	2.13
Acetophenone	C ₈ H ₈ O	1643		900 + 350 + 388	1638	0.3
Salicylaldehyde	C ₇ H ₆ O ₂		1665	900 + 350 + 900 + 388 - "870"	1668	0.18
Propiophenone	C ₉ H ₁₀ O		1712	1000 + 350 + 388	1738	1.49
<i>p</i> -Isopropylbenzaldehyde	C ₁₀ H ₁₂ O		1767	1100 + 350 + 388 - 50	1788	1.17
2'-Hydroxyacetophenone	C ₈ H ₈ O ₂		1784	1000 + 350 + 900 + 388 - "870"	1768	0.9
2-Bromobenzaldehyde	C ₇ H ₅ BrO		1838	800 + 350 + 388 + 426 - "126"	1838	0
Benzylacetone	C ₁₀ H ₁₂ O	1851		1100 + 350 + 388	1838	0.7
<i>o</i> -Anisaldehyde	C ₈ H ₈ O ₂		1941	1000 + 350 + 388 + 190	1928	0.67
2-Bromoacetophenone	C ₈ H ₇ BrO		1971	900 + 350 + 388 + 386	2024	2.62
<i>p</i> -Anisaldehyde	C ₈ H ₈ O ₂	2014	2000	1000 + 350 + 388 + 190 + 60	1988	0.6
<i>p</i> -Methoxypropiophenone	C ₁₀ H ₁₂ O ₂		2179	1200 + 350 + 388 + 190	2128	2.34
2-Aminoacetophenone	C ₈ H ₉ NO		2187	1000 + 350 + 388 + 417	2155	1.46
1-Naphthaldehyde	C ₁₁ H ₈ O		2364	1200 + 2 × 350 + 60 + 388	2348	0.68
Benzophenone	C ₁₃ H ₁₀ O	2457		1400 + 2 × 350 + 388	2488	1.25
<i>p</i> -Dimethylaminobenzaldehyde	C ₉ H ₁₁ NO	2459		1100 + 350 + 388 + 260 + "360"	2458	0.04

^a See footnote in Table III.

group. Secondary aromatic amines with two aryl substituents or with one alkyl and one aryl substituent on N atoms have $GRFs$ of +586 or +523, respectively. Tertiary aromatic amino groups with one aryl and two alkyl substituents on N atom as in

N,N-dimethylaniline, have a GRF of about +310, which may vary with the bulkiness of the substituents.

Table XVI shows the comparison of observed and predicted I values of some aromatic amines.

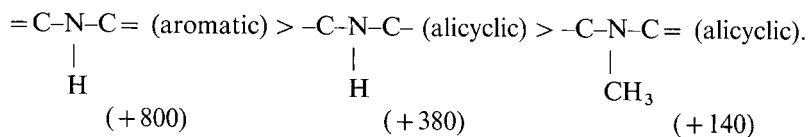
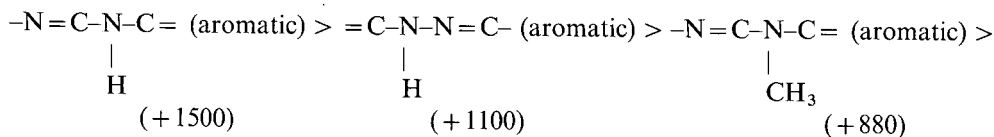
Heterocyclics

Ring compounds containing nitrogen and oxygen heteroatoms are functionally complex, which renders the prediction of *I* difficult. The number and position of aza and oxo atoms in the ring, ring size, degree of saturation, aromaticity, conjugation, position of substituents, etc. can all affect the *A* and *GRF* values. These compounds are difficult to chromatograph, because traces of moisture and unexpected interaction with the stationary phase can cause large variations. The oxo rings are less complex than the aza rings. The nitrogen atom in the ring, being trivalent, can bond as secondary and tertiary amines, and together with the ring function and conjugation, these groups can contribute differently to *I*. In comparison, the bivalent oxygen atom has its bonding orbitals completely satisfied in ring formation.

The ring oxygen is assigned a *GRF* value of +80 per atom in the 5-membered ring and +160 per atom in the 6-membered ring. Since the number of oxo compounds studied is small, these values are only tentative.

The *GRFs* of the functional groups in the aza rings are difficult to assess individually and independently because of the lack of homologs for comparative study. In the following we rank the aza moieties present in 5-membered and 6-membered rings according to their contribution to the *I* of the analyte:

(i) Aza and diaza moieties in 5-membered rings:



(ii) Aza and diaza moieties in 6-membered rings:

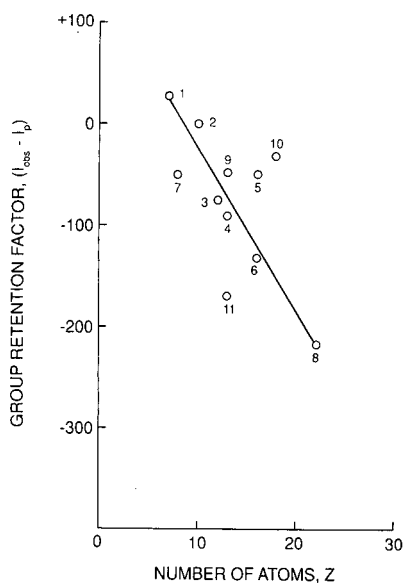
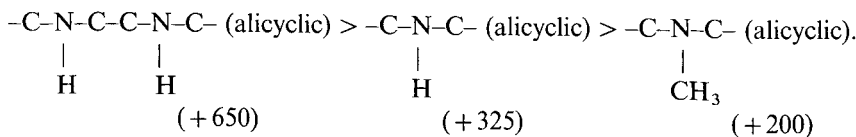
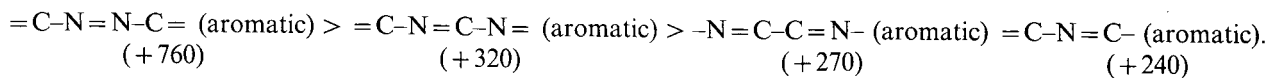


Fig. 2. The relationship between the *GRFs* of tertiary amine function and the size of substituent groups, expressed as the number of atoms (*Z*) in *N,N,N*-trisubstituted alkylamines. *Z* and *GRF* are given sequentially in parentheses following the name of the tertiary amine. The points plotted are: 1 = triethylamine (7, +27); 2 = *N,N*-dimethylbenzylamine (10, 0); 3 = *N,N*-diethylbenzylamine (12, -76); 4 = tributylamine (13, -93); 5 = *N*-methyl dibenzylamine (16, -49); 6 = tripentylamine (16, -131); 7 = *N,N*-dimethylaniline (9, -50); 8 = tribenzylamine (22, -215); 9 = 2,2',2''-trimethyltriallylamine (13, -46); 10 = *N*-methyl dioctylamine (18, -30); 11 = *N,N*-dimethylnaphthylamine (13, -170).

The *GRFs* of the aza moieties are listed in parentheses below each structural moiety. The *GRFs* of these functional groups are specific for the 5- and 6-membered ring structures. A breakdown in terms of contributions from individual functions is given in Tables XVII and XVIII. These *GRFs* have not been widely tested on other aza compounds besides those listed. The general trend is for the highly conjugated N atoms in the ring to contribute the most to the RI, followed by the imino -NH- group connected to two double bonds and then the tertiary amine nitrogen. Similar aza moieties in 5-membered rings have higher *GRFs* than in 6-membered rings,

and additional ring N atoms introduce new *GRFs* to increase *I*. The *I* values of pyridines and quinolines are more readily predicted than those of diazines and diazoles. A comparison of the observed and predicted *I* values of 5-membered and 6-membered heterocyclics is given in Tables XVII and XVIII.

Water gives a peak with a *I* of 1066 on polar column with thermal conductivity detector. This peak may appear when a hygroscopic sample is chromatographed.

Alkyl halides

The *I* values of chloroalkanes, bromoalkanes and

TABLE XV

COMPARISON OF OBSERVED AND PREDICTED *I* VALUES OF ALIPHATIC AMINES^a

The *GRFs* (*m*, and *n*) have the following values: (1) -CH₂-NH₂ group = +417, (2) tertiary amino group = +“27”, = +“27”, -“30”, -“46”, -“93” (see text), (3) -C-NH₂ group = +229, (4) -CH-NH₂ group = +350, (5) quaternary C atom = -100, (5) chain branching = -50, (6) alkyl ether -O- linkage = +70, (7) terminal C=C double bond = +40, (8) alkyl imino-NH-R group = +180.

Compound	Formula	<i>I</i> _{obs}	Lit. [16]	100Z + Σ <i>m</i> _{<i>i</i>} - Σ <i>n</i> _{<i>i</i>}	<i>I</i> _p	Difference (%)
<i>n</i> -Propylamine	C ₃ H ₉ N	816		400 + 417	817	0.12
<i>n</i> -Butylamine	C ₄ H ₁₁ N	908		500 + 417	917	0.98
<i>n</i> -Pentylamine	C ₅ H ₁₃ N	1018		600 + 417	1017	0.1
<i>n</i> -Hexylamine	C ₆ H ₁₅ N	1113		700 + 417	1117	0.36
<i>n</i> -Heptylamine	C ₇ H ₁₇ N	1213		800 + 417	1217	0.33
<i>n</i> -Decylamine	C ₁₀ H ₂₃ N	1522		1100 + 417	1517	0.33
<i>n</i> -Dodecylamine	C ₁₂ H ₂₇ N	1716		1300 + 417	1717	0.06
<i>n</i> -Octadecylamine	C ₁₈ H ₃₉ N	2330		1900 + 417	2317	0.56
Triethylamine	C ₆ H ₁₅ N	727		700 + “27”	727	0
<i>tert.</i> -Butyl amine	C ₄ H ₁₁ N	729		500 + 229	729	0
<i>sec.</i> -Butyl amine	C ₄ H ₁₁ N	864		500 + 350	850	1.62
2-Amino-3,3-dimethylbutane	C ₆ H ₁₅ N	948		700 + 350 - 100	950	0.21
Isoamylamine	C ₅ H ₁₃ N	989		600 + 417 - 50	967	2.22
2-Amino-1-methoxypropane	C ₄ H ₁₁ NO	1050		600 + 70 + 350	1020	2.86
Dibutylamine	C ₈ H ₁₉ N		1092	900 + 180	1080	1.1
2-Aminoheptane	C ₇ H ₁₇ N	1158		800 + 350	1150	0.69
3-Aminoheptane	C ₇ H ₁₇ N	1137		800 + 350	1150	1.13
Tributylamine	C ₁₂ H ₂₇ N	1207	1206	1300 - “93”	1207	0
Tripropylamine	C ₁₅ H ₃₃ N	1469		1600 - “131”	1469	0
2,2',2''-Trimethyltriallylamine	C ₁₂ H ₂₁ N		1224	1300 + 3 × 40 - 3 × 50 - “46”	1224	0
N-Ethylbenzylamine	C ₉ H ₁₃ N		1543	1000 + 350 + 180	1530	0.84
N-Propylbenzylamine	C ₁₀ H ₁₅ N		1624	1100 + 350 + 180	1630	0.37
N-Butylbenzylamine	C ₁₁ H ₁₇ N		1726	1200 + 350 + 180	1730	0.23
N-Methyldioctylamine	C ₁₇ H ₃₇ N		1770	1800 - “30”	1770	0
Dibenzylamine	C ₁₄ H ₁₅ N		2473	1500 + 2 × 350 + 180	2380	3.76

^a See footnote in Table III.

TABLE XVI

COMPARISON OF OBSERVED AND PREDICTED I VALUES OF AROMATIC AMINES^a

The GRF_s (m_i and n_i) have the following values: (1) cyclohexane ring = +123, (2) alicyclic primary $-NH_2$ group = +350, (3) chain branching = -50, (4) tertiary $Ar-NR_2$ group = +310, (5) tertiary amino group = "0", -"30", -"50", -"170", -"49" or -"215" (see text), (6) $-N-C_2H_5$ group = -60, (7) ortho effect b between $-CH_3$ and $-N(C_2H_5)_2$ = -"300", (8) aralkyl alkyl imino $-NH-$ group = +260, (9) alkyl $-NH_2$ group = +417, (10) aryl alkyl imino $-NH$ group = +523, (11) aryl $-NH_2$ group = +667, (12) ortho effect b between $-C_2H_5$ and $-NH_2$ groups = -"70", (13) aryl $-OCH_3$ group = +190, (14) ortho effect b between $-OCH_3$ and $-NH_2$ groups = "160", (15) quaternary C atom = -100.

Compound	Formula	I_{obs}	Lit. [16]	$100Z + \Sigma m_i - \Sigma n_i$	I_p	Difference (%)
Cyclohexylamine	$C_6H_{13}N$	1222	1155	$700 + 123 + 350$	1173	1.53
3-Methyl cyclohexylamine	$C_7H_{10}N$	1400		$800 + 123 + 350 - 50$	1450	3.49
N,N-Dimethylbenzylamine	$C_9H_{13}N$		1350	$1000 + 350 + "0"$	1350	0
N,N-Diethyl- <i>o</i> -toluidine	$C_{11}H_{17}N$		1428	$1200 + 350 + 310 - 2 \times 60 - 300$	1440	0.83
N,N-Dimethylaniline	$C_8H_{11}N$	1510	1538	$900 + 350 + 310 - 50$	1510	0
N-Ethylbenzylamine	$C_9H_{13}N$	1577		$1000 + 350 + 260 - 60$	1550	1.72
Phenethylamine	$C_8H_{11}N$	1638		$900 + 350 + 417$	1667	1.74
N,N-Diethylaniline	$C_{10}H_{15}N$	1660	1620	$1100 + 350 + 310 - 2 \times 60$	1640	1.2
N,N-Dimethyl- <i>o</i> -toluidine	$C_9H_{13}N$		1679	$1000 + 350 + 310$	1660	1.13
N-Methylaniline	C_7H_9N	1686	1711	$800 + 350 + 523$	1673	0.77
Aniline	C_6H_7N	1710	1740	$700 + 350 + 667$	1717	0.41
N-Ethylaniline	$C_8H_{11}N$	1761	1717	$900 + 350 + 523 - 60$	1713	2.73
N-Methyl-dioctylamine	$C_{17}H_{37}N$		1770	$1800 - "30"$	1770	0
N-Methyl- <i>p</i> -toluidine	$C_8H_{11}N$		1780	$900 + 350 + 523$	1773	0.39
<i>o</i> -Toluidine	C_7H_9N	1800	1789	$800 + 350 + 667$	1817	0.94
N-Ethyl- <i>m</i> -toluidine	$C_9H_{13}N$		1802	$1000 + 350 + 523 - 60$	1813	0.6
<i>p</i> -Toluidine	C_7H_8N	1822		$800 + 350 + 667$	1817	0.27
<i>m</i> -Toluidine	C_7H_8N	1849	1831	$800 + 350 + 667$	1817	1.73
<i>o</i> -Ethylaniline	$C_8H_{11}N$		1848	$900 + 350 + 667 - 70$	1847	0.05
N-Butylaniline	$C_{10}H_{15}N$		1893	$1100 + 350 + 523$	1973	4.05
2,4-Dimethylaniline	$C_8H_{11}N$	1903		$900 + 350 + 667$	1917	0.73
<i>o</i> -Anisidine	C_7H_9NO	1946		$900 + 350 + 190 + 667 - "160"$	1947	0.05
<i>p-tert.</i> -Butylaniline	$C_{10}H_{15}N$		2011	$1100 + 350 + 667 - 100$	2017	0.3
N,N-Dimethylnaphthylamine	$C_{12}H_{13}N$		2100	$1300 + 2 \times 350 + 60 + 310 - "170"$	2100	0
<i>m</i> -Anisidine	C_7H_9NO		2176	$900 + 350 + 190 + 667$	2107	3.17
N-Methyldibenzylamine	$C_{15}H_{17}N$	2251		$1600 + 2 \times 350 - "49"$	2251	0
N-Benzyl-N-methylaniline	$C_{14}H_{15}N$	2430		$1500 + 2 \times 350 + 260$	2460	1.22
N,N-Diphenylmethylamine	$C_{13}H_{13}N$	2450		$1400 + 2 \times 350 + 310$	2410	1.63
Dibenzylamine	$C_{15}H_{15}N$	2427	2473	$1500 + 2 \times 350 + 260$	2460	0.53
Diphenylamine	$C_{12}H_{11}N$	2586		$1300 + 2 \times 350 + 586$	2586	0
Tribenzylamine	$C_{21}H_{21}N$	3035		$2200 + 3 \times 350 - "215"$	3035	0

^a See footnote in Table III.

iodoalkanes are predicted by assuming the GRF_s for chlorine, bromine and iodine atoms to be +464, +592 and +710, respectively. These are the averages of the Δm_f values of the halo atoms in chloroalkanes, bromoalkanes and iodoalkanes, as

shown in Table XIX. The individual Δm_f values of each halo atom show a gradual increase within the series with chain lengthening. Plotting the Δm_f values against the number of carbon atoms yields a straight line, with the slope increasing from chloro-

TABLE XVII

COMPARISON OF OBSERVED AND PREDICTED I VALUES OF HETEROCYCLIC COMPOUNDS^a

In the 5-membered ring the $GRFs$ (m_i and n_i) have the following values: (1) cyclopentadiene ring = +210, (2) O atom in the ring = +80, (3) alicyclic aldehyde group = +465, (4) S atom in the ring = +200, (5) cyclopentane ring = +122, (6) $-N(CH_3)-$ group in the ring = +140, (7) imino $-NH-$ group in the ring = +380, (8) cyclopentene ring = +163, (9) one C=C bond in azole ring = +40, (10) two C=C bonds in azole ring = +190, (11) C=C-NH-C=C group in the ring = +800, (12) additional N atom at the α position of the ring = +300, (13) methyl group *ortho* to ring N = -70, (14) phenyl ring = +350, (15) additional N atom at the β position of the N-methylated azole ring = +550, (16) additional N atom at the β position of the azole ring = +700.

Compound	Formula	I_{obs}	Lit. [16]	$100Z + \Sigma m_i - \Sigma n_i$	I_p	Difference (%)
<i>Furan group</i>						
Furan	C ₄ H ₄ O	800		500 + 210 + 80	790	1.25
{Water	H ₂ O	1066		{(See text)}		
2-Furaldehyde	C ₅ H ₄ O ₂		1447	700 + 210 + 465 + 80	1455	0.51
5-Methylfuraldehyde	C ₆ H ₆ O ₂		1562	800 + 210 + 465 + 80	1555	0.45
<i>Thiophene group</i>						
Thiophene	C ₄ H ₄ S	1022	1025	600 + 210 + 200	1010	1.17
<i>Pyrrolidine group</i>						
1-Methyl pyrrolidine	C ₅ H ₁₁ N	861		600 + 122 + 140	862	0.12
Pyrrolidine	C ₄ H ₉ N	1003		500 + 122 + 380	1002	0
Perhydroindole	C ₈ H ₁₅ N	1468		900 + 123 + 122 + 380	1525	3.88
3-Pyrroline	C ₄ H ₅ N	1066		500 + 163 + 380 + 40	1083	1.57
<i>Pyrrole group</i>						
1-Methyl pyrrole	C ₅ H ₇ N	1142	1139	600 + 210 + 140 + 190	1140	0.18
Pyrrole	C ₄ H ₅ N	1511	1508	500 + 210 + 800	1510	0.07
Pyrazole (1,2-diazole)	C ₃ H ₄ N ₂	1826		500 + 210 + 800 + 300	1810	0.88
3-Methyl pyrazole	C ₄ H ₆ N ₂	1863		600 + 210 + 800 + 300 - 70	1840	1.23
4-Methyl pyrazole	C ₄ H ₆ N ₂	1929		600 + 210 + 800 + 300	1910	0.98
Indazole	C ₇ H ₆ N ₂	2556		900 + 350 + 210 + 800 + 300	2560	0.16
1-Methyl imidazole	C ₄ H ₆ N ₂	1700	1638	600 + 210 + 140 + 190 + 550	1690	0.59
2-Methyl imidazole	C ₄ H ₆ N ₂	2238		600 + 210 + 800 + 700 - 70	2240	0.09
Imidazole (1,3-diazole)	C ₃ H ₄ N ₂	2254		500 + 210 + 800 + 700	2210	1.51
4-Methyl imidazole	C ₄ H ₆ N ₂	2289		600 + 210 + 800 + 700	2240	2.14

^a See footnote in Table III.

alkanes to bromoalkanes to iodoalkanes, as shown in Fig. 3.

The increase in the slope of these linear plots of haloalkanes and the increase of the Δm_f value in ascending each series are associated with the change in polar-to-non-polar moiety ratio on chain lengthening and electronic effects of the halo atom. The halo atom can exert mesomeric and inductive effects. The mesomeric effect and hyperconjugation may dominate in the lower haloalkanes and the inductive effect in the higher ones. That the three lower iodoalkanes show marked deviation from the

linear relationship in Fig. 3 may be attributed to these factors.

The GRF of the halo atoms is influenced by the presence of other functional groups in the molecule. For example, the $GRFs$ of the halo atoms in haloarenes or haloalicyclics are smaller than those in haloalkanes. It may be noted that the $GRFs$ of the halo atoms include not only the $GRFs$ but also the carbon atom equivalency of the halo atoms. The implication of this inclusion will be discussed in a future communication [20].

TABLE XVIII

COMPARISON OF OBSERVED AND PREDICTED I VALUES OF HETEROCYCLIC COMPOUNDS^a

In the 6-membered ring the $GRFs$ (m_i and n_i) have the following values: (1) cyclohexane ring = +123, (2) O atom in the ring = +160, (3) phenyl ring = +350, (4) cyclopentane ring = +122, (5) O atom in 5-membered ring = +80, (6) $-N(CH_3)-$ in the ring = +200, (7) a second imino $-NH-$ group in the ring containing $-N(CH_3)-$ group = +240, (8) imino $-NH-$ group in the ring = +325, (9) methyl group ortho to ring N = -70, (10) chain branching = -50, (11) cycloheptane ring = +183, (12) tertiary $-N=$ in the ring = +240, (13) 1,4-diaza group = +30, (14) 1,3-diaza group = +80, (15) 1,2-diaza group = +520, (16) *trans* isomer-*cis* isomer = -60, (17) N atom in the iso position of fused heterocyclic rings = +40, (18) methyl group in *peri* position to ring N = -100, (19) methyl group in the *para* position of ring N = +70, (20) aryl ether $-O-$ linkage = +190.

Compound	Formula	I_{obs}	Lit. [16]	$100Z + \Sigma m_i - \Sigma n_i$	I_p	Difference (%)
<i>Dioxane group</i>						
1,4-Dioxane	$C_4H_8O_2$	1059		$600 + 123 + 160 \times 2$	1043	1.51
S-Trioxane	$C_3H_6O_3$	1167		$600 + 123 + 160 \times 3$	1203	2.99
1,4-Benzodioxane	$C_8H_8O_2$		1800	$1000 + 350 + 123 + 160 \times 2$	1793	0.39
1,3-Benzodioxole	$C_7H_6O_2$		1531	$900 + 350 + 122 + 80 \times 2$	1573	2.67
<i>1-Methylpiperidine group</i>						
1-Methyl piperidine	$C_6H_{13}N$	1020		$700 + 123 + 200$	1023	0.29
1-Methyl piperazine	$C_5H_{12}N_2$	1262	1204	$700 + 123 + 200 + 240$	1263	0.08
<i>Piperidine group</i>						
Piperidine	$C_5H_{11}N$	1049		$600 + 123 + 325$	1048	0.09
2-Methyl piperidine	$C_6H_{13}N$		1017	$700 + 123 + 325 - 70 - 50$	1028	1.07
2,6-Lupetidine	$C_7H_{15}N$		1009	$800 + 123 + 325 - 70 \times 2 - 50 \times 2$	1008	0.1
4-Methyl piperidine	$C_6H_{13}N$	1075		$700 + 123 + 325 - 50$	1100	2.29
3-Methyl piperidine	$C_6H_{13}N$	1081		$700 + 123 + 325 - 50$	1100	1.73
Hexamethylene imine	$C_6H_{13}N$	1178		$700 + 183 + 325$	1208	2.48
Piperazine	$C_4H_{10}N_2$	1391		$600 + 123 + 325 \times 2$	1373	1.29
Homopiperazine	$C_5H_{12}N_2$	1525		$700 + 183 + 325 \times 2$	1533	0.25
<i>Pyridine group</i>						
Pyridine	C_5H_5N	1191		$600 + 350 + 240$	1190	0.08
Pyrazine (1,4-diazine)	$C_4H_4N_2$	1224		$600 + 350 + 240 + 30$	1220	0.33
Methyl pyrazine	$C_5H_6N_2$		1259	$700 + 350 + 240 + 30 - 70$	1250	0.71
Pyrimidine (1,3-diazine)	$C_4H_4N_2$	1276	1257	$600 + 350 + 240 + 80$	1275	0.31
4-Methyl pyrimidine	$C_5H_6N_2$	1328		$700 + 350 + 240 + 80 - 70$	1300	2.11
Pyridazine (1,2-diazine)	$C_4H_4N_2$	1716		$600 + 350 + 240 + 520$	1710	0.35
3-Methyl pyridazine	$C_5H_6N_2$	1750		$700 + 350 + 240 + 520 - 70$	1740	0.57
2-Picoline	C_6H_7N		1210	$700 + 350 + 240 - 70$	1220	0.82
3-Picoline	C_6H_7N		1283	$700 + 350 + 240$	1290	0.54
4-Picoline	C_6H_7N		1300	$700 + 350 + 240$	1290	0.08
2,6-Lutidine	C_7H_9N		1241	$800 + 350 + 240 - 70 \times 2$	1250	0.72
3,5-Lutidine	C_7H_9N		1400	$800 + 350 + 240$	1390	0.71
<i>Quinoline group</i>						
Perhydro isoquinoline	$C_9H_{17}N$	1520 (<i>trans</i>)		$1000 + 123 \times 2 + 325 - 60$	1511	0.59
(<i>cis</i> + <i>trans</i>)		1560 (<i>cis</i>)		$1000 + 123 \times 2 + 325$	1571	0.7
Quinoline	C_9H_7N	1942		$1000 + 350 \times 2 + 240$	1940	0.1
Isoquinoline	C_9H_7N	1980		$1000 + 350 \times 2 + 240 + 40$	1980	0
8-Methylquinoline	$C_{10}H_9N$	1959		$1100 + 350 \times 2 + 240 - 100$	1940	0.97
Quinaldine						
(2-methylquinoline)	$C_{10}H_9N$	1970		$1100 + 350 \times 2 + 240 - 70$	1970	0
7-Methyl quinoline	$C_{10}H_9N$	2053		$1100 + 350 \times 2 + 240$	2040	0.63
6-Methyl quinoline	$C_{10}H_9N$	2062		$1100 + 350 \times 2 + 240$	2040	1.07
4-Methyl quinoline	$C_{10}H_9N$	2108	2080	$1100 + 350 \times 2 + 240 + 70$	2110	0.09
(lepidine)						
6-Methoxyquinoline	$C_{10}H_9NO$		2353	$1200 + 350 \times 2 + 240 + 190$	2330	0.98

^a See footnote in Table III.

TABLE XIX

CALCULATION OF Δm_f AND COMPARISON OF OBSERVED AND PREDICTED I VALUES OF 1-HALOALKANES^a

The *GRFs* have the following values: (1) chlorine atom in R-CH₂-Cl = +464, (2) bromine atom in R-CH₂-Br = +592, (3) bromine atom connected to secondary carbon atom = +492, (4) iodine atom in R-CH₂-I = +710.

Compound	Formula	I_{obs}	100Z	Δm_f	I_p	Difference (%)
<i>1-Chloroalkanes</i>						
1-Chloropropane	C ₃ H ₇ Cl	739	300	439	764	3.27
1-Chlorobutane	C ₄ H ₉ Cl	842	400	442	864	2.55
1-Chloropentane	C ₅ H ₁₁ Cl	945	500	445	964	1.97
1-Chlorohexane	C ₆ H ₁₃ Cl	1050	600	450	1064	1.32
1-Chloroheptane	C ₇ H ₁₅ Cl	1154	700	454	1164	0.86
1-Chlorooctane	C ₈ H ₁₇ Cl	1262	800	462	1264	0.16
1-Chlorononane	C ₉ H ₁₉ Cl	1364	900	464	1364	0
1-Chlorodecane	C ₁₀ H ₂₁ Cl	1474	1000	474	1464	0.68
1-Chlorotetradecane	C ₁₄ H ₂₉ Cl	1889	1400	489	1864	1.32
1-Chlorohexadecane	C ₁₆ H ₃₃ Cl	2094	1600	494	2064	1.43
1-Chlorooctadecane	C ₁₈ H ₃₇ Cl	2294	1800	494	2264	1.31
Average 464.27 ± 20.72						
<i>1-Bromoalkanes</i>						
1-Bromobutane	C ₄ H ₉ Br	955	400	555	992	3.87
1-Bromopentane	C ₅ H ₁₁ Br	1042	500	542	1092	4.58
1-Bromohexane	C ₆ H ₁₃ Br	1163	600	563	1192	2.43
1-Bromoheptane	C ₇ H ₁₅ Br	1256	700	556	1292	2.79
1-Bromooctane	C ₈ H ₁₇ Br	1385	800	585	1392	0.5
1-Bromononane	C ₉ H ₁₉ Br	1496	900	596	1492	0.27
1-Bromodecane	C ₁₀ H ₂₁ Br	1578	1000	578	1592	0.88
1-Bromoundecane	C ₁₁ H ₂₃ Br	1717	1100	617	1692	1.46
1-Bromododecane	C ₁₂ H ₂₅ Br	1818	1200	[618]	1792	1.43
1-Bromotetradecane	C ₁₄ H ₂₉ Br	2037	1400	637	1992	2.1
1-Bromohexadecane	C ₁₆ H ₃₃ Br	2237	1600	637	2192	2.01
1-Bromooctadecane	C ₁₈ H ₃₇ Br	2447	1800	647	2392	2.17
Average 592.00 ± 35.63						
<i>2- and 3-Bromoalkanes</i>						
2-Bromobutane	C ₄ H ₉ Br	905	400	505	892	1.44
2-Bromopentane	C ₅ H ₁₁ Br	984	500	484	992	0.81
3-Bromopentane	C ₅ H ₁₁ Br	994	500	494	992	0.2
2-Bromoheptane	C ₇ H ₁₅ Br	1173	700	473	1192	1.59
2-Bromodecane	C ₁₀ H ₂₃ Br	1493	1000	493	1492	0.07
2-Bromododecane	C ₁₂ H ₂₅ Br	1702	1200	502	1692	0.59
Average 491.83 ± 11.82						
<i>1-Iodoalkanes</i>						
1-Iodoethane	C ₂ H ₅ I	876	200	676	910	3.74
1-Iodopropane	C ₃ H ₇ I	965	300	665	1010	4.46
1-Iodobutane	C ₄ H ₉ I	1065	400	665	1110	4.05
1-Iodopentane	C ₅ H ₁₁ I	1175	500	675	1210	2.89
1-Iodohexane	C ₆ H ₁₃ I	1286	600	686	1310	1.83
1-Iodoheptane	C ₇ H ₁₅ I	1400	700	700	1410	0.71
1-Iodooctane	C ₈ H ₁₇ I	1508	800	708	1510	0.13
1-Iodononane	C ₉ H ₁₉ I	1621	900	721	1610	0.68
1-Iododecane	C ₁₀ H ₂₁ I	1734	1000	734	1710	1.38
1-Iodoundecane	C ₁₁ H ₂₃ I	1842	1100	742	1810	1.74
1-Iodododecane	C ₁₂ H ₂₅ I	1953	1200	753	1910	2.2
1-Iodohexadecane	C ₁₆ H ₃₃ I	2400	1600	800	2310	3.73
Average 710.42 ± 41.32						

^a See footnote in Table III.

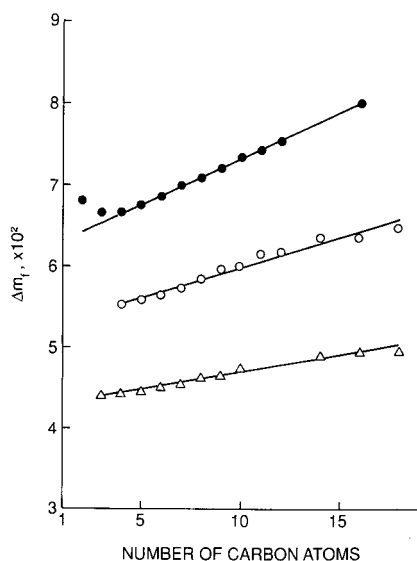


Fig. 3. Linear plots of the *GRF* increment or the functionality constant (Δm_f) vs. the number of carbon atoms in 1-haloalkanes. ● = 1-iodoalkanes; ○ = 1-bromoalkanes; △ = 1-chloroalkanes.

CONCLUSIONS

The retention mechanism in gas chromatography is complex and may involve a number of factors, such as partition between the gas phase and the stationary liquid phase, adsorption at the gas-liquid interface, H-bonding and dipolar interaction with the stationary phase, the electronic nature and configuration of the analyte molecule, etc. [5]. In a homologous series, each member differs from its near neighbors by a methylene group, which allows the same retention mechanism to prevail for all members of the series and leads to a linear relationship between *I* and the number of carbon and carbon equivalent atoms (*n* or *Z*). This is the theoretical basis for the prediction of *I*, using *A*, *Z* and *GRF* values.

Accurate *A* and *GRF* values are essential to the prediction. In many cases, the gradual change of the polar-to-non-polar moiety ratio in ascending or descending the homologous series exerts a definite effect on *GRF*. The effect is less on non-polar than on polar stationary phases and may be augmented in certain homologous series. As the polar-to-non-polar ratio decreases to near zero, the *I* value of

the analyte will approach the base value. This explains why substituted compounds such as acid esters, tertiary amines and silylated derivatives show chromatographic characteristics similar to that of aliphatic hydrocarbons.

The *I* values of a wide range of compounds, such as acids, alcohols, amines, acid esters, aldehydes, ketones, ethers, aromatic hydrocarbons, alicyclics, heterocyclics, etc. on polar column are predicted by this method to within 3% error. The procedure used for prediction of *I* is similar to that for non-polar columns. In general, the *I* values of compounds of monofunctionality are accurately predicted. The *I* values of compounds of polyfunctionality are difficult to predict, because the functional groups often interact intramolecularly to alter the *GRF* and also the *A* values, as in the case of α -amino acids and acid amides. To apply the rule of additivity without the correct *A* and *GRF* values will lead to either over- or under-estimate of *I*. For example, the free and substituted acid amides have an *A* value that is considerably less than 100 (see Table VIII); the methyl substitution at the *ortho* position to the nitrogen atom in heterocyclics contributes only a fraction of the full *I* increment. According to an early report, methyl substitutions at the α , β , and γ positions of the pyridine ring contribute differently to *I* [21]. Substituents at the *ortho* positions of the phenyl ring tend to interact with each other to lower *I* generally by hydrogen bonding or steric hindrance. Substitutions at the *para* positions may cause an increase in *I*. In addition, identical N-containing moieties in 5-membered and 6-membered aza and diaza rings yield different *GRF* values. The ring constraint in the 5-membered rings accentuates the *GRF*s of these moieties. The effect of multi-substitution and poly-functionality on *GRF* are not well understood, but studies using homologous series may clarify some of these complexities.

From the structure-retention index relationship, one can derive a set of general rules to guide the prediction of *I*. These are as follows: (i) molecules which contain multiple O and N atoms will have high *I* values in comparison to molecules that do not, (ii) molecules which have highly conjugated systems containing N and O atoms tend to give higher *I* values than those that do not, (iii) molecules which contain quaternary carbon atoms and functional groups connected to secondary or tertiary carbon

atoms have lower I values than those that do not, and (iv) highly substituted molecules tend to yield lower I values than those that are not.

Strong electron attracting and donating substituents that contain F, N and O atoms can generate unusual A and GRF values. This may also include atoms connected to multi-substituent groups. The magnitudes of the GRF value and the column difference depend upon the polarity and polarizability of the substituent group and the stationary phase. The well-known Rohrschneider and McReynolds constants may be mentioned as examples of utilizing the GRF related parameters and column differences (ΔI values) of selected compounds to characterize the selectivity and the polarity and polarizability of chromatographic stationary phases [22–24]. According to our method, the ratio of the GRF values for a given functional group or substituent on various chromatographic stationary phases can probably yield direct information about the polarity of the stationary phases and the magnitude of the I values of the analytes.

The structure retention–index relationship formulated thus far for non-polar and polar stationary phases allows us to link chemical structures to chromatographic data. It can predict from a glance of the structure the approximate I to prevent gross errors in assigning unreasonable I values to an analyte. The method of predicting I from structure and *vice versa* is useful, especially in tentatively identifying unknown products formed from parent molecules in a chemical reaction. We have applied this method with success in identifying radioactive by-products in tritium labeling by radiation-induced methods and in elucidating the associated labeling mechanisms.

ACKNOWLEDGEMENTS

This publication was made possible by grant number CA33537 from the National Cancer Insti-

tute. We thank Gloria Dela Cruz for patiently typing the manuscript.

REFERENCES

- 1 C. T. Peng, S. F. Ding, R. L. Hua and Z. C. Yang, *J. Chromatogr.*, 436 (1988) 137.
- 2 H. van den Dool and P. D. Kratz, *J. Chromatogr.*, 11 (1963) 463.
- 3 *SAS/STAT™ User's Guide, Release 6-03 Edition*, SAS Institute, Cary, NC, 1988, pp. 854–857.
- 4 E. Kováts, *Helv. Chim. Acta*, 41 (1958) 1915.
- 5 R. Kaliszan, *Quantitative Structure–Chromatographic Retention Relationship*, Wiley, New York, 1987, pp. 1–50.
- 6 F. P. Woodford and C. M. van Gent, *J. Lipid Res.*, 1 (1960) 188.
- 7 R. G. Ackman, *J. Chromatogr. Sci.*, 10 (1972) 345.
- 8 R. Aderjan and M. Bogusz, *J. Chromatogr.*, 454 (1988) 345.
- 9 T. R. Schwartz and J. D. Petty, *Anal. Chem.*, 55 (1983) 1839.
- 10 A. Gröbler, *J. Chromatogr. Sci.*, 10 (1972) 128.
- 11 S. J. Hawkes, *J. Chromatogr. Sci.*, 10 (1972) 535.
- 12 G. Tarján, Sz. Nyiredy, M. Györ, E. R. Lombosi, T. S. Lombosi, M. V. Budahegyi, S. Y. Mészáros and J. M. Takács, *J. Chromatogr.*, 472 (1989) 1.
- 13 M. B. Evans and J. K. Haken, *J. Chromatogr.*, 472 (1989) 93.
- 14 E. Kováts, *Adv. Chromatogr.*, 1 (1965) 229.
- 15 *Analabs Capillary Column Application Note No. 1*, The Foxboro Company, New Haven, CT, 1985.
- 16 *The Sadtler Standard Gas Chromatography Retention Index Library*, Vols. 1–4, Sadtler Research Libraries, Division of Bio-Rad Laboratories, Philadelphia, PA, 1986.
- 17 R. Kaliszan and H. Lamparczyk, *J. Chromatogr. Sci.*, 16 (1978) 246.
- 18 A. T. Balaban, I. Motoc, D. Bonchev and O. Mekenyan, in M. Charton and I. Motoc (Editors), *Steric Effects in Drug Design (Topics in Current Chemistry, No. 114)*, Springer, Verlag, Berlin, 1983, pp. 21–55.
- 19 L. Pauling, *The Nature of the Chemical Bond*, Cornell University Press, Ithaca, NY, 1948, p. 58.
- 20 C. T. Peng, *J. Chromatogr.*, submitted for publication.
- 21 A. L. Samusenko and R. V. Golovnya, *Chromatographia*, 25 (1988) 531.
- 22 L. Rohrschneider, *J. Chromatogr.*, 22 (1966) 6.
- 23 W. R. McReynolds, *J. Chromatogr. Sci.*, 8 (1970) 685.
- 24 S. K. Poole, B. R. Kersten, R. M. Pomaville and C. K. Poole, *LC GC*, 6 (1988) 400.

Prediction of retention indexes

III. Silylated derivatives of polar compounds

C. T. Peng* and Z. C. Yang

Department of Pharmaceutical Chemistry, School of Pharmacy, University of California, San Francisco, CA 94143-0446 (USA)

D. Maltby

Mass Spectrometry Research Laboratory and Department of Pharmaceutical Chemistry, School of Pharmacy, University of California, San Francisco, CA 94143 (USA)

(First received September 17th, 1990; revised manuscript received June 4th, 1991)

ABSTRACT

Polar compounds containing hydroxyl, amino and carboxyl groups, singly or in combination, can be chromatographed after the polar functional groups are silylated. The silylated derivatives of acids, alcohols, amines, diols, amino alcohols, amino acids are shown to behave chromatographically as hydrocarbons, and their retention indexes can be readily predicted from their base values. The column difference, namely, the difference between the retention indexes of the analyte on polar and non-polar columns is minimal for the silylated derivatives in comparison to that observed for the underivatized analytes. This minimal column difference is attributed to the hydrocarbon-like chromatographic characteristics of the silylated derivatives. The retention indexes of the silyl derivatives appear to correlate with the atom number Z of the analyte.

INTRODUCTION

Compounds containing functional groups, such as hydroxyl, amino and carboxyl groups singly or in combination in the form of alcohols, phenols, aliphatic and aromatic amines, glycols, amino alcohols, carboxylic acids and amino acids, are polar and hydrophilic. These compounds are difficult to chromatograph and often yield skewed and asymmetrical elution peaks. Sometimes these compounds may not emerge from the column at all. This difficulty can be overcome by derivatizing the polar compounds to lessen the hydrophilicity of the substituent groups.

We have shown earlier [1] that the methyl esters of aliphatic acids have retention indexes (I) identical to those of n -alkanes with an equal number of atoms when chromatographed on non-polar columns

(SE-30, DB-1). We have also shown [1] that methylation and alkylation alter the polarity and functionality of amino and hydroxyl groups, and the methylated and alkylated derivatives behave chromatographically as aliphatic hydrocarbons. In this report, we will show that silylated derivatives of compounds containing amino, hydroxyl and carboxyl groups, either singly or in combination, may also show chromatographic characteristics similar to that of n -alkanes. Silylation minimizes the intramolecular interaction between functional groups and facilitates the prediction of retention indexes.

EXPERIMENTAL

Trimethylchlorosilane (TMCS), N,O -bis(trimethylsilyl)acetamide (BSA), dimethyl-*tert*-butylsilyltrifluoroacetamide (MTBSTFA) and dimethyl-

formamide (DMF) were purchased from Pierce (Rockford, IL, USA). *tert*-Butyldimethylchlorosilane (TBDMS-CL) was purchased from Fluka (Buchs, Switzerland). All other chemicals were obtained from Aldrich (Milwaukee, WI, USA). Solvents used were of analytical grade and dry.

Silylation method A

Approximately 1.0 mg of solid or 5.0 μ l of liquid analyte is introduced into a 0.6-ml Reacti-Vial (Regis). To the reaction vials, is also added 0.1 ml of the silylating reagent consisting of a mixture of 3.0 ml MTBSTFA, 1.0 ml DMF and 80 mg TBDMS-CL. The vial is capped and heated at 75–80°C for 45 min [2,3]. After cooling the reaction mixture is injected directly into the gas chromatograph. This reaction will replace the active hydrogen in the analyte molecule with a TBDMS group.

Silylation method B

This method is similar to method A, except that a different silylating reagent consisting of 3.0 ml BSA, 1.0 ml DMF and 0.08 ml TMCS is used. The reaction mixture is heated at 75–80°C for 15 min or longer. This reagent will replace the reactive hydrogen atoms in the analyte molecule with TMS groups [2,3].

Chromatography

All chromatographic runs were performed on Hewlett-Packard Model 5890 and 5880A gas chromatographs, equipped with thermal conductivity detectors. Integration was performed by a HP Model 3393 integrator on Model 5890 and by Level 4 Integration on Model 5880A. The non-polar column used was a fused-silica capillary column DB-1 (15 m \times 0.53 mm I.D., film thickness 1.5 μ m) obtained from J&W Scientific, Folsom, CA, USA. The polar columns used were stainless-steel columns (3.05 m \times 3.175 mm I.D.) packed with 10% Carbowax 20M (CW-20M) on 80–100 mesh Supelcoport and fused-silica capillary DB-Wax columns (15 m \times 0.53 mm I.D., film thickness 1.0 μ m) from J&W Scientific. The operating conditions were similar to those described [1,4]. Briefly, the injector was at 250°C and the detector at 300°C. The oven temperature was programmed to begin at 40°C isothermally for 4 min and then linearly increased at a rate of 8°C/min to 200°C, which was the final

temperature for the DB-Wax column. The DB-1 column was maintained at 200°C for 1 min and then linearly increased again at a rate of 5°C/min to 280°C. The maximum oven temperature was maintained for additional 20 min if necessary. In some cases, the temperature program was initiated from 100°C. The early peaks overlapped in the chromatogram but their retention times were listed separately in the report by the electronic integrator.

The *I* values were calculated according to Van den Dool and Kratz [5]. The *I* values obtained with the initial temperature at 40°C differed only insignificantly from those obtained with the initial temperature at 100°C.

RESULTS AND DISCUSSION

Methods of prediction

We reported [1] that the retention index of an analyte on non-polar and polar columns can be predicted using the equation:

$$I_p = 100Z + \sum m_i - \sum n_i \quad (1)$$

where I_p is the predicted retention index; Z the total number of carbon atoms and carbon equivalent atoms such as nitrogen, oxygen, etc.; m_i and n_i represent group retention factors (*GRFs*) of substituents and functional groups the presence of which in the molecule either increases or decreases the retention index. Detailed steps for predicting the retention index from chemical structure are given in ref. 1.

When the *I* values of the series of homologues or their silylated derivatives are plotted against the total number of carbon, oxygen and nitrogen atoms (Z) in the molecule, a straight line is obtained and may be represented by linear regression equations as follows:

$$I = AZ + B \quad (2)$$

$$= AZ' + B' \quad (3)$$

and

$$B' = B - A(Z' - Z) \quad (4)$$

where the regression coefficient A represents the *I* increment for atom addition; Z and Z' are the numbers of atoms in the underivatized compound and its silylated derivative, respectively; the intercept B represents the total of the *GRF* value and the

I increment from the carbon atoms of the silylating reagent; B' differs from B in that it contains only the GRF value of the silylating group without the contribution from the carbon atoms. The relationship of B' with B is given by eqn. 4.

According to Kováts' convention, A is assigned a value of 100 for the series of normal alkanes and the m_i , n_i and B are zero. Both eqns. 1 and 2 yield a value of $100Z$ which is known as the base value. For monofunctional and monosubstituted compounds such as alcohols, amines, aldehydes, etc., the A values are close to 100 and the I values predicted from eqns. 1 and 2 are practically identical, within 3% error of the observed value. In highly polar compounds such as acids and amides the A values are significantly less than 100 [1,4], and the I values predicted by eqn. 1 may show large deviations from the observed values. It may be pointed out that the carboxyl and the amide groups are consisted of carbonyl, hydroxyl and amino groups in combination and may be considered bifunctional chromatographically.

The value of A is sensitive to multisubstitution and polyfunctionality. The presence of highly polar substituents in the molecule can depress A . The decrease in A may also affect the GRF value; as a result, the I values of polyfunctional and multisubstituted compounds cannot be accurately predicted by eqn. 1. Accurate A values can only be obtained using eqn. 2, but if the homologues of the analyte are not readily available, accurate prediction of the I values will become extremely difficult.

The strongly non-polar nature of the silylated derivatives allows their I values to be readily predicted directly from the base values [4]. If the analyte contains additional functional groups that are not affected by silylation, their group retention factors ($GRFs$) or functionality constants must be taken into consideration in predicting I .

Linear regression equations for different homologous series of silylated derivatives are listed in Table I. These equations are based on Z and B or on Z' and B' values, as defined above. The statistics of the regression coefficient (A) and the intercept (B or B') of various homologous series were calculated using the Statistical Analytical System (SAS) procedure on a 486 personal computer^a.

Polyfunctionality and derivatization

In polyfunctional compounds intramolecular interaction of the functional groups can affect the A and GRF values so that their I values cannot be readily predicted using eqn. 1. Derivatization modifies the polarity of the analyte to facilitate the prediction of I .

Silylation is one of the preferred derivatizing reactions. It is fast, attains completion readily and affords a high yield. A large number of silylating reagents are available commercially [3]. Reactivity of these silylating reagents decreases from alcohols to amines in the following order: alcohols (primary > secondary > tertiary) > phenols > carboxylic acids > primary amines > acid amides > secondary amines [2].

Silylation replaces the active hydrogen atoms in the $-OH$, $COOH$ and $-NH_2$ groups with trimethylsilyl (TMS) or *tert.*-butyldimethylsilyl (TBDMS) groups. The TMS group is less bulky than the TBDMS group and can replace both active hydrogen atoms in the primary amino ($-NH_2$) group, whereas the TBDMS can replace only one active hydrogen with ease. In general the TBDMS derivatives are more stable towards hydrolysis than the TMS derivatives.

The silicon atom in the silyl group does not make a contribution to I , as shown by the I of ethyl ester of 2-(trimethylsilyl)acetic acid (see Table X). The TMS group contains three methyl carbon atoms; its incorporation into a molecule will increase its I value by 300 units. The TBDMS group contains five methyl carbon atoms and one quaternary carbon atom and will contribute a net increment of 500 (= 600 - 100) to I . Silylation masks the functionality and eliminates the GRF value of the functional group. Unlike the underivatized compounds, the silylated derivatives of alcohols, amines and carboxylic acids exhibit comparable I values on non-polar (SE-30, DB-1) and polar (CW-20M, DB-Wax) columns.

^a The regression analysis was performed with SAS/STAT statistical analysis procedures on a 486 personal computer. Data given for each homologous series include (i) the number of data points (n), (ii) standard errors of the regression coefficient and the intercept (S.E.), (iii) the coefficient of determination (R^2), (iv) the probability of getting a greater F statistic than that observed if the hypothesis is true; *i.e.*, the significance probability (p). The meaning of these terms is given in ref. 6.

TABLE I

LINEAR REGRESSION EQUATIONS FOR COMPOUNDS OF MONOFUNCTIONALITY AND POLYFUNCTIONALITY AND THEIR SILYLATED DERIVATIVES ON NON-POLAR AND POLAR COLUMNS

I = retention index; Z = the number of C plus N and O atoms; Z' = Z + the number of C atoms in the silylating agent.

	I	
	DB-1	CW-20M, DB-Wax
<i>(I) Homologous series with monofunctional groups</i>		
<i>(A) n-Alkanoic acids</i>		
Free acids	$(93.37 \pm 0.90) Z + (257.26 \pm 9.44)^a$ ($n = 13, R^2 = 0.9990, p = 0.0001$)	$(105.60 \pm 0.88) Z + (971.50 \pm 9.59)$ ($n = 8, R^2 = 0.9996, p = 0.0001$)
O-(TMS) derivatives	$(94.79 \pm 0.53) Z + (321.17 \pm 5.50)$ $(94.79 \pm 0.53) Z' + (36.81 \pm 6.96)$ ($n = 13, R^2 = 0.9997, p = 0.0001$)	
O-(TBDMS) derivatives	$(96.41 \pm 0.82) Z + (521.31 \pm 8.89)$ $(96.41 \pm 0.82) Z' - (57.15 \pm 13.55)$ ($n = 12, R^2 = 0.9993, p = 0.0001$)	$(98.13 \pm 1.34) Z + (598.10 \pm 15.70)$ $(98.13 \pm 1.34) Z' + (9.34 \pm 23.47)$ ($n = 10, R^2 = 0.9985, p = 0.0001$)
<i>(B) n-Alkanols</i>		
Free alcohols	$(99.71 \pm 0.81) Z + (157.94 \pm 9.86)$ ($n = 11, R^2 = 0.9994, p = 0.0001$)	$(101.29 \pm 0.63) Z + (630.52 \pm 7.75)$ ($n = 11, R^2 = 0.9996, p = 0.0001$)
O-(TMS) derivatives	$(96.67 \pm 0.15) Z + (319.26 \pm 1.83)$ $(96.67 \pm 0.15) Z' + (29.26 \pm 2.24)$ ($n = 11, R^2 = 1.0000, p = 0.0001$)	
O-(TBDMS) derivatives	$(98.08 \pm 0.44) Z + (519.25 \pm 5.37)$ $(98.08 \pm 0.44) Z' - (69.21 \pm 7.81)$ ($n = 11, R^2 = 0.9998, p = 0.0001$)	$(94.98 \pm 0.50) Z + (534.30 \pm 6.05)$ $(94.98 \pm 0.50) Z' - (35.58 \pm 8.79)$ ($n = 11, R^2 = 0.9998, p = 0.0001$)
<i>(C) n-Aliphatic primary amines</i>		
Free amines	$(101.71 \pm 0.61) Z + (117.56 \pm 5.94)$ ($n = 9, R^2 = 0.9997, p = 0.0001$)	
Acetone adducts	$(99.37 \pm 1.32) Z + (350.06 \pm 11.65)$ $(99.37 \pm 1.32) Z' + (51.94 \pm 15.47)$ ($n = 6, R^2 = 0.9993, p = 0.0001$)	$(98.17 \pm 0.16) Z + (582.66 \pm 1.32)$ $(98.17 \pm 0.16) Z' + (188.14 \pm 1.78)$ ($n = 7, R^2 = 1.0000, p = 0.0001$)
N-(TMS) derivatives	$(98.46 \pm 0.25) Z + (365.98 \pm 2.39)$ $(98.46 \pm 0.25) Z' + (70.59 \pm 3.05)$ ($n = 9, R^2 = 1.0000, p = 0.0001$)	$(91.12 \pm 1.11) Z + (606.28 \pm 9.24)$ $(91.12 \pm 1.11) Z' + (332.93 \pm 12.37)$ ($n = 6, R^2 = 0.9994, p = 0.0001$)
N,N-Bis(TMS) derivatives	$(99.37 \pm 1.32) Z + (350.06 \pm 11.65)$ $(99.37 \pm 1.32) Z' + (51.94 \pm 15.47)$ ($n = 6, R^2 = 0.9993, p = 0.0001$)	
N-(TBDMS) derivatives	$(100.47 \pm 1.22) Z + (569.84 \pm 13.30)$ $(100.47 \pm 1.22) Z' + (32.95 \pm 20.20)$ ($n = 7, R^2 = 0.9993, p = 0.0001$)	
<i>(II) Homologous series with multiple functional groups</i>		
<i>(A) ω-Amino-1-alkanols</i>		
Free amino alcohols	$(106.70 \pm 8.13) Z + (321.80 \pm 50.09)$ ($n = 5, R^2 = 0.9829, p = 0.0010$)	
O-(TMS) derivatives	$(96.50 \pm 1.70) Z + (458.60 \pm 10.48)$ $(96.50 \pm 1.70) Z' + (169.10 \pm 15.49)$ ($n = 5, R^2 = 0.9991, p = 0.0001$)	
O,N,N-Tris(TMS) derivatives	$(96.30 \pm 2.72) Z + (889.80 \pm 16.78)$ $(96.30 \pm 2.72) Z' + (23.10 \pm 41.01)$ ($n = 5, R^2 = 0.9976, p = 0.0001$)	
O,N-Bis(TBDMS) derivatives	$(102.20 \pm 2.02) Z + (1045.40 \pm 12.47)$ $(102.20 \pm 2.02) Z' - (181.00 \pm 36.53)$ ($n = 4, R^2 = 0.9988, p = 0.0001$)	

(Continued on p. 117)

TABLE I (continued)

	<i>I</i>	
	DB-1	CW-20M, DB-Wax
(B) α -Amino acids		
O,N-Bis(TMS) derivatives	(70.50 \pm 2.48) <i>Z</i> + (689.50 \pm 18.80) (70.50 \pm 2.48) <i>Z'</i> + (266.50 \pm 33.59) (<i>n</i> = 4, <i>R</i> ² = 0.9975, <i>p</i> = 0.0012)	
O,N-Bis(TBDMS) derivatives	(71.80 \pm 4.31) <i>Z</i> + (1097.50 \pm 32.69) (71.80 \pm 4.31) <i>Z'</i> + (235.90 \pm 94.19) (<i>n</i> = 4, <i>R</i> ² = 0.9928, <i>p</i> = 0.0036)	
(C) Terminally substituted amino acids		
O,N,N-Tris(TMS) derivatives	(110.78 \pm 2.18) <i>Z</i> + (824.10 \pm 17.25) (110.78 \pm 2.18) <i>Z'</i> - (82.88 \pm 36.56) (<i>n</i> = 5, <i>R</i> ² = 0.9986, <i>p</i> = 0.0001)	
O,N-Bis(TBDMS) derivatives	(103.11 \pm 2.18) <i>Z</i> + (1023.95 \pm 17.21) (103.11 \pm 2.18) <i>Z'</i> - (213.40 \pm 42.97) (<i>n</i> = 5, <i>R</i> ² = 0.9987, <i>p</i> = 0.0001)	
(D) Alkane diols		
O,O-Bis(TMS) derivatives	(93.50 \pm 7.79) <i>Z</i> + (614.50 \pm 39.49) (93.50 \pm 7.79) <i>Z'</i> + (53.50 \pm 85.97) (<i>n</i> = 3, <i>R</i> ² = 0.0031, <i>p</i> = 0.0529)	
O,O-Bis(TBDMS) derivatives	(97.50 \pm 4.91) <i>Z</i> + (1007.17 \pm 24.86) (97.50 \pm 4.91) <i>Z'</i> - (162.83 \pm 83.52) (<i>n</i> = 3, <i>R</i> ² = 0.9900, <i>p</i> = 0.0320)	
(E) Acid amides		
N-(TBDMS) derivatives	(44.00 \pm 15.01) <i>Z</i> + (909.33 \pm 76.05) (44.00 \pm 15.01) <i>Z'</i> + (689.33 \pm 150.61) (<i>n</i> = 3, <i>R</i> ² = 0.8957, <i>p</i> = 0.2093)	
O,N-Bis(TBDMS) derivatives	(55.00 \pm 6.35) <i>Z</i> + (1117.33 \pm 32.17) (55.00 \pm 6.35) <i>Z'</i> + (512.33 \pm 101.75) (<i>n</i> = 3, <i>R</i> ² = 0.9868, <i>p</i> = 0.0732)	

^a The linear regression equations are given in the form of ($A \pm \text{S.E.}$) *Z* + ($GRF \pm \text{S.E.}$) where *A* is the regression coefficient, *GRF* the intercept, and S.E. the standard errors. The statistics given are the number of data points (*n*), standard errors for the regression coefficient and the intercept (S.E.), the coefficient of determination (*R*²) and the significance probability (*p*), i.e., the probability of getting a greater *F* statistic than that obtained if the hypothesis is true. It should be pointed out that all regression analysis can be seriously distorted by a single incorrect data value (see ref. 6).

Carboxylic acids

Upon silylation, the active hydrogen in the carboxylic acid group is replaced by the silyl group. The *I* values of the TMS esters on DB-1 column are approximated by their base values, and those on CW-20M column by their base values plus 150. The value of 150 represents the *GRF* for the residual polarity of the TMS ester group (-CO-O-TMS) on the polar column. The *I* values of the TBDMS esters on non-polar and polar columns can be calculated from their base values. Since the quaternary carbon atom in the TBDMS group has a *GRF* of -100 on non-polar and polar columns, this value must be subtracted from the base value. The *GRF* for the

residual polarity of the TBDMS ester group (-CO-O-TBDMS) has a value of +100 on polar column, which must be added to obtain the predicted *I*. The TBDMS ester group appears to be less polar than the TMS ester group and has a smaller *GRF* value. Table II compares the observed and predicted *I* values of TMS and TBDMS derivatives of homologous aliphatic carboxylic acids on non-polar and polar columns.

Plotting the observed *I* values of the TMS and TBDMS esters and the free acids on DB-1 and CW-20M columns against the number of atoms (*Z*) in the parent molecule yields straight lines, as shown in Fig. 1. The column difference (ΔI), defined as the

TABLE II

COMPARISON OF OBSERVED AND PREDICTED I VALUES OF SILYLATED ESTERS OF n -ALKANOIC ACIDS ON DB-1 AND CW-20MListed in the table are the following values: (1) for TMS esters: (i) I_p (on DB-1) = base value, (ii) I_p (on CW-20M) = base value + 100; (2) for TBDMS esters: (i) I_p (on DB-1) = base value - 100, (ii) I_p (on CW-20M) = base value; (3) the GRF for the silyl ester group on CW-20M = +100; (4) the GRF for the quaternary C atom in TBDMS group = -100.

Compound and silylated esters	Formula	On DB-1 column ^a			On CW-20M column ^a		
		I_{obs}	I_p	Difference (%)	I_{obs}	I_p	Difference (%)
Formic acid	CH ₂ O ₂	512					
O-(TMS)-	C ₄ H ₁₀ O ₂	612	600	3.5			
Acetic acid	C ₂ H ₄ O ₂	642					
O-(TMS)-	C ₅ H ₁₂ O ₂ Si	705	700	0.71			
O-(TBDMS)-	C ₈ H ₁₈ O ₂ Si	930	900	3.33			
Propionic acid	C ₃ H ₆ O ₂	743					
O-(TMS)-	C ₆ H ₁₄ O ₂ Si	800	800	0			
O-(TBDMS)-	C ₉ H ₂₀ O ₂ Si	1015	1000	1.5			
n -Butanoic acid	C ₄ H ₈ O ₂	823			1600		
O-(TMS)-	C ₇ H ₁₆ O ₂ Si	891	900	1	1025	1000	2.5
O-(TBDMS)-	C ₁₀ H ₂₂ O ₂ Si	1098	1100	0.18	1200	1200	0
n -Pentanoic acid	C ₅ H ₁₀ O ₂	925			1706		
O-(TMS)-	C ₈ H ₁₈ O ₂ Si	975	1000	2.5	1123	1100	2.3
O-(TBDMS)-	C ₁₁ H ₂₄ O ₂ Si	1184	1200	1.33	1294	1300	0.46
n -Hexanoic acid	C ₆ H ₁₂ O ₂	992			1834		
O-(TMS)-	C ₉ H ₂₀ O ₂ Si	1071	1100	2.64	1200	1200	0
O-(TBDMS)-	C ₁₂ H ₂₆ O ₂ Si	1276	1300	1.85	1385	1400	1.07
n -Heptanoic acid	C ₇ H ₁₄ O ₂	1103			1916		
O-(TMS)-	C ₁₀ H ₂₂ O ₂ Si	1166	1200	2.83			
O-(TBDMS)-	C ₁₃ H ₂₈ O ₂ Si	1378	1400	1.57	1474	1500	1.73
n -Octanoic acid	C ₈ H ₁₆ O ₂	1187					
O-(TMS)-	C ₁₁ H ₂₄ O ₂ Si	1260	1300	3.08	1400	1400	0
O-(TBDMS)-	C ₁₄ H ₃₀ O ₂ Si	1482	1500	1.2	1582	1600	1.13
n -Nonanoic acid	C ₉ H ₁₈ O ₂	1280			2132		
O-(TMS)-	C ₁₂ H ₂₆ O ₂ Si	1358	1400	3.01			
O-(TBDMS)-	C ₁₅ H ₃₂ O ₂ Si	1578	1600	1.38	1638	1700	1.01
n -Decanoic acid	C ₁₀ H ₂₀ O ₂	1374			2238		
O-(TMS)-	C ₁₃ H ₂₈ O ₂ Si	1455	1500	3.01			
O-(TBDMS)-	C ₁₆ H ₃₄ O ₂ Si	1674	1700	1.53	1777	1800	1.28
Lauric acid	C ₁₂ H ₂₄ O ₂	1545			2451		
O-(TMS)-	C ₁₅ H ₃₂ O ₂ Si	1651	1700	2.88			
O-(TBDMS)-	C ₁₈ H ₃₈ O ₂ Si	1872	1900	1.47	1977	2000	1.15
Myristic acid	C ₁₄ H ₂₈ O ₂	1747			2660		
O-(TMS)-	C ₁₇ H ₃₆ O ₂ Si	1845	1900	2.89			
O-(TBDMS)-	C ₂₀ H ₄₂ O ₂ Si	2075	2100	1.19	2176	2200	1.09
Palmitic acid	C ₁₆ H ₃₂ O ₂	1956					
O-(TMS)-	C ₁₉ H ₄₀ O ₂ Si	2036	2100	3.05			
O-(TBDMS)-	C ₂₂ H ₄₆ O ₂ Si	2263	2300	1.61	2370	2400	1.25

^a Base value = 100 Z , where Z is the number of carbon and carbon equivalent atoms. I_{obs} = observed I ; I_p = predicted I ; Difference (%) = (difference between I_{obs} and I_p) \times 100/(I_{obs} or I_p).

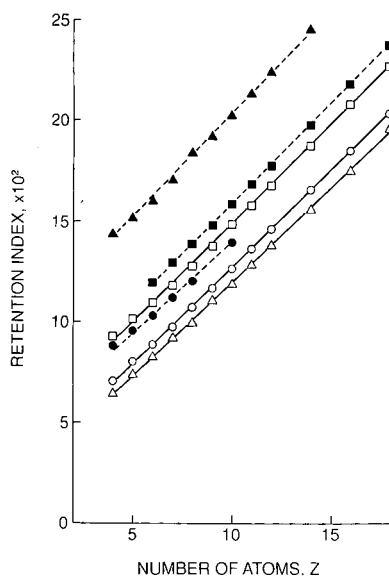


Fig. 1. Convergence of retention indexes of silylated alkanolic acid esters on non-polar and polar columns. The homologues of free acids and their TMS and TBDMS esters are given as Δ , \circ and \square on DB-1 column (solid lines) and as \blacktriangle , \bullet and \blacksquare on DB-Wax column (broken lines), respectively.

difference between I on polar and non-polar columns [4], appears to be much smaller for the silylated acid esters than for the underivatized acids. This clearly demonstrates that silylation alters the polarity and polarizability of the analyte and that the silylated derivatives mimic the chromatographic behavior of n -alkanes.

Aliphatic fatty acids are monofunctional, while the alicyclic and aromatic acids, because of the ring function, are bifunctional. Silylation may also diminish the GRF of the ring function. The decrease is more pronounced with silylated alicyclic acid esters than with silylated benzoic acid ester. In bromo- and iodobenzoic acids, silylation may also decrease the $GRFs$ of the halo atoms.

Aliphatic alcohols

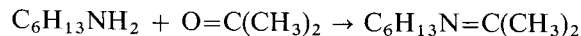
Silylated derivatives of alcohols are ethers. The ether oxygen has a GRF of zero on non-polar column and a value of +70 on polar column [4]. Silylation masks completely the polarity of the ether oxygen of the silylated ethers on polar column and reduces its GRF to practically zero. As a result, silylated derivatives of alcohols exhibit approxi-

mately the same I values on CW-20M and DB-1 columns, as shown in Table III.

Table IV shows the I values of silylated ethers of alicyclic alcohols and phenols. The GRF values of the 6-membered alicyclic rings and the phenyl ring in the silylated ethers are not affected, but the functionality of the $-\text{OH}$ group will be modified by silylation. In alicyclic silylated ethers, chain branching, due to the presence of iso-carbon, has a GRF value of -40 on DB-1 column which should be considered in obtaining the predicted I .

Primary aliphatic amines

The I values of primary aliphatic amines may be affected by the solvent used in diluting the analyte. The I values of the amines are higher by about 210 units in acetone than in ethanol. According to the structure-retention-index relationship the higher I observed in acetone should belong to a molecule with at least two more atoms than the amine molecule, suggesting the formation of Schiff's base or anil. The high temperature in the injection port accelerates the coupling of the amine and the solvent acetone. According to this scheme, the reaction product of n -hexylamine in acetone is shown as follows:



The identity of the anil was confirmed by analysis by gas chromatography-mass spectrometry.

The I values of the anils formed from amino alkanes and acetone can be predicted from the base values plus 52 which is the GRF for the anil $-\text{N}=(\text{CH}_3)_2$ group. For higher amines the anil reaction may be incomplete for the brief duration in the injection port. n -Decylamine and n -dodecylamine in acetone were found to show two chromatographic peaks each, one corresponding to the amine and the other to the acetone adduct or the anil. A comparison of the observed and predicted I values of n -alkylamines in acetone and in ethanol is given in Table V.

The primary amino $-\text{NH}_2$ group possesses two active hydrogen atoms. Depending on the condition of silylation and the molecular connectivity of the carbon atom to which the amino group is attached, one or two hydrogen may be replaced. Mono-substitution converts the primary amine to a secondary amine and disubstitution converts the primary

TABLE III

COMPARISON OF OBSERVED AND PREDICTED I VALUES OF SILYLATED ETHERS FROM n -ALKANOLS

The predicted I values for TMS ethers are: I_p (DB-1) = I_p (CW-20M) = base value. The predicted I values for TBDMS ethers are: I_p (DB-1) = I_p (CW-20M) = base value - 100, where -100 is the GRF for the quaternary C atom in TBDMS group.

Compound and silylated ethers	Formula	On DB-1 column ^a			On CW-20M column ^a		
		I_{obs}	I_p	Difference (%)	I_{obs}	I_p	Difference (%)
Ethanol	C ₂ H ₆ O	446			944		
O-(TMS)-	C ₅ H ₁₄ OSi	614	600	2.28	652	600	7.98
O-(TBDMS)-	C ₈ H ₂₀ OSi	827	800	3.38	834	800	4.08
1-Propanol	C ₃ H ₈ O	552			1025		
O-(TMS)-	C ₆ H ₁₆ OSi	705	700	0.71	730	700	4.11
O-(TBDMS)-	C ₉ H ₂₂ OSi	907	900	0.78	919	900	2.07
1-Butanol	C ₄ H ₁₀ O	659			1141		
O-(TMS)-	C ₇ H ₁₈ O	800	800	0	836	800	4.3
O-(TBDMS)-	C ₁₀ H ₂₄ OSi	1012	1000	1.2	1000	1000	0
1-Pentanol	C ₅ H ₁₂ O	767			1236		
O-(TMS)-	C ₈ H ₂₀ OSi	900	900	0	921	900	2.28
O-(TBDMS)-	C ₁₁ H ₂₆ OSi	1107	1100	0.36	1106	1100	0.55
1-Heptanol	C ₇ H ₁₆ O	974			1440		
O-(TMS)-	C ₁₀ H ₂₄ OSi	1092	1100	0.72	1108	1100	0.72
O-(TBDMS)-	C ₁₃ H ₃₀ OSi	1293	1300	0.54	1282	1300	1.38
1-Decanol	C ₁₀ H ₂₂ O	1267			1735		
O-(TMS)-	C ₁₃ H ₃₀ OSi	1379	1400	1.5	1385	1400	1.07
O-(TBDMS)-	C ₁₆ H ₃₆ OSi	1590	1600	0.63	1569	1600	1.94
1-Dodecanol	C ₁₂ H ₂₆ O	1420			1950		
O-(TMS)-	C ₁₅ H ₃₄ OSi	1575	1600	1.56	1573	1600	1.69
O-(TBDMS)-	C ₁₈ H ₄₀ OSi	1800	1800	0	1762	1800	2.11
1-Tetradecanol	C ₁₄ H ₃₀ O	1647			2157		
O-(TMS)-	C ₁₇ H ₃₈ OSi	1770	1800	1.67	1759	1800	2.28
O-(TBDMS)-	C ₂₀ H ₄₄ OSi	1987	2000	0.65	1969	2000	1.55
1-Hexadecanol	C ₁₆ H ₃₄ O	1852			2352		
O-(TMS)-	C ₁₉ H ₄₂ OSi	1965	2000	1.75	1959	2000	2.05
O-(TBDMS)-	C ₂₂ H ₄₈ OSi	2185	2200	0.68	2156	2200	2.01
1-Heptadecanol	C ₁₇ H ₃₆ O	1960			2475		
O-(TMS)-	C ₂₀ H ₄₄ OSi	2056	2100	2.1	2046	2100	2.57
O-(TBDMS)-	C ₂₃ H ₅₀ OSi	2280	2300	0.87	2244	2300	2.43
1-Octadecanol	C ₁₈ H ₃₈ O	2059			2534		
O-(TMS)-	C ₂₁ H ₄₆ OSi	2159	2200	1.86	2144	2200	2.54
O-(TBDMS)-	C ₂₄ H ₅₂ OSi	2395	2400	0.21	2339	2400	2.54

^a See footnote in Table II.

amine to a tertiary amine. The GRF for residual amino functionality of an amino group connected to a secondary carbon atom is +50. Disubstitution with two TMS silyl groups occurs only in an amino group connected to a primary carbon atom with a GRF value of zero or below zero in some cases [4].

In contrast, the TBDMS group is bulkier than the TMS group and yields only mono-silylated derivatives. Structural identities of the mono- and di-TMS derivatives of n -hexylamine have been verified by gas chromatography-mass spectrometry analysis. Table VI compares the observed and predicted

TABLE IV

COMPARISON OF OBSERVED AND PREDICTED I VALUES OF SOME SILYLATED ETHERS (ON DB-1)^a

The $GRFs$ (m_i and n_i) used for I prediction have the following values: (1) alicyclic hydroxyl group = +119, (2) cyclopentane ring = +64, (3) quaternary carbon atom in TBDMS group = -100, (4) chain branching = -40, (5) cyclohexane ring = +62, (6) cyclohexene ring = +67, (7) phenyl ring = +58, (8) phenolic hydroxyl group = +211.

Compound and silylated ethers	Formula	I_{obs}	$100Z + \sum m_i - \sum n_i$	I_p	Difference (%)
Cyclopentanol	$C_5H_{10}O$	774	$600 + 119 + 64$	783	1.15
O-(TBDMS)-	$C_{11}H_{24}OSi$	1119	$1200 + 64 - 100 - 40$	1124	0.44
Cyclohexanol	$C_6H_{12}O$	881	$700 + 62 + 119$	881	0
O-(TMS)-	$C_9H_{20}OSi$	1000	$1000 + 62 - 40$	1022	2.15
O-(TBDMS)-	$C_{12}H_{26}OSi$	1214	$1300 + 62 - 100 - 40$	1222	0.64
2-Cyclohexen-1-ol	$C_6H_{10}O$	887	$700 + 67 + 119$	886	0.11
O-(TMS)-	$C_9H_{18}OSi$	1027	$1000 + 67 - 40$	1027	0
2-Methylcyclohexanol	$C_7H_{14}O$	941	$800 + 62 + 119 - 40$	941	0
O-(TMS)-	$C_{10}H_{22}OSi$	1067	$1100 + 62 - 2 \times 40$	1082	1.39
O-(TBDMS)-	$C_{13}H_{28}OSi$	1285	$1400 + 62 - 100 - 2 \times 40$	1282	0.62
4-Methylcyclohexanol	$C_7H_{14}O$	941	$800 + 62 + 119 - 40$	941	0
O-(TMS)-	$C_{10}H_{22}OSi$	1071	$1100 + 62 - 2 \times 40$	1082	1.02
O-(TBDMS)-	$C_{13}H_{28}OSi$	1279	$1400 + 62 - 100 - 2 \times 40$	1282	0.23
Phenol	C_6H_6O	962	$700 + 58 + 211$	969	0.72
O-(TMS)-	$C_9H_{14}OSi$	1043	$1000 + 58$	1058	1.42
O-(TBDMS)-	$C_{12}H_{20}OSi$	1260	$1300 + 58 - 100$	1258	0.16
<i>m</i> -Cresol	C_7H_8O	1064	$800 + 58 + 211$	1069	0.47
O-(TMS)-	$C_{10}H_{22}OSi$	1134	$1100 + 58$	1158	2.07
O-(TBDMS)-	$C_{13}H_{22}OSi$	1348	$1400 + 58 - 100$	1358	0.74

^a See footnote in Table II.

I values of some silylated alicyclic and aromatic amines. The aromatic amino group in aniline takes only one TMS group upon silylation, and the amino group in benzylamine is also mono-substituted. Silylation modifies the amine function in cyclohexylamine to make it resemble a hydrocarbon which introduces chain branching. Chain branching in alicyclic hydrocarbons chain branching has a GRF value of -40 [1].

Polyfunctional compounds

The I values of polyfunctional compounds are difficult to predict. Their I values cannot be estimated from the $GRFs$ used for monofunctional compounds by the rule of additivity. The functional groups can interact intramolecularly among themselves to affect both A and GRF values so that the observed I and the predicted I based on the group additivity rule may be at variance. Alkylamines and

aliphatic carboxylic acids can be chromatographed alone without derivatization, but underivatized amino acids, containing both free amino and carboxyl groups in the same molecule, have infinitely large I values and do not emerge from the column.

Derivatization by silylation greatly reduces the polarity of polyfunctional molecules and allows these molecules to be chromatographed as silylated derivatives. Their I values are readily estimated from the base values. A limited number of polyfunctional compounds in the following categories have been studied.

n-Alkanediols. Underivatized alkanediols yield asymmetrical peaks. Once derivatized, the TMS and TBDMS derivatives of the diols give sharp, symmetrical peaks. The I values of the TMS derivatives can be predicted from the base values, as shown in Table VII. The I values of TBDMS derivatives are predicted from the base values minus 200 which

TABLE V

COMPARISON OF OBSERVED AND PREDICTED I VALUES OF SILYLATED DERIVATIVES OF n -ALKAMINES (ON DB-1)^a

The $GRFs$ (m_i and n_i) have the following values: (1) primary amine, $-\text{CH}_2\text{NH}_2 = +133$, (2) $-\text{NHC}_2\text{H}_5$ group = -30 , (3) $-\text{NH}-(\text{TMS})$ group = $+50$, (4) $-\text{N}=(\text{TMS})_2$ group = 0 , (5) anil group = $+52$, (6) quaternary C atom in TBDMS group = -100 , (7) chain branching = -40 .

Compound and silylated derivatives	Formula	I_{obs}	$100Z + \Sigma m_i - \Sigma n_i$	I_p	Difference (%)
Ethylamine	$\text{C}_2\text{H}_7\text{N}$	413	$300 + 133 - 30$	403	2.42
N-(TMS)-	$\text{C}_5\text{H}_{15}\text{NSi}$	660	$600 + 50$	650	1.52
n -Propylamine	$\text{C}_3\text{H}_9\text{N}$	515	$400 + 133$	533	3.38
N-(TMS)-	$\text{C}_6\text{H}_{17}\text{NSi}$	755	$700 + 50$	750	0.66
N,N-Bis(TMS)-	$\text{C}_9\text{H}_{25}\text{NSi}_2$	1031	1000	1000	3.01
n -Butylamine	$\text{C}_4\text{H}_{11}\text{N}$	626	$500 + 133$	633	1.1
Acetone adduct	$\text{C}_7\text{H}_{15}\text{N}$	835	$800 + 52$	852	1.99
N-(TMS)-	$\text{C}_7\text{H}_{19}\text{NSi}$	862	$800 + 50$	850	1.39
N,N-Bis(TMS)-	$\text{C}_{10}\text{H}_{27}\text{NSi}_2$	1115	1100	1100	1.35
N-(TBDMS)-	$\text{C}_{10}\text{H}_{25}\text{NSi}$	1085	$1100 + 50 - 100$	1050	3.23
n -Pentylamine	$\text{C}_5\text{H}_{13}\text{N}$	744	$600 + 133$	733	1.48
Acetone adduct	$\text{C}_8\text{H}_{17}\text{N}$	960	$900 + 52$	951	0.94
N-(TMS)-	$\text{C}_8\text{H}_{21}\text{NSi}$	963	$800 + 50$	850	1.39
N,N-Bis(TMS)-	$\text{C}_{11}\text{H}_{29}\text{NSi}_2$	1200	1200	1200	0
N-(TBDMS)-	$\text{C}_{11}\text{H}_{27}\text{NSi}$	1177	$1200 + 50 - 100$	1150	2.29
Isopentylamine	$\text{C}_5\text{H}_{13}\text{N}$	705	$600 + 133 - 40$	693	1.7
N-(TMS)-	$\text{C}_8\text{H}_{21}\text{NSi}$	920	$900 + 50 - 40$	910	1.09
n -Hexylamine	$\text{C}_6\text{H}_{15}\text{N}$	829	$700 + 133$	833	0.48
Acetone adduct	$\text{C}_9\text{H}_{19}\text{N}$	1046	$1000 + 52$	1052	0.57
N-(TMS)-	$\text{C}_9\text{H}_{23}\text{NSi}$	1055	$1000 + 50$	1050	0.47
N,N-Bis(TMS)-	$\text{C}_{12}\text{H}_{31}\text{NSi}_2$	1301	1300	1300	0.08
N-(TBDMS)-	$\text{C}_{12}\text{H}_{29}\text{NSi}$	1271	$1300 + 50 - 100$	1250	1.65
n -Heptylamine	$\text{C}_7\text{H}_{17}\text{N}$	937	$800 + 133$	933	0.43
Acetone adduct	$\text{C}_{10}\text{H}_{21}\text{N}$	1145	$1100 + 52$	1152	0.61
N-(TMS)-	$\text{C}_{10}\text{H}_{25}\text{NSi}$	1153	$1100 + 50$	1150	0.26
N,N-Bis(TMS)-	$\text{C}_{13}\text{H}_{33}\text{NSi}_2$	1390	1400	1400	0.71
N-(TBDMS)-	$\text{C}_{13}\text{H}_{31}\text{NSi}_2$	1373	$1400 + 50 - 100$	1350	1.68
n -Decylamine	$\text{C}_{10}\text{H}_{23}\text{N}$	1237	$1100 + 133$	1233	0.32
Acetone adduct	$\text{C}_{13}\text{H}_{27}\text{N}$	1442	$1400 + 52$	1452	0.69
N-(TMS)-	$\text{C}_{13}\text{H}_{31}\text{NSi}$	1447	$1400 + 50$	1450	0.21
N,N-Bis(TMS)-	$\text{C}_{16}\text{H}_{39}\text{NSi}_2$	1692	1700	1700	0.49
N-(TBDMS)-	$\text{C}_{16}\text{H}_{37}\text{NSi}$	1647	$1700 + 50 - 100$	1650	0.18
n -Dodecylamine	$\text{C}_{12}\text{H}_{27}\text{N}$	1444	$1300 + 133$	1433	0.76
Acetone adduct	$\text{C}_{15}\text{H}_{31}\text{N}$	1641	$1600 + 52$	1652	0.67
N-(TMS)-	$\text{C}_{15}\text{H}_{35}\text{NSi}$	1644	$1600 + 50$	1650	0.36
N,N-Bis(TMS)-	$\text{C}_{18}\text{H}_{43}\text{NSi}_2$	1893	1900	1900	0.37
N-(TBDMS)-	$\text{C}_{18}\text{H}_{41}\text{NSi}$	1879	$1900 + 50 - 100$	1850	1.54
n -Octadecylamine	$\text{C}_{18}\text{H}_{39}\text{N}$	2043	$1900 + 133$	2033	0.49
N-(TMS)-	$\text{C}_{21}\text{H}_{47}\text{NSi}$	2233	$2200 + 50$	2250	0.53
N,N-Bis(TMS)-	$\text{C}_{24}\text{H}_{55}\text{NSi}_2$	2486	2500	2500	0.56
N-(TBDMS)-	$\text{C}_{24}\text{H}_{53}\text{NSi}$	2489	$2500 + 50 - 100$	2450	1.57

^a See footnote in Table II.

TABLE VI

COMPARISON OF OBSERVED AND PREDICTED I VALUES OF SILYLATED DERIVATIVES OF SOME AMINES (ON DB-1)^a

The GRF s (m_i and n_i) have the following values: (1) cyclohexene ring = +62, (2) -NH-(TMS) group attached to secondary C atom = +25, (3) chain branching = -40, (4) -NH-(TMS) group = +50, (5) phenyl ring = +58, (6) aromatic secondary amine, Ar-NH-(TMS) group = +130, (7) aromatic tertiary amine, Ar-N(TMS)R group = +26.

Compound and silylated derivatives	Formula	I_{obs}	$100Z + \sum m_i - \sum n_i$	I_p	Difference (%)
Cyclohexylamine N-(TMS)-	$C_6H_{13}N$	851			
	$C_9H_{21}NSi$	1061	$1000 + 62 + 25 - 40$	1047	1.32
3-Aminoheptane N-(TMS)-	$C_7H_{17}N$	868		877	1.03
	$C_{10}H_{25}NSi$	1073	$1100 + 25 - 40$	1085	1.11
2-Aminopentane N-(TMS)-	$C_7H_{17}N$	868		877	1.03
	$C_{10}H_{25}NSi$	1081	$1100 + 25 - 40$	1085	0.37
3-Methylcyclohexylamine N-(TMS)-	$C_7H_{15}N$				
	$C_{10}H_{23}NSi$	1110	$1100 + 62 + 50 - 2 \times 40$	1132	1.94
Aniline N-(TMS)-	C_6H_7N	955			
	$C_9H_{15}NSi$	1186	$1000 + 58 + 130$	1188	0.17
Benzylamine N-(TMS)-	C_7H_9N				
	$C_{10}H_{17}NSi$	1212	$1100 + 58 + 50$	1208	0.33
Phenethylamine N-(TMS)-	$C_8H_{11}N$	1115		1091	2.15
	$C_{11}H_{19}NSi$	1280	$1200 + 58 + 50$	1308	2.14
<i>o</i> -Toluidine N-(TMS)-	C_7H_9N	1068			
	$C_{10}H_{17}NSi$	1244	$1100 + 58 + 130$	1288	3.41
<i>m</i> -Toluidine N-(TMS)-	C_7H_9N	1064			
	$C_{10}H_{17}NSi$	1269	$1100 + 58 + 130$	1288	1.48
N-Methylaniline N-(TMS)-	C_7H_9N	1056			
	$C_{10}H_{17}NSi$	1195	$1100 + 58 + 26$	1184	0.92
N-Ethylaniline N-(TMS)-	$C_8H_{11}N$				
	$C_{11}H_{19}NSi$	1303	$1200 + 58 + 26$	1284	1.46

^a See footnote in Table II.

represents the GRF values for the two quaternary carbon atoms in the TBDMS groups. The I values of the TMS and TBDMS derivatives of propylene glycol (*i.e.*, 1,2-propanediol) are lower than those of 1,3-propanediol, because the former contains a secondary alcoholic hydroxyl group.

ω -Amino-1-alkanols. ω -Amino-1-alkanols contain both terminal amino (-NH₂) and hydroxyl (-OH) groups. The amino groups of the amino alkanols can form anils with acetone. The hydroxyl group is more easily silylated than the primary amino group, and the TMS reagent will first react with the hydroxyl group under mild conditions to form the TMS ether with only one TMS group per molecule. A longer

reaction time silylates both hydroxyl and amino groups, with the terminal amino group disubstituted. The fully silylated amino alcohol will contain three TMS groups per molecule. The TBDMS group is bulkier than the TMS group and will replace only one hydrogen from the amino group. As a result, the fully silylated amino alcohols will contain two TBDMS groups per molecule. Table VIII lists the observed and predicted I values of the amino alcohols.

Amino groups connected to secondary and tertiary carbon atoms are not readily silylated.

Amino acids. Underivatized amino acids are non-volatile and cannot be analyzed by gas chromato-

TABLE VII

COMPARISON OF OBSERVED AND PREDICTED I VALUES OF O,O-BIS(TMS)- AND O,O-BIS(*tert.*-BUTYLDIMETHYLSILYL)ALKANEDIOLS (ON DB-1)^aThe GRF s (m_i and n_i) have the following values: (1) quaternary C atom in TBDMS group = -100, (2) the difference between primary and secondary alcohol function = -70.

Compound and silylated ether	Formula	I_{obs}	$100Z + \sum m_i - \sum n_i$	I_p	Difference (%)
Ethylene glycol	$C_2H_6O_2$				
O,O-Bis(TMS)-	$C_8H_{22}O_2Si_2$	993	1000,	1000	0.7
O,O-Bis(TBDMS)-	$C_{14}H_{34}O_2Si_2$	1400	$1600 - 2 \times 100$	1400	0
Propylene-1,2-diol	$C_3H_8O_2$				
O,O-Bis(TMS)-	$C_9H_{24}O_2Si_2$	1013	$1100 - 70$	1013	1.65
O,O-Bis(TBDMS)-	$C_{15}H_{36}O_2Si_2$	1424	$1700 - 200 - 70$	1430	0.42
1,3-Propanediol	$C_3H_8O_2$				
O,O-Bis(TMS)-	$C_9H_{24}O_2Si_2$	1073	1100,	1100	2.45
O,O-Bis(TBDMS)-	$C_{15}H_{36}O_2Si_2$	1489	$1700 - 200$	1500	0.73
1,4-Butanediol	$C_4H_{10}O_2$				
O,O-Bis(TMS)-	$C_{10}H_{26}O_2Si_2$	1180	1200,	1200	1.67
O,O-Bis(TBDMS)-	$C_{16}H_{38}O_2Si_2$	1595	$1800 - 200$	1600	0.31

^a See footnote in Table II.

graphy. Amino acids can be chromatographed as TMS or TBDMS derivatives. The I values of silylated amino acids are determined by the number of silyl groups in the molecule and the proximity of the amino and carboxyl groups. The amino group at the α or β position to the carboxyl group is only monosubstituted, but the amino group connected to a methylene carbon at the terminal carbon atom is unhindered and will be disubstituted. The amino group in glycine is known to be disilylated by the TMS reagent [7].

Table IX lists the observed and predicted I values of TMS and TBDMS derivatives of some amino acid homologues containing ω , α or β amino groups. The terminal ω amino groups are disubstituted with TMS groups. The molecule that contains a silylated ester group and a terminal amino group with two TMS groups may further decrease its I by -60. Amino groups attached to secondary carbon atoms can only be monosubstituted, and the residual polarity of the resulting secondary amino group will have a GRF value of +50.

In α -amino acids, the close proximity of the silylated amino and carboxyl groups will reduce the I by -80 and decrease the value of A to about 71. In comparison, the isomeric ω -amino acids with the

amino and carboxyl groups at each end of an alkane chain have normal A values near 100. Linear plots of I vs. Z of the TMS and TBDMS derivatives of isomeric α - and ω -amino acids are shown in Fig. 2. The α -amino acids have a smaller A value than the ω -amino acids. A small A value is associated with high polarity and the steric factor that reduces I . The statistical data for the regression coefficients and the intercepts are given in Table I.

Acid amides. Acid amides can accept one or two TBDMS groups. The first TBDMS group will be attached to the amide N atom and the second TBDMS group to the amide O atom. This result agrees with those of others [2].



The acid amide group is highly polar and will affect the A values of mono- and di-TBDMS-substituted derivatives. The A for the monosubstituted derivatives is 44 and that for the disubstituted derivatives 55. Because the true value of A is so different from the assigned value of 100, the base value can no longer be used to predict I of these silylated derivatives. Accurate prediction can be

TABLE VIII

COMPARISON OF OBSERVED AND PREDICTED I VALUES OF SILYLATED DERIVATIVES OF ω -AMINO- n -ALKANOLS (ON DB-1)^a

The $GRFs$ (m_i and n_i) have the following values: (1) primary alcohol group in a molecule with terminal $-NH_2$ group = +210, (2) primary alcohol $-CH_2OH$ = +156, (3) primary amine $-CH_2NH_2$ = +133, (4) quaternary C atom in TBDMS group = -100, (5) anil group = +52, (6) $-N=(TMS)_2$ group = 0, (7) $-NH$ (TBDMS) group = +50.

Compound and silylated derivatives	Formula	I_{obs}	$100Z + \Sigma m_i - \Sigma n_i$	I_p	Difference (%)
2-Amino-ethanol	C_2H_7NO	739	400 + 210 + 133	743	0.54
O-(TMS)-	$C_5H_{15}NOSi$	842	700 + 133	833	0.12
O,N,N-Tris(TMS)-	$C_{11}H_{31}NOSi_3$	1281	1300	1300	1.46
O,N-Bis(TBDMS)-	$C_{14}H_{35}NOSi_2$	1448	1600 - 200 + 50	1450	0.14
3-Amino-1-propanol	C_3H_9NO	842	500 + 210 + 133	843	0.12
O-(TMS)-	$C_6H_{17}NOSi$	948	800 + 133	933	1.58
O,N,N-Tris(TMS)-	$C_{12}H_{33}NOSi_3$	1371	1400	1400	2.07
O,N-Bis(TBDMS)-	$C_{15}H_{37}NOSi_2$	1560	1700 - 200 + 50	1550	0.64
4-Amino-1-butanol	$C_4H_{11}NO$	998	600 + 210 + 133	943	5.51
Acetone adduct	$C_7H_{15}NO$	1115	900 + 156 + 52	1108	0.63
O-(TMS)-	$C_7H_{19}NOSi$	1032	900 + 133	1033	0.1
O,N,N-Tris(TMS)-	$C_{13}H_{35}NOSi_3$	1459	1500	1500	2.73
O,N-Bis(TBDMS)-	$C_{16}H_{39}NOSi_2$	1666	1800 - 200 + 50	1650	0.96
5-Amino-1-pentanol	$C_5H_{13}NO$	1075	700 + 210 + 133	1043	2.97
Acetone adduct	$C_8H_{17}NO$	1219	1000 + 156 + 52	1208	0.9
O-(TMS)-	$C_8H_{21}NOSi$	1135	1000 + 133	1133	0.18
O,N,N-Tris(TMS)-	$C_{14}H_{37}NOSi_3$	1558	1600	1600	2.63
O,N-Bis(TBDMS)-	$C_{17}H_{41}NOSi_2$	1760	1900 - 200 + 50	1750	0.57
6-Amino-1-hexanol	$C_6H_{15}NO$	1156	800 + 210 + 133	1143	1.12
Acetone adduct	$C_9H_{17}NO$	1307	1100 + 156 + 52	1308	0.08
O-(TMS)-	$C_9H_{23}NOSi$	1231	1100 + 133	1233	0.16
O,N,N-Tris(TMS)-	$C_{15}H_{39}NOSi_3$	1669	1700	1700	1.82
O,N-Bis(TBDMS)-	$C_{18}H_{43}NOSi_2$	1859	2000 - 200 + 50	1850	0.48

^a See footnote on Table II.

made, based on the true values of A and the regression equations. The A and GRF values for these derivatives are given in Table I under acid amides. Comparison of the predicted and observed I values is given in Table X.

Aliphatic dicarboxylic acids. Dicarboxylic acids such as oxalic acid, succinic acid, etc., can be silylated to yield disilylated acid esters. Their I values on non-polar column can be predicted from the base values minus 60. A GRF value of -60 is assigned to account for the presence of two terminal silyl groups in the di-acid molecule. The validity of this assumption will be further investigated. A comparison of the observed and predicted I values of these silyl derivatives is given in Table X.

Miscellaneous. The I values of miscellaneous silylated compounds may also be predicted from the base values according to the rules outlined above. Table X gives the comparison of the observed and predicted I values of some silylated derivatives. The presence of a silyl group in the molecule may diminish the $GRFs$ of other substituents and functional groups. The vanishingly small $GRFs$ for the alicyclic rings in the alicyclic hydrocarbon carboxylic acids and the reduced $GRFs$ of the bromo (from +276 to +240) and iodo (from +380 to +325) substituents in halobenzoic acids are such examples.

Chain branching refers to branching from the main alkyl chain. At the point of branching a

TABLE IX

COMPARISON OF OBSERVED AND PREDICTED I VALUES OF SILYLATED DERIVATIVES OF α - AND ω -AMINO ACIDS (ON DB-1)^aThe $GRFs$ (m_i and n_i) have the following values: (1) $-\text{CH}_2-\text{N}(\text{TMS})_2$ group = -60 , (2) $=\text{CH}-\text{NH}(\text{TBDMS})$ group = $+50$, (3) proximity of $=\text{CH}-\text{NH}(\text{TBDMS})$ and $=\text{CH}-\text{COO}(\text{TBDMS})$ groups = -80 , (4) quaternary C atom in TBDMS reagent = -100 .

Compound and silylated derivatives	Formula	I_{obs}	$100Z + \sum m_i - \sum n_i$	I_p	Difference (%)
2-Amino acetic acid (glycine)	$\text{C}_2\text{H}_5\text{NO}_2$				
O,N,N-Tris(TMS)-	$\text{C}_{11}\text{H}_{29}\text{NO}_2\text{Si}_3$	1317	$1400 - 60$	1340	1.72
O,N-Bis(TBDMS)-	$\text{C}_{14}\text{H}_{33}\text{NO}_2\text{Si}_2$	1551	$1700 + 50 - 200$	1550	0.06
3-Amino-1-propionic acid (β -alanine)	$\text{C}_3\text{H}_7\text{NO}_2$				
O,N,N-Tris(TMS)-	$\text{C}_{12}\text{H}_{31}\text{NO}_2\text{Si}_3$	1434	$1500 - 60$	1440	0.42
O,N-Bis(TBDMS)-	$\text{C}_{15}\text{H}_{35}\text{NO}_2\text{Si}_2$	1629	$1800 + 50 - 200$	1650	1.27
4-Amino-1-butanoic acid	$\text{C}_4\text{H}_9\text{NO}_2$				
O,N,N-Tris(TMS)-	$\text{C}_{13}\text{H}_{33}\text{NO}_2\text{Si}_3$	1542	$1600 - 60$	1540	1.3
O,N-Bis(TBDMS)-	$\text{C}_{16}\text{H}_{37}\text{NO}_2\text{Si}_2$	1744	$1900 + 50 - 200$	1750	0.34
6-Amino-1-hexanoic acid	$\text{C}_6\text{H}_{13}\text{NO}_2$				
O,N,N-Tris(TMS)-	$\text{C}_{15}\text{H}_{37}\text{NO}_2\text{Si}_3$	1726	$1800 - 60$	1740	0.8
O,N-Bis(TBDMS)-	$\text{C}_{18}\text{H}_{41}\text{NO}_2\text{Si}_2$	1955	$2100 + 50 - 200$	1950	0.26
8-Amino-1-octanoic acid	$\text{C}_8\text{H}_{17}\text{NO}_2$				
O,N,N-Tris(TMS)-	$\text{C}_{17}\text{H}_{41}\text{NO}_2\text{Si}_3$	1931	$2000 - 60$	1940	0.46
O,N-Bis(TBDMS)-	$\text{C}_{20}\text{H}_{45}\text{NO}_2\text{Si}_2$	2159	$2300 + 50 - 200$	2150	0.42
2-Amino-1-propionic acid (alanine)	$\text{C}_3\text{H}_7\text{NO}_2$				
O,N-Bis(TMS)-	$\text{C}_9\text{H}_{23}\text{NO}_2\text{Si}_2$	1114	$1200 - 80$	1120	0.54
O,N-Bis(TBDMS)-	$\text{C}_{15}\text{H}_{35}\text{NO}_2\text{Si}_2$	1532	$1800 - 200 - 80$	1520	0.79
2-Amino-1-butanoic acid	$\text{C}_4\text{H}_9\text{NO}_2$				
O,N-Bis(TMS)-	$\text{C}_{10}\text{H}_{25}\text{NO}_2\text{Si}_2$	1184	$1300 - 80$	1220	2.95
O,N-Bis(TBDMS)-	$\text{C}_{16}\text{H}_{37}\text{NO}_2\text{Si}_2$	1600	$1900 - 200 - 80$	1620	1.64
3-Amino-1-butanoic acid	$\text{C}_4\text{H}_9\text{NO}_2$				
O,N-Bis(TMS)-	$\text{C}_{10}\text{H}_{25}\text{NO}_2\text{Si}_2$	1218	$1300 - 80$	1220	0.16
O,N-Bis(TBDMS)-	$\text{C}_{16}\text{H}_{37}\text{NO}_2\text{Si}_2$	1647	$1900 - 200 - 80$	1620	1.64
2-Amino-1-pentanoic acid (DL-norvaline)	$\text{C}_5\text{H}_{11}\text{NO}_2$				
O,N-Bis(TMS)-	$\text{C}_{11}\text{H}_{27}\text{NO}_2\text{Si}_2$	1247	$1400 - 80$	1320	5.53
O,N-Bis(TBDMS)-	$\text{C}_{17}\text{H}_{39}\text{NO}_2\text{Si}_2$	1661	$2000 - 200 - 80$	1720	3.88
2-Amino-1-hexanoic acid (DL-norleucine)	$\text{C}_6\text{H}_{13}\text{NO}_2$				
O,N-Bis(TMS)-	$\text{C}_{12}\text{H}_{29}\text{NO}_2\text{Si}_2$	1328	$1500 - 80$	1420	6.48
O,N-Bis(TBDMS)-	$\text{C}_{18}\text{H}_{41}\text{NO}_2\text{Si}_2$	1751	$2100 - 200 - 80$	1820	3.79

^a See footnote in Table II.

methylene carbon atom is converted into a tertiary carbon atom; this change alters the molecular connectivity of the carbon atom and decreases the GRF by 40. In cyclohexanol, silylation not only eliminates the alcohol functionality but also reduces I due to effective chain branching, resulting from the added silyl group.

In a homologous series the A value may be strongly affected by large GRF values. Derivatiza-

tion will generally reduce the latter but increase the former. There are indications that the $GRFs$ of other functional groups in the molecule may be affected by the presence of highly polar and polarizable substituent groups. This may be one of the reasons that the I values of compounds of polyfunctionality are difficult to predict based on the A and GRF values alone.

TABLE X

MISCELLANEOUS COMPOUNDS ON NON-POLAR AND POLAR COLUMNS^a**On DB-Wax column**

The *GRFs* (m_i and n_i) have the following values: (1) -COOCH₃ group = +295, (2) phenyl ring = +350, (3) the N in pyridine ring = +240, (4) C-NH-(TBDMS) group = +50, (5) quaternary C atom in TBDMS group = -100.

Compound	Formula	I_{obs}	$100Z + \sum m_i - \sum n_i$	I_p	Difference (%)
Methyl (trimethylsilyl)acetate	C ₆ H ₁₄ O ₂ Si	1093	800 + 295	1095	0.18
Nicotinamide, O,N-Bis(TBDMS)-	C ₁₈ H ₃₄ N ₂ O ₅ Si ₂	2513	2100 + 350 + 240 + 50 - 2 × 100	2540	1.06
Nicotinic acid, O-(TBDMS)-	C ₁₂ H ₁₉ NO ₂ Si	2002	1500 + 350 + 240 - 100	1990	0.59

On DB-1 column

The *GRFs* (m_i and n_i) have the following values: (1) phenyl ring = +58, (2) chain branching = -40, (3) two terminal silyl groups in a molecule = -60, (4) double bond in alkyl chain = +27, (5) alicyclic ring connected to silylated carboxyl group = +0, (6) aryl Br = +240, (7) aryl I = +325 (see text under *Miscellaneous*).

Compound	Formula	I_{obs}	$100Z + \sum m_i - \sum n_i$	I_p	Difference (%)
Hexamethyldisiloxane	C ₆ H ₁₈ OSi	667		700	3.29
Methyl (trimethylsilyl)acetate	C ₆ H ₁₄ O ₂ Si	852		800	6.1
Oxalic acid, O,O-Bis(TBDMS)-	C ₁₄ H ₃₀ O ₄ Si ₂	1531	1800 - 2 × 100 - 60	1540	0.58
Succinic acid, O,O-Bis(TBDMS)-	C ₁₆ H ₃₄ O ₄ Si ₂	1739	2000 - 2 × 100 - 60	1740	0.06
2-Butene-1,4-dicarboxylic acid, O,O-Bis(TBDMS)-	C ₁₈ H ₃₆ O ₄ Si ₂	1944	2200 + 27 - 2 × 100 - 60	1967	1.17
1,5-Dimethylhexylamine, N-(TBDMS)-	C ₁₄ H ₃₃ NSi	1354	1500 - 2 × 40 + 25 - 100	1345	0.66
Cyclobutane carboxylic acid, O-(TMS)-	C ₈ H ₁₆ O ₂ Si	1009	1000	1000	0.89
Cyclopentane carboxylic acid, O-(TMS)-	C ₉ H ₁₈ O ₂ Si	1096	1100	1100	0.36
Cyclohexane carboxylic acid, O-(TMS)-	C ₁₀ H ₂₀ O ₂ Si	1188	1200	1200	1.01
Cyclohexane carboxylic acid, O-(TBDMS)-	C ₁₃ H ₂₆ O ₂ Si	1410	1500 - 100	1400	0.71
Benzoic acid, O-(TMS)-	C ₁₀ H ₁₄ O ₂ Si	1232	1200 + 58	1258	2.07
Benzoic acid, O-(TBDMS)-	C ₁₃ H ₂₀ O ₂ Si	1458	1500 + 58 - 100	1458	0
<i>o</i> -Bromobenzoic acid, O-(TMS)-	C ₁₀ H ₁₃ O ₂ BrSi	1466	1200 + 240 + 58	1498	2.14
<i>m</i> -Bromobenzoic acid, O-(TMS)-	C ₁₀ H ₁₃ O ₂ BrSi	1472	1200 + 240 + 58	1498	1.74
<i>p</i> -Bromobenzoic acid, O-(TMS)-	C ₁₀ H ₁₃ O ₂ BrSi	1479	1200 + 240 + 58	1498	1.27
<i>o</i> -Iodobenzoic acid, O-(TMS)-	C ₁₀ H ₁₃ O ₂ ISi	1579	1200 + 325 + 58	1583	0.25
<i>m</i> -Iodobenzoic acid, O-(TMS)-	C ₁₀ H ₁₃ O ₂ ISi	1582	1200 + 325 + 58	1583	0.06
<i>p</i> -Iodobenzoic acid, O-(TMS)-	C ₁₀ H ₁₃ O ₂ ISi	1591	1200 + 325 + 58	1583	0.05
3,4,5-Triiodobenzoic acid, O-(TMS)-	C ₁₀ H ₁₁ O ₂ I ₃ Si	2381	1200 + 3 × 325 + 58 + 2 × 70	2273	0.29

(Continued on p. 128)

TABLE X (continued)

Compound	Formula	I_{obs}	$100Z + \sum m_i - \sum n_i$	I_p	Difference (%)
Formamide, O,N-Bis(TBDMS)- N-(TBDMS)-	$C_{13}H_{31}NOSi_2$	1341	(calc. from eqns. in Table I)	1337	0.82
	$C_7H_{16}NOSi$	1094	(calc. from eqns. in Table I)	1085	0.82
Acetamide, O,N-Bis(TBDMS)- N-(TBDMS)-	$C_{14}H_{33}NOSi_2$	1385	(calc. from eqns. in Table I)	1392	0.5
	$C_8H_{18}NOSi$	1112	(calc. from eqns. in Table I)	1129	1.51
Propionamide, O,N-Bis(TBDMS)- N-(TBDMS)-	$C_{15}H_{35}NOSi_2$	1451	(calc. from eqns. in Table I)	1447	0.28
	$C_9H_{20}NOSi$	1182	(calc. from eqns. in Table I)	1173	0.76
Hydroxylamine, N,O-Bis(TBDMS)-	$C_{12}H_{31}NOSi_2$	1266	$1400 + 50 - 2 \times 100$	1250	1.26
Hydroxylamine, N,N,O-Tris(TMS)-	$C_9H_{27}NOSi_3$	1123	1100	1100	2.05

^a See footnote in Table II.

CONCLUSIONS

Substituents that yield large column differences are carboxyl, phenolic and alcoholic hydroxyls, amino groups, etc. These highly polar groups in the

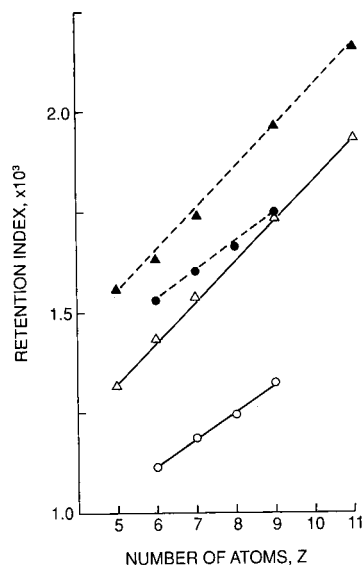


Fig. 2. Linear plots of retention indexes of TMS and TBDMS derivatives of α -amino acids (\circ , \bullet) and ω -amino acids (Δ , \blacktriangle) vs. the number of atoms (Z) on non-polar and polar columns. The I values of the homologues on non-polar column are connected by a solid line (—) and those on polar column by a broken line (---). The plots of TMS and TBDMS derivatives of the α -amino acids on DB-1 and DB-Wax columns have almost identical slopes; so have those of the ω -amino acids. The slopes of the silylated α -amino acids are less steep than those of the silylated ω -amino acids.

form of acids, alcohols and amines, can be chromatographed underivatized, but when present in polyfunctional molecules, such as amino acids, these groups may interact intramolecularly to increase I , rendering the chromatography of the polyfunctional molecules extremely difficult without derivatization.

Derivatization, especially silylation, masks the functionality of substituent groups, minimizes their intramolecular interaction and allows the polyfunctional compounds to revert to a virtual hydrocarbon state. In this "reduced" state the silylated molecules exhibit chromatographic characteristics similar to that of aliphatic hydrocarbons, thus facilitating the prediction of their I values from base values. According to convention, the n -alkanes are assigned identical I values on polar and non-polar columns. Substituent groups retaining residual polarity and polarizability after silylation will show higher I values on polar than on non-polar columns. The convergence of the I values of silylated derivatives on these columns is a manifestation of their hydrocarbon-like chromatographic characteristics. From the I values of the silylated derivatives one can deduce the molecular size in terms of the number of atoms in the skeleton of the analyte molecule.

The relationship between retention index and molecular size of non-polar molecules and the relationship between structure and retention index will be useful for estimating the number of silylated groups in an analyte molecule. The size of the molecular skeleton and possibly the kind and number of functional groups in an analyte molecule can be derived from the I values and the column

differences before and after derivatization. Silylation, methylation and acetylation give different derivatives but may yield a core of useful shared information. In this manner, one can gain structural information from chromatographic data. Application of the method is straightforward and may be useful for routine separation, analysis, and tentative identification of unknown components in mixtures prior to detailed structural analysis by mass spectrometry.

ACKNOWLEDGEMENTS

This publication was made possible by grant number CA33537 from National Cancer Institute. We acknowledge the Mass Spectrometry Facility, University of California, San Francisco, supported

by NIH Division of Research Resources grants RR01614 and RR04112.

REFERENCES

- 1 C. T. Peng, S. F. Ding, R. L. Hua and Z. C. Yang, *J. Chromatogr.*, 436 (1988) 137.
- 2 A. E. Pierce, *Silylation of Organic Compounds*, Pierce Chemical Co., Rockford, IL, 1982, pp. 7-71.
- 3 *Handbook and General Catalog*, Pierce Chemical Co., Rockford, IL, 1988.
- 4 C. T. Peng, Z. C. Yang and S. F. Ding, *J. Chromatogr.*, 585 (1991) 85.
- 5 H. van den Dool and P. D. Kratz, *J. Chromatogr.*, 11 (1963) 463.
- 6 *SAS/STAT TM User's Guide, Release 6.03 Edition*, SAS Institute Inc., Cary, NC, 1988, pp. 854-857.
- 7 J. Hils, V. Hagen, H. Ludwig and K. Ruhlmann, *Chem. Ber.*, 99 (1967) 776.

Gas chromatography for measurement of hydrogen isotopes at tritium processing

Tatsuhiko Uda^{*,*}, Kenji Okuno, Takumi Suzuki and Yuji Naruse

Japan Atomic Energy Research Institute, Tokai-mura, Naka-gun, Ibaraki-ken 319-11 (Japan)

(Received July 1st, 1991)

ABSTRACT

Analysis characteristics of the hydrogen isotopes H₂, HD, HT, D₂, DT and T₂ were experimentally studied using gas chromatography. A liquid nitrogen cooling column was employed for isotope separation, along with a thermal conductivity detector and a small-volume ionization chamber. The intensity ratio of the six hydrogen isotopes as measured by the thermal conductivity detection was H₂:HD:HT:D₂:DT:T₂ = 100:73:61:57:49:43. When the sampling volume was 1 cm³, the estimated detection limits for H₂ and T₂ were, respectively, 20 and 50 Pa partial pressure and 200 and 500 ppm concentration. The 0.16-cm³ ionization chamber could measure only the tritiated molecules, and the estimated detection limit for T₂ gas was 1 ppm. The retention time was reduced when the concentration was greater than 1%. In particular, when it was increased above 10%, identification of neighboring peaks tended to be difficult.

INTRODUCTION

To develop a fusion fuel gas-processing technology, various experimental studies have been performed in the Tritium Process Laboratory (TPL) [1] at the Japan Atomic Energy Research Institute (JAERI). To analyze experimental gases, including tritium, an analysis and measurement system (AMS) is installed in the TPL. Gas chromatography (GC) has conventionally been used as the gas analyzer, with the fundamental measurement method for isotopes of molecular hydrogen [2]. Primary studies have been performed by Moore and Ward [3] using non-radioactive hydrogen isotopes such as H₂, HD and D₂. They have separated not only hydrogen and deuterium but also their nuclear spin isomers on alumina at -196°C. While the separation of the *p*-H₂ and *o*-H₂ from *o*-D₂ and *p*-D₂ can be accomplished, the *o*-H₂ peak overlaps or is very close to the HD peak [4-6]. However, to analyze quantitatively

only hydrogen isotope gases, the separation of isomers becomes rather a hindrance. Fujita and Kwan [6] reported that nuclear spin isomers can be separated only when catalysts causing their equilibration at the temperature used are absent. When a catalyst is present, both spin isomers are eluted as a single zone corresponding to the average of the two isomers. A suitable catalyst of column packing, activated alumina covered with ferric hydroxide or manganese chloride, and carrier gas, neon, have been identified [6,7].

Many experimental reports have described H₂, HD and D₂, but only a few have provided an analytical study of hydrogen isotopes including tritium [7-9]. Genty and Schott [7] reported quantitative analysis of hydrogen isotopes, H₂, D₂, T₂, HD, HT and DT, as a mixed gas.

Although the principal method for the analysis of hydrogen isotopes has been established, the following characteristics still require clarification: those to measure high-concentration tritium and other hydrogen isotopic mixed gases, which constitute fusion fuel gas; and those to identify all six hydrogen isotopes in various ratios. Therefore we experi-

* Permanent address: Energy Research Laboratory, Hitachi Ltd., 1168 Moriyama-cho, Hitachi-shi, Ibaraki-ken 316, Japan.

mentally measured the hydrogen isotopic mixed gases by GC and tried to identify and obtain their measurement characteristics.

EXPERIMENTAL

Tritium and tritiated isotopic gas analyses have been performed using GC in the analysis and measurement system (AMS) of the TPL. The AMS is made up of four gas-handling lines for: (1) preparation of isotopically equilibrated hydrogen isotopes; (2) the ionization chamber test; (3) isotopic hydrogen gas recovery by metal beds; and (4) analysis by GC [7]. Fig. 1 shows the AMS flow system, in which experimental gases were prepared. At first the vessel was filled with pure H_2 , D_2 and T_2 gases. The purities of these isotopic hydrogen molecules were more than 99.9% for H_2 , more than 99% for D_2 and about 99% for T_2 . Then a fixed volume of the pure gas was sampled and analyzed by GC. Next, three gaseous mixtures of pure isotopic hydrogen, H_2 - D_2 , H_2 - T_2 and D_2 - T_2 , each in a ratio of 1:1, were prepared. These gas mixtures were passed through an isotopic equilibrator packed with platinum black-coated alumina catalyst. The equilibrator temperature was about 295 K. Three hydrogen species, HD, HT and DT, were produced accordingly by the isotopic exchange reaction.

Fig. 2 show the experimental flow line for GC. Four sampling tube volumes were possible: 1, 5, 10 or 20 cm^3 . The volume chosen depended on the gas

concentration. In this study, the 1- cm^3 sampling tube was selected, because it was expected to give less radioactive waste gas. Neon was used as the carrier gas.

Sampled gas was carried to the chromatography column packed with manganese chloride-coated alumina particles (Yanako Hydroisopack, made by Yanagimoto Kogyo). The column was kept cold using liquid nitrogen. At the same time only the carrier gas was passed to the reference column, which was heated up to 120°C. After passing through the column, the gas was detected with the thermal conductivity detector (TCD), and then the tritium concentration was measured using an ionization chamber. There were two ionization chambers having volumes of about 0.16 and 21.6 cm^3 . The characteristics of these ionization chamber are reported elsewhere [10]. We used the smaller ionization chamber, because the holding time of the detecting gas was short and sharp peaks could be obtained. The analyzed gas was carried to the effluent tritium gas removal system (ERS) at the TPL. Most of the remaining experimental gas was recovered by a metal bed, in which isotopic hydrogen gas getter was packed. Experimental conditions are summarized in Table I.

RESULTS AND DISCUSSION

Gas chromatograms of hydrogen isotopes

Fig. 3 shows gas chromatograms measured with

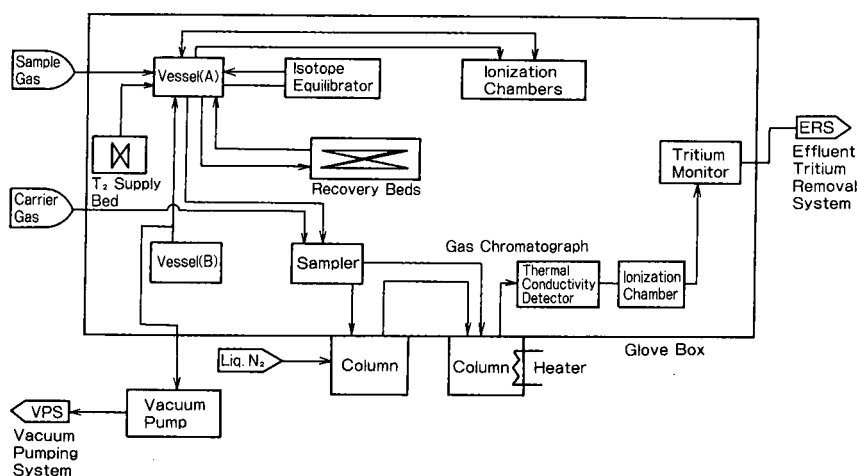


Fig. 1. Flow diagram of experimental gas preparation line. This loop is the AMS installed at the TPL.

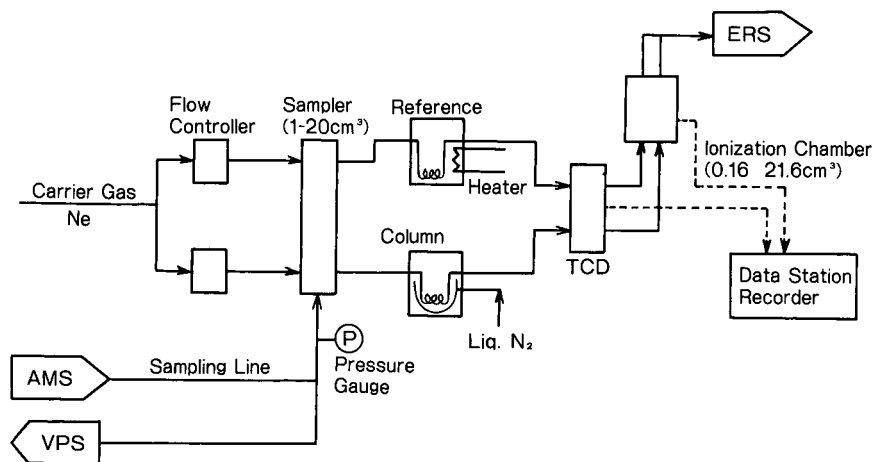


Fig. 2. Flow diagram of gas chromatography for hydrogen isotopes analysis.

the TCD for pure H_2 , D_2 and T_2 gases. The gas chromatogram of H_2 does not show peaks of other molecular hydrogen isotopes. In the D_2 gas chromatogram, a small HD peak was detected as an impurity. The D_2 :HD peak-area ratio was 99.54:0.46. On the other hand, pure T_2 gas includes HT, as well as a little helium and a trace of H_2 . The T_2 :HT peak-area ratio obtained was 98.6:1.4. The source of hydrogen is considered to be residual gas in the process line or at the metal bed, because pure H_2 gas was used previously to activate the metal.

Fig. 4 shows a gas chromatogram of pure T_2 gas at 1.8 kPa. The upper chromatogram was measured with the 0.16-cm³ ionization chamber and the lower with the TCD. When the partial pressure of T_2 gas

sample is low and its peak height is small, a peak for the impurity DT is observed. When the T_2 gas pressure is high, the DT peak might be hidden by the T_2 peak. Fig. 5 shows gas chromatograms of the mixture of H_2 , D_2 and T_2 gases after passing through the equilibrator. The six isotopes of molecular hydrogen can be detected individually with the TCD. On the other hand, only the three tritium-bonding hydrogen molecules, T_2 , HT and DT, are detected with the ionization chamber.

Calibration

Fig. 6 shows calibration curves for H_2 , HD, HT, D_2 , DT and T_2 as plots of partial pressure *versus* TCD intensity. Linearity is confirmed for each isotope of molecular hydrogen. The intensity order is obtained as $H_2 > HD > HT > D_2 > DT > T_2$. Detection limits as measured with the TCD are between 20 and 50 Pa, *i.e.*, between 200 and 500 ppm. Fig. 7 shows linear calibration of the six isotopes of molecular hydrogen obtained with the TCD. The slopes of the lines are the proportional coefficients of TCD sensitivity to partial pressures of isotopic hydrogen gas. Using the individual proportional coefficients the sensitivity ratio obtained is H_2 :HD:HT: D_2 :DT: T_2 = 100:73:61:57:49:43. This sensitivity ratio should be proportional to the thermal conductivity balance of each hydrogen isotope and neon gas. The thermal conductivities of pure H_2 , D_2 , T_2 and neon gases are presented in Table II [11–13]. Although the theoretical sensitivity ratio

TABLE I

EXPERIMENTAL CONDITIONS OF GAS CHROMATOGRAPHY FOR HYDROGEN ISOTOPES ANALYSIS

Specification of analyzer	Measurement conditions
Column diameter, 1/8 in.	Carrier gas, neon
Length, 3 m	Carrier gas flow-rate, 50 cm ³ /min
Absorber, manganese chloride-coated alumina (Yanako Hydroisopack)	Sampling gas volume, 1 cm ³
Detector, TCD, ionization chamber (effective volume 0.16 cm ³)	Column temperature, 77 K
	TCD temperature, 393 K
	Filament current, 70 mA
	Ionization chamber, applied voltage, 40 V; electric field strength, 200 V/cm

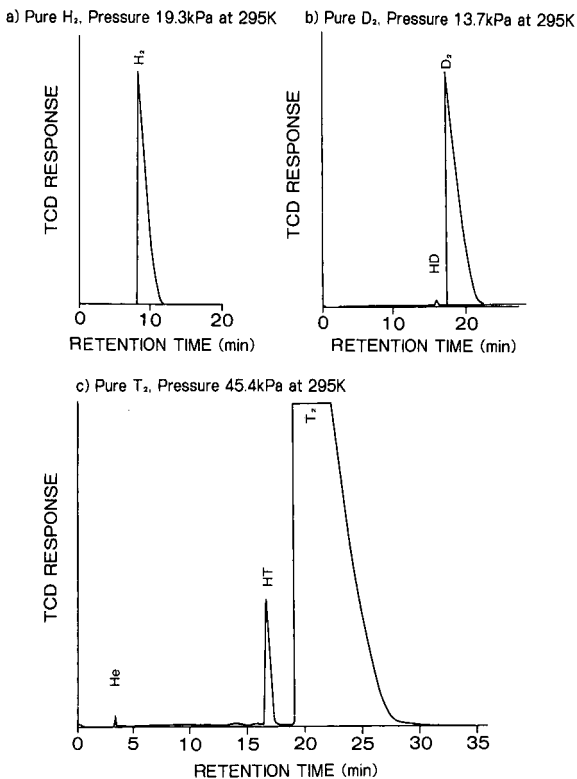


Fig. 3. Gas chromatograms of pure hydrogen isotopes, H_2 , D_2 and T_2 , obtained with the TCD.

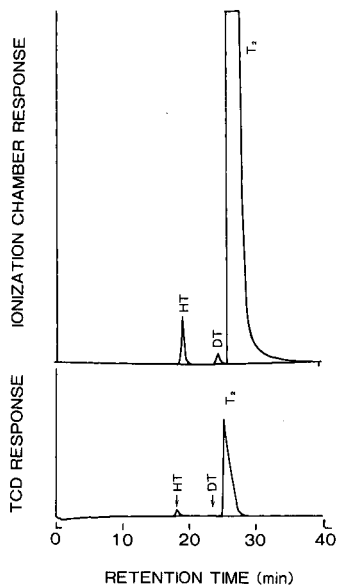


Fig. 4. Gas chromatograms of pure T_2 gas (pressure, 1.8 kPa at 295 K) detected by the 0.16-cm^3 ionization chamber and TCD.

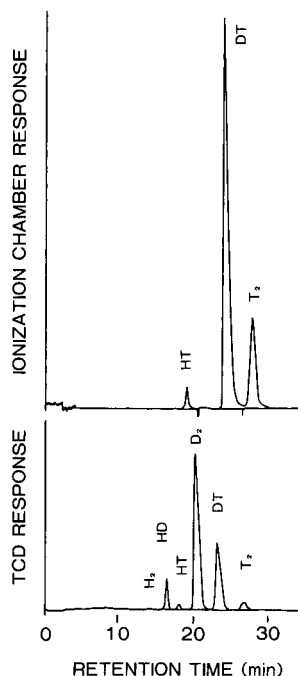


Fig. 5. Gas chromatograms of a mixture of gaseous hydrogen isotopes (pressure, 2.1 kPa at 295 K) detected by the 0.16-cm^3 ionization chamber and TCD. Mixing ratio is $H_2:HD:HT:D_2:DT:T_2 = 0.1:4.7:1.4:58.6:30.9:4.4$.

is $H_2:D_2:T_2 = 100:69:41$, the measured ratio is $100:57:43$, representing a difference of about 20%. The reason for this is unclear, but it is thought that thermal conduction to the gas layer from the sensor wire is affected by radiation or circulation of flow gas. However, this ratio might be constant for this detector. So this ratio can be used for quantitative analysis of hydrogen isotopes as proportional coefficients. Using this calibration coefficient, the purity of T_2 is estimated to be 99.05% and that of D_2 is 99.6%.

Fig. 8 shows the calibration curves for tritium and tritiated hydrogens in the 0.16-cm^3 ionization chamber. There is a linear relation between partial pressure and ionization current. The detection limit depends on the sensitivity of the ionization chamber and chamber volume, for example when using the 21.6-cm^3 chamber sensitivity might increase, and the retention time would be longer and the peak width would be broadened. For radio-GC, a smaller volume seems to be a better choice. The detection limit for T_2 gas is about 0.1 Pa (1.0 ppm concentra-

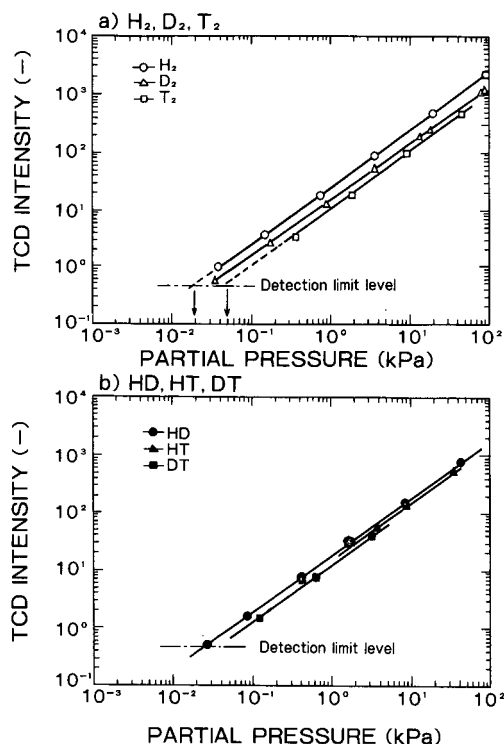


Fig. 6. Relationships between partial pressures of hydrogen isotopes and TCD intensity.

tion and $4.0 \cdot 10^{-10}$ mol mass). The ionization chamber shows a response to lower concentrations of tritium gas, and the limit can be expected to be lowered by decreasing the noise level. But it is difficult to obtain a higher signal-to-noise ratio

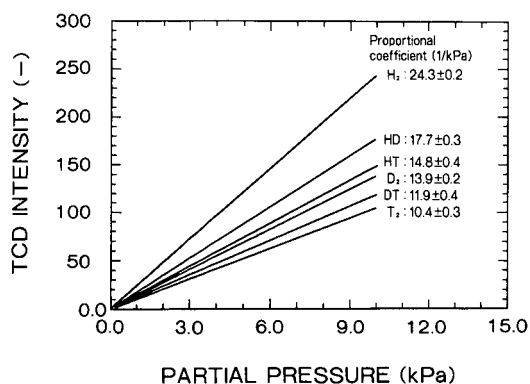


Fig. 7. Proportional coefficients of hydrogen isotopes measured for TCD intensity per unit partial pressure.

TABLE II

THERMAL CONDUCTIVITIES (TC) OF ISOTOPIC HYDROGEN AND CARRIER GASES AT 300 K

Molecular gas	TC (10^{-4} J/s · mK)
H ₂	1815
D ₂	1406
T ₂	1036
Helium	1499
Neon	493

because of the memory effect due to contamination inside the chamber.

Concentration effect

Generally peak separation ability depends on the retention time interval and peak width. When column conditions are constant, retention time, t_R , is expressed as [14]:

$$t_R = \frac{k \cdot K_A \cdot z}{v} \quad (1)$$

where k is a coefficient, K_A is the adsorption equilibrium coefficient [concentration in adsorption phase (mol/g)/concentration in carrier gas (mol/cm³)], z is the length of the column bed (cm) and v is the flow-rate of carrier gas (cm/s).

Of course, a long retention time gives a good separation, so it is useful to activate the column packing, *i.e.*, to increase adsorption ability, and to employ a longer column and decreased flow-rate of the carrier gas. In our experiments the same column was used and the flow-rate of carrier gas was fixed. The relationships between partial pressures of hydrogen isotopes and retention times are shown in Fig. 9. On increasing the partial pressure, the retention time is shortened. On the other hand, when the partial pressure is decreased, the retention time gradually becomes longer, and finally it becomes constant at extremely low partial pressure. This means that the adsorption equilibrium coefficient is dependent on partial pressure, *i.e.*, on concentration. It is considered that the ratio of the hydrogen isotopic concentration in the adsorption layer and in the carrier gas layer must be constant at low concentrations. But the ratio might decrease on increasing the objective gas concentration.

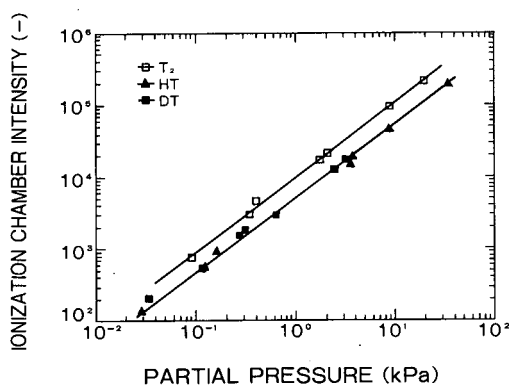


Fig. 8. Relationships between partial pressures of tritiated hydrogen isotopes and the 0.16-cm³ ionization chamber intensity.

When analyzing a mixed gas of low and high concentrations of hydrogen isotopes, the retention times of both isotopes of hydrogen might overlap. A remarkable shift of retention time occurs at partial pressures above 1 kPa. To avoid peak overlapping, longer retention time would be effective, and the following two methods may be considered. One is to increase the activity of the absorber by aging at high temperature for a long time, and the other is to decrease the carrier gas flow-rate. However, too much aging shortens the life of the column packing and a lower gas flow-rate needs a much longer analysis time, so that more than half an hour would be needed to separate all the isotopes of hydrogen. It then becomes difficult to measure a small amount of one isotopic gas mixed with a large amount of another.

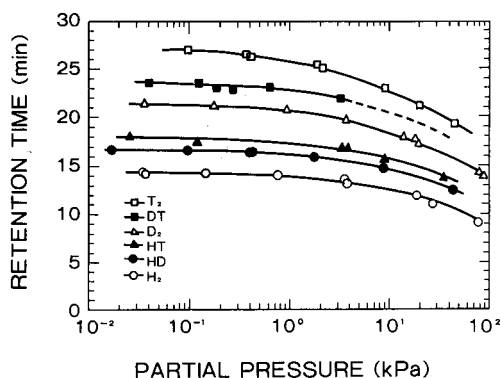


Fig. 9. Effect of hydrogen isotopic gases partial pressures on retention times.

Improvement of detection limits

To apply GC to the tritium gas-processing system, higher sensitivity is required. Generally, GC output *versus* unit concentration gas is expressed as [15]:

$$S = \frac{A \cdot FR}{RS \cdot CS \cdot W} \quad (2)$$

where S is the intensity of a peak (V cm³/g), A is the peak area on the recorder chart (cm²), FR is the flow-rate of carrier gas (cm³/s), RS is the sensitivity of the recorder (V/cm), CS is the chart speed (cm/s) and W is the quantity of sample gas (g).

As shown in Fig. 5, a gas mixture of the six hydrogen isotopes can be detected by GC using the TCD. The detection limit with the TCD is 20 Pa for H₂ and 50 kPa for T₂. To improve these limits it might be useful to increase the sampling volume or to decrease the carrier gas flow-rate, as indicated by eqn. 2. However, increasing the sampling volume increases the amount of radioactive waste gas effluent. On the other hand, as pointed out in the previous section, decreasing the carrier gas flow-rate means a longer analysis time. Another important way of improving the sensitivity is to have an extremely high signal-to-noise ratio. However, with the present commercially available measurement equipment, it does not seem to be easy to achieve a higher ratio.

Future study must look at ways of avoiding these shortcomings of GC and developing an improved gas measurement system for the fusion fuel gas process.

CONCLUSIONS

The characteristics of GC when applied to isotopic hydrogen analyses were experimentally obtained using a liquid nitrogen cooling column, with a TCD and an ionization chamber. The following results were obtained.

(1) The intensity ratio for hydrogen isotopes measured with the TCD was H₂:HD:HT:D₂:DT:T₂ = 100:73:61:57:49:43.

(2) When the sampling volume was 1 cm³, the detection limits for H₂ and T₂ were estimated to be, respectively, 20 and 50 Pa partial pressure and 200 and 500 ppm concentration.

(3) Using the 0.16-cm³ ionization chamber, the intensity ratio obtained for T₂:HT:DT was 2:1:1

according to the atomic fraction in the isotopic molecules. The detection limit for T₂ gas was estimated to be 1 ppm concentration and 4 · 10⁻¹⁰ mol mass.

(4) On increasing the hydrogen isotope concentration above 1%, the retention time tended to drop. Furthermore, when the concentration was increased to more than 10%, neighboring peak identification became difficult.

REFERENCES

- 1 Y. Naruse, Y. Matsuda and K. Tanaka, *Fusion Eng. Des.*, 12 (1990) 293.
- 2 J. Janak, *Chromatography*, Reinhold, New York, 1975, p. 899.
- 3 W. R. Moore and H. R. Ward, *J. Am. Chem. Soc.*, 80 (1958) 2909.
- 4 W. R. Moore and H. R. Ward, *J. Phys. Chem.*, 64 (1960) 382.
- 5 H. A. Smith and P. P. Hunt, *J. Phys. Chem.*, 64 (1960) 383.
- 6 K. Fujita and T. Kwan, *Bunseki Kagaku (Japan Analyst)*, 12 (1963) 15.
- 7 C. Genty and R. Schott, *Anal. Chem.*, 42 (1970) 7.
- 8 D. K. Warner, C. Kinard and D. R. Bohl, *Chromatographic Measurement of Hydrogen Isotopic and Permanent Gas Impurities in Tritium*, ML-2308, Monsanto Research Corp., Miamisburg, OH, 1976.
- 9 M. Tanase, K. Kurosawa, M. Fujie, H. Sugai, S. Okane and M. Kato, *Fusion Technol.*, 14 (1988) 1090.
- 10 T. Uda, K. Okuno, Y. Matsuda and Y. Naruse, *J. Nucl. Sci. Technol.*, 28 (1991) 451.
- 11 Kagaku Binran, *Kiso Hen II*, Maruzen, Tokyo, 3rd ed., 1984, p. 71 (in Japanese).
- 12 R. C. Reid and T. K. Sherwood, *The Properties of Gases and Liquids*, McGraw Hill, New York, 1966, p. 459.
- 13 R. A. Svehla, *Estimated Viscosities and Thermal Conductivities of Gases at High Temperature*, NASA Technical Report R-132, Cleveland, OH, 1962.
- 14 R. Schneider and J. M. Smith, *AIChE J.*, 14 (1968) 762.
- 15 J. E. Willett, *Gas Chromatography, Analytical Chemistry by Open Learning*, Wiley, London, 1987, p. 24.

Enantiomeric separation of α -phenylethylamine and its substituted isomers by gas chromatography

Xianwen Lou, Xueliang Liu, Suizhi Zhang and Liangmo Zhou*

Dalian Institute of Chemical Physics, Chinese Academy of Sciences, Dalian 116012 (China)

(First received May 1st, 1991; revised manuscript received June 21st, 1991)

ABSTRACT

α -Phenylethylamine, *o*, *m*, *p*-methoxy- α -phenylethylamines and *o*, *m*, *p*-methyl- α -phenylethylamines were enantiomerically separated with four different diamide chiral stationary phases (CSPs) [monobenzyl succinate-L-Val-*tert*-butylamide (CSP-1), undecenoyl-L-Val-*S*- α -phenylethylamide (CSP-2), undecenoyl-L-Val-*R*- α -phenylethylamide (CSP-3) and cross-linked polycyanoethyl vinyl siloxane-L-Val-*tert*-butylamide (CSP-4)] using capillary gas chromatography. The *ortho*-effect of the methoxy group on the enantiomeric separation was investigated. The elution order of the enantiomers on CSP-3 is reversed with respect to that on the other CSPs studied. The enantiomeric separation of α -phenylethylamine and its methoxy- and methyl-substituted isomers is illustrated.

INTRODUCTION

α -Phenylethylamine and its derivatives can be used for the syntheses of anti-cancer drugs and asymmetric catalysts [1–3]. The enantiomeric separation of these compounds is of great importance in biochemistry, asymmetric synthesis and pharmacology. Racemic amines can be enantiomerically separated using chiral stationary phases (CSPs) [4,5], although the separation of substituted α -phenylethylamine enantiomers has not yet been fully investigated. It has been reported that the methoxy group shows a considerable *ortho*-effect in the enantiomeric separation of N-trifluoroacetyl (TFAc)-*o*-methoxy- α -phenylethylamine [6]. This paper reports an investigation of the mechanism of this *ortho*-effect.

EXPERIMENTAL

Materials

Fused-silica capillary tubes (0.25 mm I.D.) were obtained from Yongnian Optical Fibre Manufacture (China). Monobenzyl succinate-L-Val-*tert*-butylamide (CSP-1) was kindly supplied by Professor

X. Xu (Shanghai Institute of Materia Medica, Academia Sinica, Shanghai, China). The preparations and properties of undecenoyl-L-Val-*S*- α -phenylethylamide (CSP-2), undecenoyl-L-Val-*R*- α -phenylethylamide (CSP-3) and polycyanoethyl vinyl siloxane-L-Val-*tert*-butylamide (CSP-4) have been described previously [7,8].

Syntheses of the solutes

Syntheses of methyl-substituted acetophenones. For the synthesis of *o*- and *m*-methylacetophenones, Grignard reagents of *o*- and *m*-halotoluenes were reacted with acetonitrile and hydrolysed in acid solution [9]. The Friedel–Crafts reaction of toluene was used to prepare *p*-methylacetophenone [10].

Syntheses of methoxy-substituted acetophenones. Fries rearrangement of phenyl acetate was used to prepare *o*- and *p*-methoxyacetophenones, which then reacted with dimethylsulphate in alkaline solution [11]. *m*-Methoxyacetophenone was prepared by the methylation of *m*-hydroxyacetophenone [12].

Syntheses of methyl- and methoxy-substituted α -phenylethylamines. All six of the amines were synthesized by the Leukart reaction of their methyl- and methoxy-substituted acetophenones with am-

monium formate [13]. *d,l-p*-Methoxy- α -phenylethylamine was partly resolved with 1-tartaric acid in methanol [14].

Derivatization

The amines were derivatized with trifluoroacetyl anhydride according to the method of Feibush and Gil-Av [15]. The mass spectra of the derivatized amines are shown in Fig. 1.

Chromatographic conditions

Fused-silica capillary columns were coated or cross-linked as described previously [7,16]. The chromatographic separations were carried out with a GC R1A gas chromatograph equipped with a split injector and a flame ionization detector. The elution order of the amine enantiomers was determined by comparison with the retention times of chirally pure standards.

RESULTS AND DISCUSSION

The structures of the amines studied are shown in Fig. 2. The capacity factors (k') and separation factors (α) of N-TFAc- α -phenylethylamine and its methoxy and methyl-substituted isomers are listed in Table I. The elution order of the enantiomers on CSP-3 is reversed with respect to the other CSPs studied. CSP-2 and CSP-3 have two asymmetric centres and are diastereoisomers. On CSP-2 and CSP-3 the α -values of N-TFAc-*m*-methoxy- α -phenylethylamine are slightly larger than those of the *p*-isomer, and on CSP-1 and CSP-4 the α values are almost equal. Except for the *p*-isomers on CSP-3, the α values of *m*- and *p*-N-TFAc-methoxy- α -phenylethylamines are slightly larger than those of the corresponding *m*- and *p*-N-TFAc-methyl- α -phenylethylamines. All the α values of *o*-, *m*-, *p*-methyl-substituted and *m*-, *p*-methoxy-substituted N-TFAc- α -phenylethylamines, except for the *p*-isomers on CSP-3, are not less than the α values of unsubstituted N-TFAc- α -phenylethylamine. N-TFAc-*o*-methoxy- α -phenylethylamine has the lowest α values of the amines tested and is eluted faster than its *m*- and *p*-isomers.

From these results, the following conclusions can be made:

(1) For CSP-2 and CSP-3, the configuration of the α -phenylethylamide moiety of the CSPs deter-

mines the elution order of the enantiomers. On CSP-3, the two chiral centres have opposite rotational directions and the solutes show lower α values than those on its diastereoisomer, CSP-2.

(2) Except for N-TFAc-*o*-methoxy- α -phenylethylamine and CSP-3, none of the methyl- and methoxy-substituted isomers showed lower α values than those of unsubstituted N-TFAc- α -phenylethylamine.

(3) The *o*-methoxy group shows a pronounced *ortho*-effect on the α and k' values on the four CSPs studied.

In the *o*-position of a benzene ring, a methyl group shows greater steric hindrance than a methoxy group. However, the α values of N-TFAc-*o*-methyl- α -phenylethylamine are comparable with those of its *m*- and *p*-isomers and are much larger than those of N-TFAc-*o*-methoxy- α -phenylethylamine. In this instance the steric hindrance cannot reasonably be used to explain the lowest α values of N-TFAc-*o*-methoxy- α -phenylethylamine listed in Table I.

It is suggested that, in the N-TFAc-*o*-methoxy- α -phenylethylamine molecule, the oxygen atom of the methoxy group and the hydrogen atom of the amide group are at such positions that they could form a six membered ring through intramolecular hydrogen bonding (see Fig. 3). This intramolecular hydrogen bonding considerably decreases the hydrogen bonding of the N-TFAc-*o*-methoxy- α -phenylethylamine with the CSPs, resulting in much lower α values and faster elution than its *m*- and *p*-isomers.

It has been reported that chiral amines can be separated on monoamide CSPs such as N-lauroyl-*S*- α -(1-naphthyl)ethylamine. The separation mechanism suggests that the solute is intercalated between two solvent molecules [4]. If this mechanism is assumed, the interaction between the amide groups of the solute and solvent is very important for chiral recognition.

When the amide groups of the solutes cannot sufficiently interact with the diamide CSPs, such as for N-TFAc-*o*-methoxy- α -phenylethylamine, very low α values or even no separation is obtained. This implies that the amide group of the N-TFAc chiral amine is also an important interaction site for chiral recognition on diamide CSPs. The introduction of a methyl group to *o*-, *m*-, *p*-position and a methoxy

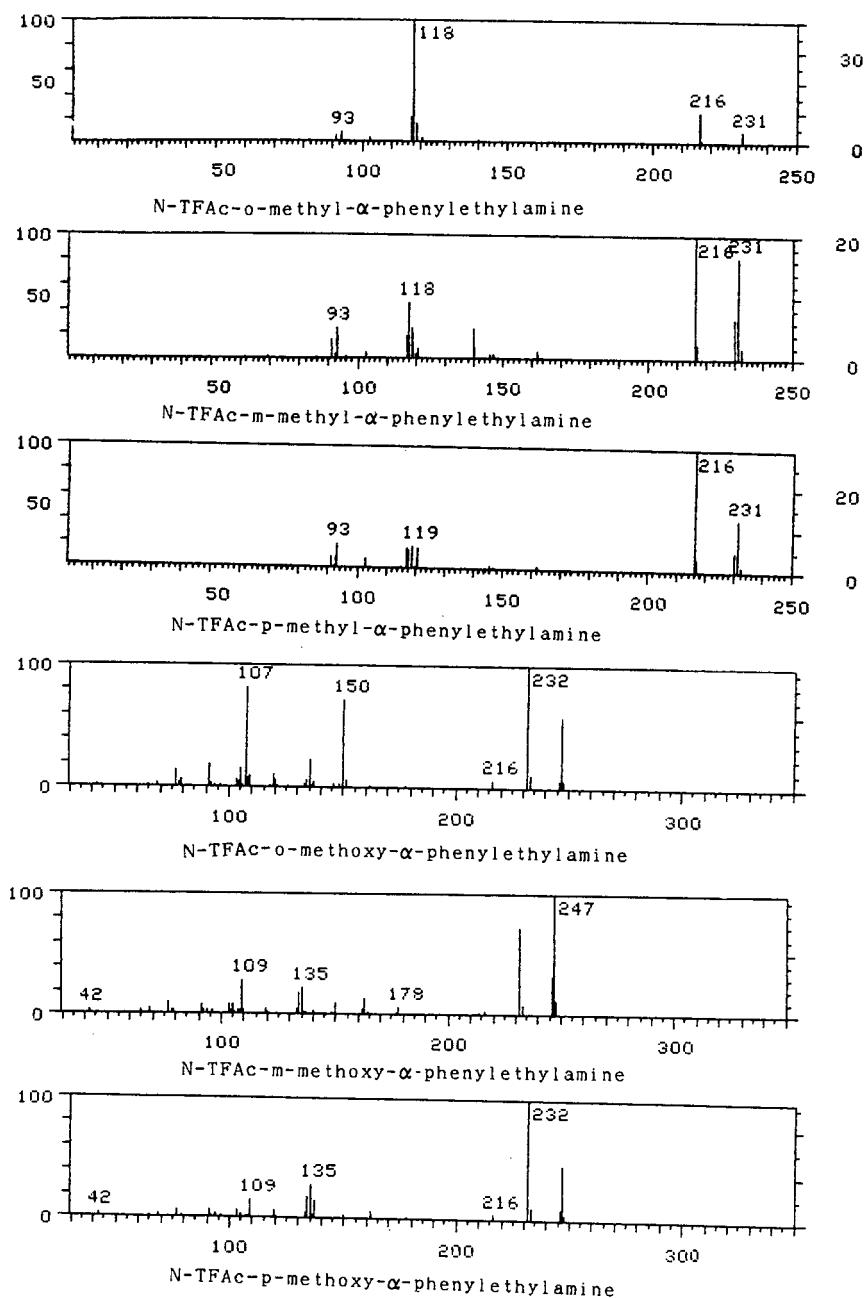


Fig. 1. Mass spectra of the N-TFAC-aminos.

group to *m*, *p*-position on the benzene ring of N-TFAC- α -phenylethylamine slightly improved the selectivity of enantiomers on CSP-1, CSP-2 and CSP-4. This is probably because the introduced

group (methyl or methoxy) enhances the interaction of the benzene ring of the solutes with the CSPs.

The enantiomeric separation of the amines on the four CSPs is shown in Fig. 4. Except for N-TFAC-*o*-

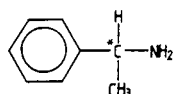
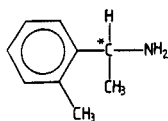
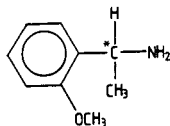
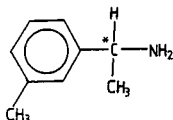
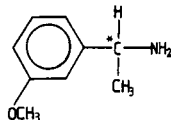
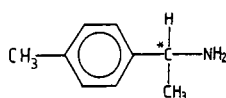
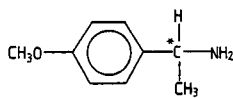
 α -phenylethylamine*o*-methyl- α -phenylethylamine*o*-methoxy- α -phenylethylamine*m*-methyl- α -phenylethylamine*m*-methoxy- α -phenylethylamine*p*-methyl- α -phenylethylamine*p*-methoxy- α -phenylethylamine

Fig. 2. Structures of racemic amines examined.

TABLE I

 α - AND k' VALUES OF N-TFAC- α -PHENYLETHYLAMINE AND ITS METHOXY- AND METHYL-SUBSTITUTED ISOMERS

Isomer	Temperature (°C)	CSP-1		CSP-2		CSP-3		CSP-4	
		α	k' (<i>S</i>)	α	k' (<i>S</i>)	α	k' (<i>R</i>)	α	k' (<i>S</i>)
<i>α-Phenylethylamine</i>									
	130	1.044	5.74	1.045	9.24	1.028	5.98	1.026	5.78
	150	1.039	2.68	1.040	4.34	1.023	2.98	1.024	2.38
<i>Methyl-substituted α-phenylethylamine</i>									
<i>o</i> -Isomer	130	1.044	6.14	1.048	10.9	1.029	7.08	1.025	6.05
	110	1.049	14.9			1.036	15.8	1.030	16.2
<i>m</i> -Isomer	130	1.046	6.98	1.048	12.2	1.028	7.93	1.030	6.62
	110	1.055	17.2			1.034	18.1	1.034	18.2
<i>p</i> -Isomer	130	1.050	7.45	1.051	13.1	1.024	8.50	1.032	6.93
	110	1.058	18.3			1.032	19.2	1.038	19.2
<i>Methoxy-substituted α-phenylethylamine</i>									
<i>o</i> -Isomer	130	— ^a	9.59	1.015	14.2	— ^a	10.2	— ^a	8.87
	150	— ^a	4.28	1.013	6.88	— ^a	4.88	— ^a	3.62
<i>m</i> -Isomer	130	1.053	22.7			1.040	23.3	1.032	23.7
	150	1.045	10.9	1.052	16.7	1.032	11.6	1.024	8.44
<i>p</i> -Isomer	130	1.053	24.5			1.022	24.3	1.033	25.4
	150	1.046	12.0	1.047	18.1	1.018	12.6	1.026	9.08

^a No separation.

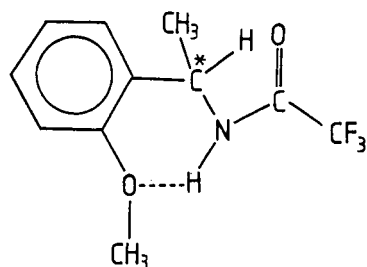


Fig. 3. Intramolecular hydrogen bonding of N-TFAc-*o*-methoxy- α -phenylethylamine.

methoxy- α -phenylethylamine, all the amines can be readily separated into their antipodes on CSP-1, CSP-2 or CSP-4.

CONCLUSIONS

The methoxy group of N-TFAc-*o*-methoxy- α -phenylethylamine shows a considerable *ortho*-effect on the selectivity of enantiomers, probably due to the formation of intramolecular hydrogen bonding

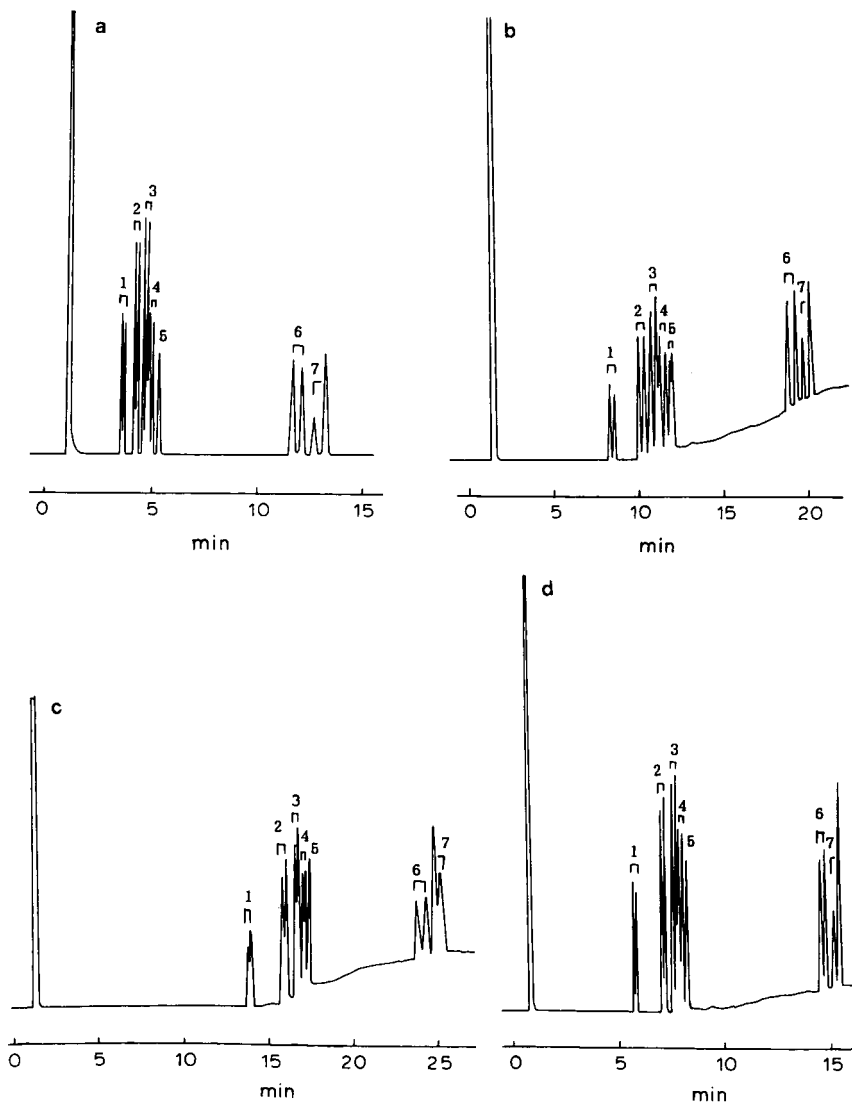


Fig. 4. Chromatogram of N-TFAc-chiral amines. Fused-silica capillary column (20 m \times 0.25 mm) coated as given for each part. (a) Coated with CSP-1; temperature 150°C; carrier gas hydrogen; *R*-enantiomers eluted first. (b) Coated with CSP-2; temperature 130°C (5 min), then 4°C/min to 150°C; carrier gas hydrogen; *R*-enantiomers eluted first. (c) Coated with CSP-3; temperature 110°C (10 min), then 4°C/min to 150°C; carrier gas hydrogen; *S*-enantiomers eluted first. (d) Cross-linked with CSP-4; temperature 130°C (5 min), then 4°C/min to 150°C; carrier gas hydrogen; *R*-enantiomers eluted first. Peaks: 1 = *d,l*- α -phenylethylamine; 2 = *d,l*-*o*-Methyl- α -phenylethylamine; 3 = *d,l*-*m*-methyl- α -phenylethylamine; 4 = *d,l*-*p*-methyl- α -phenylethylamine; 5 = *d,l*-*o*-methoxy- α -phenylethylamine; 6 = *d,l*-*m*-methoxy- α -phenylethylamine; 7 = *d,l*-*p*-methoxy- α -phenylethylamine.

between the oxygen atom in the methoxy group with the hydrogen atom in the amide group. Both substituents and their positions in the benzene ring can to some extent affect the α -values of substituted- α -phenylethylamine antipodes. The amines tested, except for *o*-methoxy- α -phenylethylamine, can be readily separated into their enantiomers in a single run on CSP-1, CSP-2 or CSP-4 under selected conditions.

ACKNOWLEDGEMENTS

The authors thank Mr. Jianing Wang and Mr. Yuzhen Tian for carrying out the gas chromatographic-mass spectrometric experiments. This work was supported by the National Natural Sciences Foundation of China and the Youth Sciences Foundation of the Dalian Institute of Chemical Physics.

REFERENCES

- 1 B. Rosenberg, L. Vancamp, J. E. Trosko and V. H. Mansour, *Nature (London)*, 222 (1969) 385.
- 2 M. Fiorini and G. M. Giongo, *J. Mol. Catal.*, 5 (1979) 303.
- 3 C. F. J. Barnard, *Platinum Metal. Rev.*, 33 (1989) 162.
- 4 S. Weinstein, B. Feibush and E. Gil-Av, *J. Chromatogr.*, 126 (1976) 97.
- 5 B. Koppenhoefer and E. Bayer, in F. Bruner (Editor), *The Science of Chromatography (J. Chromatogr. Library, Vol. 32)*, Elsevier, Amsterdam, 1985, p.1.
- 6 X. Lou, X. Liu and L. Zhou, *Proceedings of the 13th International Symposium on Capillary Chromatography, Riva del Garda, 1991*, Hüthig, Heidelberg, 1991, p. 169.
- 7 Z. Zhang, X. Lou and L. Zhou, *Proceedings of the 6th Chinese National Symposium on Chromatography, Shanghai, 1987*, Huadong Institute of Chemical Engineering, Shanghai, 1987, p. 126.
- 8 L. Zhou, X. Qu, X. Lou, Y. Liu and X. Xu, *Proceeding of the 2nd Chinese National Symposium on Biomedical Chromatography, Nanjing, 1990*, Nanjing University of Medicine, Nanjing, 1990, p. 377.
- 9 G. Jones, *J. Chem. Soc.*, (1960) 1918.
- 10 R. Adams and C. R. Noller, *Org. Synth. Coll.*, 1 (1932) 109.
- 11 J. A. Scarrow and C. F. H. Allen, *Org. Synth., Coll.*, (1943) 387.
- 12 J. C. E. Simpson and C. M. Atkinson, *J. Chem. Soc.*, (1945) 656.
- 13 A. W. Ingersoll, *Org. Synth., Coll.*, 2 (1943) 503.
- 14 A. W. Ingersoll, *Org. Synth., Coll.*, 2, (1943) 506.
- 15 B. Feibush and E. Gil-Av, *J. Gas Chromatogr.*, 5 (1967) 257.
- 16 X. Lou, Y. Liu and L. Zhou, *J. Chromatogr.*, 552 (1991) 153.

Short Communication

High-performance liquid chromatography of peptides at reduced temperatures: separation of isomers

Michal Lebl[☆], Sunan Fang and Victor J. Hruby*

Department of Chemistry, University of Arizona, Tucson, AZ 85721 (USA)

(First received January 21st, 1991; revised manuscript received June 6th, 1991)

ABSTRACT

Cholecystokinin analogues containing N-methyl amino acids were studied by reversed-phase high-performance liquid chromatography at reduced temperatures. A reduction in temperature to -17°C led to lower efficiency, but at the same time separations of *cis* and *trans* isomers (and some impurities) were achieved. The velocity constants for *cis-trans* equilibria were calculated.

INTRODUCTION

The effect of increased temperature on the chromatographic separation of peptides has been examined in several papers [1,2]. Usually, increased temperature leads to higher efficiency of the column and the separation of peptides is improved [3]. Lower temperatures generally decrease the efficiency of the column owing to the increased viscosity of the mobile phase, but it can be used for various physico-chemical studies of peptides. Increased energetic barriers allows for the separation of isomers which are otherwise inseparable [4-8]. For example, rapidly interconverting species were observed in the case of muramyldipeptides, and the chromatographic trace was used for calculation of the velocity constants of interconversion [9]. Detailed theoretical studies of this phenomenon were later performed by Melander *et al.* [10]. However, where rapid interconversion of two or more forms of the analyzed com-

pound is likely (*e.g.*, anomers of sugars or glycopeptides or peptide conformers), we can expect to separate these forms only if the interconversion is slowed by decreasing the temperature. Mixtures of isomers often can be observed with peptides containing secondary amino groups (*e.g.*, proline or N-alkylated amino acids). We have applied this thinking to the separation of *cis* and *trans* peptide bond conformers of the cholecystokinin-related pentapeptide Gly-Trp-MeNle-Asp-Phe-NH₂ [11,12]. A decrease in temperature led not only to separation of the expected conformers, but also the separation of impurities present in the sample which were not observed under normal room temperature conditions of chromatography. We were able to show which peaks are conformers by their separation and re-equilibration to the original equilibrium mixture. We could also calculate the velocity constant of the *cis-trans* interconversion [9].

[☆] Present address: Selectide Corporation, 10 900 N. Stallard Pl., Tucson, AZ 85737, USA.

EXPERIMENTAL

Materials

The peptide Gly-Trp-MeNle-Asp-Phe-NH₂ was synthesized by solid-phase peptide synthesis using a Boc-benzyl (Bzl) strategy on a *p*-methylbenzhydrylamine polystyrene resin [11,12]. The peptide was purified by high-performance liquid chromatography (HPLC) on a Vydac-C₁₈ column (25 × 1 cm I.D.) using a gradient elution with 0.1% trifluoroacetic acid and acetonitrile and/or methanol as the organic modifier.

Methods

Chromatography was performed on a Spectra-Physics SP-8700 instrument using a Spectra-Physics SP-8400 variable-wavelength detector. For the low-temperature experiments, the columns was jacketed in a Tygon tube (40 × 2 cm I.D.) connected to a thermostat adjustable from +60 to -20°C. Two columns were used: a Vydac C₁₈ peptides and proteins column (7 μm; 25 × 0.4 cm I.D.) and an ED-MA 40 column (10 μm; 8 × 0.8 cm I.D., Tessek, Prague, Czechoslovakia). Velocity constants were calculated according to published methods [9].

RESULTS AND DISCUSSION

Analogs of the C-terminal pentapeptide of cholecystokinin were synthesized in connection with studies of the receptor selectivity and central activities of these compounds [11,12]. The analogues containing N-methylnorleucine such as Gly-Trp-MeNle-Asp-Phe-NH₂ had an interesting range of biological activities and therefore were studied by ¹H NMR spectroscopy [11,12]. These studies have shown that these peptides exist as both *cis* and *trans* conformers about the Trp-MeNle peptide bond [12]. Therefore, we decided to try to separate them by HPLC. Under normal conditions (at room temperature) we observed only a single symmetrical peak (Fig. 1A). A decrease in temperature led to the broadening of this peak and at 0°C four peaks could be detected, although baseline separation was not achieved (Fig. 1B). We initially used acetonitrile as the chromatographic organic solvent, and therefore we could not decrease the temperature further. For this reason, we changed the organic modifier to a mixture of methanol and acetonitrile. In this system

we could go down to -20°C, even though under these conditions the flow had to be decreased to 0.8 ml/min owing to the very high back-pressure (260 bar). At -17°C the mixture clearly contained five components (Fig. 1C). We were able to separate in a pure form the three main peaks. The fractions were collected into containers cooled in a bath containing a dry-ice-ethanol mixture. Analytical evaluation at -17°C showed their purity (Fig. 1D-F). When the fractions were heated to room temperature and reinjected into the same column kept at -17°C (Fig. 1G-I), fraction 1 did not change, but fractions 2 and 3 afforded an identical mixture of the two peaks of the peptide conformers. It may be predicted [13] that the fraction containing the less retained compound has the *trans* conformation-containing peptide.

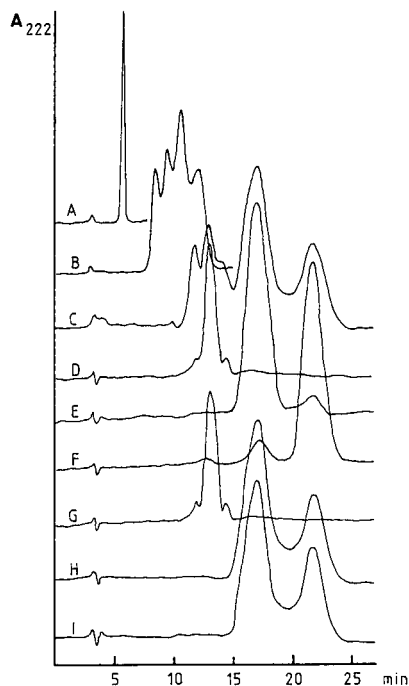


Fig. 1. Chromatography of an HPLC-purified sample of Gly-Trp-MeNle-Asp-Phe-NH₂ at various temperatures. Conditions: column, Vydac C₁₈ peptides and proteins (25 × 0.4 cm I.D.); eluent, methanol-acetonitrile-0.1% trifluoroacetic acid (50:13:37); flow-rate 1 ml/min; detection at 222 nm. (A) 23°C; (B) 0°C; (C) -17°C; (D) fraction one (from C) kept frozen, analyzed at -17°C; (E) fraction two kept frozen, analyzed at -17°C; (F) fraction three kept frozen, analyzed at -17°C; (G) fraction one heated to room temperature, analyzed at -17°C; (H) fraction two heated to room temperature, analyzed at -17°C; (I) fraction three heated to room temperature, analyzed at -17°C.

On closer inspection, the low-temperature HPLC of the conformational mixture reveals (Fig. 2) that the trace contains a plateau between peaks B and A. This is similar to previous observations [4–9,13] and provides the possibility of calculating the velocity constant for interconversion of the *cis* and *trans* conformations of the peptide. In the present situation, however, it is not feasible to determine exactly the equilibrium constant because faster elution could not be achieved owing to the high back-pressures. The determination of the areas A, B and C [9] was also complicated by the fact that the peaks were not sharp. Therefore, we performed approximate calculations with the best data we could obtain. Two values of K were obtained; the first did not include areas A' and B' with the area C, and the second (in our opinion the more correct, because it reflects in part the computer-simulated situation) included these areas (for the theory of the calculation [9]). The value of K was roughly estimated to be 0.47. According to our calculation, the velocity constant of *cis*–*trans* interconversion at -17°C is between $1.7 \cdot 10^{-2}$ and $2.9 \cdot 10^{-2} \text{ min}^{-1}$. Even though our calculation is much simpler than that suggested by Melander *et al.* [10], the results are comparable.

The peaks eluted earlier from the Vydac C_{18} column at -17°C are probably impurities that were not observed or separated in the runs performed at room temperature. We decided to test different chromatographic materials to see if the separation of these impurities could be achieved. An alterna-

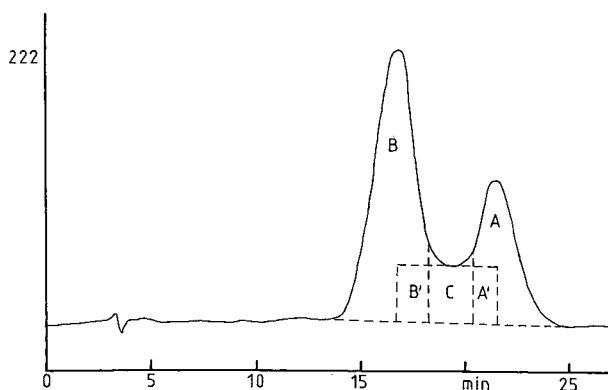


Fig. 2. Chromatographic trace of re-equilibrated mixture of *cis* and *trans* conformers of Gly-Trp-MeNle-Asp-Phe-NH₂ used for the calculation of velocity constants. For details see ref. 9. Conditions as in Fig. 1; temperature, -17°C .

tive hydrophobic material used for reversed-phase HPLC is a modified polystyrene in which the polystyrene is coated with ethylene dimethylacrylate (EDMA 40). This column was made available to us in the form of a small ($8 \times 0.8 \text{ cm I.D.}$) experimental column, courtesy of Tessek. This column clearly separates the impurities from the main product, but a decrease in temperature does not lead to an improvement in the separation. On the contrary, the efficiency of the column is decreased and at -6°C unacceptably broad peaks with very high retention times were obtained. Hence, no complete separation of the conformers was achieved, and only shoulders on the broad peak of the main component of the mixture were observed (Fig. 3). However, it is important to note that this column provides an alternative to the usual C_{18} and other hydrocarbon-modified supports for reversed phase chromatography.

To observe the influence of reduced temperature on the separation of peptides having similar retention times, we tested the separation of oxytocin analogues containing D- and L-tetrahydroisoquinoline-carboxylic acid in position 2 [14]. In this instance, the separation was completely lost at decreased temperature owing to the poorer efficiency of the column (the situation was the same using either a Vydac C_{18} or a EDMA-40 column; the latter result

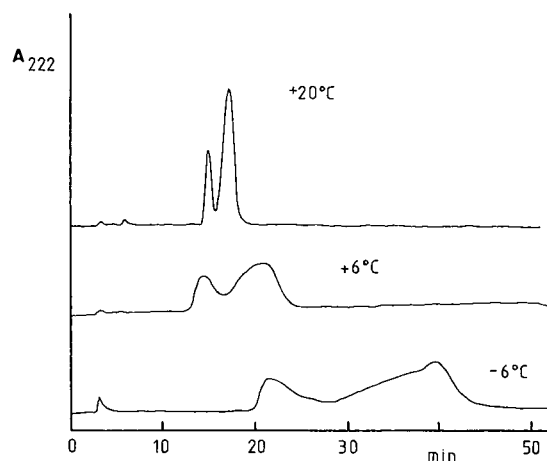


Fig. 3. Chromatography of HPLC-purified sample of Gly-Trp-MeNle-Asp-Phe-NH₂ at various temperatures. Conditions: columns, EDMA 40 ($8 \times 0.8 \text{ cm I.D.}$); eluent, methanol-acetonitrile-0.1% trifluoroacetic acid (50:3:47); flow-rate 1 ml/min; detection at 222 nm.

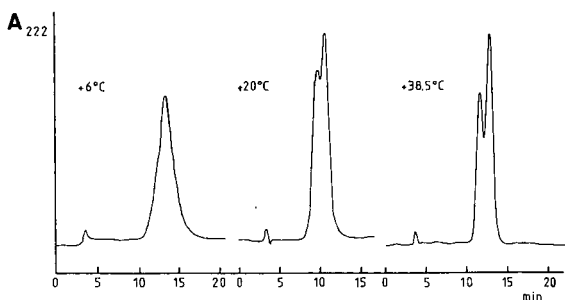


Fig. 4. Influence of temperature on the separation of [2-(D- and L-tetrahydroisoquinolinecarboxylic acid)]oxytocin. Conditions: column, EDMA 40 (8 × 0.8 cm I.D.); eluent, methanol-acetonitrile-0.1% trifluoroacetic acid (50:3:47); flow-rate 1 ml/min; detection at 222 nm.

is illustrated in Fig. 4), but was improved by heating the column.

In conclusion, it is hard to predict *a priori* the influence of lowering the temperature on the separation of peptides. Decreased efficiency and increased retention times may be expected. However, in some instances, as in the separation of isomers that interconvert at room temperature and thus require reduced temperature to slow the rate of interconversion, separation can only be achieved by lowering the temperature. The use of alternative solid supports for reversed-phase HPLC is strongly recommended for verification of the purity of synthetic peptides.

ACKNOWLEDGEMENTS

This work was supported by US Public Health Grant DK 36289 and the National Science Foundation.

REFERENCES

- 1 M. Dizdaroglu, H. C. Krutzsch and M. G. Simic, *Anal. Biochem.*, 123 (1982) 190.
- 2 T. Nagao and T. Tanimura, *J. Chromatogr.*, 496 (1989) 39.
- 3 O. Mikes, *High-Performance Liquid Chromatography of Biopolymers and Biooligomers, Part A*, Elsevier, Amsterdam, 1988, p. A44.
- 4 D. E. Henderson, S. J. Saltzman, P. C. Uden and Z. Cheng, *Polyhedron*, 7 (1988) 369.
- 5 D. E. Henderson and Cs. Horváth, *J. Chromatogr.*, 368 (1986) 203.
- 6 J. Jacobson, W. R. Melander, G. Valsnys and Cs. Horváth, *J. Phys. Chem.*, 88 (1984) 4536.
- 7 D. E. Henderson and D. J. O'Connor, *Adv. Chromatogr.*, 23 (1984) 65.
- 8 N. Delaet, M. Elseviers, D. Tourwé and G. Van Binst, in R. Epton (Editor), *Innovation and Perspectives in Solid Phase Synthesis*, SPCC, Birmingham, 1990, p. 473.
- 9 M. Lebl and V. Gut, *J. Chromatogr.*, 260 (1983) 478.
- 10 W. R. Melander, H. J. Lin, J. Jacobson and Cs. Horváth, *J. Phys. Chem.*, 88 (1984) 4527.
- 11 V. J. Hruby, S. Fang, R. Knapp, W. Kazmierski, G. K. Lui and H. I. Yamamura, *Int. J. Pept. Protein Res.*, 35 (1990) 566.
- 12 V. J. Hruby, S. Fang, R. Knapp, W. Kazmierski, G. K. Lui and H. I. Yamamura, in J. E. Rivier and G. R. Marshall (Editors), *Peptides: Chemistry, Structure and Biology*, ESCOM, Leiden, 1990, p. 53.
- 13 W. R. Melander, J. Jacobson and Cs. Horváth, *J. Chromatogr.*, 234 (1982) 269.
- 14 M. Lebl, P. Hill, L. Karaszova, J. Slaninova, I. Fric, W. Kazmierski and V. J. Hruby, *Int. J. Pept. Protein Res.*, 36 (1990) 321.

Short Communication

Determination of cimetidine and related impurities in pharmaceutical formulations by high-performance liquid chromatography

P. Betto, E. Ciranni-Signoretti* and R. Di Fava

Istituto Superiore di Sanità, Viale Regina Elena 299, 00161 Rome (Italy)

(First received March 22nd, 1991; revised manuscript received July 11th, 1991)

ABSTRACT

The analytical characteristics of cimetidine tablets were studied. A high-performance liquid chromatographic method was developed in order to assay cimetidine and its related impurities simultaneously. A reversed-phase system and diode-array detector were used.

INTRODUCTION

Cimetidine is a histamine H₂-receptor antagonist. It inhibits gastric acid secretion and other actions of histamine, mediated by H₂-receptors. Clinical trials have shown cimetidine to be of value in the treatment of gastric and duodenal ulcers and in other conditions where gastric acid is involved [1–14]. It is widely used by the oral, intramuscular and intravenous routes. Also, a large number of cimetidine products are commercially available, especially oral products, and in particular tablet formulations. The impurities profiles in these preparations have been widely investigated [15–17]; the maximum acceptable limits of these impurities are reported in some Pharmacopoeias [18–20].

In the pharmaceutical dosage forms, some degradation products can be present. Cimetidine undergoes decomposition through two pathways: hydrolysis and oxidation [21], with the production of N-cyano-N'-methyl-N''-[2-(5-methyl-1*H*-imidazol-4-yl)methyl]sulphonylethylguanidine (**I**), N-methyl-

N'-[2-(5-methyl-1*H*-imidazol-4-yl)methylthio]ethylguanidine (**II**) and N-carbamoyl-N'-methyl-N''-[2-(5-methyl-1*H*-imidazol-4-yl)methylthio]ethylguanidine (**III**). As a related impurity, commercial cimetidine contains also N-cyano-N'-[2-(5-methyl-1*H*-imidazol-4-yl)methylthioethyl]-S-methylisothiourea (**IV**), which is the immediate precursor in the synthesis [15].

Different high-performance liquid chromatographic (HPLC) methods have been utilized for determining compounds **I–IV** in cimetidine dosage forms [15–17]. Nevertheless, these are not suitable for determining all the mentioned impurities simultaneously [16–17] and they also need two different mobile phases for their separation [15]. Therefore, it was deemed of interest to develop an HPLC method in order to determine simultaneously the above-mentioned impurities and the drug, using only one mobile phase. An HPLC system equipped with a photodiode-array UV detector was utilized for the on-line determination of impurity profiles. The method was used to verify the quality of cimetidine

tablet formulations commercially available in Italy with respect to their drug and impurity contents.

EXPERIMENTAL

Materials

Twelve different formulations of cimetidine which are commercially available in Italy were studied. The tablets were composed of 200, 400 or 800 mg of cimetidine and several other ingredients.

Cimetidine and related impurities (I–IV) were supplied by Smith Kline & French (Milan, Italy). Sodium 1-pentanesulphonate was from Fluka (Buchs, Switzerland). Acetonitrile (HPLC grade) and all the other reagents were from Carlo Erba (Milan, Italy). All solvents used in the HPLC system were solubilized with distilled water treated with a Milli-Q system (Millipore, Milford, MA, USA).

Apparatus

Analytical HPLC was performed using an LKB Model 2249 gradient pump and an LKB Model 2140 rapid spectral detector (Pharmacia–LKB, Uppsala, Sweden) connected to a personal computer (Personal System 2, mod. 30, IBM, Portsmouth, UK). The column was a μ Bondapak C_{18} (10 μ m) (30 cm \times 3.9 mm I.D.) from Waters–Millipore (Milford, MA, USA).

Chromatographic conditions

The separation of the tested compounds was achieved using a linear gradient. Solvent A was 0.025 M sodium acetate, adjusted to pH 3.50, containing 0.003 M sodium 1-pentanesulphonate. Solvent B was 0.025 M sodium acetate (pH 3.50) containing 0.003 M sodium 1-pentanesulphonate plus 20% (v/v) of acetonitrile. The gradient was linear for 25 min (from 10% to 90% B), then returned to 10% B to allow the column to re-equilibrate. The elution of the compounds was carried out at room temperature with a flow-rate of 1.0 ml/min. The volume injected was 5–50 μ l. Detection was effected at 220, 230, 240 and 250 nm.

Sample preparation

Ten tablets were accurately weighed and ground to a fine powder. An amount of the powder that contained *ca.* 100 mg of cimetidine was weighed

and transferred to a volumetric flask where it was stirred with 180 ml of mobile phase A. After sonication for 15 min, the mixture was made up to volume (200 ml) with mobile phase A and filtered.

The impurities I–IV were dissolved in mobile phase A (I, III and IV at 2 μ g/ml and II at 4 μ g/ml).

Assay procedure

Volumes of 5 μ l of the sample solution were injected into the chromatograph under the conditions described. For comparison, an identical amount of the cimetidine standard solution was injected. The standard solution contained the same concentrations of the drug (based on the label claim). The impurities were determined by injecting 50 μ l of the sample solution and comparing the areas of impurity peaks with those of the peaks obtained by injecting known amounts of each impurity.

RESULTS AND DISCUSSION

The method described for determining cimetidine and related impurities, employing HPLC with a photodiode-array detector, was shown to be selective and sensitive. Simultaneous detection, at different wavelengths, and measurements of the UV spectrum of each separated compound during elution make it possible to identify the impurities easily and rapidly.

A representative chromatogram illustrating the resolution of a standard mixture and a sample are

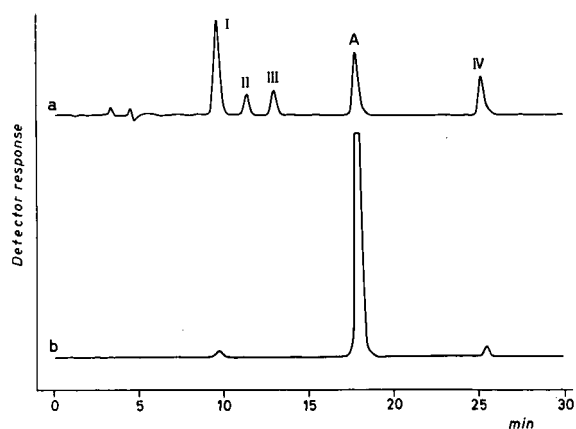


Fig. 1. Chromatograms of (a) standard mixture of cimetidine (a) (0.4 μ g), I (0.4 μ g), II (0.8 μ g), III (0.4 μ g) and IV (0.4 μ g); (b) sample L. Column: μ Bondapak C_{18} . Detection at 220 nm.

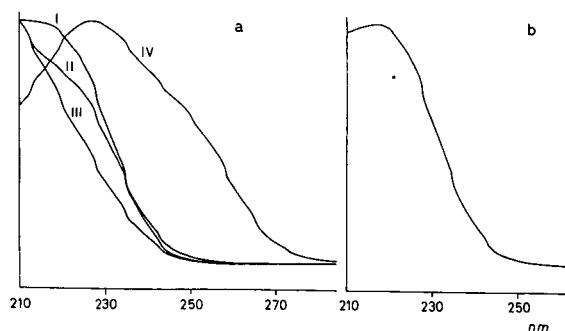


Fig. 2. Photodiode-array UV spectra of the components of a standard mixture after chromatographic separation (see Fig. 1). (a) Spectra of impurities I, II, III and IV; (b) spectrum of cimetidine.

shown in Fig. 1. Fig. 2 shows the spectra of the main compound cimetidine and of the impurities I-IV as obtained by photodiode-array detection. Although the spectra are similar, the slight but characteristic differences are of diagnostic value in the identification of I-IV.

The reproducibility of the method was satisfactory, as shown in Table I, which reports the response

TABLE I
REPRODUCIBILITY OF DETERMINATION OF CIMETIDINE IN TABLET FORMULATIONS

Sample	Cimetidine concentration ± S.D. (%)	Coefficient of variation (%)	
		Within-assay ^a	Between-assay ^b
A	101.2 ± 1.6	1.8	2.3
B	91.7 ± 1.1	2.1	2.9
C	92.6 ± 1.8	2.7	3.2

^a Average of five determinations.

^b Average of ten determinations.

to repeated injections of three of the samples analysed.

Linearity was checked statistically, and Table II shows the data obtained for the calibration graphs of cimetidine and the impurities.

Recovery was determined by preparing synthetic mixtures, simulating three tablet formulations, containing known amounts of standard and impurities

TABLE II
STATISTICAL DATA FOR CALIBRATION GRAPHS FOR CIMETIDINE AND IMPURITIES I, II, III AND IV

Compound	Range tested (µg)	Correlation coefficient	Slope	Intercept
Cimetidine	0.40-20.0	0.9996	3.057	0.058
I	0.02-1.60	0.9997	1.770	0.006
II	0.04-3.20	0.9986	0.518	0.029
III	0.02-1.60	0.9983	1.403	0.030
IV	0.02-1.60	0.9951	2.301	0.127

TABLE III
RECOVERY STUDY

Synthetic mixture	Amount injected (µg)					Recovery (%) ± S.D. ^a				
	Cimetidine	I	II	III	IV	Cimetidine	I	II	III	IV
a	12.5	0.04	0.08	0.04	0.04	99.5 ± 2.1	96.3 ± 4.5	97.6 ± 3.9	95.8 ± 4.1	98.1 ± 4.3
b	15.0	0.04	0.08	0.04	0.04	98.7 ± 2.7	95.6 ± 3.1	94.9 ± 4.3	96.1 ± 3.7	97.1 ± 3.8
c	17.5	0.05	0.10	0.05	0.05	97.8 ± 1.8	93.8 ± 3.5	96.8 ± 4.4	95.1 ± 4.3	94.9 ± 4.7

^a Average of five determinations.

TABLE IV

ASSAY (% OF DECLARED) OF CIMETIDINE AND RELATED IMPURITY LEVELS IN COMMERCIAL DOSAGE FORMS

Each value represents the mean (\pm S.D.) of five determinations. The impurity levels not reported were less than 0.01%.

Sample	Cimetidine concentration \pm S.D. (%)	Impurity concentration (%)				
		I	II	III	IV	I + II + III + IV
A	101.2 \pm 1.6	—	—	—	0.05	0.05
B	91.7 \pm 1.1	—	—	—	—	—
C	92.6 \pm 1.8	—	—	—	0.20	0.20
D	90.0 \pm 0.4	0.20	—	—	—	0.20
E	91.3 \pm 2.0	0.13	—	—	—	0.13
F	99.2 \pm 0.8	—	—	—	0.09	0.09
G	102.8 \pm 1.2	0.09	—	—	—	0.09
H	109.5 \pm 0.9	—	—	—	—	—
I	110.0 \pm 0.8	—	—	—	0.20	0.20
L	91.5 \pm 2.1	0.11	—	—	0.10	0.21
M	93.7 \pm 2.2	0.05	—	—	0.07	0.12
N	93.1 \pm 0.8	—	—	—	0.17	0.17

and subjecting them to the procedure (Table III).

The detection limit was *ca.* 2 ng, calculated on a response of twice the noise level.

The results obtained for cimetidine and impurities in commercial dosage forms are reported in Table IV. The amount of active ingredient found experimentally is within 10% of the amount declared, in agreement with Italian regulations. The percentages of the related impurities, for all the formulations examined, met pharmacopoeial standards.

The described HPLC method appears to be reproducible and sensitive and provides a reliable quality control of cimetidine tablet formulations.

REFERENCES

- R. W. Brimblecombe, W. A. M. Duncam, G. J. Durant, C. R. Ganellin, M. E. Pearson and J. W. Black, *Pharmacology*, 53 (1975) 435.
- R. W. Brimblecombe, W. A. M. Duncam, G. J. Durant, J. C. Ennett, C. R. Ganellin and M. E. Pearson, *J. Int. Med. Res.*, 3 (1975) 86.
- W. L. Burland, W. A. M. Duncan, T. Hesselbo, J. G. Mills, P. C. Sharpe, S. J. Haggie and J. H. Willie, *Br. J. Clin. Pharmacol.*, 2 (1975) 481.
- C. T. Richardson, J. H. Walsh and M. I. Hicks, *Gastroenterology*, 71 (1976) 19.
- R. M. Henn, J. I. Isemberg and V. Laxwell, *N. Engl. J. Med.*, 293 (1976) 371.
- R. E. Pounder, J. G. Willimas, G. J. Milton-Thompson and J. J. Misiewicz, *Lancet*, ii (1975) 1069.
- R. E. Pounder, J. G. Willimas, G. J. Milton-Thompson and J. J. Misiewicz, *Gut*, 17 (1976) 133.
- R. E. Pounder, J. G. Willimas, C. G. Russel, G. J. Milton-Thompson and J. J. Misiewicz, *Gut*, 17 (1976) 161.
- D. Hollander, Z. Hossain and A. M. Sufi, *Am. J. Dig. Dis.*, 21 (1976) 361.
- G. F. Longstreth, V. L. W. Go and J. R. Malagelada, *N. Engl. J. Med.*, 294 (1976) 801.
- G. Bodemar and A. Walan, *Lancet*, ii (1976) 161.
- W. S. Blackwood, D. P. Maudgal, R. G. Pickard, D. Lawrence and T. C. Northfield, *Lancet*, ii (1976) 174.
- J. F. Groarke and O. Fitzgerald, *Ir. J. Med. Sci.*, 145 (1976) 172.
- S. J. Haggie, D. C. Fermont and J. H. Wyllie, *Lancet*, i (1976) 983.
- E. G. Lovering and N. M. Currann, *J. Chromatogr.*, 319 (1985) 235.
- S. E. Walker, T. W. Paton, T. M. Fabian, C. C. Liu and P. E. Coates, *Am. J. Hosp. Pharm.*, 38 (1981) 881.
- P. M. G. Bavin, A. Post and E. Zarembo, in K. Florey (Editor), *Analytical Profiles of Drug Substances*, Vol. 13, Academic press, New York, 1984, p. 127.
- Unites States Pharmacopeia*, US Pharmacopoeial Convention, Rockville, MD, 21st Revision, 6th Suppl., 1985, p. 2530.
- Farmacopea Ufficiale della Repubblica Italiana*, Istituto Poligrafico e Zecca dello Stato, Rome, IX ed., 1985, p. 458.
- European Pharmacopoeia*, Vol. II, Maisonneuve, Saint Rufine, 1985, p. 458.
- H. A. Rosemberg, J. T. Dougherty, S. Mayron and J. G. Baldinus, *Am. J. Hosp. Pharm.*, 37 (1980) 390.

Short Communication

High-performance liquid chromatography of thiazolidinic compounds obtained by condensation of pyridoxal 5'-phosphate or pyridoxal with aminothiols (L- or D-cysteine, cysteamine, L-cysteine ethyl ester)

L. Terzuoli, R. Leoncini, D. Vannoni, E. Marinello* and R. Pagani

Institute of Biochemistry and Enzymology, University of Siena, Piano dei Mantellini 44, I-53100 Siena (Italy)

(First received March 19th, 1991; revised manuscript received July 16th, 1991)

ABSTRACT

We investigated six thiazolidine 4-carboxylic acids of biological interest, obtained by condensation of pyridoxal 5'-phosphate or pyridoxal with L- or D-cysteine, cysteamine or L-cysteine ethyl ester. A reversed-phase high-performance liquid chromatographic method, using a C₁₈ column for their separation, was developed by sequential optimization of the pH and the gradient of the mobile phase. Resolution of the compounds was obtained with an analysis time of less than 20 min.

INTRODUCTION

Thiazolidine compounds are formed by condensation of either aliphatic or aromatic moieties, containing a -CHO group, with different aminothiols [1,2]. We obtained several thiazolidine 4-carboxylic acids (TAs) by condensation [3–8] of pyridoxal 5'-phosphate (PLP) or pyridoxal (PL) (the other aldehyde form of vitamin B₆), with L- or D-cysteine, cysteamine or L-cysteine ethyl ester (Fig. 1, compounds I–VI).

Interest in these compounds arose following the observation that several aminothiols, such as L- or D-cysteine, cysteamine, and L-cysteine ethyl ester, exert a high degree of inhibition on certain PLP-dependent enzymes, such as rat liver L-threonine deaminase, the properties of which we have extensively studied [9–11]. Inhibition is due to the forma-

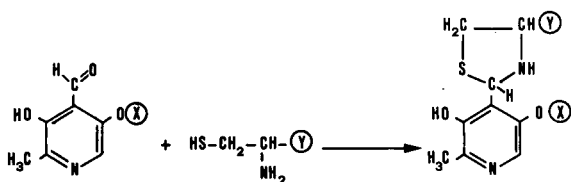
tion of a thiazolidinic ring, from condensation of L-cysteine and the enzyme-bound PLP.

Since the thiazolidine compounds are easily formed under physiological conditions (pH 7 and 37°C), it seems likely that they also form *in vivo*. If so, it is important to identify their biological role in the cell. To solve this problem, a procedure was needed for the isolation and determination of TAs, which would also be valid in the presence of tissue extract. Accordingly we developed the selective high-performance liquid chromatographic (HPLC) procedure, described in this paper.

EXPERIMENTAL

Chemicals

PLP, PL, L- and D-cysteine, cysteamine, L-cysteine ethyl ester, potassium dihydrogenphosphate



I	Y = C OOH	X = PO ₃ H ₂
II	Y = H	X = PO ₃ H ₂
III	Y = C OOC ₂ H ₅	X = PO ₃ H ₂
IV	Y = C OOH	X = H
V	Y = H	X = H
VI	Y = C OOC ₂ H ₅	X = H

Fig. 1. Formation of thiazolidine 4-carboxylic acids through condensation of PLP and L-cysteine (I), cysteamine (II), and L-cysteine ethyl ester (III); or PL and L-cysteine (IV), cysteamine (V), and L-cysteine ethyl ester (VI).

and potassium monohydrogenphosphate were obtained from Merck (Darmstadt, Germany). Norit A was purchased from Fisher Scientific (Fair Lawn, NJ, USA). Methanol (HPLC grade) was obtained from Baker (Phillipsburg, NJ, USA).

Preparation of thiazolidine 4-carboxylic acids (I–VI)

Compounds I–VI were synthesized from PLP or PL with L- or D-cysteine, cysteamine, or L-cysteine ethyl ester, by known methods [3,4,6]. Their purity was tested through elemental analysis, and IR and NMR spectra.

IR analysis was performed using a Perkin-Elmer (Garden Grove, CA, USA) Model 782 spectrometer; NMR spectra were obtained using a Perkin-Elmer Model R600 instrument.

Aqueous solutions of the compounds showed a specific UV spectrum with an absorption maximum at 330 nm with $\epsilon = 6.41$ (I), 6.98 (II), 4.05 (III), 6.08 (IV), 1.49 (V), 5.92 (VI) l mmol⁻¹ cm⁻¹. The spectra were obtained using a Shimadzu (Kyoto, Japan) UV-160 spectrophotometer.

Preparation and use of rat liver supernatant

Rat liver supernatant was prepared as previously reported [12]. Male albino rats, 9 weeks old, 250 g body weight, were decapitated and their livers rapidly removed; a 10% homogenate (in 50 mM potassium phosphate, pH 7.5) was prepared and centrifuged at 260 000 g for 1 h at 4°C. A 10-ml volume of

the supernatant was treated with 1.5 ml of 50% Norit A suspension (v/v) according to Hershko *et al.* [13], for 15 min and centrifuged at 1000 g for 15 min.

A 0.5-ml volume of 4 mM solution of compounds I–VI was added to 0.5 ml of supernatant, immediately deproteinized with 2 M hydrochloric acid (0.5 M final concentration), centrifuged at 8000 g and diluted with a 50 mM potassium phosphate buffer (pH 7.5) to 1 mM final concentration of TAs. The blank was obtained by replacement of the supernatant with 0.5 ml of the same buffer, and 20 μ l of this solution (20 nmol of each) was submitted to HPLC analysis.

Apparatus and chromatographic conditions

We used a Beckman (San Ramon, CA, USA) System Gold high-performance liquid chromatograph equipped with a 126 programmable solvent module, a scanning detector module 167 and a Beckman Ultrasfere XL C₁₈ column (70 × 4.6 mm I.D., 3- μ m particle size) protected by a precolumn.

The mobile phase was a mixture of 0.05 M potassium phosphate buffer [adjusted to pH 5.5 with 0.5 M potassium hydroxide (buffer A)], 0.01 M potassium phosphate buffer pH 5.5 (buffer B) and methanol. The programme for the mobile phase gradient is given in Table I. The flow-rate was 1 ml/min and the detection wavelength was 254 nm.

RESULTS AND DISCUSSION

Optimal conditions

Under these conditions we ignored the free aminothiols (L- and D-cysteine, cysteamine, and L-cysteine ethyl ester) because they did not interfere with the chromatography.

We carried out a preliminary study to obtain the best separation of TAs from the starting products (PLP and PL): the effects of different pH values of the mobile phase are reported in Fig. 2. The pH chosen for the chromatography was 5.5. Moreover, we varied the relative proportions of buffers A and B and methanol in order to obtain the best separation of the six TAs, PLP and PL, as shown in Fig. 3.

Good linearity was obtained for TAs I, II, IV and VI, PLP and PL in the range 0.3–20 nmol and for TAs III and V at 1–40 nmol and 5–40 nmol, respec-

TABLE I
GRADIENT PROGRAMME FOR MOBILE PHASE COMPOSITION

Time (min)	Mobile phase (% v/v) ^a			Duration (min)
	Buffer A	Buffer B	Methanol	
0 (start)	97	—	3	3
3	—	97	3	2
5	—	60	40	3
16	—	97	3	2
18	97	—	3	2
25 (stop)	97	—	3	—

^a Buffer A: 0.05 M potassium phosphate buffer (adjusted to pH 5.5 with 0.5 M potassium hydroxide); buffer B: 0.01 M potassium phosphate buffer (adjusted to pH 5.5 with 0.5 M potassium hydroxide).

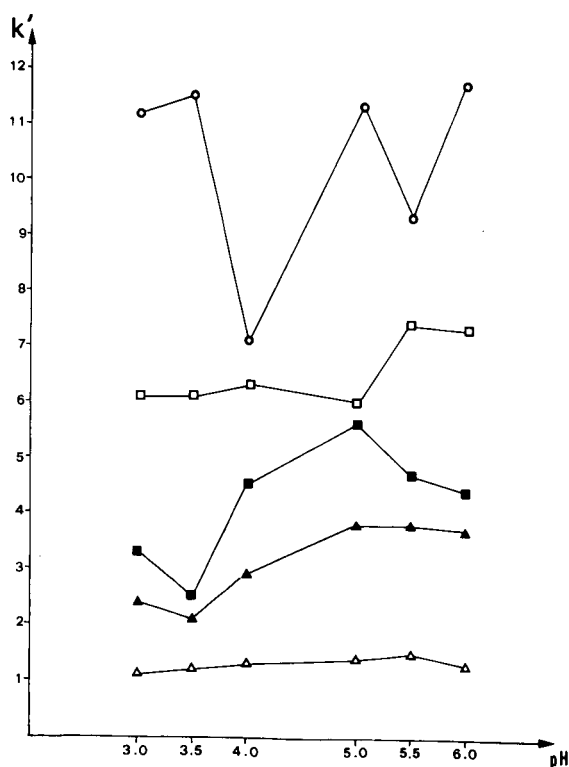


Fig. 2. Effect of pH on capacity factors (k') values of (■) PLP, (▲) PL, (△) I, (□) II, (○) IV. The data relating to compounds III, V and VI are not shown because these compounds were not eluted under the experimental conditions used, but only after addition of methanol to the mobile phase.

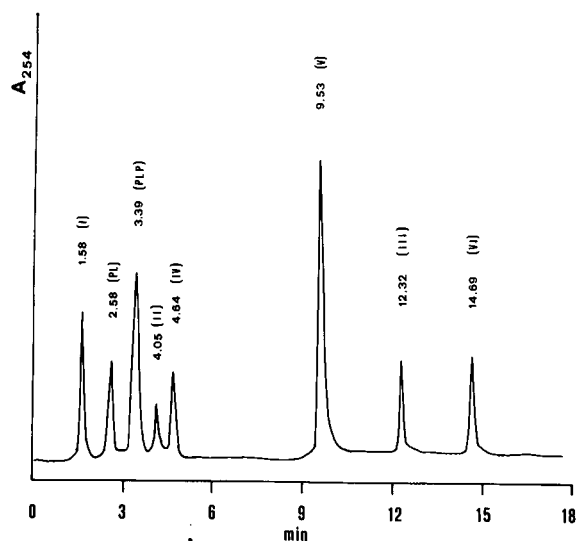


Fig. 3. Separation of PLP, PL, I, II, III, IV, V and VI. Injected amount: 20 nmol of each standard.

tively. Correlation coefficients and regression equations are reported in Table II.

The overall between-run and between-day precisions of the retention times and peak areas were studied, and the results are presented in Table III.

Behaviour of TAs in the presence of tissue extracts

Rat liver supernatant was added to the solution of these compounds, as indicated in Experimental. As shown in Fig. 4, their chromatographic behaviour did not change. These data demonstrate that there were no biological compounds in the supernatant affecting the determination of TAs, and that

TABLE II
CORRELATION COEFFICIENTS AND REGRESSION EQUATIONS OF PLP, PL, I, II, III, IV, V AND VI

Compound	Regression equation	Correlation coefficient (r)
PL	$y = 5.59x - 1.58$	0.9994
PLP	$y = 3.27x + 1.05$	0.9993
I	$y = 3.28x - 0.51$	0.9999
II	$y = 3.78x - 0.70$	0.9999
III	$y = 0.19x + 0.10$	0.9989
IV	$y = 3.26x - 0.84$	0.9998
V	$y = 1.09x - 1.03$	0.9992
VI	$y = 2.70x - 0.17$	0.9999

TABLE III

PRECISION OF RETENTION TIME AND PEAK AREAS OF PLP, PL, I, II, III, IV, V AND VI

Parameter	Compound	Retention time (min)	S.D. (n=5)	Relative S.D. (%)	Peak area (arbitrary units)	S.D. (n=5)	Relative S.D. (%)
Between-run precision (within 1 day)	I	1.50	0.02	1.13	6.29	0.04	0.63
	PL	2.46	0.01	0.24	10.76	0.13	1.21
	PLP	3.12	0.03	0.96	7.31	0.19	2.59
	II	4.05	0.01	0.15	6.37	0.04	0.63
	IV	4.48	0.01	0.24	12.13	0.07	0.62
	V	9.71	0.01	0.06	3.18	0.04	1.26
	III	12.27	0.00	0.00	20.31	0.06	0.29
Between-day precision (7 days)	VI	14.46	0.00	0.00	12.17	0.15	1.23
	I	1.48	0.05	3.31	5.86	0.32	5.46
	PL	2.48	0.03	1.17	10.20	0.42	4.12
	PLP	3.11	0.07	2.25	7.33	0.26	3.55
	II	4.05	0.05	1.16	6.50	0.43	6.61
	IV	4.54	0.07	1.49	13.60	2.34	17.20
	V	9.67	0.07	0.70	3.65	0.31	8.49
III	12.18	0.05	0.40	20.16	1.14	5.65	
VI	14.56	0.10	0.69	13.95	0.76	5.44	

it can be carried out in the presence of tissue extracts.

Our results show that TAs I–VI can be easily separated from each other and from their precursors (PLP or PL) by HPLC. The same procedure can be used when tissue extracts are added to the assay mixture. Only compound IV showed irregular behaviour during HPLC separation, as evidenced by

the high S.D. value (Table III): this was not due to contamination, since its purity had been carefully controlled, as reported in Experimental. In spite of this however, compound IV can be easily separated from the others and determined in the presence of tissue extracts.

We conclude that our procedure facilitates investigation of the biological role of all these com-

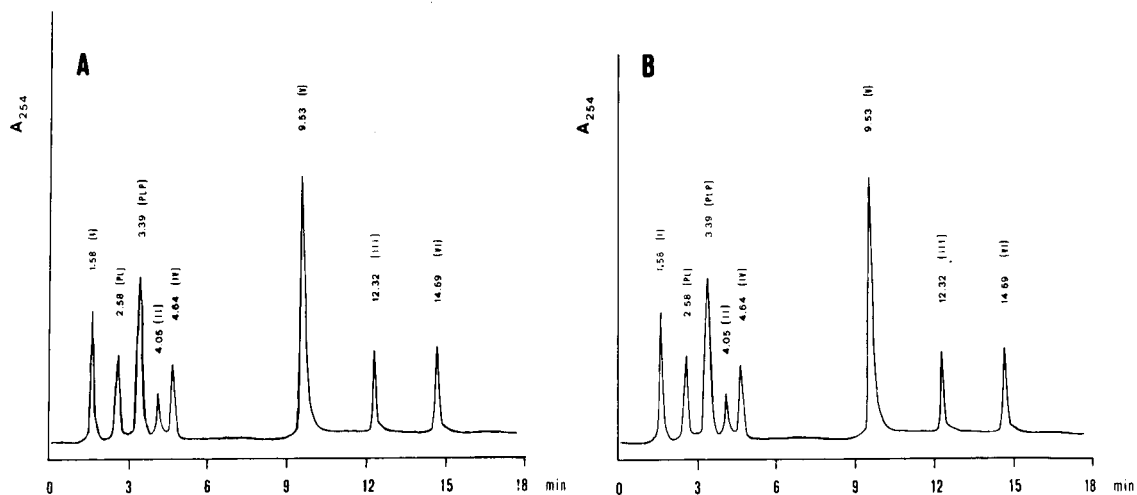


Fig. 4. Behaviour of TAs in (A) the absence and (B) the presence of tissue extract.

pounds, and in particular can be used to ascertain:

(1) if they are present in cellular extracts or in biological fluids;

(2) if they undergo quantitative fluctuations under different conditions;

(3) if they are synthesized from the cell or undergo metabolic transformations;

(4) if they interfere only in the PLP-dependent reactions or also in other enzymic transformations.

REFERENCES

- 1 M. P. Schubert, *J. Biol. Chem.*, 114 (1936) 341.
- 2 S. Ratner and H. T. Clarke, *J. Am. Chem. Soc.*, 59 (1937) 200.
- 3 D. Heyl, S. A. Harris and K. Folkers, *J. Am. Chem. Soc.*, 70 (1943) 429.
- 4 M. V. Buell and R. E. Hansen, *J. Am. Chem. Soc.*, 82 (1960) 6042.
- 5 D. Mackay, *Arch. Biochem. Biophys.*, 99 (1962) 93.
- 6 E. Angeletti and M. Haertlet, *Boll. Chim. Farm.*, 105 (1965) 867.
- 7 E. H. Abbot and A. E. Martell, *J. Am. Chem. Soc.*, 92 (1970) 1754.
- 8 M. Z. A. Badr, M. M. Aly, A. M. Fahmy and M. E. Y. Mansour, *Bull. Chem. Soc. Jpn.*, 54 (1981) 1844.
- 9 R. Pagani, A. Casella, F. Beffa and E. Marinello, *Biosci. Rep.*, 1 (1981) 955.
- 10 E. Marinello, R. Pagani and F. Ponticelli, *Quad. Ric. Sci.*, 113 (1984) 139.
- 11 R. Leoncini, R. Pagani, E. Marinello and T. Keleti, *Biochim. Biophys. Acta*, 984 (1989) 52.
- 12 L. Terzuoli, R. Pagani, R. Leoncini, D. Vannoni and E. Marinello, *J. Chromatogr.*, 514 (1990) 80.
- 13 A. Hershko, A. Razin and G. Mager, *Biochim. Biophys. Acta*, 184 (1969) 64.

Short Communication

Liquid chromatographic determination of ethylenethiourea using pulsed amperometric detection

Daniel R. Doerge* and Austin B. K. Yee

Department of Environmental Biochemistry, University of Hawaii, Honolulu, HI 96822 (USA)

(First received March 15th, 1991; revised manuscript received June 11th, 1991)

ABSTRACT

A liquid chromatographic method was developed using pulsed amperometric detection at a gold working electrode to measure residue levels of ethylenethiourea (ETU) in crops and groundwater. Use of the sequential pulsing program eliminates electrode fouling while preserving the sensitive and selective detection of ETU. Minimum detection limits in crops were 5–10 ppb (1.25–2.5 ng on-column) and 5 ppb (0.5 ng) in groundwater. The commercial availability of the pulsed electrochemical detector and its gold working electrode that remains functional with a minimum of conditioning is an improvement in method simplicity.

INTRODUCTION

Ethylenethiourea (ETU) is a formulation contaminant and environmental metabolite of ethylene bisdithiocarbamate (EBDC) fungicides, the most widely used fungicides worldwide [1]. The presence of ETU residues in food crops is of regulatory concern because high doses of ETU cause thyroid enlargement (goiter) and cancer (thyroid and liver) in experimental animals [2].

ETU has been determined by a variety of gas (GC) and liquid chromatographic (LC) methods [3,4]. The low volatility of ETU necessitates derivatization for analysis by GC and the low UV absorbance maximum (232 nm) makes LC with UV detection susceptible to interferences found in typical environmental samples. The most successful LC method published uses amperometric detection with a mercury–gold amalgam working electrode to determine ETU at levels ≥ 10 ppb in many crops [5]. However, the gold electrode supplied by the manufacturer must be modified prior to use in the

analysis. Briefly, the electrode surface was treated with liquid mercury and subsequently equilibrated in air for extended times (≥ 2 days) [5]. In addition, the modified working electrode has a finite period of consistent response (≤ 21 days), after which the electrode surface must be reconditioned as described above. These limitations provided the impetus to explore other electrochemical techniques for the sensitive and selective detection of ETU.

Pulsed amperometric detection has been used successfully to measure thiourea derivatives at low levels using gold or platinum working electrodes [6,7]. This technique is not limited, as is d.c. amperometry on these electrodes, by poisoning of the electrode surface by oxidized sulfur species and metal oxide formation. The ability to use a sequence of potential pulses allows for measurement of electron transfer at the working electrode followed by an oxidative “cleaning” potential and a subsequent reductive “reconditioning” potential to regenerate an active and stable electrode surface [8]. The commercial availability of such instrumentation led us

to use this technique for the determination of ETU in crops and groundwater.

EXPERIMENTAL

ETU was obtained from Aldrich (Milwaukee, WI, USA) and recrystallized from water before use. LC solvents were prepared from acetonitrile (Optima, Fisher Scientific, Fairlawn, NJ, USA) and water purified with a Milli-Q system (Millipore, Bedford, MA, USA) and were degassed by helium sparging. LC separation of ETU was performed using a quaternary gradient pump module (Dionex, Sunnyvale, CA, USA) equipped with a Rheodyne Model 7125 injector and a 25 cm \times 4 mm I.D. OmniPac PAX 500 column (Dionex) using 5% acetonitrile in 25.0 mM KH_2PO_4 (Sigma, St. Louis, MO, USA), pH 7.0, at a flow-rate of 1.5 ml/min. Pulsed amperometry was measured using the potential-time waveform defined in Fig. 1 produced by a pulsed electrochemical detector (Dionex) equipped with a Ag/AgCl reference electrode and recorded on an LCI-100 recording integrator (Perkin-Elmer, Norwalk, CT, USA). The gold working electrode was used as received from Dionex following an initial polishing by hand (*ca.* 1 min) using a fine abrasive compound. A UV detector (UVIS 200, Linear Instruments, Reno, NV, USA) was used for in-line detection of ETU at 232 nm to monitor the column performance and detector response. Method validation was provided by particle beam LC-mass spectrometry (LC-MS) using [^{13}C]ETU as an internal standard [9].

Extraction and purification of ETU residues from papaya and banana samples obtained from commercial grocery stores were performed by using the AOAC method as revised by Krause [5]. Briefly, a 50-g portion of fruit (peel or pulp) was homogenized with aqueous methanol and filtered and an aliquot corresponding to 10 g of fruit was processed further. The bulk of the solvent was removed *in vacuo* and the remainder was applied to Gas-Chrom S. The ETU residues were eluted through a column of alumina with 2% methanol in methylene chloride, which was removed *in vacuo*. The samples were dissolved in water (4 ml) and filtered (0.45 μm) prior to LC analysis of 100- μl aliquots. ETU concentrations were determined from comparison of peak areas or heights with those generated by au-

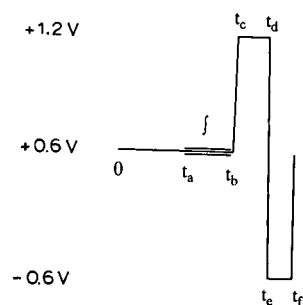


Fig. 1. Potential-time waveform used for pulsed amperometric detection of ETU. $t_a = 0.3$, $t_b = 0.5$, $t_c = 0.51$, $t_d = 0.59$, $t_e = 0.6$, $t_f = 0.65$ s. Current is integrated from t_a to t_b .

thentic standards injected immediately after the crop extract.

RESULTS AND DISCUSSION

Sensitive and selective detection of ETU in Hawaiian fruits and groundwater was accomplished using a commercial pulsed electrochemical detector and a polymer-based LC column. This column has been found to give reproducible retention time and peak shape for ETU in crops and groundwater with sufficient retention ($k' = 1.3$) for amperometric detection. The waveform used (Fig. 1) was based on that described by Johnson and co-workers [6,7] and the detector response to ETU standards was optimized by variation of potential and times. Integrated amperometry has been reported to give enhanced response to thioureas relative to simple potential-time waveforms such as that shown in Fig. 1 [7]. However, integrated amperometric waveforms corresponding to those previously published did not enhance the detection limit for ETU under the conditions of this study. It was also determined that varying the pH in the range 3–10 did not enhance the detector response to ETU. After several days of analyzing crop samples, an increase in the background signal and a decrease in the signal from ETU were observed. The sensitivity of the electrode was restored by polishing the working electrode surface as described above. After a short equilibration time (≤ 30 min), the detector was ready for use.

The use of an in-line UV detector allowed the assessment of the effect of the electrochemical detector on peak asymmetry. Determination of the peak asymmetry factor (B/A) by measuring the ar-

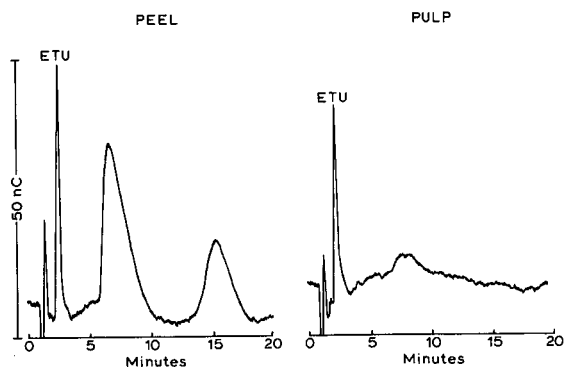


Fig. 2. Determination of ETU in papaya peel and pulp by LC with pulsed amperometric detection.

eas of the front and back portions of the peaks from both detectors showed that the electrochemical detector did not introduce significant tailing effects ($\leq 1\%$).

Fig. 2 shows the analysis of papaya pulp and peel for samples spiked with 20 ppb of ETU prior to homogenization, which corresponds to 5 ng injected on-column. The ETU detected corresponds to recoveries of 112 and 80% for the peel and pulp, respectively. These recoveries, and those from banana pulp (93%), are typical of the modified AOAC procedure and are comparable to those obtained in this laboratory from a variety of crops analyzed by a particle beam LC-MS method [9]. The detection limits (signal-to-noise ratio = 3) varied depending on the sample, but were typically 5–10 ppb (1.25–2.5 ng on-column). The major components of the total noise were baseline disturbances from unretained components and the presence of electroactive interferences, especially in papaya peel, the most complex matrix encountered. These limits compare favorably with those obtained using the mercury-gold amalgam working electrode reported by Krause (1.25–2.5 ng) [5]. While no tolerances are set for ETU levels in food crops, typical laboratory detection limits are 10 ppb.

The chromatogram in Fig. 2 shows the presence of at least two electroactive components in the papaya peel sample. The presence of sulfur-containing compounds in papaya skin has been reported previously [10]. The papaya pulp sample is essentially free from electroactive components except ETU. Chromatograms of control papaya samples showed no ETU and had similar elution profiles of coextractive components.

ETU was also determined in groundwater obtained from the Palolo section of the Pearl Harbor, Honolulu basin aquifer. Control injections showed no detectable ETU, so samples were fortified with varying amounts of ETU prior to analysis. The amperometric detector response to ETU in groundwater was linear over more than two orders of magnitude (0.5–100 ng, $r^2 = 0.9995$). The detection limit in groundwater was estimated to be 5 ppb (0.5 ng) with no sample preparation using 100- μ l injections.

This study demonstrates the utility of pulsed amperometric detection for the detection of ETU in environmental samples at levels comparable to those previously obtained using d.c. amperometry with a mercury-treated gold electrode [5]. The use of the pulsed waveform permits analyte detection and the working electrode reconditioning required for extended use with typical environmental samples and minimum variation in detector response. In addition, the commercial availability of the gold working electrode used in this study, which remains functional with a minimum of conditioning, *i.e.*, occasional polishing that is easily incorporated into a daily routine, represents an improvement in method simplicity.

ACKNOWLEDGEMENTS

The authors thank Drs. Roy Rocklin and Carl J. Miles for helpful discussions. This paper is submitted as Journal Series No. 3754 from the Hawaii Institute of Tropical Agriculture and Human Resources.

REFERENCES

- 1 National Research Council, *Regulating Pesticides in Food*, National Academy Press, Washington, DC, 1987, p. 208.
- 2 US EPA, *Fed. Reg.*, 54 (1989) 52158.
- 3 P. Bottomly, R. A. Hoodless and N. A. Smart, *Residue Rev.*, 95 (1985) 45.
- 4 C. J. Miles and D. R. Doerge, *J. Agric. Food Chem.*, 39 (1991) 214.
- 5 R. T. Krause, *J. Assoc. Off. Anal. Chem.*, 72 (1989) 975.
- 6 T. Z. Polta and D. C. Johnson, *J. Electroanal. Chem.*, 209 (1986) 159.
- 7 G. G. Neuburger and D. C. Johnson, *Anal. Chem.*, 60 (1988) 2288.
- 8 R. Rocklin, *Conductivity and Amperometry*, Dionex, Sunnyvale, CA, 1989, pp. 28–41.
- 9 D. R. Doerge and C. J. Miles, *Anal. Chem.*, 63 (1991) 1999.
- 10 C. S. Tang, *Phytochemistry*, 12 (1973) 769.

Short Communication

Determination of specific retention volumes at 20°C for hydrocarbons on microporous carbons

Xu-Liang Cao^{*}

Department of Chemistry, Brunel University, Uxbridge, Middlesex UB8 3PH (UK)

(First received June 11th, 1991; revised manuscript received July 31st, 1991)

ABSTRACT

Gas chromatography was used to determine the specific retention volumes at 20°C, $V_g(20^\circ\text{C})$, for various hydrocarbons on different microporous carbons. It was found that all microporous carbons can be used for the diffusive sampling of hydrocarbons with more than four carbon atoms. Those hydrocarbons with more than seven carbon atoms have extremely high $V_g(20^\circ\text{C})$ values on these adsorbents, whereas the $V_g(20^\circ\text{C})$ values for very light hydrocarbons ($\leq C_3$) are almost all less than 100 l/g, which shows that diffusive sampling may not be suitable for them. It was also found that the adsorption of molecules occurs readily in those micropores which give the highest isosteric heats of adsorption.

INTRODUCTION

The uptake rate of a diffusive sampler (DA/L) [1] should be constant in an ideal case before the saturation of adsorbents, as it depends only on the geometry of the sampler (cross-sectional area, A , and diffusion length, L) and the individual pollutant vapour which has a particular diffusion coefficient in air, D . However, this is true only for an optimized adsorbent–adsorbate system. In practice, non-constant sampling rates were observed [2,3], which are related to the characteristics of the adsorption of the adsorbate–adsorbent system concerned. Therefore, in diffusive sampling, the optimum adsorbent has to be selected for a particular analyte in order to keep the analyte concentration at the adsorbent surface as low as possible.

The adsorbent for diffusive sampling can be selected by determining the experimental uptake rate [4], which should be similar to the ideal uptake rate for the optimized adsorbate–adsorbent system. It can also be selected by a much simpler method as suggested by Brown and Walkin [3]. They proposed that the strength of an adsorbent should be expressed as the retention volume of a particular analyte at 20°C per gram of adsorbent, *i.e.*, the specific retention volume at 20°C. If this value exceeds 100 l/g, the adsorbent should prove satisfactory for diffusive sampling.

Microporous carbons are potential adsorbents for diffusive sampling, especially for the sampling of light hydrocarbons. In this paper, the results of the specific retention volumes at 20°C for various hydrocarbons on different microporous carbons are reported; these can be used as a guide for the selection of adsorbents in the future diffusive sampling work.

* Present address: Environmental Science Division, Lancaster University, Lancaster LA1 4YQ, UK.

EXPERIMENTAL

Gas chromatographic measurements were made using a Perkin-Elmer F30 gas chromatograph fitted with a flame ionization detector. The carrier gas was nitrogen (supplied by British Oxygen) at a flow-rate of 35 cm³/min, which was controlled by the make-up needle valve throughout the course of the experiments. The column inlet pressure was measured by a septum pressure gauge and the outlet pressure was measured to be atmospheric. Retention measurements were made over the temperature range 40–380°C. The gas hold-up time (t_0) was determined by the homologous series method [5].

The hydrocarbons used were 1% calibration standards for *n*-alkanes (methane to *n*-butane) and *n*-alkenes (ethylene to *n*-butylene) from Phase Separations and *n*-pentane to *n*-nonane, cyclohexane, benzene, isopentane, 2-methylpentane and 2,2-dimethylbutane from Aldrich. The details of the sample preparation have been described previously [6].

The adsorptive vapours were injected into the carrier gas stream by means of a gas-tight syringe. The on-line computer was started simultaneously with injection. Sequences of injections were made until retention volumes were reproducible to within 2% for at least three consecutive injections. The specific retention volume, V_g , was calculated from the following equation:

$$V_g = 273 (t_R - t_0) F_c / T w \quad (1)$$

where t_R is the retention time of the adsorptive (min), t_0 is the gas hold-up time (min), T is the absolute temperature (K), w is the weight of adsorbent in the column (g) and F_c is the volumetric carrier gas flow-rate reduced to column temperature and mean pressure (cm³/min).

The following microporous carbons were used. Carbosieve B is a polymer-based molecular sieve carbon, obtained from JJ's Chromatography (King's Lynn, Norfolk, UK). Two charcoal cloths, CC1, a high burn-off charcoal with a much wider range of pore size, and CC2, a low burn-off charcoal cloth, were kindly supplied by Dr. J. J. Freeman of Brunel University. The surface properties of these carbons are given in Table I. The details of the column preparation and conditioning have been described previously [6].

TABLE I

SURFACE PROPERTIES OF ADSORBENTS

A_{BET} = BET specific surface area; A_s = external area; V_p and V_s = primary and secondary micropore volumes respectively, from nitrogen α_s plot. For definition of α_s see ref. 9.

Adsorbent	A_{BET} (m ² /g)	A_s (m ² /g)	V_p [cm ³ (liq.)/g]	V_s [cm ³ (liq.)/g]
Carbosieve B	1174	51.5	0.45	0
CC1	2074	60.5	0.23	0.98
CC2	1039	16.5	0.41	0

RESULTS AND DISCUSSION

It was found that under the conditions employed almost all hydrocarbons gave nearly symmetrical chromatographic peaks, except in a few instances, such as 2,2-dimethylbutane on Carbosieve B and *n*-octane and *n*-nonane on Carbosieve B and CC2.

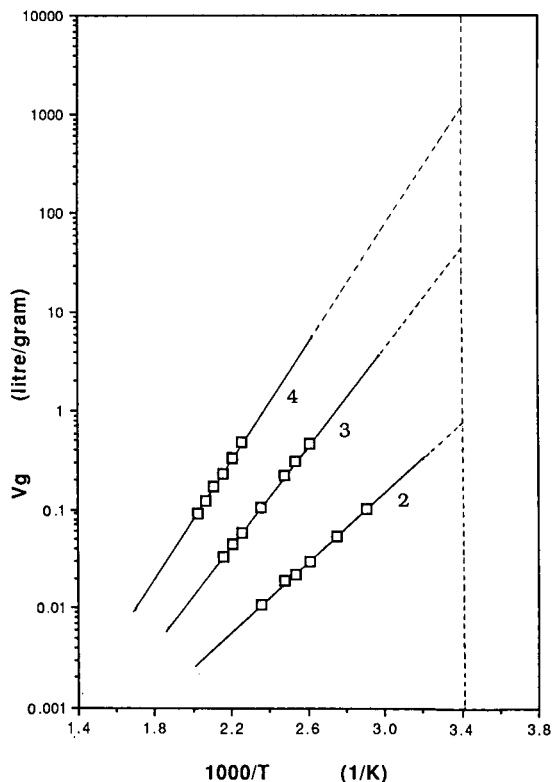


Fig. 1. Plots of $\log V_g$ against $1/T$ for *n*-alkenes on Carbosieve B. Numbers on lines indicate number of carbon atoms.

The specific retention volumes were calculated according to eqn. 1 from the retention times. The logarithms of the derived specific retention volumes (l/g) were then plotted against the reciprocal of the absolute column temperature. Representative $\log V_g$ vs. $1/T$ plots of different hydrocarbons for Carbosieve B, CCl1 and CC2 are shown in Figs. 1-5. These plots are almost all linear over a wide range of temperature, although there is a slight curvature in some instances.

The specific retention volumes at 20°C were obtained for each hydrocarbon by extrapolating the slope of each line in the $\log V_g$ vs. $1/T$ plots. The derived values of the specific retention volumes at 20°C for each hydrocarbon are given in Table I. The V_g (20°C) values for 2,2-dimethylbutane on Carbosieve B and *n*-octane and *n*-nonane on Carbosieve B and CC2 cannot be determined because of

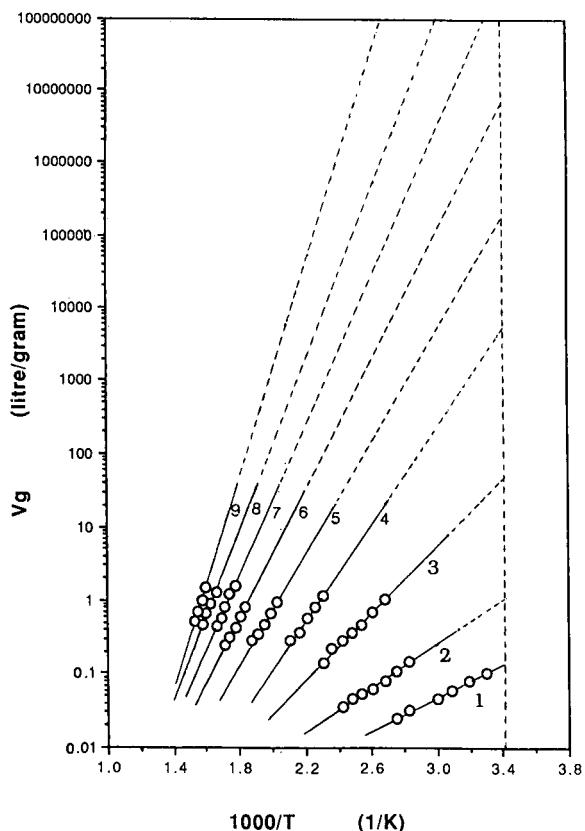


Fig. 2. Plots of $\log V_g$ against $1/T$ for *n*-alkanes on CCl1. Numbers on lines indicate number of carbon atoms.

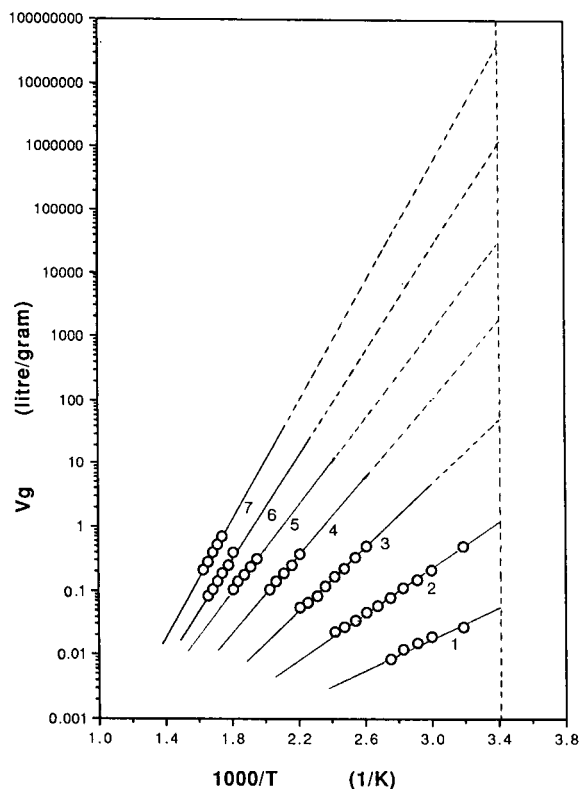


Fig. 3. Plots of $\log V_g$ against $1/T$ for *n*-alkanes on CC2. Numbers on lines indicate number of carbon atoms.

the severe asymmetry of the chromatographic bands (tailing) and the problem of irreproducible retention data.

It can be seen from the results in Table II that the specific retention volumes at 20°C generally increase with increasing molecular weight of the hydrocarbons. The values of V_g (20°C) for hydrocarbons with more than four carbon atoms all exceed 100 l/g, which indicates that all these adsorbents can be used for the diffusive sampling of these hydrocarbons. However, owing to difficulties with desorption, polymer adsorbents that have much lower specific surface areas (such as Tenax) should be used for the diffusive sampling of hydrocarbons with more than seven carbon atoms instead of microporous carbons on which these hydrocarbons have extremely high V_g (20°C) values. In contrast, even for CCl1, which has the highest specific surface area (2074 m²/g) of the adsorbents, the values of V_g (20°C) for hydrocarbons with less than three carbon atoms, *i.e.*, methane

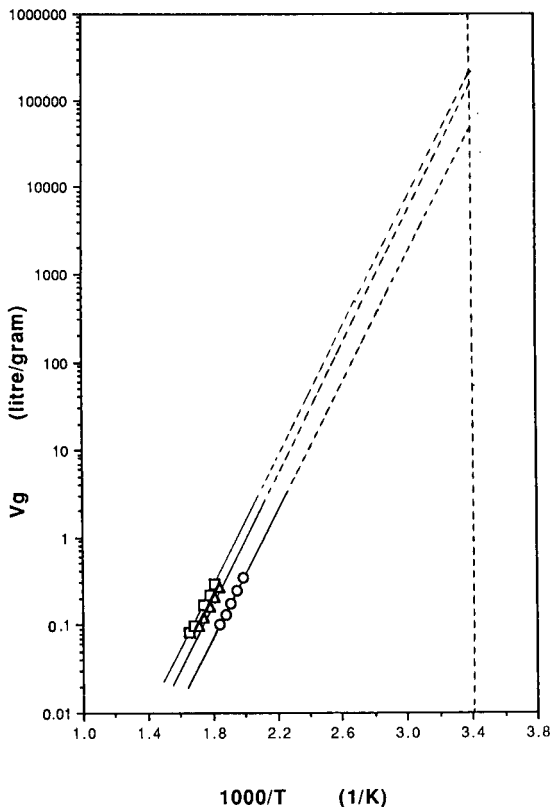


Fig. 4. Plots of $\log V_g$ against $1/T$ for hydrocarbons on CC2. \circ = Isopentane; \square = benzene; \triangle = 2,2-dimethylbutane.

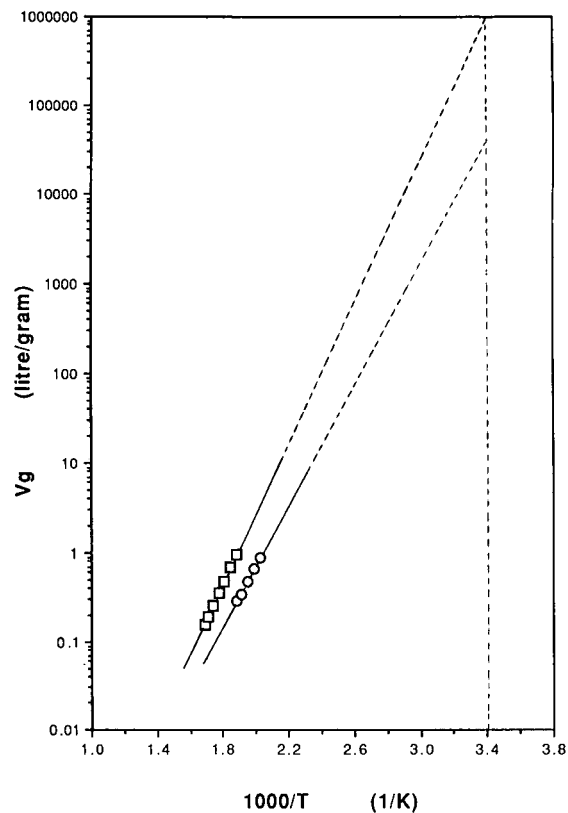


Fig. 5. Plots of $\log V_g$ against $1/T$ for hydrocarbons on CC1. \circ = Isopentane; \square = cyclohexane.

to propane, ethylene and propylene, are still far less than 100 l/g, except for propane on Carbosieve B, which shows that diffusive sampling may not be suitable for these very light hydrocarbons or the accuracy of their diffusive sampling measurement will be very poor compared with the pumped method.

It is interesting that, similarly to the findings for the isosteric heats of adsorption values, q^{st} [6], the corresponding V_g (20°C) values for *n*-alkanes and *n*-alkenes generally decrease in the order Carbosieve B > CC1 > CC2, *i.e.*, Carbosieve B, which possesses a homogeneous pore structure, gives higher V_g (20°C) values than CC1, which has a much broader range of pore sizes, which indicates that adsorption occurs readily in those micropores which give the highest isosteric heat of adsorption. In contrast, the V_g (20°C) values for hydrocarbons with

branched chains or bulky shapes on CC1 are higher than those on the other two adsorbents. This may be due to the wider micropores in CC1, in which there may be an enhancement of the adsorption energy for adsorption of bulkier molecules, because the enhancement in q^{st} depends on the ratio of micropore width to molecular diameter [7], and the adsorptive molecules of different size will tend to adsorb preferentially in slightly different parts of the micropore structure [8].

The other phenomenon which is also similar to previous findings for q^{st} [6] is that the V_g (20°C) values of straight-chain hydrocarbons are higher than those of hydrocarbons with branched chains or bulky shapes, which may indicate the molecular sieving properties of these adsorbents. For all adsorbents, the V_g (20°C) values generally decrease in the order *n*-pentane > isopentane, *n*-hexane >

TABLE II
SPECIFIC RETENTION VOLUMES AT 20°C FOR HYDROCARBONS ON DIFFERENT ADSORBENTS

Hydrocarbon	V_g (20°C)		
	Carbosieve B	CC1	CC2
Methane	0.12	0.13	0.05
Ethane	5.8	1.1	1.2
Propane	330	50	52
<i>n</i> -Butane	$1.9 \cdot 10^4$	$5.1 \cdot 10^3$	$1.8 \cdot 10^3$
<i>n</i> -Pentane	$5.0 \cdot 10^5$	$1.7 \cdot 10^5$	$2.8 \cdot 10^4$
<i>n</i> -Hexane	$7.6 \cdot 10^6$	$6.1 \cdot 10^6$	$1.2 \cdot 10^6$
<i>n</i> -Heptane	$4.0 \cdot 10^9$	$3.9 \cdot 10^8$	$4.2 \cdot 10^7$
<i>n</i> -Octane	—	$1.8 \cdot 10^{10}$	—
<i>n</i> -Nonane	—	$1.5 \cdot 10^{13}$	—
Ethylene	0.80	0.68	0.62
Propylene	45	33	34
<i>n</i> -Butylene	$1.2 \cdot 10^3$	$1.1 \cdot 10^3$	$1.0 \cdot 10^3$
Benzene	$2.8 \cdot 10^5$	$9.2 \cdot 10^5$	$2.0 \cdot 10^5$
Cyclohexane	$2.6 \cdot 10^5$	$1.0 \cdot 10^6$	$1.2 \cdot 10^5$
Isopentane	$2.3 \cdot 10^5$	$3.7 \cdot 10^4$	$4.2 \cdot 10^4$
2-Methylpentane	$2.8 \cdot 10^6$	$3.3 \cdot 10^6$	$2.6 \cdot 10^5$
2,2-Dimethylbutane	—	$2.2 \cdot 10^6$	$1.6 \cdot 10^5$

2-methylpentane > 2,2-dimethylbutane > cyclohexane \approx benzene, which may be explained by assuming that generally a linear conformation will allow the greatest interactions between surface and adsorbate, whereas with a branched structure the interaction between surface and adsorbate is weakened because some carbon atoms are relatively far away from the surface.

CONCLUSIONS

The specific retention volumes at 20°C provide a very simple method for the selection of adsorbents for diffusive sampling. The results show that all microporous carbons can be used for the diffusive sampling of hydrocarbons with more than four carbon atoms. However, for hydrocarbons with more than seven carbon atoms, which have extremely high V_g (20°C) values, these adsorbents may not be suitable owing to the difficulties with desorption. The V_g (20°C) values for hydrocarbons with less than three carbon atoms are almost all less than 100 l/g, which indicates that diffusive sampling may not be suitable for these very light hydrocarbons. The results also show that the adsorption of molecules occurs readily in those micropores which give the highest isosteric heats of adsorption.

REFERENCES

- 1 W. J. Lautenberger, E. V. Kring and J. A. Morello, *Am. Ind. Hyg. Assoc. J.*, 4 (1980) 737.
- 2 R. H. Brown, R. P. Harvey, C. J. Purnell and K. J. Saunders, *Am. Ind. Hyg. Assoc. J.*, 45 (1984) 67.
- 3 R. H. Brown and K. T. Walkin, *American Industrial Hygiene Conference*, Houston, TX, 18–23 May, 1980, Abstract 231.
- 4 N. Van Den Hoed and M. T. H. Halmans, *Am. Ind. Hyg. Assoc. J.*, 48 (1987) 364.
- 5 J. R. Conder and C. L. Young, *Physicochemical Measurement by Gas Chromatography*, Wiley, Chichester, 1979, p. 91.
- 6 X.-L. Cao, B. A. Colenutt and K. S. W. Sing, *J. Chromatogr.*, 555 (1991) 183.
- 7 D. H. Everett and J. C. Powl, *J. Chem. Soc., Faraday Trans. 1*, 72 (1976) 619.
- 8 P. J. M. Carrott and K. S. W. Sing, *J. Chromatogr.*, 518 (1990) 53.
- 9 S. J. Gregg and K. S. W. Sing, *Adsorption, Surface Area, and Porosity*, Academic Press, London, 2nd ed., 1982, p. 98.

Short Communication

Identification of enzymatic degradation products from synthesized glucobrassicin by gas chromatography–mass spectrometry

L. Latxague and C. Gardrat*

Laboratoire Chimie Appliquée, Université Bordeaux 1, 351 Cours de la Libération, 33405 Talence Cedex (France)

J. L. Coustille

ITERG, rue Monge, 33600 Pessac (France)

M. C. Viaud and P. Rollin

Laboratoire de Chimie Bioorganique et Analytique, Université d'Orléans, BP 6759, 45067 Orléans Cedex 2 (France)

(First received May 28th, 1991; revised manuscript received July 19th, 1991)

ABSTRACT

Synthesized glucobrassicin, an indole glucosinolate present in rape, was submitted to exogenous enzymatic degradation with commercial myrosinase at two different pH values. Organic products were analysed after silylation by gas chromatography using a thermoionic detector. Three products (3-indolemethanol, 3-indoleacetonitrile and 3,3'-diindolylmethane) were identified by comparison with the retention times of silylated authentic materials and by gas chromatography–mass spectrometry. Two different degradation schemes were proposed according to the pH conditions: 3-indoleacetonitrile was obtained at acidic pH and 3,3'-diindolylmethane at neutral pH. The synthetic glucobrassicin thus behaved in the same manner as the natural product.

INTRODUCTION

Glucosinolates are an important class of compounds widely distributed in all crucifer plants [1–3]. Much work has been devoted to the rape: the meal remaining after oil extraction can be fed to livestock, but in limited amounts as it contains some of these glucosinolates. During processing of seeds, they are broken down by an endogenous enzyme, myrosinase (E.C. 3.2.3.1) to give, in particular, organic isothiocyanates, nitriles, oxazolidi-

nethiones and thiocyanate ion [1–3]. These derivatives have been found to be harmful when consumed by humans and animals [1–3]. Thyroid, liver and kidney diseases are known to occur in monogastric animals [1–5].

Nowadays, new varieties named double low rapeseed (00 rapeseed), which contain less glucosinolates, are cultivated. However, this genetic improvement has affected only the aliphatic fraction. The indole glucosinolates (Fig. 1) represent the major part of the total glucosinolate content [6].

It has been shown that they are susceptible to thermal degradation leading to the formation of thiocyanate ions [6–8]. Nitriles have also been obtained in rape seeds and meals [9,10]. Enzymatic degradation of natural glucobrassicin has been described [11]. Nevertheless, the separation and purification of indole glucosinolates are very tedious [12] and it seems that complete degradation schemes are to be found only by using pure compounds. We took advantage of a recently developed synthesis of glucobrassicin [13] to make an exogenous enzymatic degradation study of this glucosinolate at acidic and neutral pH.

EXPERIMENTAL

Materials

Glucobrassicin was synthesized as described by Viaud and Rollin [13] with a slight modification: the intermediate 3-(2-nitrovinyl)indole was prepared by the condensation of indole and 1-dimethylamino-2-nitroethylene [14]. 3-Indoleacetonitrile and pyridine were obtained from Merck, myrosinase from Sigma and bis(trimethylsilyl)trifluoroacetamide (BSTFA) from Pierce. 3-Indolemethanol was obtained by sodium borohydride reduction of the corresponding aldehyde [15].

To prepare 3,3'-diindolylmethane, 3-indolemethanol hydrate (1 g) (Aldrich) and distilled water (50 ml) were placed in a 100-ml flask equipped with a condenser and heated with magnetic stirring for 18 h under reflux. The solid was dissolved in ethyl acetate and the solution was dried (magnesium sulphate), filtered and concentrated *in vacuo*. Recrystallization from methanol afforded an orange solid (490 mg; m.p. 162–163°C; lit. [16] m.p., 164–165°C). ^1H NMR (300 MHz, DMSO- d_6), δ (p.p.m.): 4.12 (s, 2H, CH_2); 6.90 (dd, 2H, H_5 , $J_{\text{H}_5-\text{H}_6} = 7.1$ Hz); 7.02 (dd, 2H, H_6); 7.11 (d, 2H, H_2 , $J_{\text{H}_2-\text{NH}} = 1.5$ Hz); 7.31 (d, 2H, H_7 , $J_{\text{H}_6-\text{H}_7} = 8.2$ Hz); 7.51 (d, 2H,

H_4 , $J_{\text{H}_4-\text{H}_5} = 7.9$ Hz); 10.72 (m, 2H, NH). ^{13}C NMR (62 MHz, DMSO- d_6), δ (p.p.m.): 20.87 (C_{10}); 111.25 (C_7); 114.14 (C_3); 117.97 (C_5); 118.62 (C_4); 120.67 (C_6); 112.71 (C_2); 127.13 (C_8); 136.33 (C_9).

Enzymatic hydrolysis of glucobrassicin

Glucobrassicin (10 mg) was weighed into a 10-ml tube. Buffer solution (5 ml; pH 3 or 7) and a few milligrams of myrosinase were then added. The homogenized solution was kept at 37°C for 4 h. Organic products were extracted with hexane (2×5 ml). The extracts were concentrated under a slow flow of nitrogen and the residue was silylated with 50 μl of pyridine and 50 μl of BSTFA at room temperature. Analysis was performed after 5 min.

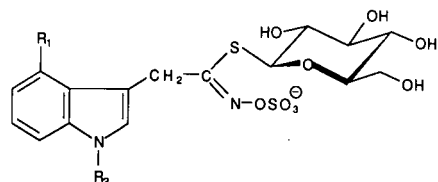
Gas chromatographic conditions

Gas chromatographic analysis was carried out on a Delsi DI-700 gas chromatograph with thermoionic detection (TID). A fused-silica column (25 m \times 0.32 mm I.D.) with a 0.2- μm coating of SE-30 was used. The carrier gas (helium) pressure was 0.8 bar; the splitting ratio was 1:50. The oven temperature was programmed from 100 to 280°C at 5°C min^{-1} . The injector and detector temperatures were 320°C.

Gas chromatography–mass spectrometry

The instrument used was an Intersmat IGC 121 M gas chromatograph linked via a direct inlet to a Micromass VG 16-F mass spectrometer. The column was a 25 m \times 0.22 mm I.D. fused-silica capillary column with a 0.25- μm coating of BP-1. The injection port temperature was 280°C, helium was used as the carrier gas at a pressure of 1.0 bar and the oven temperature was programmed from 130 to 300°C at 4°C min^{-1} . Positive-ion electron impact mass spectra were recorded at 70 eV. Spectra were swept from 20 to 700 u at 0.5 s per decade.

Mass spectra of silylated reference products are



$\text{R}_1 = \text{R}_2 = \text{H}$	glucobrassicin
$\text{R}_1 = \text{OH}$ $\text{R}_2 = \text{H}$	4-hydroxyglucobrassicin
$\text{R}_1 = \text{OCH}_3$ $\text{R}_2 = \text{H}$	4-methoxyglucobrassicin
$\text{R}_1 = \text{H}$ $\text{R}_2 = \text{OCH}_3$	neoglucobrassicin

Fig. 1. Major indole glucosinolates in rapeseed.

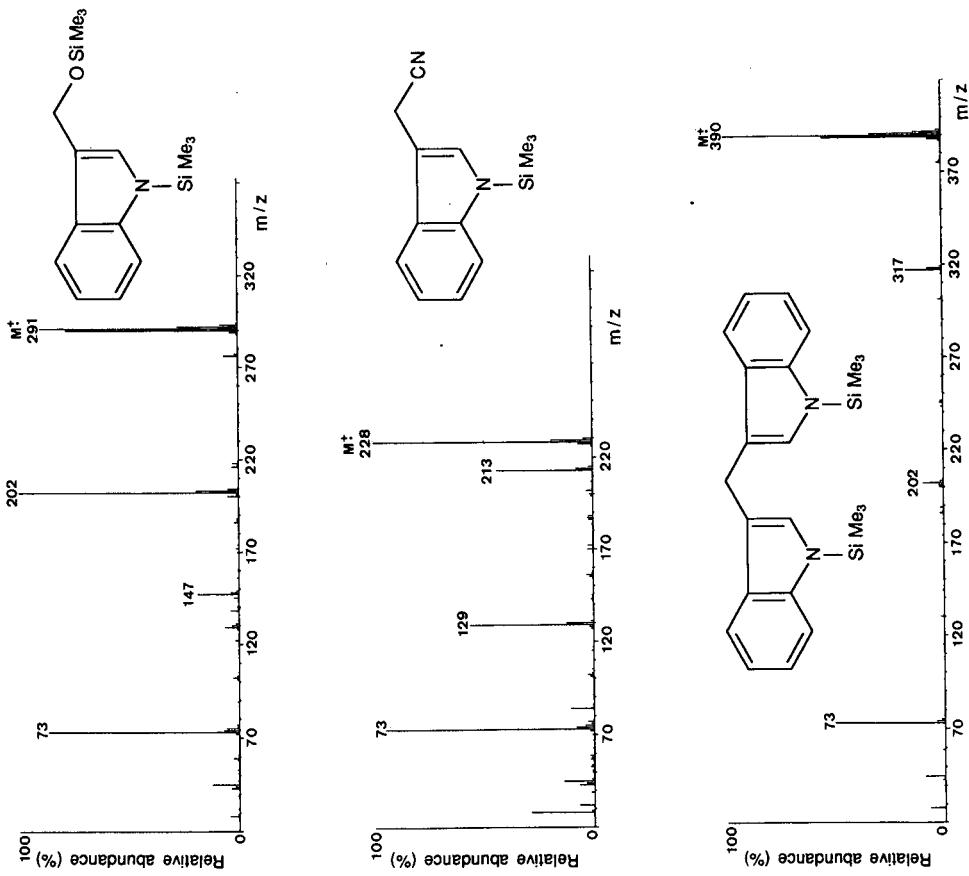


Fig. 2. Mass spectra (70 eV) of putative silylated reference products. Me = Methyl.

Fig. 3. Gas chromatograms of (A) enzymatic degradation products of glucobrassicin at pH 3; (B) enzymatic degradation products of glucobrassicin at pH 7; (C) a mixture of pure silylated products. For conditions, see Experimental. Peaks: 1 = 3-indolemethanol; 2 = 3-indoleacetonitrile; 3 = 3,3'-diindolylmethane.

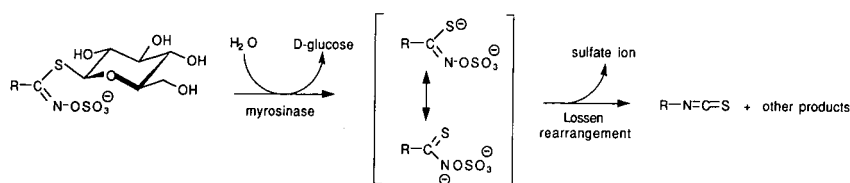


Fig. 4. General breakdown of glucosinolates.

given in Fig. 2. (The mass spectrum of the trimethylsilyl derivative of 3-indolemethanol differs considerably from that in the *Wiley/NBS Registry of Mass Spectral Data* [17]).

RESULTS AND DISCUSSION

Gas chromatograms of the trimethylsilylated derivatives of enzymatic degradation products of glucobrassicin are shown in Fig. 3. Hydrolysis products at pH 3 and 7 are shown in Fig. 3A and B, respectively, followed by a mixture of pure silylated products (Fig. 3C). Identification was confirmed by gas chromatography-mass spectrometry.

As can be seen, two different mechanisms were evidenced in the enzymatic degradation of glucobrassicin: at pH 3, the only detected product was 3-indoleacetonitrile; at pH 7, the predominant com-

pound (>98%) was 3,3'-diindolylmethane, with a trace (<2%) of 3-indolemethanol.

Unambiguously, 3,3'-diindolylmethane comes from the self-condensation of the corresponding alcohol, certainly via a mechanism described previously [18]. It is well documented that myrosinase (thioglucoside glucohydrolase) cleaves the S-glucose bond to give, after desulphation, an isothiocyanate (Fig. 4), commonly observed with aliphatic glucosinolates [1-3].

With glucobrassicin, this compound has never been evidenced despite many trials [8]. (Nevertheless, in recent work dealing with the degradation of neoglucobrassicin, the corresponding isothiocyanate was evidenced under particular experimental conditions [19]). It appears that it is unstable and immediately yields 3-indolemethanol and thiocyanate ion.

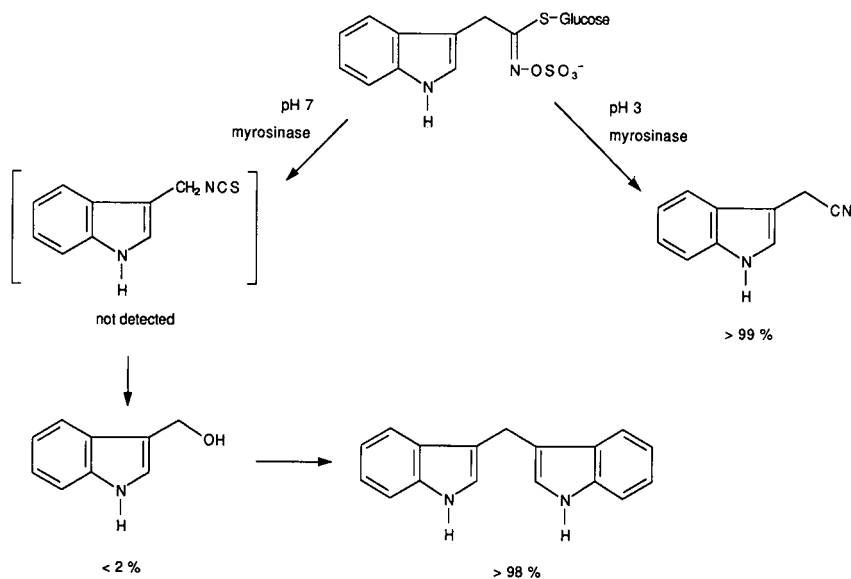


Fig. 5. Enzymatic hydrolysis of synthesized glucobrassicin.

A general scheme of the enzymatic degradation of synthesized glucobrassicin is given in Fig. 5.

In conclusion, during enzymatic hydrolysis, the synthesized glucobrassicin showed the same behavior as the natural product [11].

ACKNOWLEDGEMENT

C. Vitry (CESAMO, Université Bordeaux I) is gratefully thanked for the mass spectrometric study.

REFERENCES

- 1 H. L. Tookey, C. H. van Etten and M. E. Daxenbichler, in I. E. Liener (Editor), *Toxic Constituents of Plant Foodstuffs*, Academic Press, New York, 2nd ed., 1980, p. 103.
- 2 C. H. Van Etten and H. L. Tookey, in M. Rechcigl, Jr. (Editor), *CRC Handbook of Naturally Occurring Food Toxicants*, CRC Press, Boca Raton, FL, 1983, p. 15.
- 3 G. R. Fenwick, R. K. Heaney and W. J. Mullin, *CRC Crit. Rev. Food Sci. Nutr.*, 18 (1983) 123.
- 4 M. Vermorel, R. K. Heaney and G. R. Fenwick, *J. Sci. Food Agric.*, 44 (1988) 321.
- 5 M. Vermorel, M. J. Davicco and J. Evrard, *Reprod. Nutr. Dev.*, 27 (1987) 57.
- 6 B. A. Slominski and L. D. Campbell, *J. Sci. Food Agric.*, 40 (1987) 131.
- 7 B. A. Slominski and L. D. Campbell, *J. Sci. Food Agric.*, 47 (1989) 75.
- 8 R. McDanell, A. E. M. McLean, A. B. Hanley, R. K. Heaney and G. R. Fenwick, *Food Chem. Toxicol.*, 26 (1988) 59.
- 9 B. A. Slominski and L. D. Campbell, *J. Chromatogr.*, 454 (1988) 285.
- 10 C. Gardrat and J. L. Coustille, *J. High Resolut. Chromatogr.*, 12 (1989) 626.
- 11 R. Gmelin and A. I. Virtanen, *Suom. Kemistil. B*, 34 (1961) 15.
- 12 A. B. Hanley, C. L. Curl, G. R. Fenwick and R. K. Heaney, *Cruciferae Newsl.*, 9 (1984) 66.
- 13 M. C. Viaud and P. Rollin, *Tetrahedron Lett.*, 31 (1990) 1417.
- 14 G. Büchi and C. P. Mak, *J. Org. Chem.*, 42 (1977) 1784.
- 15 R. M. Silverstein, E. E. Ryskiewicz and S. W. Chaikin, *J. Am. Chem. Soc.*, 76 (1954) 4485.
- 16 E. Leete and L. Marion, *Can. J. Chem.*, 31 (1953) 775.
- 17 F. W. MacLafferty and D. S. Stauffer, *The Wiley/NBS Registry of Mass Spectral Data*, Vol. 3, Wiley, New York, p. 2606.
- 18 J. N. Bemiller and W. Colilla, *Phytochemistry*, 11 (1972) 3393.
- 19 A. B. Hanley, K. R. Parsley, J. A. Lewis and G. R. Fenwick, *J. Chem. Soc., Perkin Trans. 1*, (1990) 2273.

Short Communication

Fast separation of polymethoxylated flavones by carbon dioxide supercritical fluid chromatography

Ph. Morin*

Laboratoire de Chimie Bioorganique et Analytique, Université d'Orléans, 45067 Orléans Cédex 2 (France)

A. Gallois[☆] and H. Richard

Laboratoire de Chimie, ENSIA, Massy (France)

E. Gaydou

Laboratoire de Phytochimie, Faculté des Sciences et Techniques de Saint-Jérôme, Marseille (France)

(First received March 27th, 1991; revised manuscript received July 16th, 1991)

ABSTRACT

The application of supercritical fluid chromatography (SFC) with modified carbon dioxide for the separation of polymethoxylated flavones (PMFs) is reported. The chromatographic system consists of a bare silica column (250 × 4.6 mm I.D.) with a carbon dioxide-methanol mobile phase and UV detection (313 nm). Selectivities are found to be different with this SFS system than with high-performance liquid chromatography (HPLC). All these naturally occurring PMFs (sinensetin, nobiletin, tangeretin, heptamethoxyflavone, tetramethylscutellarein) could be satisfactorily determined using an internal standard. The method was applied to the determination of PMFs in several *Citrus* oils. The SFC procedure is considerably faster than HPLC with good resolution and an adequate accuracy for the quantitative identification of PMFs.

INTRODUCTION

Flavones, which are widespread in the vegetable kingdom, generally occur as hydroxylated or glycosylated derivatives [1]. Polymethoxylated flavones (PMFs) constitute a special group which are present in certain *Citrus* species. The peel of these fruits contains higher concentrations of PMFs than their leaves or juices. Flavonoid determination is useful

in chemiotaxonomic studies on *Citrus* and to authenticate *Citrus* oils. Many papers have been published on the determination of PMFs by high-performance liquid chromatography (HPLC) [2–11].

The results of supercritical fluid chromatographic (SFC) separations of PMFs with carbon dioxide on silica-packed columns are described in this paper.

EXPERIMENTAL

Separations were performed on a stainless-steel column (250 mm × 4.6 mm I.D.) packed with Du-

* Present address: Dionex S.A., 103 av. Grenier, 92100 Boulogne, France.

Pont Zorbax silica (5 μm) equipped with a pre-column (50 mm \times 4.6 mm I.D.) filled with the same silica. The mobile phase, carbon dioxide (N 45 grade, 99,995% purity) (Air Liquide, Bois d'Arcy, France) was pumped through the system by a Varian (Palo Alto, CA, USA) Model 2510 pump. The polar modifier (HPLC-grade methanol; Rathburn Chemicals, Walkerburn, UK) was added using a Gilson (Villiers-le-Bel, France) Model 302 pump. The two solvents were mixed in a Gilson mixing chamber. The pump heads were cooled at 4°C to promote filling of the pump with liquid mobile phase from the carbon dioxide tank. Samples were introduced onto the column via a Rheodyne Model 7010 injector fitted with a 20- μl sample loop. A Varian Model 2550 variable-wavelength UV detector, equipped with an 8- μl high-pressure flowcell, was set at 313 nm (range 0.08 a.u.f.s.). The pressure was controlled by a manual back-pressure regulator (Model 26-3220-24004, Tescom, MN, USA) connected in series after the detector and maintained at 40°C by a water-bath. All stainless-steel tubing between the injector and the column, and also between the outlet of the column and the pressure regulator, was immersed in a water-bath at 40°C to reduce detector noise.

The PMFs used as standards in this work were donated from several sources.

RESULTS AND DISCUSSION

The major aim of this study was to investigate the ability of packed columns for SFC separation of the PMFs. These compounds have the basic flavone structure shown in Table I. As they differ only in the position and the number of methoxy groups on the A, B and C rings of the flavone, differences in polarity and solubility are weak and difficult to interpret. Owing to the similar chemical structures of these compounds, a bare silica stationary phase with a high specific surface area was considered to give higher selectivity than a partitioning stationary phase, and used for this work. All these flavones have their UV absorbance maxima in the range 310–350 nm range [2].

A pure carbon dioxide mobile phase was first tested, but none of the PMFs in Table I could be eluted from Zorbax silica-packed columns at 40°C and 300 atm. As expected on such a column, the

TABLE I
STRUCTURES OF POLYMETHOXYLATED FLAVONES [1]

PMF	Systematic name
Tangeretin	5,6,7,8,4'-Pentamethoxyflavone
Heptamethoxyflavone	3,5,6,7,8,3',4'-Heptamethoxyflavone
Nobiletin	5,6,7,8,3',4'-Hexamethoxyflavone
Sinensetin	5,6,7,3',4'-Pentamethoxyflavone
Tetramethylisoscuteellarein	5,8,7,4'-Tetramethoxyflavone
Isosinensetin	5,7,8,3',4'-Pentamethoxyflavone
Tetramethylscuteellarein	5,6,7,4'-Tetramethoxyflavone
Hexamethoxyflavone	3,5,6,7,3',4'-Hexamethoxyflavone

flavonoids were strongly adsorbed on the activated silanol sites present in the column and the elution strength of pure carbon dioxide was not sufficient for these medium-polarity compounds.

Methanol-carbon dioxide mixtures as mobile phase

The addition of methanol to supercritical carbon dioxide alters the retention in packed-column SFC by masking the active silanol sites. A preliminary of the separation of a test mixture containing five PMFs was carried out to determine their retention behaviour on a bare silica column using supercritical carbon dioxide modified with methanol in the range 5–30%. The capacity factor of each flavone (tangeretin, nobiletin, sinensetin, tetramethylisoscuteellarein and isosinensetin) on a Zorbax silica column was determined at the constant temperature (40°C) for several different methanol contents in carbon dioxide (Table II). Each solute was injected four times and the relative standard deviation (R.S.D.) of the capacity factor was less than 0.5%. The elution order obtained on a silica column with a carbon dioxide-methanol mixture as mobile phase is the same that observed in adsorption HPLC with heptane-ethanol or heptane-isopropanol mixtures [1], and the opposite of the elution order in reversed-phase HPLC [9,10]. In our work, the retention behaviour observed on the silica column confirms that the retention mechanism is based on adsorption of solutes on silanol groups. Tangeretin and heptamethoxyflavone, which contain five and seven methoxy groups, respectively, elute before nobiletin and tetramethylisoscuteellarein, which contain six and four methoxy groups, respectively.

TABLE II

INFLUENCE OF METHANOL ADDED TO CARBON DIOXIDE ON THE CAPACITY FACTORS OF POLYMETHOXYLATED FLAVONES

Stationary phase, Zorbax silica (250 mm × 4.6 mm I.D.); outlet pressure, 200 atm; temperature, 40°C.

Methanol (%, v/v)	Capacity factor (k')				
	Tangeretin	Nobiletin	Sinensetin	Isoscutellarein	Isosinensetin
5	3.94	5.64	15.35	21.00	—
7	2.40	3.34	5.75	8.35	11.00
10	1.55	2.25	3.60	4.75	5.00
20	0.56	0.73	1.17	1.52	—
30	0.40	0.50	0.76	0.99	—

This indicates that the flavonoid retention is determined not only by the number of methoxy groups present, but also by steric effects to an extent that becomes greater as the number of methoxy groups increases. Similar effects were observed in HPLC and reported by Bianchini and Gaydou [1], who studied the retention of seventeen polymethoxylated flavones on a silica packing (LiChrosorb Si 60) using mainly *n*-heptane-ethanol (75:25, v/v) or *n*-heptane-isopropanol (60:40, v/v) as mobile phase. They discussed the influence of both position and number of methoxy groups in the flavonoid skeleton on the retention. We observed in SFC the same sequence for the capacity factors as obtained by Bianchini and Gaydou using adsorption HPLC.

An increase in methanol content results in enhanced solute solubility, a decreased solute adsorption and, consequently, a decrease in retention (Table II); nevertheless, no improvement in selectivity occurred in the 5–20% methanol range for these solutes.

Retention effects could be simply discussed in terms of additivity rules. For example, consider the

logarithms of retention values with 7% modifier. A hypothetical 5,7,4'-trimethoxyflavone would have a log k' of 1.16. Introducing the increments $I_6 = -0.53$, $I_8 = -0.24$ and $I_3 = +0.13$ for substituents in positions 6, 8 and 3', respectively, experimental and calculated log k' values compared as shown in Table III. A methoxy group in position 3 decreases the retention (see the elution order of heptamethoxyflavone and nobiletin), whereas a methoxy group in position 3' increases the retention (see the capacity factors of tangeretin and nobiletin). Finally, methoxy groups in positions 3' and 4' contribute to an increase in the capacity factors (tangeretin and heptamethoxyflavone).

The SFC analysis of a standard mixture of six polymethoxylated flavones was carried out in less than 12 min using silica as the stationary phase, as shown in Fig. 1. The resolution between nobiletin and heptamethoxyflavone is greater than 1.5, whereas reversed-phase HPLC needed the use of water-tetrahydrofuran solvent to resolve these two compounds satisfactorily [8,9].

Fig. 2a and b show chromatograms of the same

TABLE III

EXPERIMENTAL AND CALCULATED LOG k' VALUES FOR POLYMETHOXYLATED FLAVONES

Stationary phase, Zorbax silica (250 mm × 4.6 mm I.D.); outlet pressure, 200 atm; temperature, 40°C; mobile phase, carbon dioxide modified with 7% of methanol.

Parameter	5,7,4'-Trimethoxy-flavone	Tangeretin	Nobiletin	Sinensetin	Tetramethylisoscuteallarein	Isosinensetin
(Log k') _{exp.}	—	0.380	0.524	0.760	0.922	1.04
(Log k') _{calc.}	1.160	0.390	0.520	0.760	0.920	1.05

flavonoid mixtures with different carbon dioxide and methanol flow-rates; at high flow-rate these solutes elute in 2 min without any significant loss of efficiency and resolution.

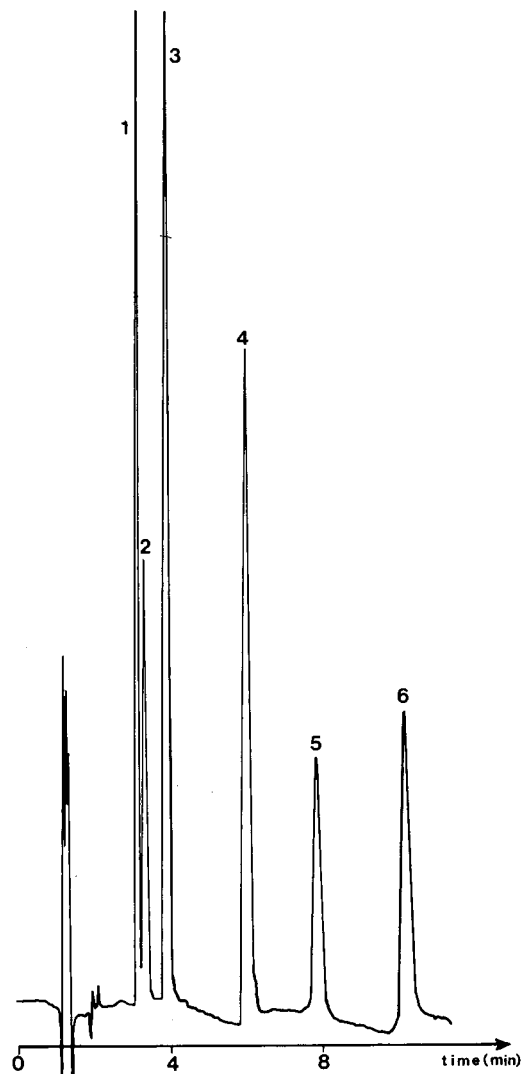


Fig. 1. SFC separation of synthetic mixture of polymethoxylated flavones. Column, 250 mm \times 4.6 mm I.D.; stationary phase, Zorbax (5 μ m) silica; mobile phase, carbon dioxide modified with 10% of methanol; inlet pressure, 220 atm; outlet pressure, 200 atm; column temperature, 40°C; carbon dioxide flow-rate, 3 ml/min; methanol flow-rate, 0.3 ml/min; UV detection at 313 nm. Solutes: 1 = tangeretin; 2 = heptamethoxyflavone; 3 = nobiletin; 4 = sinensetin; 5 = tetramethylisoscuteellarein; 6 = isosinensetin.

Linearity of response and detection limits

The determination of the flavones was achieved using the described SFC system. Linearity ranges of peak area *versus* PMF concentration were established for the UV detector set at 313 nm by injecting 20 μ l of the first sinensetin standards of various concentrations (238, 166, 142, 119, 100, 71, 47 and 25 p.p.m.) and second the tangeretin standards (196, 153, 130, 96, 65, 48 and 24 p.p.m.) (Fig. 3). The UV detector responses of these two flavones were linear in this concentration range up to 5 μ g. Detection

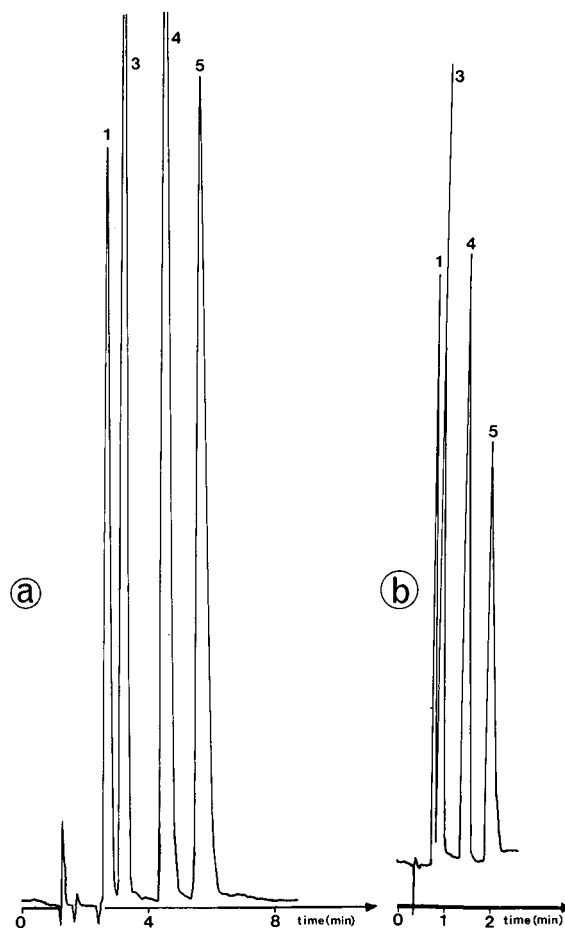


Fig. 2. Rapid separation of polymethoxylated flavones by packed-column SFC. Conditions as in Fig. 1, except as follows: (a) carbon dioxide flow-rate 3 ml/min, methanol flow rate 0.3 ml/min, inlet pressure 220 atm; (b) carbon dioxide flow-rate 9 ml/min, methanol flow-rate 0.9 ml/min, inlet pressure 258 atm. Solutes: 1 = tangeretin; 3 = nobiletin; 4 = sinensetin; 5 = tetramethylisoscuteellarein.

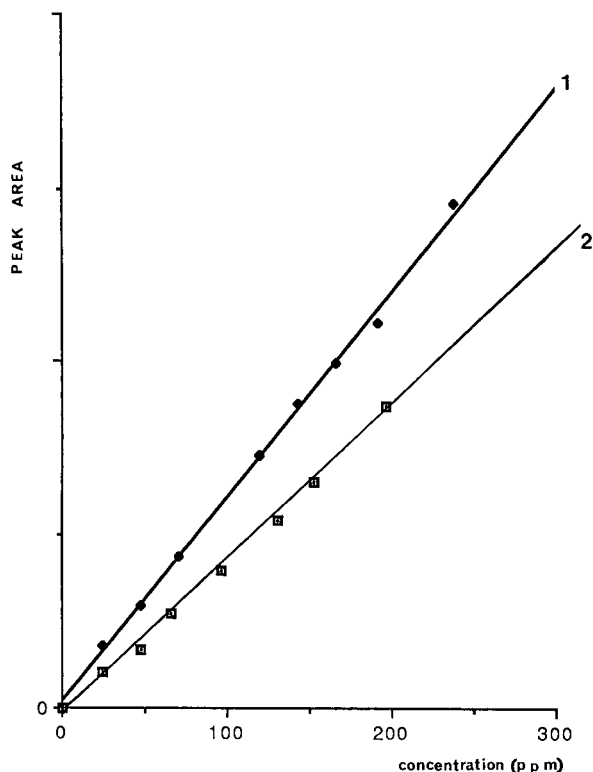


Fig. 3. Quantitative relationship between flavone peak area and concentration. Inlet pressure, 220 atm; outlet pressure, 200 atm; column temperature, 40°C; UV detection at 313 nm; Volume injected, 20 μ l; sample dissolved in ethanol. Solutes: 1 = sinensetin; 2 = tangeretin.

limits (signal-to-noise ratio = 2) were 2.5 p.p.m. for tangeretin (50 ng) and 1.6 p.p.m. for sinensetin (32 ng).

Analysis of Citrus oils

In some instances, an internal standard (coumarin) was added to the *Citrus* oils in order to facilitate the identification of the peaks by comparison of their capacity factors. Finally, PMFs were determined in an orange oil (Fig. 4) and a tangerine oil (Fig. 5).

CONCLUSIONS

Packed-column carbon dioxide SFC appears to be useful for rapid analyses of the main polymethoxylated flavones in *Citrus* oils. Carbon dioxide

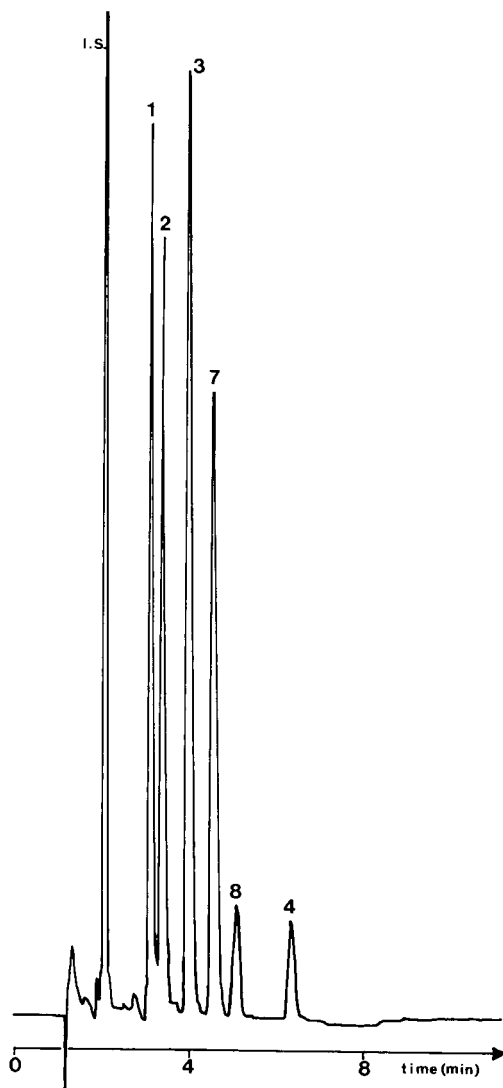


Fig. 4. SFC of the polymethoxylated flavones in orange oil. Conditions as in Fig. 1; orange oil diluted 1:15 in ethanol. Solutes: I.S. = internal standard (coumarin); 1 = tangeretin; 2 = heptamethoxyflavone; 3 = nobiletin; 4 = sinensetin; 7 = tetramethylscutellarein; 8 = hexamethoxyflavone.

modified with 10% of methanol was found to elute all the PMFs from a bare silica stationary phase. The SFC analysis is faster than reversed-phase HPLC, with a fair resolution and accurate and reproducible retention times and peak-area determinations.

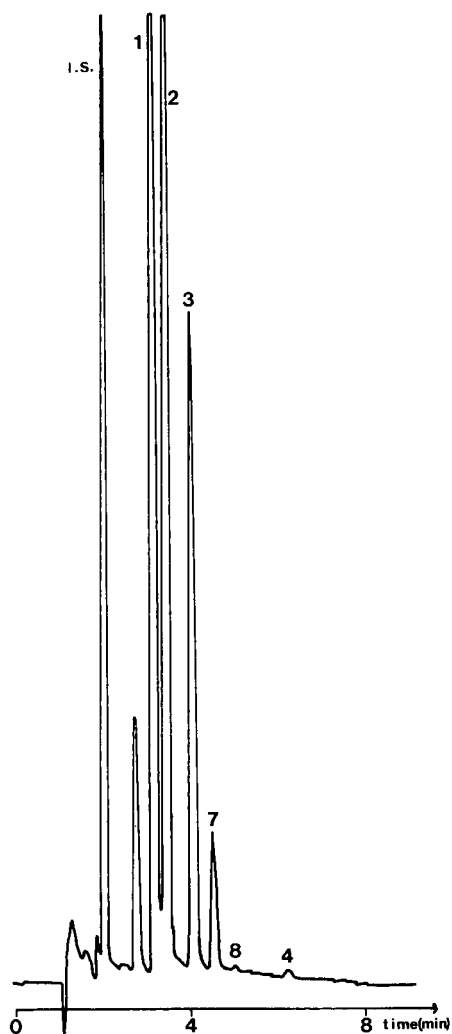


Fig. 5. SFC of the polymethoxylated flavones in tangerine oil. Conditions as in Fig. 1; tangeretin oil diluted 1:15 in ethanol. Solutes as in Fig. 4.

REFERENCES

- 1 J. P. Bianchini and E. M. Gaydou, *J. Chromatogr.*, 211 (1981) 61.
- 2 J. M. Sendra, J. L. Navarro and L. Izquierdo, *J. Chromatogr. Sci.*, 26 (1988) 443.
- 3 M. K. Veldhuis, L. J. Swift and W. C. Scott, *J. Agric. Food Chem.*, 18 (1970) 590.
- 4 R. Galensa and K. Herrmann, *J. Chromatogr.*, 189 (1980) 217.
- 5 B. Heimburger, R. Galensa and K. Herrmann, *J. Chromatogr.*, 439 (1988) 481.
- 6 E. M. Gaydou, J. P. Bianchini and R. Randriamiharisoa, *J. Agric. Food Chem.*, 35 (1987) 525.
- 7 M. Hadj-Mahammed and B. Y. Meklati, *Lebensm.-Wiss. Technol.*, 20 (1987) 111.
- 8 R. Rouseff and S. Ting, *J. Chromatogr.*, 176 (1979) 75.
- 9 S. V. Ting, R. L. Rouseff, M. H. Dougherty and J. A. Attaway, *J. Food Sci.*, 44 (1979) 69.
- 10 J. P. Bianchini, E. M. Gaydou, A. M. Siouffi, G. Mazerolles, D. Mathieu and R. Phan Tan Luu, *Chromatographia*, 23 (1987) 15.
- 11 J. P. Bianchini and E. M. Gaydou, *J. Chromatogr.*, 190 (1980) 233.

Short Communication

Determination of cimetidine in pharmaceutical preparations by capillary zone electrophoresis

Susan Arrowood and A. M. Hoyt, Jr.*

Department of Chemistry, University of Central Arkansas, Conway, AR 72032 (USA)

(First received May 2nd, 1991; revised manuscript received August 9th, 1991)

ABSTRACT

A method was developed for the determination of cimetidine (the active ingredient in the ulcer medication Tagamet) in the commercial preparations in which it is sold. Samples were dissolved, diluted and extracted with petroleum ether before capillary zone electrophoresis in 20 mM phosphate buffer at pH 7. Analysis of over 60 samples from commercially available formulations gave relative standard deviations of 1.9 to 6.4%.

INTRODUCTION

Cimetidine is a first-generation anti-ulcer drug manufactured by Smith Kline and French (Beecham), and sold under the trade name Tagamet. Many analytical procedures for cimetidine are available, and these methods have been applied commonly to body fluids. The most widely used is high-performance liquid chromatography (HPLC), typically employing UV absorbance detection at 228–229 nm [1–5]. Differences in the cited procedures are in extraction, sample type, internal standard, or interfering compounds. Less-commonly employed procedures use colorimetry [6,7], titration [8], polarography [9], and even ion-selective electrodes [10].

Most pharmaceutical work with capillary zone electrophoresis (CZE), and its relative, micellar electrokinetic capillary chromatography (MECC), has been of a qualitative nature [11–13]. CZE was investigated as the basis of a method, in the present application, in order to take advantage of the speed,

separating capability, and small sample requirement of the technique. The underutilized quantitative potential of this technique is also thus illustrated.

EXPERIMENTAL

Chemicals and reagents

Phosphoric acid, potassium hydroxide, hydrochloric acid, light petroleum (b.p. 30–75°C) and phenol were ACS grade and purchased from VWR Scientific (Irving, TX, USA). Cimetidine was obtained from ICN Biomedicals (Costa Mesa, CA, USA) and kept in refrigerated storage. Commercial cimetidine pharmaceuticals were obtained at a local pharmacy.

Electrophoretic system

The electrophoretic system employed a Hipotronics 840A 0-30KVDC (Hipotronics, Brewster, NY, USA) power supply. The 80-cm, 50 μ m I.D. capillary (No. TSP050375, Polymicro Technolo-

gies, Phoenix, AZ, USA) was fitted with an on-column detector (model CV⁴, ISCO, Lincoln, NE, USA) 24 cm from the negative (grounded) terminus. The positive electrode was enclosed in a plexiglass box to prevent electrical shock. Signals were detected concurrently by a 0–1 mV recorder (BD40, Kipp en Zonen, Delft, Netherlands) and an integrator (Model 4290, Varian Associates, Walnut Creek, CA, USA). Sample degassing was accomplished using a Branson 2200 (Branson Ultrasonics, Danbury, CT, USA) ultrasonic cleaner.

Instrumental and chemical parameters for electrophoresis

Resolution and peak symmetry were found to be optimized in a buffer of 20 mM phosphate at pH 7, prepared by titrating a 20 mM solution of H₃PO₄ to neutrality with 20% potassium hydroxide. Initially, the capillary was forcibly syringe-purged, and the reservoirs at the capillary termini were filled with buffer, following degassing of the phosphate solution for 15 min using sonication and aspirator vacuum. Subsequently, degassing the reservoirs only was usually sufficient.

The UV spectrum of cimetidine showed a single peak at the wavelength employed, 220 nm. An electropherogram of a mixture of cimetidine ($5.6 \cdot 10^{-5}$ g/ml) and the chosen internal standard, phenol ($8 \cdot 10^{-5}$ g/ml) in buffer is shown in Fig. 1. Separations, performed at 25 kV, gave currents of 25–40 μ A.

Samples were introduced by 10-s immersions of the entrance end of the capillary into sample solution elevated 25 cm above the exit reservoir level. Estimates of sample size, using a method previously reported [14] indicated that *ca.* 5 nl was injected in the 10-s period.

Pharmaceuticals assay

Preparation of the calibration curve for use in assaying the pharmaceutical preparations was accomplished by first preparing stock solutions of cimetidine (*ca.* 0.07 g/100 ml) and phenol (*ca.* 0.08 g/100 ml) in pH 7 phosphate buffer. Five standards, each containing 5 ml of the phenol solution, and 2, 4, 6, 8, and 10 ml, respectively, of the cimetidine solution were placed in 50-ml volumetric flasks, then made to volume with phosphate buffer. Duplicate 10-s injections of each were made after degass-

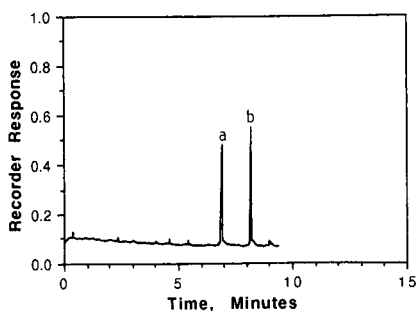


Fig. 1. Electropherogram of CZE separation of (a) cimetidine and (b) phenol in 20 mM phosphate buffer, pH 7.

ing. The average peak area ratios, when graphed *vs.* concentration, showed the expected linearity.

The amount of cimetidine in tablets was determined by placing one tablet in a 250-ml volumetric flask, adding phosphate buffer to the mark, and stirring overnight on a magnetic stirrer. A 10-ml aliquot was transferred to a 100-ml volumetric flask, 10 ml of phenol solution added, and the flask made to volume with phosphate buffer. A 50-ml aliquot of this final solution was extracted twice with 25 ml light petroleum, and the extracts were discarded. Duplicate 10-s injections were made after degassing. The only variation to be noted is that 5-ml aliquots of the 250-ml initial solutions were used on the 800-mg tablet samples, in order to keep the peak area ratios within the limits of the calibration curve.

Tagamet liquid preparations (label claim 300 mg/5 ml) were assayed by pipetting 5 ml of the liquid into 250-ml volumetric flasks, then diluting to volume with phosphate buffer. Aliquots of 10 ml of this solution were then treated the same as the 10-ml aliquots of the tablet solutions above.

Injectable preparations followed a similar protocol to the liquids described above. The entire 2 ml contents of each vial were emptied into 250-ml volumetric flasks which were made to volume with phosphate buffer; 10 ml aliquots were used for determination as before. The results of over 60 assays of commercial preparations are summarized in Table I. Tabular values were calculated from the average of duplicate peak area ratios, using the slope and intercept of the best-fit line for the cimetidine standard solutions.

RESULTS AND DISCUSSION

Assay parameters

The linear range of instrument response, as shown by increases in peak area ratios with increasing cimetidine concentration, is demonstrated in Fig. 2. Above approximately $1.8 \cdot 10^{-4}$ g/ml, direct proportionality is lost. At this concentration, the detector response is maximized, and further increases are not able to be measured.

Initial quantitation attempts utilized measurement of relative peak heights as an estimate of cimetidine level. Much more consistent values were obtained if relative peak areas are used. Twenty duplicate injections of the same sample (heights hand-measured from the recorder trace, areas taken from the electronic integrator) gave a relative standard deviation of 3.3% for peak height ratios, 1.8% for peak area ratios.

Since the internal standard, phenol, was neutral at the chosen pH, it migrates with the electroosmotic flow; however, no problems associated with this coincidence were noted. All pharmaceutical preparation types were analyzed, and no problems with interferences were encountered.

Capillary performance deterioration

When pharmaceuticals were diluted and the solutions introduced into the capillary without pretreatment, successive electropherograms showed poorer resolution, smaller peaks, and a more erratic baseline. The light petroleum extraction in the procedure eliminated this problem; after extraction, cap-

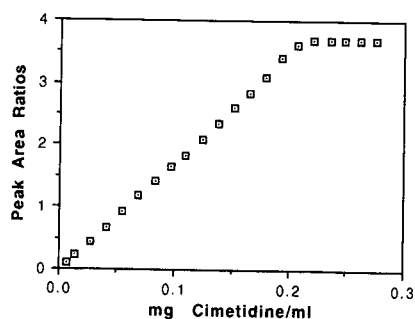


Fig. 2. CZE linearity response test: cimetidine peak area/phenol peak area as a function of cimetidine concentration.

illary performance remained constant over hundreds of samples. Repeated light petroleum extractions of pure solutions of cimetidine and internal standard showed the peak area ratio is unaffected by this step.

Sample dissolution time

Tablet samples which stood in buffer solution showed cimetidine peaks which increased in size for several hours. After standing overnight, the peaks stabilized at a maximum, therefore tablet samples were stirred overnight before dilution, extraction and assay. Similar observations were not noted in the liquid and injectable preparations; they could be determined immediately.

Comparison with existing methods

One HPLC method for cimetidine and its degradation products in preparations which included

TABLE I
SUMMARY OF ANALYSES OF PHARMACEUTICAL PREPARATIONS

Preparation	Number of samples	Amount (mg) ^a	CZE method results (mg)			R.S.D. ^b (%)
			Avg.	High	Low ^a	
Tablet	14	200	212	232	196	6.4
Tablet	14	300	314	335	290	3.9
Tablet	14	400	402	411	380	2.3
Tablet	15	800	830	870	790	3.5
Liquid	10	300/5 ml	327	339	314	2.7
Injectable	10	300/2 ml	324	332	314	1.9

^a Manufacturer's stated amount.

^b R.S.D. = Relative standard deviation.

tablets [15] had relative standard deviations which ranged up to 7.1%, while another in biological fluids had coefficients of variation of as much as 20% [16]. Therefore, CZE is at least comparable in precision, while requiring fewer manipulations, a much smaller sample, and less time than the more common methods. Extraction and pretreatment, usual in HPLC, is simple here, and the CZE method requires less operator skill.

ACKNOWLEDGEMENT

This research was supported by grant No. 90-B-08 from the Arkansas Science and Technology Authority.

REFERENCES

- 1 M. Abdel-Rahim, D. Ezra, C. Peck and J. Lazar, *Clin. Chem.*, 31 (1985) 621.
- 2 R. Chiou, R. J. Stubbs and W. F. Bayne, *J. Chromatogr.*, 377 (1986) 441.
- 3 H. Kubo, Y. Kobayashi and K. Tokunaga, *Anal. Lett.*, 18 (1985) 245.
- 4 C. W. Lloyd, W. J. Martin, J. Nagle and A. R. Hauser, *J. Chromatogr.*, 339 (1985) 139.
- 5 H. A. Strong and M. Spino, *J. Chromatogr.*, 422 (1987) 301.
- 6 C. Aromdee, K. Raksrivong and A. Vathanasanti, *Analyst (London)*, 112 (1987) 1523.
- 7 M. V. S. Krishnan and A. S. Rao, *Indian Drugs*, 23 (1986) 469.
- 8 K. N. Raut, S. D. Sabnis and S. S. Vaidya, *Indian J. Pharm. Sci.*, 48 (1986) 49.
- 9 A. Sanchez-Perez, J. Hernandez-Mendez and J. E. Fuentes de Frutos, *J. Assoc. Off. Anal. Chem.*, 68 (1985) 1060.
- 10 A. Mitsana-Papazoglou, E. P. Deamandis and T. P. Hadjiannou, *J. Pharm. Sci.*, 76 (1987) 485.
- 11 S. Fujiwara and S. Honda, *Anal. Chem.*, 59 (1987) 2773.
- 12 H. Nishi, N. Tsumagari, T. Kakimoto and S. Terabe, *J. Chromatogr.*, 477 (1989) 259.
- 13 A. Wainwright, *J. Microcolumn Sep.*, 2 (1990) 166.
- 14 A. M. Hoyt, Jr. and M. J. Sepaniak, *Anal. Lett.*, 22 (1989) 861.
- 15 E. G. Lovering and N. M. Curran, *J. Chromatogr.*, 319 (1985) 235.
- 16 A. Adedoyin, L. Aarons and J. B. Houston, *J. Chromatogr.*, 345 (1985) 192.

PUBLICATION SCHEDULE FOR 1992

Journal of Chromatography and Journal of Chromatography, Biomedical Applications

MONTH	O 1991	N 1991	D 1991	J	
Journal of Chromatography	585/1	585/2 586/1 586/2 587/1	587/2 588/1+2	589/1+2 590/1 590/2	The publication schedule for further issues will be published later
Cumulative Indexes, Vols. 551-600					
Bibliography Section					
Biomedical Applications				573/1 573/2	

INFORMATION FOR AUTHORS

(Detailed *Instructions to Authors* were published in Vol. 558, pp. 469-472. A free reprint can be obtained by application to the publisher, Elsevier Science Publishers B.V., P.O. Box 330, 1000 AH Amsterdam, The Netherlands.)

Types of Contributions. The following types of papers are published in the *Journal of Chromatography* and the section on *Biomedical Applications*: Regular research papers (Full-length papers), Review articles and Short Communications. Short Communications are usually descriptions of short investigations, or they can report minor technical improvements of previously published procedures; they reflect the same quality of research as Full-length papers, but should preferably not exceed five printed pages. For Review articles, see inside front cover under Submission of Papers.

Submission. Every paper must be accompanied by a letter from the senior author, stating that he/she is submitting the paper for publication in the *Journal of Chromatography*.

Manuscripts. Manuscripts should be typed in double spacing on consecutively numbered pages of uniform size. The manuscript should be preceded by a sheet of manuscript paper carrying the title of the paper and the name and full postal address of the person to whom the proofs are to be sent. As a rule, papers should be divided into sections, headed by a caption (*e.g.*, Abstract, Introduction, Experimental, Results, Discussion, etc.). All illustrations, photographs, tables, etc., should be on separate sheets.

Introduction. Every paper must have a concise introduction mentioning what has been done before on the topic described, and stating clearly what is new in the paper now submitted.

Abstract. All articles should have an abstract of 50-100 words which clearly and briefly indicates what is new, different and significant.

Illustrations. The figures should be submitted in a form suitable for reproduction, drawn in Indian ink on drawing or tracing paper. Each illustration should have a legend, all the *legends* being typed (with double spacing) together on a *separate sheet*. If structures are given in the text, the original drawings should be supplied. Coloured illustrations are reproduced at the author's expense, the cost being determined by the number of pages and by the number of colours needed. The written permission of the author and publisher must be obtained for the use of any figure already published. Its source must be indicated in the legend.

References. References should be numbered in the order in which they are cited in the text, and listed in numerical sequence on a separate sheet at the end of the article. Please check a recent issue for the layout of the reference list. Abbreviations for the titles of journals should follow the system used by *Chemical Abstracts*. Articles not yet published should be given as "in press" (journal should be specified), "submitted for publication" (journal should be specified), "in preparation" or "personal communication".

Dispatch. Before sending the manuscript to the Editor please check that the envelope contains four copies of the paper complete with references, legends and figures. One of the sets of figures must be the originals suitable for direct reproduction. Please also ensure that permission to publish has been obtained from your institute.

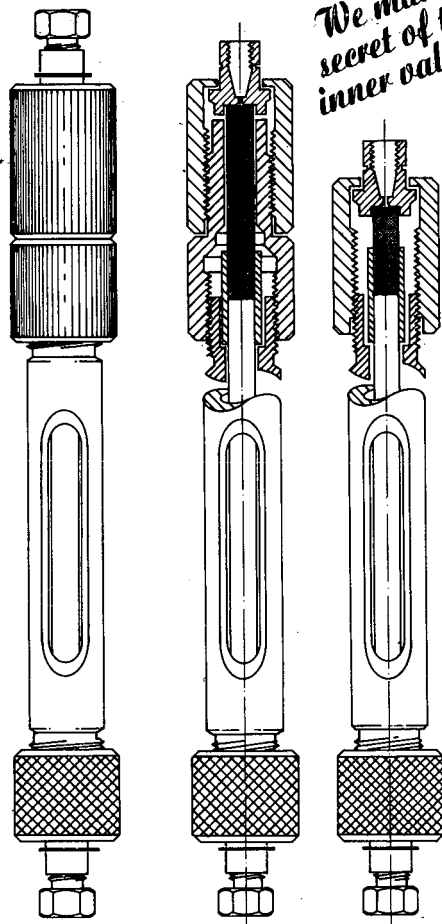
Proofs. One set of proofs will be sent to the author to be carefully checked for printer's errors. Corrections must be restricted to instances in which the proof is at variance with the manuscript. "Extra corrections" will be inserted at the author's expense.

Reprints. Fifty reprints of Full-length papers and Short Communications will be supplied free of charge. Additional reprints can be ordered by the authors. An order form containing price quotations will be sent to the authors together with the proofs of their article.

Advertisements. The Editors of the journal accept no responsibility for the contents of the advertisements. Advertisement rates are available on request. Advertising orders and enquiries can be sent to the Advertising Manager, Elsevier Science Publishers B.V., Advertising Department, P.O. Box 211, 1000 AE Amsterdam, Netherlands; courier shipments to: Van de Sande Bakhuysenstraat 4, 1061 AG Amsterdam, Netherlands; Tel. (+31-20) 515 3220/515 3222, Telefax (+31-20) 6833 041, Telex 16479 els vi nl. *UK:* T. G. Scott & Son Ltd., Tim Blake, Portland House, 21 Narborough Road, Cosby, Leics. LE9 5TA, UK; Tel. (+44-533) 753 333, Telefax (+44-533) 750 522. *USA and Canada:* Weston Media Associates, Daniel S. Lipner, P.O. Box 1110, Greens Farms, CT 06436-1110, USA; Tel. (+1-203) 261 2500, Telefax (+1-203) 261 0101.

HPLC cartridges packed with NUCLEOSIL®

with new guard column
holder for 11 and 30 mm
guard columns



- Economical
- Mounted in seconds
- Convenient operation
- Versatile column range

Please ask for further information.

MACHEREY-NAGEL 

MACHEREY-NAGEL GmbH & Co. KG · P.O. Box 101352 · D-5160 Düren
West Germany · Tel. (0 24 21) 6 98-0 · Telex 8 33 893 mana d · Fax (0 24 21) 6 20 54
Switzerland: MACHEREY-NAGEL AG · P.O. Box 224 · CH-4702 Oensingen
Tel. (0 62) 76 20 66 · Telex 9 82 908 mnag ch · Fax (0 62) 76 28 64

FOR ADVERTISING INFORMATION PLEASE CONTACT OUR ADVERTISING REPRESENTATIVES

USA/CANADA

Weston Media Associates

Mr. Daniel S. Lipner

P.O. Box 1110, GREENS FARMS, CT 06436-1110

Tel: (203) 261-2500, Fax: (203) 261-0101

GREAT BRITAIN

T.G. Scott & Son Ltd.

Tim Blake

Portland House, 21 Narborough Road
COSBY, Leicestershire LE9 5TA

Tel: (0533) 753-333, Fax: (0533) 750-522

Mr. M. White or Mrs. A. Curtis

30-32 Southampton Street, LONDON WC2E 7HR

Tel: (071) 240 2032, Fax: (071) 379 7155,

Telex: 299181 adsale/g

JAPAN

ESP - Tokyo Branch

Mr. S. Onoda

20-12 Yushima, 3 chome, Bunkyo-Ku
TOKYO 113

Tel: (03) 3836 0810, Fax: (03) 3839-4344

Telex: 02657617



REST OF WORLD

ELSEVIER

SCIENCE

PUBLISHERS

Ms. W. van Cattenburch

P.O. Box 211, 1000 AE AMSTERDAM,

The Netherlands

Tel: (20) 515.3220/21/22, Telex: 16479 els vi nl

Fax: (20) 683.3041